Sandy Solutions for Rising Challenges

Evaluating the Suitability of Nourishments in Mitigating European Coastal Erosion by 2100

MSc Thesis Hydraulic Engineering

Juul Hemmes

Deltares

TU Delft

Sandy Solutions for Rising Challenges

Evaluating the Suitability of Nourishments in Mitigating European Coastal Erosion by 2100

by

Juul Hemmes

to obtain the degree of Master of Science
at the Delft University of Technology
to be defended publicly on Thursday July 3, 2025 at 15:00.

Supervisors:	Dr. Ir. M. A. de Schipper	TU Delft
	Dr. Ir. A.P. Luijendijk	TU Delft & Deltares
	Dr. J.E.A. Storms	TU Delft
	F.R. Calkoen	TU Delft & Deltares
Project Duration:	November, 2024 - July, 2025	
Faculty:	Faculty of Civil Engineering and Geo-sciences, TU Delft	

Cover: Aerial view of Tisvilde, on the Danish Riviera, ALAMY (Modified)

Deltares

TU Delft

Preface

This thesis represents the final milestone of my Master's in Hydraulic Engineering at TU Delft, concluding a journey defined by curiosity, collaboration, and a growing commitment to addressing coastal challenges.

My passion for engineering began in high school, when our team was one of the few secondary school groups allowed to participate in the Shell Eco-marathon, competing alongside TU Delft students. That experience inspired me to pursue Civil Engineering in Delft, initially drawn to nearly every aspect of the field except hydraulic engineering. Ironically, it's that very subfield that ended up capturing my interest the most

My appreciation for its relevance truly emerged during my minor in Misungwi, Tanzania, where I co-designed a water management system for a remote farm in collaboration with local communities and fellow students. That project combined technical application with tangible impact, and taught me the importance of aligning engineering solutions with local context, needs, and equity.

During my Master's, I gravitated toward coastal engineering, a field that captivated me with its complexity, urgency, and societal relevance. Sea-level rise and climate change are not future problems; they are already reshaping coastlines and communities. I became especially interested in beach nourishment, not just as a technical solution, but as a strategic, long-term adaptation tool operating at the interface of policy, geomorphology, and governance. This thesis allowed me to explore those intersections and contribute to understanding where and how nourishment can be suitable.

Along the way, I've come to value the importance of integrating long-term thinking into spatial planning and making data-driven decisions under uncertainty. This work challenged me to think critically, balance theory and practice, and reflect on the role of engineering in shaping resilient, future-oriented coastlines.

I am deeply grateful to those who supported me throughout this journey. Arjen, thank you for your mentorship, clear questions, and open conversations. Matthieu, your expertise and critical feedback truly elevated this thesis. Joep, your interdisciplinary perspective helped me keep sight of the broader context. Floris, thank you for being in my corner, your support with data and your collaborative spirit made a big difference.

To my family and friends, thank you for your unwavering support. Joska, thanks for turning my ideas into visuals that actually told the story, and looked good too. And to my hydraulic friends: thank you for enduring six months of non-stop thesis talk, I promise we'll talk about something else soon!

Looking back, I'm truly happy with the direction I've taken. I will continue working in this field, where innovation and nature go hand in hand.

Juul Hemmes
Delft, June 2025

Abstract

Climate change is accelerating coastal erosion, posing growing risks to infrastructure, ecosystems, and livelihoods across the world's coastal zones. While global and regional studies increasingly provide projections of physical shoreline change, they often fail to integrate these with the spatial distribution of exposed assets or the potential for adaptation measures. As a result, their utility for informing where and how interventions, such as beach nourishment, could serve as viable adaptation options remains limited. Current research typically treats coastal erosion, exposure, and adaptation in isolation, leaving a critical gap in support for strategic coastal planning, where cross-country and cross-boundary insights could enable more coordinated and effective responses.

Here we present a continental-scale framework that integrates shoreline-change modelling, infrastructure exposure, and nourishment suitability to inform coastal adaptation across Europe. We first compile a novel database of 1,060 historical nourishment interventions spanning 70 years, capturing the spatial distribution, implementation motives, and coastal contexts, including borrow area, nourishment type, and coastal type, under which nourishments have been applied. These insights inform a Nourishment Suitability Assessment Model (NSAM), which evaluates future nourishment potential based on four key factors: coastal type, policy context, sediment availability, and prior experience. We then project shoreline retreat by combining ensemble-based sea-level rise scenarios with ambient erosion trends derived from multi-decadal satellite imagery. The analysis applies the Bruun Rule with spatially variable coastal slopes and probabilistically combines sea-level rise-induced retreat with ambient trends. Applied to over 27,000 km of sandy coastline, this produces spatially explicit retreat projections that are intersected with exposure data to identify high-risk beaches.

Our results show that over 98% of transects are projected to erode under sea-level rise by 2100, with median shoreline retreat reaching −80 m under SSP5-8.5. In contrast, ambient change alone shows strong regional variation, with 41% of historically unstable coasts eroding but a median accretion of 17 m at the European scale. Combined projections indicate that while 85% of European sandy coasts are projected to erode by mid-century under SSP2-4.5, only 11.6% of these coincide with direct infrastructure exposure. By focusing on high-risk beaches, defined as stretches with over 1 km of exposed assets, this research identifies up to 841 exposure hotspots (covering 1,497 km) under SSP5-8.5 in 2100, helping to prioritise sites in need of adaptation. Among these exposed sites, nourishment suitability varies considerably, shaped by both physical conditions and institutional capacity. The NSAM's traffic light classification offers a first-order indication of where nourishment could form part of context-specific adaptation strategies, with suitability highest where conditions align with historical precedent and institutional barriers are low.

Key uncertainties are identified, particularly in slope representation and the assumed independence between ambient and sea-level rise-induced retreat. These highlight priorities for future model refinement. The framework demonstrates how integrated hazard, exposure, and adaptation assessment can enable more targeted and context-specific coastal management. By synthesizing forward-looking erosion risk with backward-looking adaptation practice, this work helps bridge the gap between impact assessment and action, showing that while many coasts are at risk, not all are equally suitable for nourishment, and a context-specific approach is necessary.

Contents

Nomenclature

Abbreviations

Abbreviation	Definition
AC	Ambient Change
CEED	Coastal European Exposure Database
DoC	Depth of Closure
EDA	Exploratory Data Analysis
GCTR	Global Coastal Transect Repository
GCTS	Global Coastal Transect System
GIA	Glacial Isostatic Adjustment
IPCC	Intergovernmental Panel on Climate Change
LECZ	Low Elevation Coastal Zone
MSL	Mean Sea Level
NDWI	Normalized Difference Water Index
NSAM	Nourishment Suitability Assessment Model
OSM	OpenStreetMap
RCP	Representative Concentration Pathway
RMSE	Root Mean Square Error
RSLR	Relative Sea Level Rise
R^2	Coefficient of Determination
SDS	Satellite Derived Shorelines
SE	Standard Error
SLR	Sea Level Rise
SSP	Shared Socioeconomic Pathway

Symbols

Symbol	Definition	Unit
D	Depth	[m]
D_c	Depth of closure	[m]
dx	Shoreline change	[m]
L	Length	[m]
n	Number of observations	[-]
N	Normal distribution	[-]
p_x	Percentile	[-]
R	Retreat	[m]
T	Trend	[m/year]
V	Volume	[m^3]
$\tan(\beta)$	Beach slope	[-]
β_0	Regression coefficient (intercept)	[-]
β_1	Regression coefficient (slope)	[-]

1

Introduction

Research Context

Coastal zones are among the most dynamic and vulnerable environments on Earth, supporting critical ecosystems, infrastructure, and livelihoods (Barbier et al., 2024). Climate change has intensified threats to these regions, particularly through rising sea levels and increased storm activity (Griggs & Reguero, 2021). These changes have already contributed to widespread coastal erosion, either newly occurring or accelerating along previously vulnerable shorelines, and are expected to drive permanent shoreline retreat and inundation over longer timescales (Cazenave & Cozannet, 2014; Nicholls & Cazenave, 2010).

Between 1901 and 2018, the global mean sea level (GMSL) rose by 0.20 m, with the rate of rise accelerating to 3.7 mm/yr since the 1960s (IPCC, 2023a). Currently, 24 % of the world's sandy beaches are eroding at rates exceeding 0.5 m/yr (Luijendijk et al., 2018), and stable coasts may also become increasingly exposed as sea levels continue to rise (Zhang et al., 2004).

In Europe, more than 8200 km of sandy coastline have already experienced significant retreat in recent decades, with consistent observations of shoreline loss across the continent (van de Wal et al., 2024). This trend is driven by a combination of natural coastal dynamics and anthropogenic pressures, and is projected to intensify under future climate conditions. In many locations, the presence of hard infrastructure landward of the beach constrains natural retreat, leading to coastal squeeze and threatening the long-term persistence of sandy beaches (Lansu et al., 2024). These developments are not only associated with ecological, social, and economic consequences, but are also expected to increase the risk of coastal flooding (van de Wal et al., 2024).

At the same time, the coastal population in Europe is projected to grow by 57 % by 2040 (IPCC, 2023a), further increasing exposure. This combination of accelerating environmental risks and growing socio-economic pressure underscores the urgency of advancing sustainable management of coastal erosion for the future.

These developments can be understood as part of a broader climate adaptation chain, linking socio-economic and environmental drivers to physical impacts and the need for appropriate adaptation responses (IPCC, 2023a). Figure 1.1 illustrates this chain and highlights the final stages, impacts & risks, and adaptation, as the focus of this thesis.

Research Problem

Despite increasing awareness of the risks posed by sea-level rise and coastal erosion, traditional hard infrastructure, such as seawalls and groynes, continues to be widely used, even though these structures often have negative ecological impacts and may become less stable as sea levels rise and foundation scouring intensifies (IPCC, 2023a; Schoonees et al., 2019).

Beach nourishment has emerged as a promising, nature-based alternative that aligns with, rather than disrupts, natural sediment transport processes. By redistributing sand to eroding coastlines, nour-

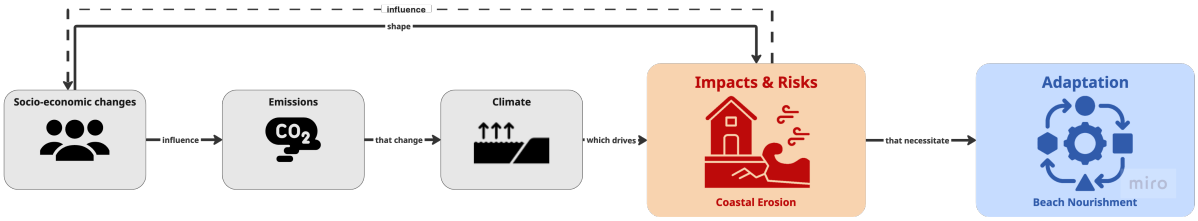

Figure 1.1: Causal chain from socio-economic drivers to coastal adaptation responses. This thesis focuses on the final stages: quantifying shoreline retreat and exposure, and evaluating beach nourishment as an adaptive strategy. Adapted from IPCC (2023a).

ishment strategies aim to enhance coastal resilience while reducing reliance on rigid, often disruptive engineering solutions (Dean, 1991; Hanson et al., 2002; Staudt et al., 2021). However, there is still limited understanding of where, when, and under what conditions nourishment is a suitable mitigation strategy, particularly in the context of future climate. Additionally, the scalability and regional adaptability of nourishment remain under-explored, in part due to data limitations and the lack of harmonised frameworks across Europe.

An initial global assessment of coastal erosion under sea-level rise was conducted by Hinkel et al. (2013) using the DIVA model, an integrated framework for evaluating biophysical and socio-economic impacts. While this study marked a major advance at the time, it relied on coarse, global-scale datasets and simplifying assumptions, such as uniform beach slopes, that limit its relevance for regional or site-specific analyses. For instance, recent meta-analyses of over 2,000 field measurements have shown that beach-face slopes vary significantly with grain size, sediment type, and local conditions (Bujan et al., 2019). With the availability of higher-resolution datasets, improved satellite observations, and more advanced modelling approaches, there is now an opportunity to refine and extend these early findings with greater accuracy and contextual detail.

Recently, projections by Vousdoukas et al. (2020) represent an important step forward by incorporating satellite-derived shoreline change data. However, some methodological steps, such as the processing of input data, are only briefly described, limiting transparency and reproducibility. The study also imposes a uniform retreat limit of 100 m, rather than accounting for actual spatial constraints such as existing infrastructure, which reduces the applicability of the results for exposure and risk assessments.

This research seeks to bridge these gaps by integrating physical shoreline change projections with exposure assessments and evaluating the potential of beach nourishment as a nature-based erosion mitigation strategy across Europe. By combining high-resolution satellite-derived data with climate scenarios, this study aims to identify high-risk coastal areas, based on erosion trends and exposure of assets, while also developing a framework for assessing where nourishment could be suitable as an adaptive response.

Research Objective. Develop a Nourishment Suitability Assessment Model (NSAM) to assess where beach nourishment could be a suitable strategy for mitigating coastal erosion across Europe, for different climate scenarios.

Research Scope

This research focuses exclusively on sandy coastlines in Europe, as these areas are particularly prone to sediment loss and shoreline retreat. Other shore types, such as rocky shores, estuaries, or mudflats, and alternative defence measures like seawalls or groynes fall outside the scope of this study.

The primary hazard considered is coastal erosion; flood risk is explicitly excluded from the analysis. By narrowing the focus to erosion-related processes, the study aims to generate detailed insights into the drivers of shoreline change and the suitability of nourishment as a mitigation strategy.

The temporal scope extends to the year 2100, combining historical records with scenario-based projections to capture both past trends and future developments. This time frame ensures the findings are directly applicable to short- and long-term coastal planning

Research Question

The main research question that this thesis seeks to answer is:

> **Main Question.** Where and to what extent are nourishments suitable to mitigate coastal erosion under changing climate conditions?

To answer this question, four sub questions are formulated:

1. What are the characteristics and governance-related motives of previous nourishment interventions on European coasts?
2. How can satellite-derived and geospatial data be used to assess existing coastal erosion and predict future shoreline evolution under moderate and extreme climate scenarios?
3. Which European beaches, along with their assets, are most exposed to future erosion?
4. How can insights from the historical nourishment database shape a Nourishment Suitability Assessment Model for evaluating at-risk European coastlines?

Research Structure

This thesis adopts a systems perspective on coastal adaptation, focusing on the final stages of the socio-environmental causal chain (Figure 1.1): the impacts and risks associated with future shoreline change, and the corresponding adaptation response of beach nourishment.

The analysis is structured around one main research question and four sub-questions, which together bridge the gap between future coastal risk and nourishment-based adaptation. As shown in Figure 1.2, these sub-questions are operationalised through four key deliverables and mapped to the corresponding results chapters.

The chapters follow a progression from data and method development to analysis, integration, and reflection:

- **Chapters 2–3** establish the theoretical and methodological foundations, including dataset construction, shoreline modelling, and exposure assessment.
- **Chapters 4–5** present the results of the two core components: historical nourishment practices and future shoreline projections with associated exposure.
- **Chapter 6** integrates both strands using the Nourishment Suitability Assessment Model to evaluate nourishment potential at selected high-risk beaches.
- **Chapters 7–9** provide the discussion, main conclusions, and future outlook.

Overview

By addressing the research questions, this thesis bridges the gap between shoreline change projections, exposure assessment, and the role of nourishment in coastal adaptation.

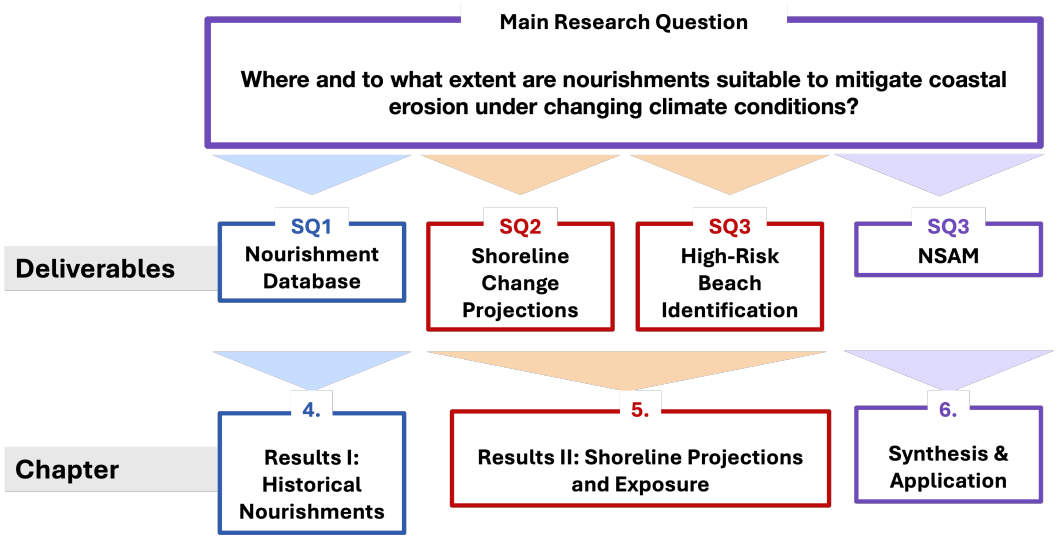

Figure 1.2: Research framework linking shoreline change, exposure, and adaptation via beach nourishment. Each sub-question results in a deliverable, with chapters structured to reflect this progression.

2

Literature Review

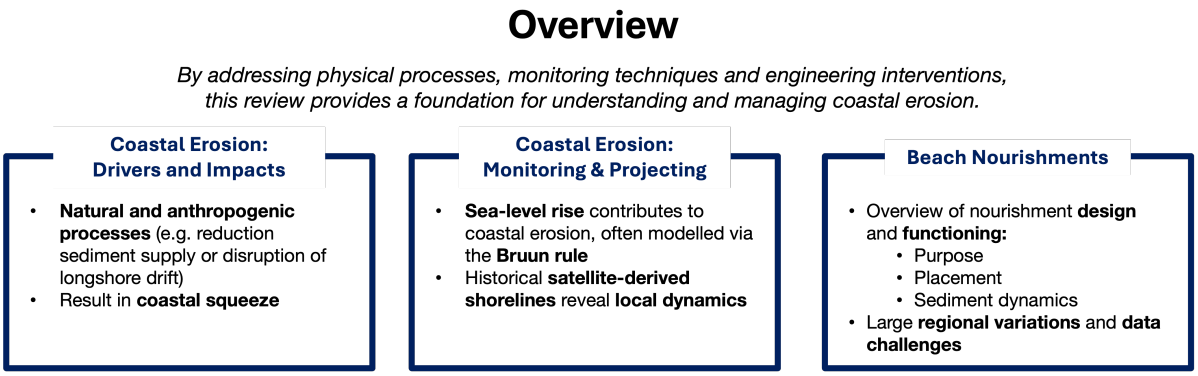

This chapter provides the contextual foundation for the study. It begins by examining the drivers and impacts of coastal erosion, followed by recent developments in shoreline monitoring and the projection of future coastal change. Beach nourishment is then introduced as a key adaptation strategy, with attention given to the physical processes underlying its design and implementation. The chapter concludes by identifying current gaps in the integration of shoreline change modelling, exposure assessment, and adaptation planning, gaps which motivate the research methodology developed in this thesis.

2.1. Coastal Erosion: Drivers and Impacts

Coastal zones offer vital ecological, economic, and cultural value, attracting dense human settlement and infrastructure development (Neumann et al., 2015). Approximately 10% of the global population lives in low-lying coastal zones (LECZs), defined as areas less than 10 meters above mean sea level (McGranahan et al., 2007). This share is expected to grow substantially, especially in Europe. By 2100, population growth in the LECZ could increase by up to 96% under high-emission pathways such as SSP5 (Merkens et al., 2016).

In Europe, approximately 23% of the coastline consists of sandy beaches (Luijendijk et al., 2018). These beaches are inherently dynamic and especially prone to erosion due to their mobile sediment composition and exposure to wave energy (EUROSION, 2004). Figure 2.1 shows observed erosion and accretion trends across Europe, highlighting spatial variability in shoreline change. This analysis includes both natural and engineered beaches, offering a comprehensive view of long-term shoreline dynamics.

Coastal erosion refers to the landward retreat of the shoreline caused by a net loss of sediment. It is distinct from, though often linked to, coastal flooding and submergence. While flooding and submergence occur due to rising relative water levels without changes in absolute land elevation, erosion is a

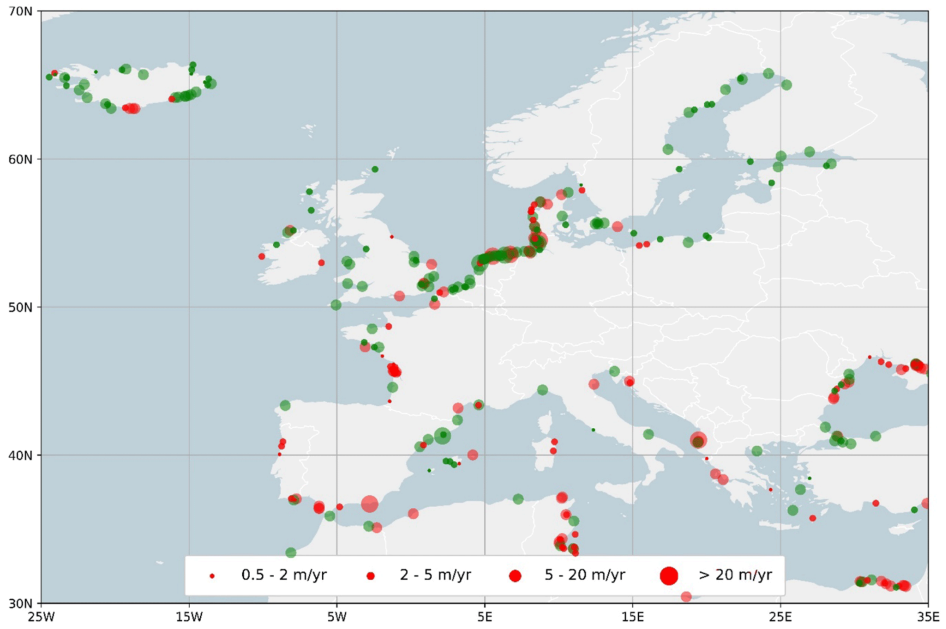

Figure 2.1: Hotspots of long-term shoreline change along European beaches from 1984 onward. Red circles indicate erosion, green circles indicate accretion. The analysis includes both natural and engineered (e.g. nourished) beaches. Based on Luijendijk et al. (2018), figure reprinted from van de Wal et al. (2024).

morphodynamic process driven by sediment removal by waves, currents and other hydrodynamic forces (Hinkel et al., 2013; Stive et al., 2002).

Drivers of Coastal Erosion

Erosion is caused by a combination of natural and anthropogenic processes, acting across different temporal and spatial scales. On decadal timescales, shoreline retreat can result from sediment imbalances along the coast (i.e., alongshore sediment transport gradients) and long-term sea-level rise (Vousdoukas et al., 2020). On shorter timescales, storms can lead to episodic erosion, followed by partial recovery in calmer conditions (Coco et al., 2014).

Figure 2.2 summarizes the mechanisms contributing to sediment gains and losses. These include fluvial inputs, offshore sediment availability, and anthropogenic interventions.

Bird and Lewis (2014) identify 15 contributing factors to erosion (see Appendix A.1), including reduction in sediment supply (e.g., from rivers or cliffs), disruption of longshore drift by coastal structures, extraction of beach sediment, and the increasing intensity of storm events. These complex and often location-specific interactions highlight the need for tailored and adaptive mitigation strategies.

Impacts on Society and Infrastructure

The consequences of coastal erosion extend beyond physical land loss. Retreating coastlines pose a direct risk to infrastructure, tourism-dependent economies, ecosystems, and cultural heritage. Lansu et al. (2024) report that 93% of unprotected coastlines globally have infrastructure within 25 km of the shore. On sandy coasts between 32° and 45°N, such as those in Italy, France, and Spain, this distance shrinks to a median of just 70 meters.

This narrow margin leaves little room for natural shoreline migration. The resulting phenomenon, known as ”coastal squeeze,” is visualized in Figure 2.3, where development prevents beaches and dunes from adapting to sea-level rise, amplifying erosion and flooding risks.

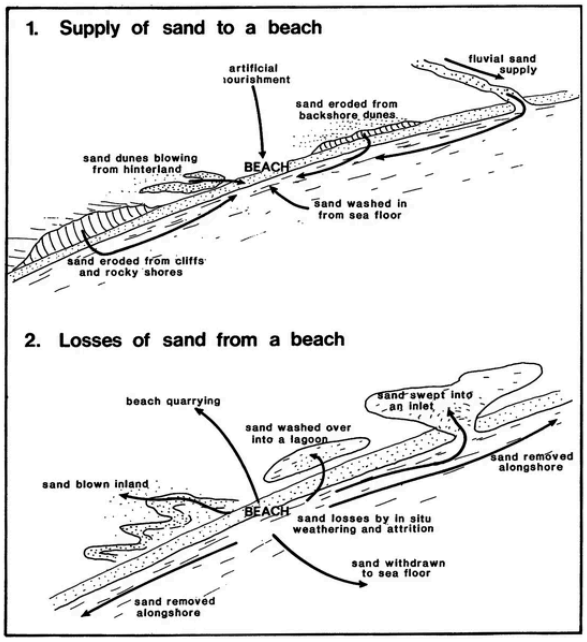

Figure 2.2: Mechanisms of sand supply and loss affecting coastal sediment balance. Reprinted from Bird and Lewis (2014).

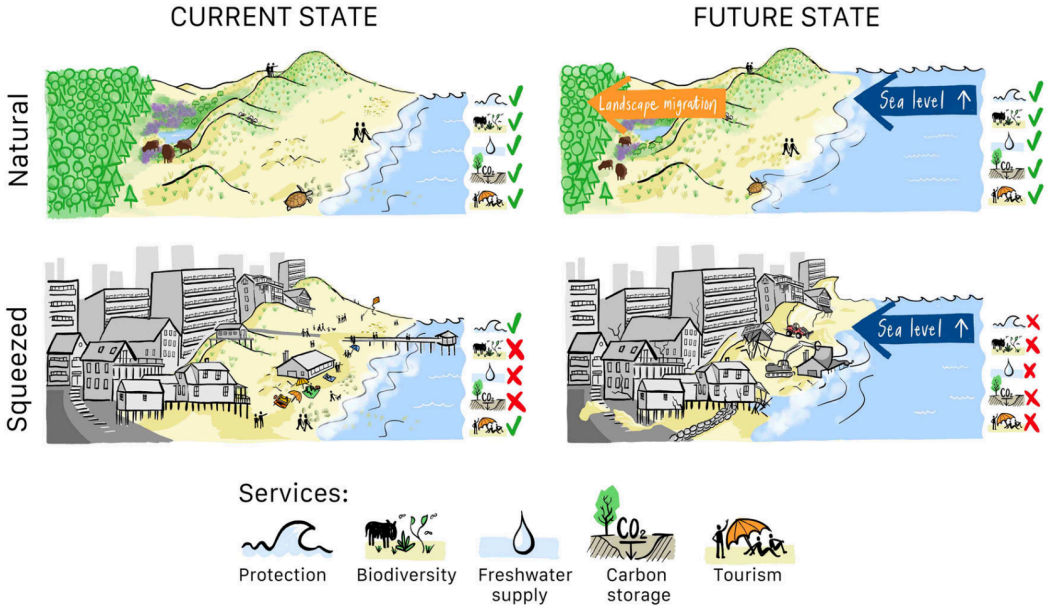

Figure 2.3: Consequences of coastal squeeze in current and future conditions. As development constrains inland migration of dunes and beaches, natural adaptation is suppressed, heightening vulnerability to erosion and flooding. Reprinted from Lansu et al. (2024).

2.2. Monitoring and Projecting Coastal Change

Until recently, observing coastal change at decadal to multi-decadal timescales was restricted to a limited number of well-instrumented sites. Methods such as Global Navigation Satellite Systems, Real-Time Kinematic GPS, and video monitoring (e.g., ARGUS stations) provided high-resolution data, but spatial coverage remained sparse (Goncalves & Awange, 2017; Pianca et al., 2015).

The advent of satellite remote sensing has transformed the field, shifting it from data-poor to data-rich

(Vitousek et al., 2023). Freely available optical satellite imagery, particularly from the Landsat and Sentinel programs, has enabled the global and long-term monitoring of coastal dynamics. The Landsat archive, dating back to 1972, offers consistent 30-meter spatial resolution with 16-day revisit intervals, making it invaluable for reconstructing historical shoreline evolution (Wulder et al., 2022). More recently, ESA's Sentinel-2 constellation provides imagery with similar resolution but higher temporal frequency (5-day revisit), improving the granularity of modern shoreline monitoring (Spoto et al., 2012).

A groundbreaking contribution to the field was made by Luijendijk et al. (2018), who developed the first global dataset of Satellite-Derived Shorelines (SDS). This dataset combines annual observations with transect spacing of 200–500 meters, offering a consistent framework for detecting long-term shoreline change across thousands of kilometers.

This breakthrough accelerated the adoption of satellite-based methods for large-scale coastal analysis (Castelle et al., 2024; Vitousek et al., 2023; Vos et al., 2023). Today, SDS datasets, especially those derived from Google Earth Engine (GEE), are considered the state of the art for tracking and forecasting sandy coastline dynamics. Recent advances have also seen the integration of machine learning techniques with SDS data to predict shoreline trajectories, outperforming traditional interpolation methods on decadal timescales (Calkoen et al., 2021).

2.2.1. Climate Change and Coastal Erosion

Climate change intensifies coastal erosion primarily through sea-level rise (SLR), but also through changes in storm regimes, sediment supply, and wave patterns (Coelho et al., 2022; Slott et al., 2006). The Intergovernmental Panel on Climate Change (IPCC) projects that global mean sea level could rise by up to 1.01 m by 2100 and 1.88 m by 2150 under high-emission scenarios (SSP5-8.5), significantly increasing risks for low-lying coastal regions (IPCC, 2023b).

While tide gauges and altimetry data provide reliable insights into historical trends, projecting future shoreline change remains a challenge due to uncertainties in both climatic and geomorphological drivers. Two recent studies offer complementary approaches to forecasting coastal erosion: Athanasiou et al. (2020) focus solely on sea-level rise as a driver, while Vousdoukas et al. (2020) combine SLR with ambient shoreline dynamics and storm-driven erosion.

At the heart of many large-scale erosion models lies a core assumption about how sea-level rise translates into shoreline retreat, typically framed through simplified equilibrium concepts.

2.2.2. Sea-Level Rise and the Bruun Rule

Sea-level rise occurs on both global and regional scales due to thermal expansion, glacial melt, and land subsidence. While global sea-level rise reflects large-scale climate-driven changes, regional sea-level rise (RSLR) incorporates local effects such as vertical land movement, gravitational redistribution of meltwater, and ocean circulation patterns. A foundational model linking SLR to shoreline retreat on long timescales is the Bruun Rule (Bruun, 1962). It holds that rising sea levels lead to the upward and landward migration of the beach profile to preserve equilibrium with the waterline. Erosion of the upper beach compensates for the increased accommodation space offshore, as illustrated in Figure 2.4.

This behavior can be conceptualized as a sediment continuity problem, where the retreat distance R must satisfy:

$$R_{RSLR} = RSLR \times \left(\frac{L}{d}\right) \tag{2.1}$$

Here, L is the cross-shore length of the active profile, and d is the vertical extent from the dune crest or berm height to the depth of closure (Zhang et al., 2004). Typical L/d values range from 50–150.

The Bruun Rule rests on several simplifying assumptions:

- The beach profile is in dynamic equilibrium and adjusts only in the cross-shore direction.
- There is no net loss or gain of sediment from the system (i.e., sediment is conserved).
- Sediment eroded from the upper beach is deposited offshore within the active profile.

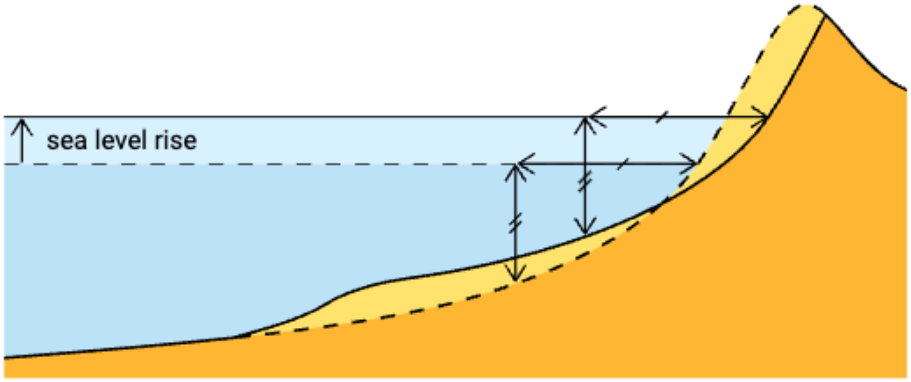

Figure 2.4: Illustration of the Bruun effect: the profile migrates upward and landward in response to rising sea levels, maintaining sediment volume continuity (Bosboom & Stive, 2023).

- The depth of closure (below which no significant sediment movement occurs) remains constant.
- No longshore sediment transport, human interventions, or complex morphological features influence the profile.
- There are no obstructions (e.g., seawalls or revetments) that inhibit sediment transport or prevent natural profile adjustment across the active beach zone.

Due to these assumptions, the Bruun Rule is most applicable to gently sloping, sandy, open coasts with minimal human interference and negligible longshore transport. It is less reliable in settings such as cliffed coastlines, barrier islands, inlet-dominated shores, and engineered or sediment-starved systems, where the actual shoreline response to SLR involves complex sediment dynamics and structural controls (Ranasinghe, 2016).

2.2.3. Future Projections of Shoreline Retreat

An initial global assessment by Hinkel et al. (2013) was conducted using the DIVA model, an integrated global framework that simulates the biophysical and socio-economic impacts of sea-level rise, including erosion and adaptation responses. This is done by dividing the world's coastlines into thousands of segments linked to climatic and socio-economic scenarios. While pioneering at the time, this assessment relied on outdated data, considered only sea-level rise as a driver of erosion, and incorporated several simplifying assumptions, such as constant beach slopes, that can now be addressed more accurately using modern datasets and modelling techniques.

Building on these early efforts, more recent studies have sought to quantify expected shoreline retreat under future climate scenarios. Athanasiou et al. (2020), for example, applied the Bruun Rule in combination with satellite-derived nearshore slopes and sea-level rise projections. Their results project that European coastlines will retreat by approximately 97 m on average under the high-emission RCP8.5 scenario and 54 m under the more moderate RCP4.5 scenario by 2100, as shown in Figure 2.5. However, these estimates are subject to considerable uncertainty, largely due to uncertainty in estimates of cross-shore slope and the omission of other important erosion drivers (e.g. local dynamics).

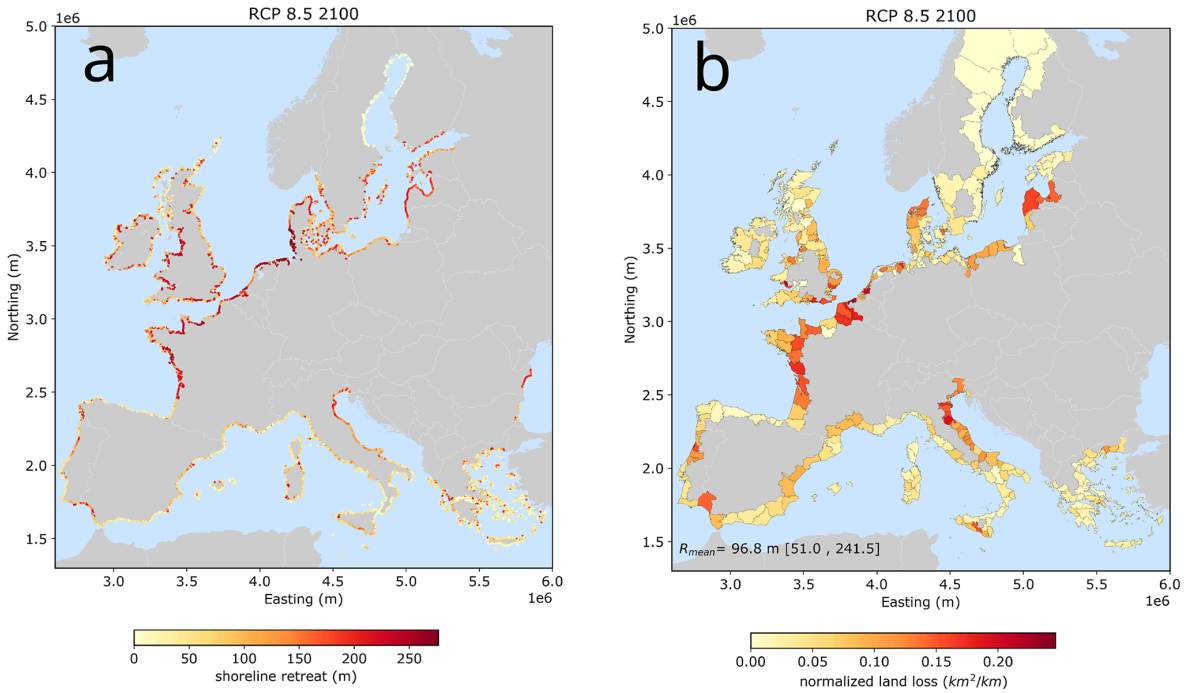

Figure 2.5: Projected shoreline retreat (in meters) and land loss (in km^2/km coastline) for Europe by 2100 under RCP8.5. Based on satellite-derived slopes and the Bruun Rule (Athanasiou et al., 2020).

In contrast, Vousdoukas et al. (2020) adopt a more comprehensive and process-based approach. Their framework integrates three key components: (1) ambient shoreline change (AC), (2) sea-level rise-induced retreat (R), and (3) storm-induced erosion (S). Each component is projected independently using physical and empirical models and then combined probabilistically to assess future shoreline change under multiple climate scenarios. A more detailed description of their modelling approach is provided in Appendix A.2. The results, visualized in Figure 2.6, reveal substantial regional variation in the relative importance of each erosion driver across Europe by 2100 under RCP8.5.

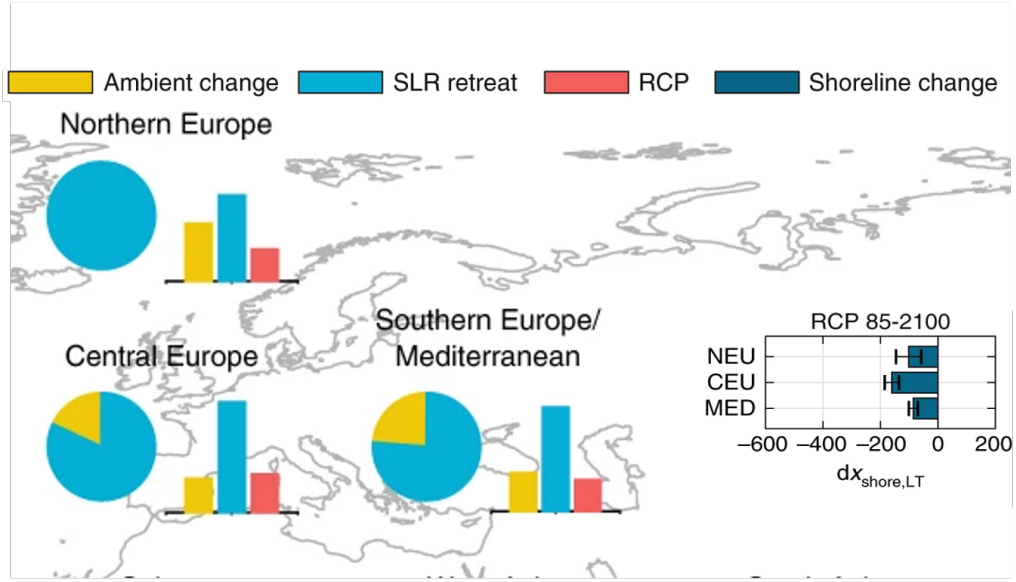

Figure 2.6: Projected shoreline change under RCP8.5 by 2100 across IPCC SREX subregions in Europe. Black bars show 5–95% uncertainty. Pie charts illustrate relative contributions from sea-level rise (R) and ambient change (AC) (Vousdoukas et al., 2020).

Shoreline Datasets and Analytical Frameworks

While the global shoreline projections by Vousdoukas et al. (2020) represent the most comprehensive forecasts currently available, opportunities for improvement remain, particularly in terms of spatial resolution and input data. A significant development in global shoreline monitoring was introduced by Calkoen et al. (2025), who extended and refined the ShorelineMonitor framework originally developed by Luijendijk et al. (2018). While the original dataset provided global shoreline change estimates at 500 m resolution between 1984 and 2016, Calkoen's update expands the time series through to 2024, increases spatial resolution to 100 m, and applies stricter quality criteria to shoreline detections. The resulting dataset integrates over 350 million Satellite-Derived Shoreline (SDS) observations, each extracted from annual Landsat composites using dynamic detection methods based on the Normalized Difference Water Index (NDWI).

These shorelines are mapped onto the Global Coastal Transect System (GCTS) to form the *ShorelineMonitor* dataset, which includes 7.5 million uniformly spaced transects along the global coastline.

In addition to the time series, another dataset, the Global Coastal Transect Repository (GCTR), includes 11 million transects with a machine-learning-based coastal typology classification that distinguishes between shore type (e.g., sandy, muddy, no sediment) and coastal type (e.g., dune, cliff, sediment plain), as well as other coastal attributes (Calkoen et al., 2025).

Its open, cloud-native architecture and rich metadata structure make the dataset both highly accessible and analytically flexible. This thesis adopts the data from Calkoen et al. (2025) as its core source.

2.3. Beach Nourishment as a Coastal Adaptation Strategy

Coastal adaptation strategies can generally be classified into three main categories: retreat, accommodation, and protection (Nicholls, 2011), which are described in more detail in Appendix A.3.

As shown in Figure 2.7, effective coastal risk management requires long planning horizons. Sea-level rise unfolds gradually, and timely responses depend on anticipatory, adaptive planning. All strategies come with trade-offs related to cost, effectiveness, environmental impact, and societal acceptance (Borchert et al., 2018; Mongelli et al., 2024; Roy et al., 2023).

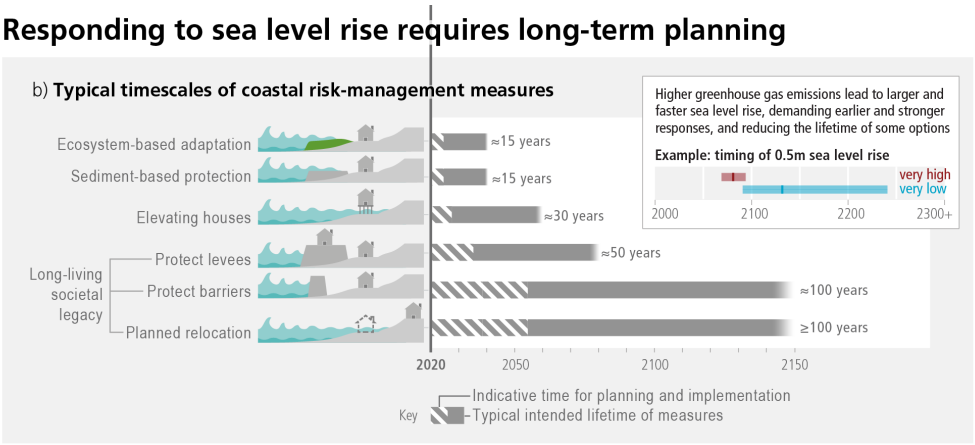

Figure 2.7: Coastal risk management timelines. Reprinted from IPCC (2023b). Typical time scales for the planning, implementation (dashed bars) and operational lifetime of current coastal risk-management measures (blue bars). Higher rates of sea level rise demand earlier and stronger responses and reduce the lifetime of measures (inset). As the scale and pace of sea level rise accelerates beyond 2050, long-term adjustments may in some locations be beyond the limits of current adaptation options and for some small islands and low-lying coasts could be an existential risk.

Among the range of strategies, beach nourishment has emerged as a widely adopted approach, particularly along sandy coastlines. Its appeal lies in its ability to enhance coastal resilience while simultaneously providing ecological and recreational benefits (de Schipper et al., 2021). In contrast to hard protection methods, nourishment is an adaptable intervention that can be integrated into broader sediment management frameworks.

It has become a common practice in many coastal protection programmes (Bontje et al., 2016), offering a flexible, nature-based alternative to traditional hard engineering approaches. It involves the placement of sediment, typically sand, on beaches to restore sediment budgets, increase beach width, or reinforce dune systems (Dean, 2002). Unlike fixed structures such as seawalls or groynes, nourishment maintains the morphodynamic behaviour of sandy coastlines and often provides co-benefits for ecosystems and recreation (Bird & Lewis, 2014; Nordstrom, 2005; Speybroeck et al., 2006).

2.3.1. Physical Design and Functioning of Beach Nourishments

Beach nourishment aims to mitigate shoreline retreat by artificially replenishing sediment, addressing erosion's effects rather than stopping the process itself (Lodder & Slinger, 2022). Effective design depends on local coastal conditions and governance goals, and increasingly requires a multidisciplinary approach that considers both performance and environmental impact de Schipper et al. (2021).

The diversity in the purposes, types and sediment sources of nourishments is reflected in the classification scheme developed in the methodology (see section 3.1).

Implementation Objectives

The versatility of beach nourishment lies in its capacity to address multiple coastal management objectives simultaneously. Building on classification frameworks by Hamm et al. (2002) and Pinto et al. (2020), nourishment practices can generally be grouped into five main categories:

1. **Shoreline stabilization:** Replenishing sediments to offset long-term erosion and restore sediment budgets.
2. **Flood and storm mitigation:** Reinforcing beaches and dunes to reduce overtopping and breaching risk.
3. **Infrastructure protection:** Acting as a buffer to dissipate wave energy before it reaches coastal assets.
4. **Recreation and tourism:** Expanding dry beach areas to support economic activity and public use.
5. **Environmental and cultural preservation:** Safeguarding habitats and heritage sites from marine encroachment.

In practice, a single nourishment project may serve multiple purposes. For example, a dune-reinforcement scheme may simultaneously reduce flood risk, protect infrastructure and support recreation by maintaining accessible beaches, while also delivering ecosystem services (van Oudenhoven et al., 2018).

Types of Nourishment Placement

Beach nourishment types are defined by the placement of sediment relative to mean sea level (MSL), which governs their morphodynamic behaviour, performance and longevity. As illustrated in Figure 2.8, dune nourishments, either landward or seaward, enhance storm resilience by reinforcing the dune system through wind-driven redistribution, often in combination with vegetation planting.

Beach nourishments place sediment on the visible portion of the beach, typically around or above MSL. This approach offers immediate recreational and aesthetic benefits but is highly susceptible to rapid erosion, especially during the first post-construction storms, due to the steep and non-equilibrium profile it initially creates (Dean, 2002).

Shoreface nourishments are positioned below MSL on the submerged nearshore slope. Although their impact on the dry beach is more gradual and less visible, they cause minimal disruption to beach users and tend to have longer retention times. These nourishments depend on natural, wave-driven transport to gradually move sediment landward. Two conceptual models explain this process: the *lee-side accretion mechanism*, where the nourishment creates a sheltered zone of deposition but may cause downdrift erosion due to transport gradients; and the *feeder mechanism*, where sediment migrates onshore over time and directly contributes to beach accretion (Figure 2.9) (de Schipper et al., 2021; van Duin et al., 2004; van der Werf et al., 2025).

Across all nourishment types, the initial morphology is far from equilibrium. This results in significant edge erosion and sediment redistribution until a more stable profile is reached. Strategically designing

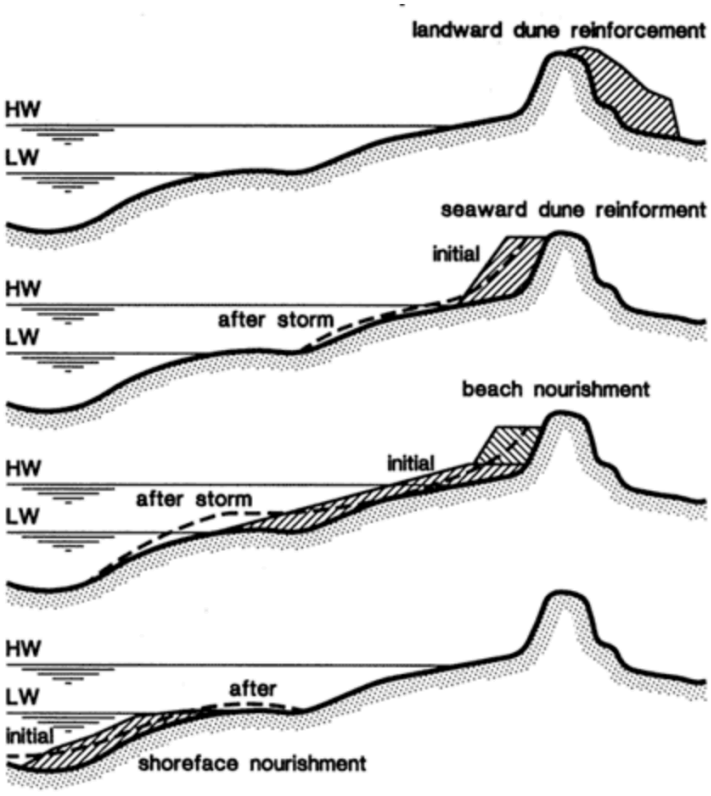

Figure 2.8: Schematic cross-shore profiles of different nourishment types. Dune nourishments are placed either landward or seaward of the active beach to enhance storm resilience, beach nourishments directly widen the visible beach, and shoreface nourishments are positioned below mean sea level to feed the beach over time via natural transport processes. Reprinted from Marchand (n.d.).

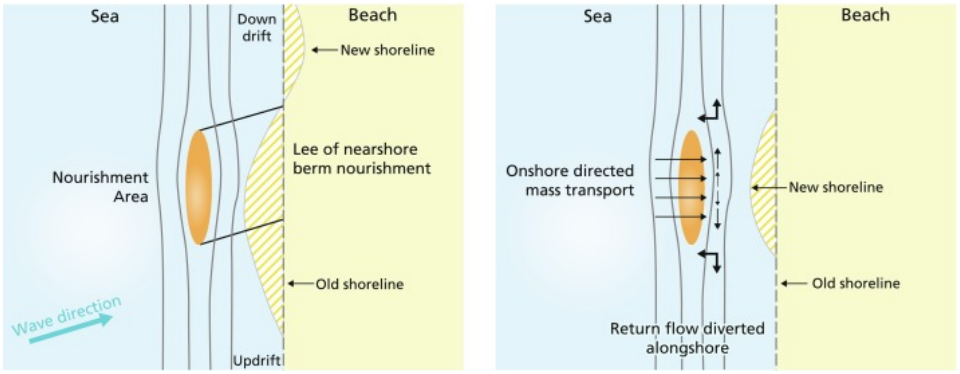

Figure 2.9: Effects expected to occur as a consequence of the placement of a shoreface nourishment. Reprinted from van der Werf et al. (2025).

this adjustment phase is critical for achieving intended outcomes while minimizing adverse downdrift impacts.

Sediment Dynamics

Nourishment sediment is typically sourced from offshore borrow areas or navigation channels and often differs in grain size from native beach material (Hanson et al., 2002; Pinto et al., 2020). Coarser sand tends to create a steeper, wider beach profile that is initially out of equilibrium with prevailing wave and current conditions (Dean, 2002; Hanson et al., 2002), as shown in Figure 2.10a.

Sediment redistribution occurs through both cross-shore and longshore transport, with high erosion rates common in the initial adjustment phase, particularly on steep profiles (Anthony et al., 2011; Elko & Wang, 2007; Gares et al., 2006). These morphodynamic responses, including planform spreading and profile flattening, are illustrated in Figure 2.10b. Over time, sediment may form offshore bars, nourish adjacent coasts or support dune growth, highlighting the need to account for broader sediment-sharing systems.

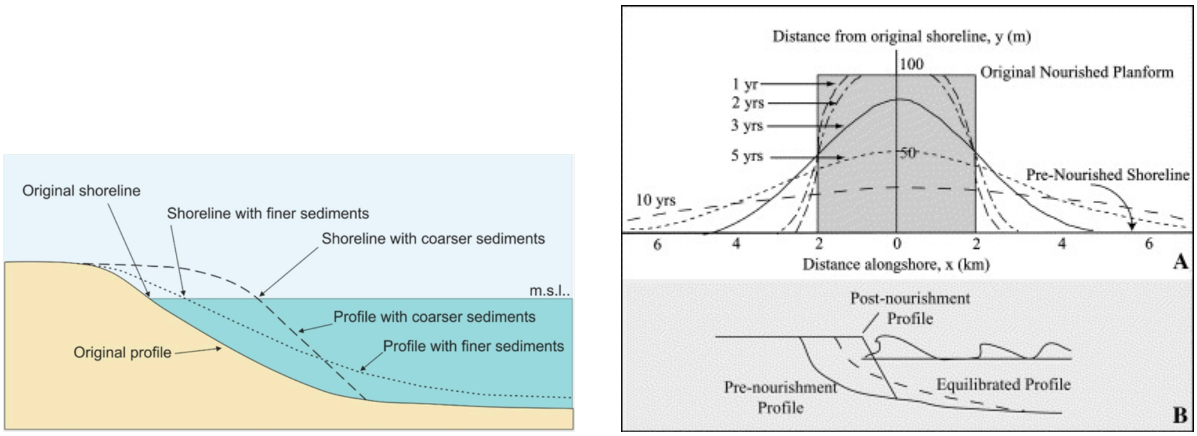

(a) Profile adjustment due to grain size differences (Adriadapt, 2022).

(b) Planform and profile evolution post-nourishment (Dean, 2002; Elko & Wang, 2007).

Figure 2.10: Morphodynamic adjustment of nourished beaches due to sediment characteristics and transport processes.

Interactions with Hard Structures

In some regions, especially the Mediterranean, nourishment is combined with hard structures like groynes or breakwaters (Hanson et al., 2002; Pranzini, 2018). Groynes trap sand and limit longshore loss, while breakwaters dissipate wave energy and encourage deposition. While they may enhance nourishment longevity, they also introduce trade-offs. Downdrift erosion, sediment shadowing and changes in nearshore circulation are common risks (Ranasinghe & Turner, 2006).

2.3.2. Regional Variations, Data Challenges and Implications

The implementation of beach nourishment varies considerably across Europe, shaped by differences in geomorphology, governance traditions and socio-economic priorities. A comprehensive overview by Hanson et al. (2002) and more recent work by Pinto et al. (2020) highlight several regional distinctions.

In North Sea countries such as the Netherlands, Germany and Denmark, nourishment is primarily deployed for coastal protection. These nations operate under national safety standards and long-term strategic frameworks, often applying nourishment proactively and cyclically, even in the absence of visible erosion, as part of broader sediment management programmes. Such projects typically rely on fully soft solutions without the use of supporting hard structures.

In contrast, Mediterranean countries like France, Italy and Spain tend to implement nourishment for recreational or economic reasons. These projects are often reactive, following erosion events, and frequently combined with hard structures to prolong their effectiveness (Hanson et al., 2002).

Given the diversity in regional approaches, developing universally applicable nourishment design criteria remains challenging (Gijsman et al., 2018). Not only do physical and policy conditions vary, but data

availability is also highly uneven across countries. The scope of many existing studies is often dictated by where consistent and detailed nourishment records exist (Qiu et al., 2020).

2.3.3. Ecological Considerations and Debates

While beach nourishment is often promoted as a softer and more adaptable alternative to hard structures, its ecological consequences are still debated. Nonetheless, many potential adverse effects can be reduced through thoughtful planning and timing (Speybroeck et al., 2006). Properly designed projects can enhance habitat heterogeneity and even create new ecological niches for species such as seabirds and intertidal invertebrates (van Egmond et al., 2018). However, if poorly matched in timing or sediment characteristics, nourishments can cause habitat burial, alter feeding conditions, or disrupt recruitment of sensitive fauna, as illustrated in Figure 2.11 (Staudt et al., 2021).

Mitigation strategies, such as grain-size matching, seasonal restrictions, and staggered nourishment placement, are commonly recommended, but environmental impacts are still frequently observed (Staudt et al., 2021). While ecological effects are outside the scope of this thesis, acknowledging these debates remains important for future applications.

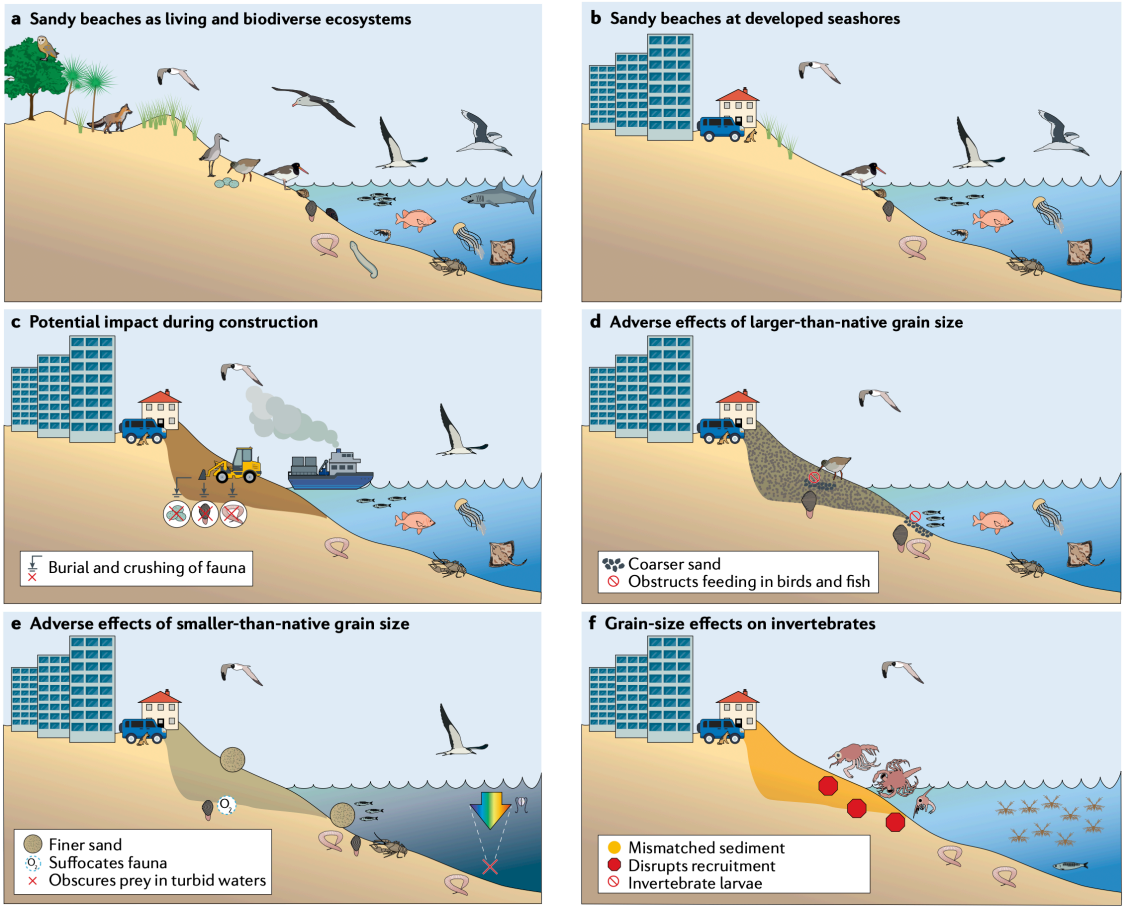

Figure 2.11: Potential ecological changes during and following beach nourishment. Reprinted from de Schipper et al. (2021). (a) Ocean beaches without significant human stressors are rich in species and individuals. (b) Human activity along developed, eroding shorelines often reduces beach fauna. (c) Nourishment can cause habitat disruption through direct mechanical impacts such as burial and crushing. (d) Placement of coarser-than-native material can obstruct foraging by birds and fish. (e) Finer material may lead to turbidity, suffocating infauna and obscuring prey. (f) Mismatched grain sizes can disrupt invertebrate recruitment and reduce biodiversity. Note: Panels are conceptual and not to scale.

2.4. Framing Future Coastal Risk and Adaptation

The causal chain from socio-economic drivers to coastal adaptation (Figure 1.1) serves as the conceptual backbone of this work, illustrating how global changes progress into local impacts and responses. However, despite advances in climate and shoreline modelling, a persistent gap remains: the disconnect between projected erosion risk and observed adaptation practice. In particular, large-scale models often fail to consider the spatial distribution of fixed assets (such as buildings) or the implementation of soft protection strategies like beach nourishment. As a result, projections may misrepresent both exposure and the potential for effective response.

At the same time, existing research on nourishment remains fragmented. Most studies are national or local in scope, vary in classification and terminology, and offer limited comparability. This fragmented understanding hinders efforts to identify consistent drivers, assess suitability, or align adaptation strategies with the areas of greatest risk.

Taken together, these gaps point to a critical need for integrated, spatially explicit assessments that:

- Connect shoreline retreat projections with exposure of buildings,
- Contextualise adaptation suitability within both physical and institutional settings,
- And move beyond isolated studies to enable broader comparative insights.

2.4.1. Research Contribution

Responding to these needs, this thesis develops a unified analytical framework to link coastal impacts and adaptation responses across Europe. Its contributions are threefold:

- **Historical Analysis:** A harmonised spatial database of beach nourishment interventions is compiled across eight European countries using grey literature, expert input, and official sources.
- **Cross-National Insights:** Differences in nourishment purpose, sediment type, and institutional context are examined in relation to coastal typologies and erosion patterns.
- **Forward-Looking Integration:** Shoreline retreat projections are combined with building exposure and evaluated against a multi-criteria nourishment suitability model under multiple time frames and SSPs.

By operationalising the final stages of the causal chain, from hazard to response, this thesis offers a replicable, spatially grounded framework for evaluating where beach nourishment may be most suitable to mitigate coastal erosion. It thereby helps bridge the gap between large-scale erosion modelling and context-specific, actionable adaptation planning.

3

Data & Methodology

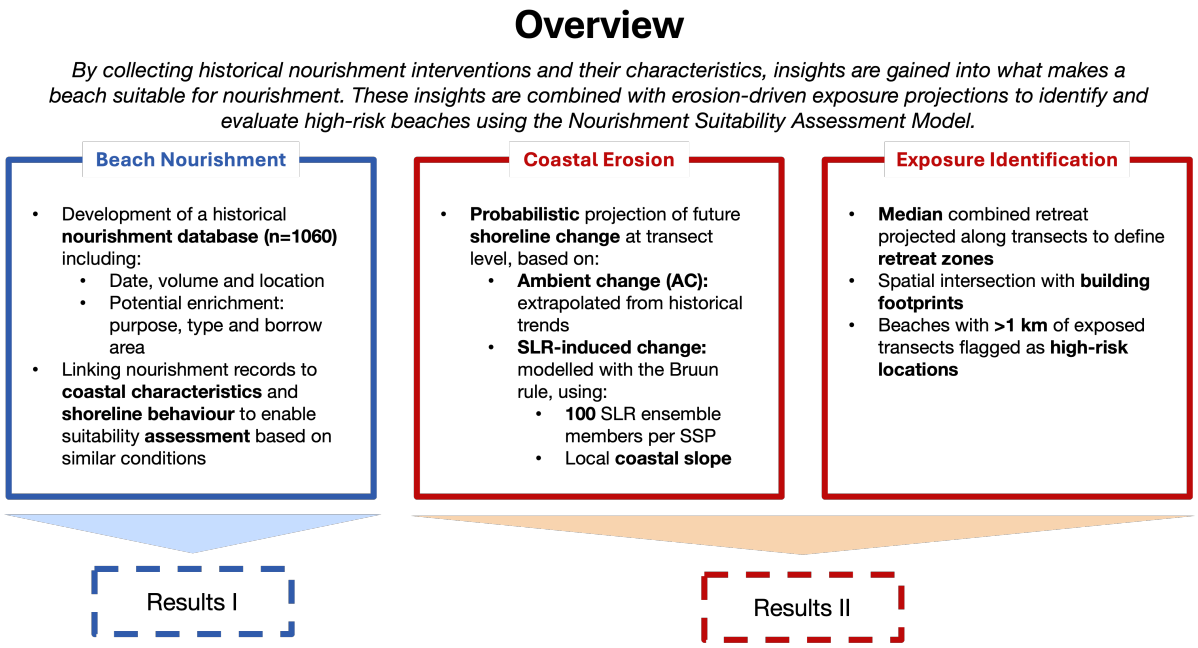

This chapter outlines the data sources and methodological framework used to assess shoreline retreat, quantify building exposure, and investigate historical coastal nourishment practices. Together, these components address both climate-driven risks and the adaptation responses they necessitate, capturing the end of the causal chain of climate change to policy.

The approach consists of two parallel strands:

- **Adaptation** (left): Compilation and enrichment of a harmonized nourishment database, linked to coastal characteristics to inform suitability evaluation.
- **Impacts and Risks** (right): Probabilistic modelling of shoreline retreat from sea-level rise and historical trends, used to identify exposed buildings and high-risk beach stretches.

Figure 3.1 illustrates the structure of each strand. Numbered blocks correspond to the section of this chapter.

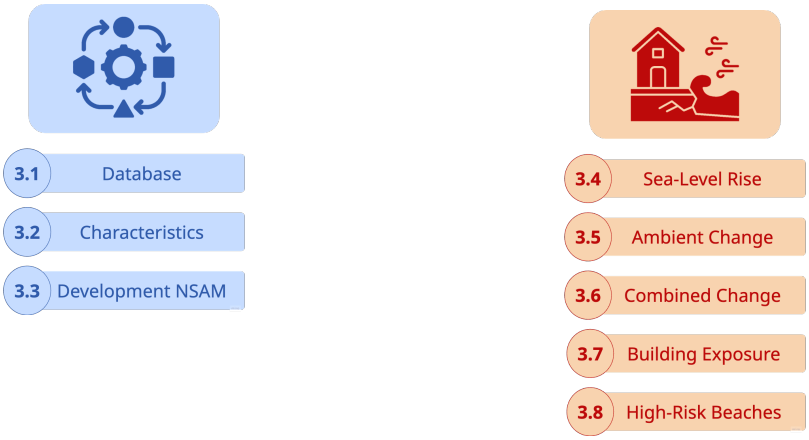

(a) Adaptation: nourishment data, coastal characterization, and suitability assessment.

(b) Impacts and risks: shoreline change projections and exposure analysis.

Figure 3.1: Structure of the methodological framework. Step numbers refer to sections within this chapter

Within this methodology, four core datasets are used and integrated to support the shoreline change modelling, exposure analysis, and nourishment characterization. These datasets form the analytical backbone of the study, providing spatial, temporal, and typological information at transect level. The ShorelineMonitor and GCTR datasets are partially derived from Landsat imagery, providing an effective shoreline positioning precision of approximately 15 m (Hagenaars et al., 2017). A summary of their key attributes and corresponding acronyms is presented in Figure 3.2.

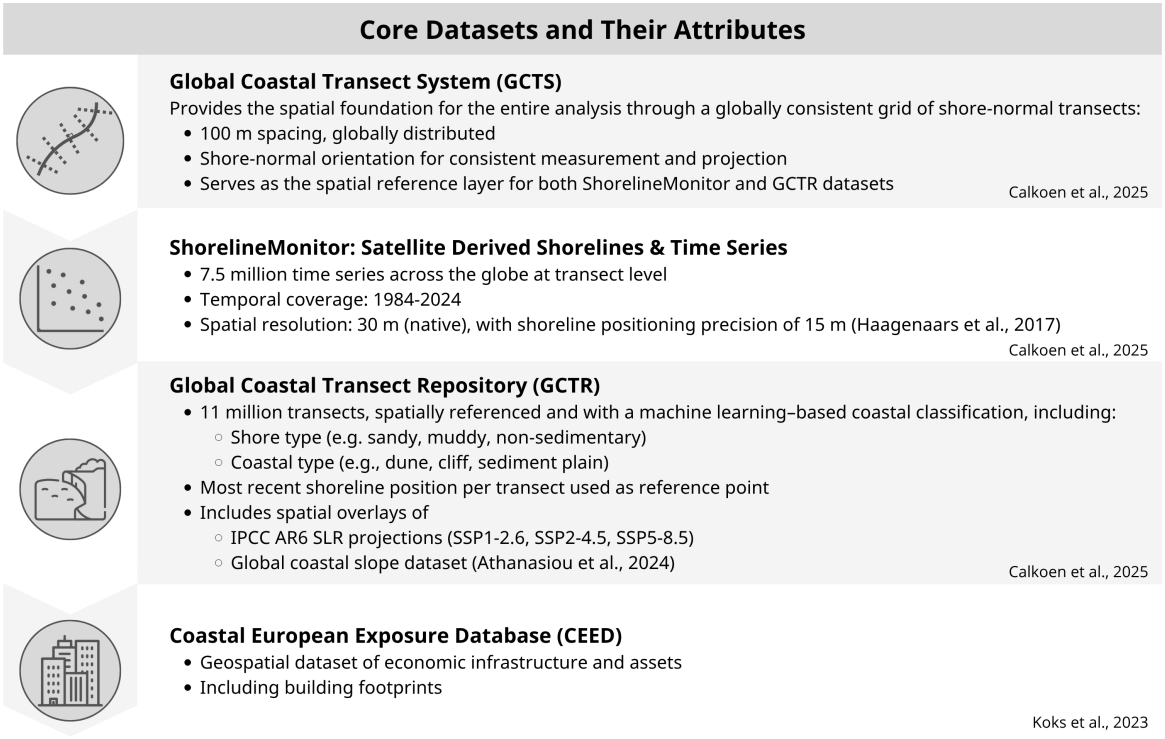

Figure 3.2: Overview of the four core datasets used in this study, including their spatial structure and key attributes. These datasets support both the exposure analysis and the nourishment suitability assessment.

The spatial extent of this research is bounded by the continental limits of Europe. A geographic bounding box, spanning from 30°W to 40°E longitude and from 35°N to 70°N latitude, was used to isolate the European region. This bounding box is visualized in Figure 3.3.

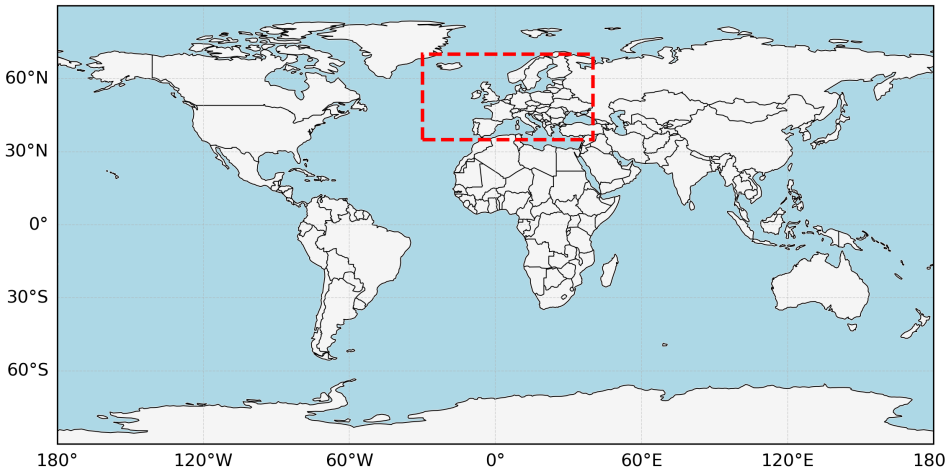

Figure 3.3: Global map with a dashed red bounding box indicating the spatial extent of the European coastal study area.

Using the continent attribute from the GCTR dataset, only transects located within this bounding box and tagged as part of Europe were retained. This results in 1,388,990 transects covering 138,899 km across Europe, of which 412,818 transects (41,282 km) are classified as sandy, approximately 30%. Additional filtering criteria used throughout the analysis are discussed in subsequent sections.

3.1. Development of the Historical Nourishment Database

To support large-scale shoreline analysis, this section describes the development of a harmonized, spatially-referenced nourishment database for European coasts. Fragmented national datasets were standardized and integrated into a single structure that captures the key temporal and spatial attributes of nourishment activities, such as volume, timing, location, and stated purpose.

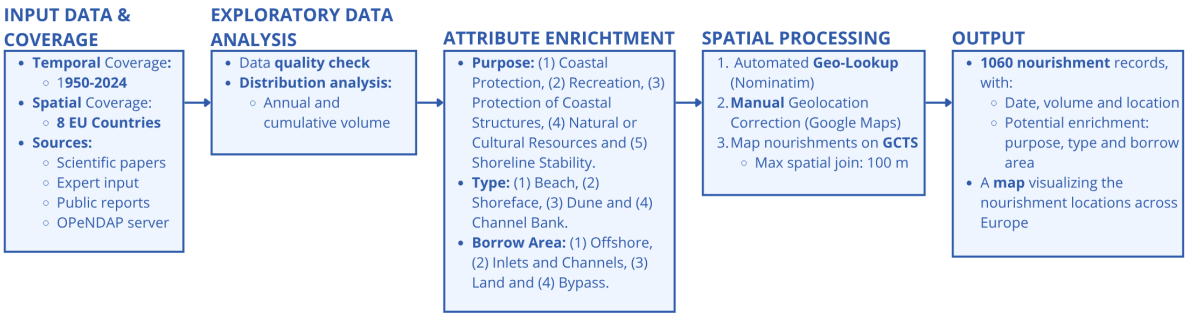

Figure 3.4: Overview of the processing steps used to construct the historical nourishment database.

3.1.1. Input Data and Coverage

The nourishment database compiles data from a range of sources, including governmental agencies, scientific literature, and direct expert input. Table 3.1 summarizes the sources used per country, the time periods covered, number of nourishment projects, and the original data formats. Formats varied widely, from scanned reports and spreadsheets to shapefiles and online web services, necessitating tailored processing and standardization steps.

In total, the compiled raw dataset includes nourishment records from eight European countries, covering 1109 individual projects.

Data Standardization and Preprocessing

To unify the diverse national datasets listed in Table 3.1, a set of standardization and preprocessing steps was applied. The objective was to bring all records into a consistent structure, standardizing

Table 3.1: Raw Data Sources for the Historical Nourishment Database

Country	Years Covered	Raw Number of Nourishments Records	Source	Format
Denmark	1974–1998	14	Hanson et al. (2002)	Scientific paper
France	1962–1998	28	Hanson et al. (2002)	Scientific paper
	1998–2016	17	Cerema (2023)	Public research report
Germany	1950–2024	278	Courtesy of Theide Wöffler (LKN.SH) and Simon Hillmann (NLWKN), 2025	Expert input (Leaflet, Excel, Shapefiles)
Italy	1969–1998	29	Hanson et al. (2002)	Scientific paper
Netherlands	1952–2023	507	Deltares and Rijkswaterstaat (n.d.)	OPeNDAP server
Portugal	1950–2017	134	Pinto et al. (2020)	Scientific paper
	2018–2024	65	Courtesy of Celso Pinto, 2025	Expert input (Excel)
Spain	1985–1998	12	Hanson et al. (2002)	Scientific paper
Sweden	2000–2024	25	Courtesy of Caroline Hallin, 2025	Expert input (Excel)

formats, coordinate systems, and attribute naming, so they could be used for spatial analysis and later integration with other geospatial datasets.

Initially, raw nourishment records were compiled in a central Excel workbook, with a separate sheet for each country. This format allowed for easier organization and identification of country-specific formatting issues or missing data. The Excel file was imported into a Python environment and processed using `pandas`. A data type dictionary ensured correct parsing of all columns (e.g., dates, strings, floats, integers). An overview of the metadata fields and types is provided in section B.1.

Some datasets required additional preprocessing:

- **Netherlands:** Nourishment data was retrieved via the OPeNDAP server and merged with a separate `.json` file containing geospatial geometries. Merging was based on matching attributes, including `start_date`, `end_date`, `vol`, and `geometry`. A known limitation is that the geometries near Maasvlakte 2 (MV2) are inaccurate and were flagged accordingly.
- **Germany (Sylt):** Data was provided as polygon shapefiles. Since the working format required Point geometries (Shapely objects), polygons were converted to their centroids. These points were then snapped to the nearest OpenStreetMap (OSM) coastline to ensure proper coastal alignment.

Each nourishment record was assigned a unique `nourishment_id`, allowing all related attributes to be easily queried, referenced, and traced back through the pipeline. These preprocessing steps enabled uniform comparison across countries and formed the foundation for the attribute enrichment and spatial georeferencing stages described next.

3.1.2. Exploratory Data Analysis

An initial round of exploratory data analysis (EDA) was performed after standardizing column data types. The main objectives were to detect missing values, identify outliers, and examine the distribution of key variables within the nourishment dataset.

The first step involved checking for missing values in essential fields. Four records lacked start dates, and five were missing nourishment volumes. Since these values could not be reliably reconstructed from external documentation or geospatial sources, these records were excluded to preserve data integrity.

Next, a boxplot of the volume field was used to identify outliers. One extreme value corresponded to

the Maasvlakte 2 land reclamation project in the Netherlands. Although related to coastal processes, this intervention differs substantially from typical beach or shoreface nourishments due to its scale and port-focused purpose. Excluding this record prevents distortion in statistical summaries and supports more meaningful comparisons across interventions.

To further explore the distribution of nourishment volumes, a histogram was generated. The raw distribution is right-skewed, reflecting a wide range in project scales. This step was included to check for additional outliers or unusual distribution patterns beyond the known extreme case. To normalize the distribution, a Box–Cox transformation was tested, yielding a parameter value of $\lambda = 0.108$ (Box & Cox, 1964). This supports the use of a base-10 logarithmic transformation, which reduces skewness and results in a distribution that more closely approximates normality. (Osborne, 2010).

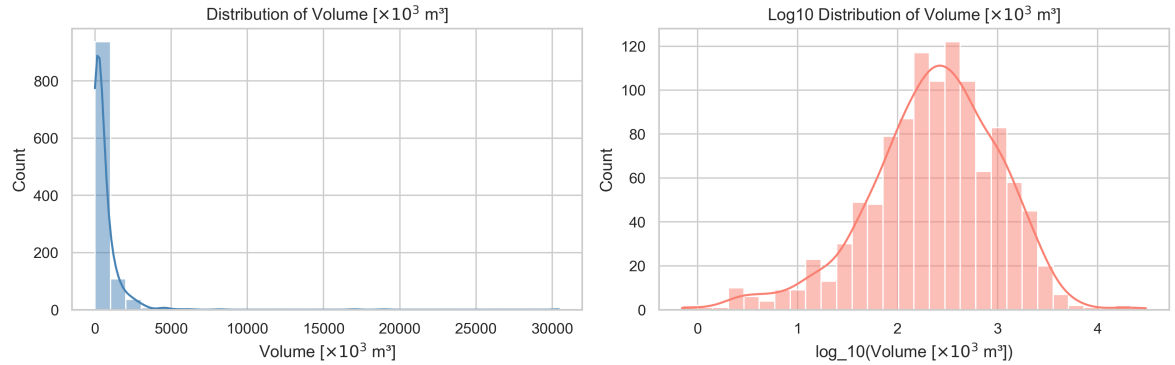

Figure 3.5: Histogram of nourishment volumes. Left: Raw distribution showing strong right skew. Right: Log_{10}-transformed distribution approximating normality, enabling clearer visual and statistical comparison.

After filtering missing values and removing extreme outliers, the dataset used for further analysis, attribute enrichment and spatial processing, includes 1,100 nourishment records.

An overview of annual and cumulative nourishment volumes is shown in Figure 3.6, based on the filtered dataset.

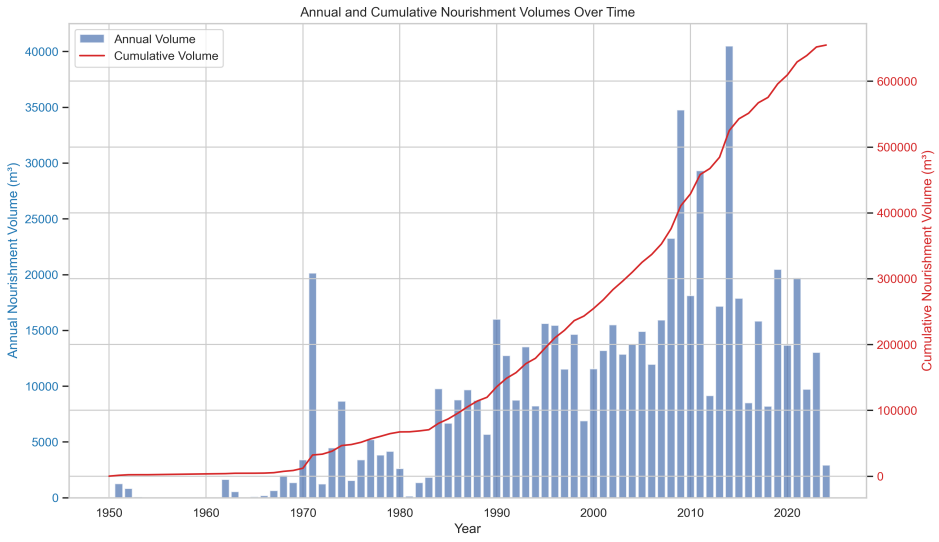

Figure 3.6: Annual and cumulative nourishment volumes over time. The chart shows a rising trend in both annual nourishment activity and cumulative volumes, with an increase in recorded interventions starting in the 1980s and continuing into the 21st century.

3.1.3. Attribute Enrichment

To improve the interpretability and consistency of the nourishment records, categorical fields such as `purpose`, `type`, and `borrow_area` were standardized. These fields were originally coded or inconsistently labelled across countries.

Because classification systems varied, or were absent altogether, a uniform scheme was developed. This classification follows the structure of the Dutch Rijkswaterstaat database and is stored in new columns with a `_flag` suffix.

Many records contained multiple values for these fields. To support structured analysis, each was reduced to a single "primary" value per record, using predefined hierarchies that reflect both functional relevance and frequency in the dataset. The rationale for each hierarchy is described below.

Nourishment Purpose

The purpose of each nourishment was categorized using a refined version of the framework introduced by Hamm et al. (2002) and expanded by Pinto et al. (2020). The classification used in this study is shown in Table 3.2.

Table 3.2: Classification of Beach Nourishment Purposes

Purpose	Purpose Flag	Description
Shoreline Stability	1	Sediment is added to restore the sediment budget and reduce long-term erosion. This may involve nearshore placement (as a feeder to the beach or to provide lee-side shelter) or direct placement on the subaerial beach.
Coastal Protection	2	Aimed at reducing the risk of overwash and flooding by strengthening natural coastal defences such as beaches and dunes. These nourishments reinforce dune systems, increasing resilience to storm surge and wave run-up.
Protection of Coastal Structures	3	Acts as a buffer in front of hard structures (e.g., seawalls, revetments), absorbing wave energy and reducing structural wear. Nourishment extends the lifespan and effectiveness of engineered defences.
Recreation	4	Expands the dry beach to improve usability and visitor capacity. Sediment is placed on the beach to shift the shoreline seaward, creating more space for recreational use.
Protection of Natural or Cultural Resources	5	Designed to prevent erosion or sea-level rise from damaging ecologically or culturally important sites, such as dune habitats, marine nurseries, or archaeological features.

Primary Purpose Hierarchy: (1) Coastal Protection, (2) Recreation, (3) Protection of Coastal Structures, (4) Natural or Cultural Resources and (5) Shoreline Stability.

"Shoreline Stability" was listed in 490 records (434 as the sole purpose), but often appears alongside more targeted goals such as Coastal Protection or Recreation. To prevent overrepresentation of this general category, it was placed lowest in the hierarchy. This ensures more functionally specific purposes are prioritised when classifying each record.

Nourishment Type

Types of nourishment were standardised based on the Rijkswaterstaat classification, which categorises interventions by the location of sediment placement (e.g., beach, shoreface, dune). The classification used is shown in Table 3.3.

Table 3.3: Classification of Nourishment Types

Nourishment Type	Type Flag	Description
Beach Nourishment	1	Direct placement of sediment on the subaerial beach to restore width, elevation, or recreational capacity. Typically used to counteract erosion or to expand dry beach area.
Shoreface Nourishment	2	Sediment placed in the nearshore zone, landward of the depth of closure, where wave-induced sediment transport is still active. Nourishment in this zone promotes natural redistribution of sediment toward the beach and enhances wave dissipation. Also used in combination with beach nourishment.
Dune or Dike Reinforcement	3	Placement of sediment to reinforce coastal dunes and, where relevant, dikes. Includes both landward and seaward dune expansion, often in combination with beach nourishment.
Channel Bank Nourishment	4	Sediment placed along the banks of a tidal inlet, estuary, or river channel to stabilize and reduce erosion.

Primary Type Hierarchy: (1) Beach, (2) Shoreface, (3) Dune and (4) Channel Bank.

Beach nourishment is the most frequently applied method, appearing in 771 single-type records and 789 mixed-type records. In mixed cases, beach nourishment is typically the main intervention, with dune or shoreface components being either secondary or a result of redistribution. This hierarchy helps avoid misclassification based on minor components and ensures consistent identification of the dominant intervention type.

Borrow Area

The source of nourishment material, termed the borrow area, was categorized based on classifications used by Hanson et al. (2002) and Pinto et al. (2020). Table 3.4 provides the complete list.

Table 3.4: Classification of Borrow Areas Used in Nourishment Projects

Borrow Area Type	Type Flag	Description
Inlets and Channels	1	Sediment sourced from tidal inlets, estuaries, or navigation channels. This often involves dredging accumulated sand deposits, which simultaneously maintains navigational access and supplies material for nourishment.
Offshore	2	Sand extracted from offshore seabeds, typically at depths where sediment is more available and environmental impacts are reduced. Offshore sources are commonly used for large-scale nourishment projects.
Bypass	3	Sediment artificially transferred around coastal structures (e.g., jetties or harbor mouths) to restore sediment continuity and nourish down-drift beaches.
Land	4	Material sourced from terrestrial deposits such as inland quarries, dunes, or sediment stockpiles. Used primarily where marine sources are unavailable or unsuitable.

Primary Borrow Area Hierarchy: (1) Offshore, (2) Inlets and Channels, (3) Land and (4) Bypass.

Offshore sources dominate the dataset, with 554 records, followed by inlets and channels (208 records). Land-based and bypass sources are rare and typically appear in combination with other sources. This hierarchy reflects the dominant sediment sourcing practices and supports consistent assignment of primary borrow areas across projects.

The resulting fields, `primary_purpose`, `primary_type`, and `primary_borrow_area`, form the foundation for all subsequent classification and analysis in this study. Full multi-value data remains preserved in the raw dataset for reference and transparency.

Attribute Availability by Country

Not all source datasets included full attribute information. Table 3.5 summarizes which classifications were available per country, which is important to consider when interpreting subsequent analyses. From this point forward, all analyses are based on the `primary_purpose`, `primary_type`, and `primary_borrow_area` fields, as defined above.

Table 3.5: Availability of Nourishment Attribute Classifications by Country. An `X` indicates that the original dataset included information on the respective attribute. Blank cells indicate missing or undefined fields.

Country	Type	Purpose	Borrow Area
Denmark	X		X
France	X		X
Germany	X		
Italy			X
Netherlands	X	X	X
Portugal	X	X	X
Spain	X	X	
Sweden	X	X	X

3.1.4. Spatial Processing

To enable spatial analysis and integration with external geospatial datasets, all location data were standardized to decimal degrees, including the conversion of any coordinates originally provided in degrees-minutes-seconds (DMS) format.

For entries lacking valid coordinates, the `geo_lookup` function from the Nominatim geocoding service was used to retrieve approximate locations based on place names. After this automated step, 132 records remained without valid geometries. These were manually geo-referenced using Google Maps, with coordinates stored in a custom dictionary and added back to the dataset.

During quality control, one record, Bas-Champ (France), was found to be incorrectly located inland. Despite verification efforts, no matching beach location could be identified, and the record was therefore excluded from the final dataset.

To geographically locate each nourishment, records were linked to the nearest transect in the Global Coastal Transect System developed by Calkoen et al. (2025). The GCTS consists of evenly spaced transects (100 m intervals) along the European coastline and provides a consistent spatial reference framework across multiple datasets. Linking nourishment records to transects enables harmonized cross-dataset analysis and access to standardized transect-level attributes.

Before performing the spatial join, both the nourishment data and GCTS were reprojected to a common coordinate reference system: EPSG:3035 (ETRS89 / LAEA Europe). This projection minimizes distortion across continental Europe and supports accurate distance-based calculations.

Each nourishment was then matched to its nearest transect within a 100 m radius, equivalent to the GCTS transect spacing. A smaller threshold (e.g., 50 m) would be suitable for well-defined shoreline placements but was deemed too restrictive given potential inaccuracies introduced during geocoding and manual entry.

To verify the spatial join, the distance between each nourishment point and its matched transect was calculated. Records exceeding the 100 m threshold were flagged for manual review. Most unmatched records were found to originate from known issues in the Dutch Maasvlakte 2 dataset, where spatial geometries were incomplete or unreliable.

In total, 39 nourishment records could not be confidently linked to a transect and were excluded from further analysis. These records are listed in Appendix B.2 for transparency. The remaining dataset was

then reprojected to EPSG:4326 (WGS 84) to provide standard latitude–longitude coordinates for use in web-based mapping tools and downstream spatial analysis.

3.1.5. Output

After all preprocessing, enrichment, and spatial processing steps were completed, the final nourishment dataset was saved in `.json` format. This format was selected for its flexibility and compatibility with Python-based workflows, particularly for handling geospatial and attribute-rich data.

The final dataset contains 1,060 nourishment records, each of which includes a valid start date, nourishment volume, geographic location, and a matched transect from the Global Coastal Transect System. Where available, records are also enriched with standardized attributes for nourishment purpose, type, and borrow area, based on the classification schemes described earlier.

3.2. Characterizing Nourished Coastlines Using Shoreline Trends and Coastal Typologies

To better understand the physical context and observed shoreline behaviour at nourished sites, this section describes how nourishment records were linked to transect-level classifications and shoreline trend data. By combining the nourishment database with the Global Coastal Transect Repository and the ShorelineMonitor time series, key coastal characteristics, such as shore type, coastal typology, and pre-nourishment shoreline trends, were extracted for each intervention. Both datasets by Calkoen et al. (2025) provide the spatial foundation for this analysis.

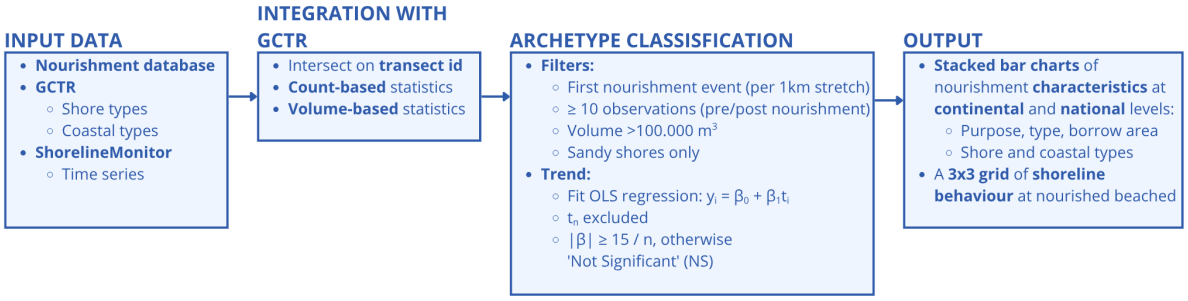

Figure 3.7: Overview of the data sources and processing steps used to extract nourishment site characteristics and pre/post-nourishment shoreline trends.

3.2.1. Input Data

Nourishment Database. The nourishment records form the basis of this analysis. Each entry includes at minimum a start year, nourishment volume, and location. Where available, attributes such as nourishment type, borrow area, and purpose are included. The dataset is stored in `.geojson` format and contains 1,060 records with standardized fields and GCTS transect IDs.

Global Coastal Transect Repository. As shown in Figure 3.2, the GCTR extends the GCTS by adding coastal and shore type classifications derived from satellite imagery and machine learning. It enables consistent morphological characterization of the European coastline.

ShorelineMonitor Time Series. Also introduced in Figure 3.2, the ShorelineMonitor dataset provides shoreline positions from 1984–2024 at 15 m resolution. It includes over 7.5 million transects, quality flags, and is fully aligned with the GCTR via shared `transect_ids`.

Together, these inputs enable consistent coastal classification and trend extraction at each nourishment location.

3.2.2. Integration of Nourishment Data with Coastal Transect Classifications

To contextualize nourishment locations within their physical and environmental setting, the nourishment database was enriched with attributes from the GCTR (Calkoen et al., 2025). The datasets were linked

using a shared `transect_id`, previously assigned during the spatial processing step.

To interpret patterns in nourishment practices, two metrics were considered: the number of nourishment records and the total volume of nourished sediment. These offer complementary perspectives:

- **Count-based statistics** indicate how frequently nourishment occurs in specific coastal settings. This can provide insight into policy and management approaches, such as whether a region favors frequent small-scale interventions or relies on fewer, larger-scale projects.
- **Volume-based statistics** reflect the physical scale of intervention and the likely associated investment. Larger volumes may represent substantial engineering efforts, but can also result from opportunistic sediment placement (e.g., reuse of dredged material from nearby navigation channels or ports). As such, volume data can help differentiate between proactive adaptation strategies and sediment redistribution linked to other coastal operations.

While both metrics are valuable, each has limitations. Record counts may over represent areas with more granular reporting or frequent minor works, while volume-based data can be skewed by a small number of very large interventions. By considering both, this study aims to provide a more balanced and comprehensive understanding of nourishment practices across the European coastline.

3.2.3. Nourishment Trend Archetype Classification

This section outlines the method used to identify shoreline trend archetypes based on the observed behaviour of nourished coasts before and after intervention. Archetypes allow for typological classification of nourishment outcomes and support comparison across coastal settings.

Event Filtering Criteria

To ensure reliable trend detection, a series of spatial, temporal, and geomorphic filters was applied to the nourishment dataset. Only the first nourishment event within each 1 km coastal stretch was considered, with any prior nourishment activity in neighbouring transects (± 500 m) leading to exclusion. Further filters included:

- **Minimum intervention year:** Nourishments before 1990 were excluded due to limited satellite coverage.
- **Minimum nourishment volume:** Only interventions exceeding $100.000\,\mathrm{m}^3$ were retained.
- **Shore type:** Only sandy transects were considered, consistent with the study's scope.
- **Observation threshold:** At least 10 primary shoreline observations were required both before and after nourishment.

Shoreline Trend Estimation

Shoreline change trends were derived from the ShorelineMonitor dataset (Calkoen et al., 2025), using Ordinary Least Squares (OLS) regression on annual shoreline positions. To avoid compositional artifacts, the nourishment year was excluded from trend fitting. The regression model:

$$y = \beta_0 + \beta_1 t$$

was applied separately to the pre- and post-nourishment time windows. Trends were considered meaningful if the slope exceeded a resolution-based threshold:

$$T = \frac{15}{n}$$

where n is the number of observations. The threshold incorporates the spatial resolution of Landsat-derived shorelines and scales with the temporal density of observations.

Archetype Assignment

Each transect was assigned a two-part classification based on the direction and significance of the pre- and post-nourishment trends:

- **Erosion:** $\beta_1 < 0$ and $|\beta_1| > T$
- **Accretion:** $\beta_1 > 0$ and $|\beta_1| > T$
- **Not Significant:** $|\beta_1| \leq T$

This yielded trend archetypes such as *Erosion → Accretion* or *Accretion → Not Significant*. Trend lines were visualized by archetype group, using standardized colour coding: red for erosion, green for accretion, and gray for non-significant trends.

Accounting for Repeated Nourishments

To support interpretation, each transect was tagged with the number of post-nourishment interventions. This allowed the identification of transects influenced by repeated nourishment, helping to distinguish single-event responses from cumulative effects. This metric is used descriptively and does not affect the core classification.

3.2.4. Output

The final output of this analysis includes a series of visualizations that summarize nourishment characteristics and classify shoreline response archetypes. These consist of:

- Stacked bar charts showing the distribution of nourishment attributes (purpose, type, borrow area) by coastal and shore type at both global and national levels.
- A 3×3 grid illustrating pre- and post-nourishment trend combinations, supported by counts of repeated interventions and spatial distribution maps of initial shoreline trends.

These outputs are further analysed in chapter 4, where they are used to explore patterns in nourishment practices and associated shoreline responses across Europe.

3.3. Development of the Nourishment Suitability Assessment Model

The development of the NSAM is grounded in the preceding analysis of historical nourishment practices across Europe. Rather than relying on a purely theoretical framework, the model leverages empirical patterns in intervention types, coastal settings, governance structures, and observed outcomes that have historically supported the implementation of nourishment.

Specifically, the number of interventions and the total sediment volumes associated with each category are used as proxies for suitability. These metrics reflect both the frequency and the scale of nourishment efforts, offering a first-order approximation of where nourishment is most likely to be viable under future shoreline retreat scenarios.

The assessment framework is structured around four key factors, derived from the nourishment database and integrated typologies:

- **Coastal Type:** Physical characteristics of the coastline, such as sandy sediment plains or dune-backed systems.
- **Coastal Policy:** National or regional governance frameworks that influence nourishment frequency and scale.
- **Sediment Availability:** Access to borrow areas such as offshore deposits.
- **Knowledge and Experience:** Historical presence of nourishment projects and associated institutional capacity.

These four factors form the empirical basis for evaluating nourishment suitability. Their relevance and explanatory strength are examined in the results chapter and subsequently formalised into a traffic light classification framework in the synthesis and application chapter (chapter 6).

3.4. Modelling Shoreline Change from Sea-Level Rise

Following the analysis of historical nourishment interventions and coastal characteristics, the next stage addresses the projection of future shoreline retreat. This section focuses on retreat driven by sea-level rise, estimated using ensemble-based climate projections and the Bruun Rule. The objective is to generate probabilistic samples of future shoreline positions for each transect across multiple climate scenarios. These outputs are later combined with the results of ambient change (AC) modelling, described in the following section, to assess exposure and risk.

Figure 3.8: Workflow for estimating shoreline retreat under sea-level rise using ensemble-based projections and the Bruun Rule.

3.4.1. Input Data and Mapping to Transects

Sea-Level Rise Projections. Sea-level rise (SLR) projections from the IPCC AR6 (based on CMIP6 ensembles) were used for SSP1-2.6, SSP2-4.5, and SSP5-8.5, with target years 2030, 2050, and 2100. The data were originally provided on a coarse 1° grid. To assign projections to GCTR transects, ensemble rasters were converted to points and spatially joined using a nearest-neighbour match in EPSG:3035, with a maximum radius of 100 km.

Coastal Slope. Each transect was assigned a local cross-shore coastal slope derived from Athanasiou et al. (2024). The slope represents the elevation difference between the depth of closure (DoC) and the nearest inland elevation peak along a shore-normal transect, as calculated from DeltaDTM.

To ensure a reliable spatial association between shoreline transects and slope data, while maintaining broad spatial coverage, slope values were first constrained to naturally occurring ranges for sandy coasts, between 1:300 and 1:5 (Vousdoukas et al., 2020). A maximum spatial join radius of 750 m was then applied to match slope values to transects. This threshold represents a compromise between maximizing transect inclusion and maintaining physical representativeness, ensuring that assigned slope values closely reflect local shoreline morphology. In total, 98.8% of the transects matched a suitable slope. Transects for slope data could not be matched within this distance were excluded from further analysis. A full exploratory data analysis of the slope filtering and matching procedure, including diagnostic plots, is provided in Appendix B.3.

Global Coastal Transect Repository. The GCTR forms the spatial backbone of the analysis and already integrates the SLR projections and coastal slope values via the methods described above. Only transects classified as sandy were retained for downstream analysis.

An overview of all filtering steps applied to SLR-relevant transects is provided in Table 3.6.

Table 3.6: Sequential filtering of SLR-relevant transects located on sandy shores within Europe. Source: GCTR (global coverage of over 11 million transects).

Step	Description	Transects
0a	All transects in Europe	1,388,990
0b	Of which: sandy transects	412,818
1	Retain only transects with coastal slope between 1/300 and 1/5	286,863
2	Exclude transects failing 750 m spatial join threshold	283,479

3.4.2. Application of the Bruun Rule

SLR-induced shoreline change was estimated using the Bruun Rule, applied separately for each SLR ensemble member:

$$dx = -\frac{\text{SLR}}{\tan(\theta)} \tag{3.1}$$

where:

- dx: shoreline change (m),
- SLR: sea-level rise (m),
- $\tan(\theta)$: cross-shore coastal slope (-).

This formulation assumes sediment is redistributed in the cross-shore to maintain an equilibrium profile, without net loss. It also neglects alongshore processes and assumes no coastal defences, vegetation effects, or human interventions.

For each SSP-year-transect combination, the equation was applied to all 100 SLR ensemble members, generating a probabilistic distribution of retreat estimates. An example is included in Figure B.9.

3.4.3. Output

For every transect and scenario, the full distribution of 100 modelled change values was retained. Summary statistics (5th, 50th, and 95th percentiles) were extracted to support comparison and integration with ambient shoreline change (Section 3.5).

3.5. Probabilistic Shoreline Change from Ambient Drivers

This section describes the modelling approach for ambient shoreline change (AC), which captures shoreline trends resulting from wave climate, sediment transport processes, and anthropogenic influences. Historical shoreline observations are used to estimate long-term trends, which are extrapolated probabilistically into the future using Monte Carlo sampling. The resulting distributions represent future shoreline change under present-day ambient conditions.

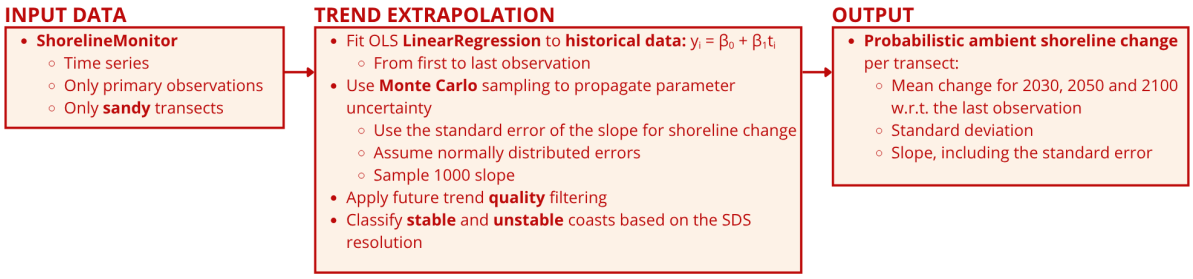

Figure 3.9: Workflow for estimating ambient shoreline change using a probabilistic method to extrapolate the historic trend

3.5.1. Input Data

Annual shoreline positions were obtained from the *ShorelineMonitor* dataset (Calkoen et al., 2025), covering the period 1984–2024. To ensure data reliability, only primary observations, the most reliable observations per transect, were retained. The outliers are also removed from the data. Transects of the time series are matched to the sandy transects in Europe of the GCTR.

3.5.2. Trend Extrapolation via Monte Carlo Sampling

To estimate future shoreline change, a linear regression model was applied to historical shoreline positions from 1984 to 2024 for each transect. The regression slope represents the observed rate of shoreline

movement during this period, while the standard error of the slope captures uncertainty in the parameter estimate. This parameter uncertainty is propagated forward using Monte Carlo simulations, where a distribution of slope values is sampled and extrapolated to future target years.

Although shoreline change processes were likely ongoing before 1984, this approach does not attempt to reconstruct long-term historical trends. Instead, it focuses on projecting change from a recent observational baseline forward in time. The model assumes that the trend observed over the last four decades is representative of near-future dynamics (until 2100). Shoreline change is thus expressed relative to the final year of the observed record, with projected changes calculated as deviations from this reference point.

This method explicitly accounts for parameter uncertainty in the slope estimate but does not incorporate model uncertainty (e.g., how well the linear model fits the data) or structural sources of error. These additional uncertainties are discussed further in chapter 7.

To propagate uncertainty in trend estimation, shoreline change was modelled as a linear function of time:

$$y_t = \beta_0 + \beta_1 t \tag{3.2}$$

where:

- β_0: intercept (initial shoreline position),
- β_1: linear slope (rate of shoreline change).

A linear regression was fit to each valid shoreline time series. Uncertainty in the slope estimate $\hat{\beta}_1$ was assumed normally distributed, with the regression standard error used as the standard deviation. For each transect, 1,000 slope samples were drawn from a normal distribution:

$$\hat{m} \sim \mathcal{N}(\hat{\beta}_1, \mathrm{SE}_{\hat{\beta}_1}) \tag{3.3}$$

Projected shoreline change was then calculated for the years 2030, 2050, and 2100 using:

$$\Delta y = \hat{m} \cdot (t - t_0) \tag{3.4}$$

where:

- $\hat{m}$: sampled slope (in meters per year),
- t_0: final year of observation (typically between 2021-2024),
- t: target year.

Each simulation produces a distribution of shoreline change values per transect and time horizon, capturing uncertainty in both the magnitude and direction of the projected trend. Due to the linear propagation of normally distributed slopes, the projected shoreline change distribution is also approximately normal. Its mean and standard deviation are retained for use in the combined shoreline change simulations.

To illustrate the result of this trend extrapolation approach, Figure 3.10 presents two example transects. The first shows an eroding shoreline in Blokhus Denmark, while the second represents an accreting coast in the Netherlands. In both cases, the black dashed line denotes the median projection, and the shaded region shows the 90% confidence interval derived from the Monte Carlo sampling. These examples highlight how observed historical variability influences the range and direction of future projections.

Trend Quality Filtering

To ensure robustness, only transects meeting minimum data quality criteria were retained:

- At least five valid years of *primary* shoreline observations,
- Unique and finite timestamps and shoreline positions,

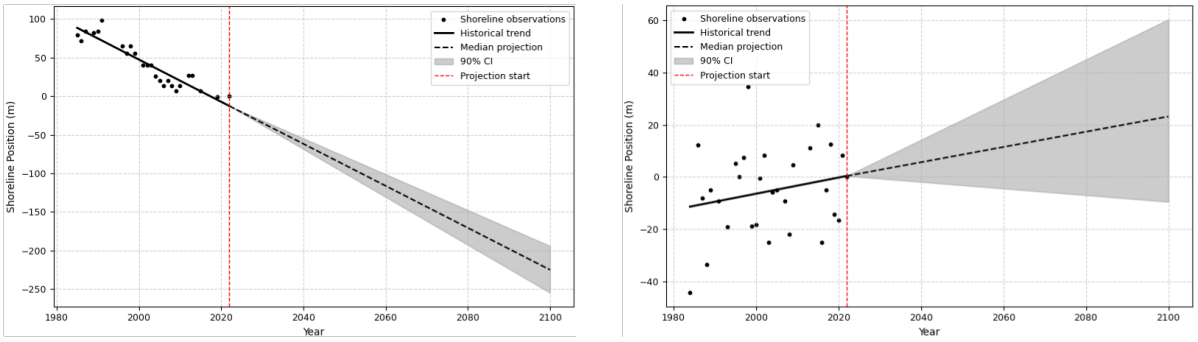

(a) Eroding transect (Blokhus, Denmark)

(b) Accreting transect (Holland coast, near the North–South Holland provincial boundary, the Netherlands)

Figure 3.10: Examples of ambient shoreline change projections based on linear regression and Monte Carlo sampling. The fan charts show observed shoreline positions, historical trends, and projected change with 90% confidence intervals.

- Non-zero variance in position (to enable trend detection),

A summary of all filtering steps is provided in Table 3.7.

Focus on Shoreline Change (Δy) Rather Than Absolute Position

This analysis explicitly models relative shoreline change (Δy) rather than absolute shoreline position. This choice enables the combination of sea-level rise and ambient change by referencing all projections to a fixed spatial point.

Because the model focuses solely on change, the uncertainty of the intercept term becomes irrelevant and falls out of the equation. This improves interpretability and aligns with the structure of SLR-induced change projections.

Where applicable, we incorporate slope parameter uncertainty through the ambient change confidence intervals, and SLR uncertainty via 100 ensemble members across multiple Shared Socio-economic Pathways. Uncertainties related to the coastal slope and the exact detection of the reference point are considered out of scope for this analysis but are briefly discussed in chapter 7.

Model Choice Validation

The linear regression model used in this study reflects commonly applied methods for estimating historical shoreline trends. To validate its performance, model fit was assessed based on its ability to reliably detect and quantify shoreline change over time.

As a first step, transects were classified as either *stable* or *unstable*, based on the resolution threshold of Landsat-derived shorelines, which is approximately 15 m (Hagenaars et al., 2017). Stable coasts were defined as having a net shoreline change of less than 15 m over the observation period, while unstable coasts exceeded this threshold.

To evaluate model performance, the coefficient of determination (R^2) and Root Mean Squared Error (RMSE) were calculated for the full dataset and for the unstable subset separately. Results show a lower mean R^2 value of 0.22 for the full set of transects, compared to 0.42 for the unstable subset, indicating better model fit when meaningful trends are present. In contrast, mean RMSE values were lower for the full set (13.5 m) compared to the unstable subset (22.8 m), which is expected due to the smaller magnitude of trends in the stable group.

In this case, the comparison confirms that the model is more reliable in detecting meaningful shoreline trends, while low-magnitude changes result in lower explained variance but also smaller errors.

Density plots for the R^2 and RMSE distributions, along with example trend fits for a stable and an unstable shoreline, are provided in Appendix section B.4.

Table 3.7: Sequential filtering of Ambient Change (AC)-relevant transects located on sandy shores within Europe. Source: ShorelineMonitor (global coverage of over 7.5 million transects).

Step	Description	Transects
0a	All transects in Europe	1,233,617
0b	Of which: sandy transects	380,064
1	Retain only transects with primary shoreline observations	380,064
2	Exclude transects failing quality criteria	377,208
3	Classify remaining transects as stable / unstable based on AC trend	195,836 / 141,372

3.5.3. Output

For each valid transect, the following outputs were computed for the years 2030, 2050, and 2100 (relative to the final year of observation):

- Mean and standard deviation of projected ambient change at each time horizon,
- Estimated linear trend slope (β_1) and its standard error,
- A binary flag indicating whether the ambient trend is valid, used to classify coasts as stable or unstable

All results were stored in a spatially referenced GeoDataFrame, with one row per transect per year. These outputs were then passed to the next stage for combination with sea-level rise-induced change.

3.6. Projecting Combined Shoreline Change

This section describes the integration of shoreline change due to sea-level rise with ambient shoreline change driven by observed historical trends. A probabilistic Monte Carlo approach is used to combine these two components for each transect, producing joint shoreline change projections that reflect both climate-driven and ambient processes. The complete workflow is illustrated in Figure 3.11.

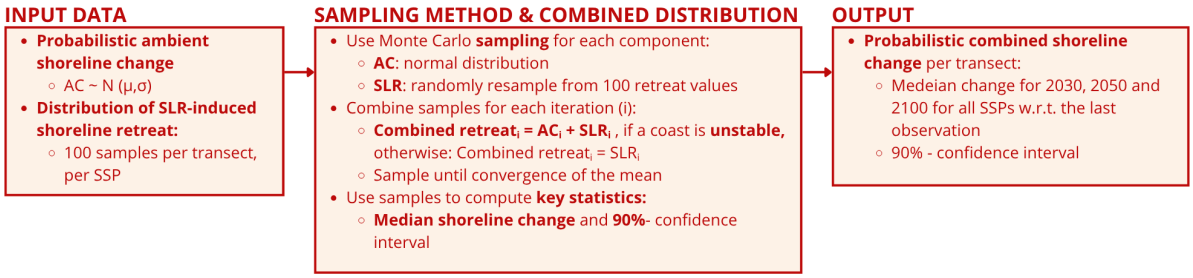

Figure 3.11: Workflow for combining ambient shoreline change (AC) with sea-level rise (SLR)-induced retreat into a shared probabilistic shoreline change distribution.

3.6.1. Input Data

This step integrates all sandy transects included in the independent analyses of SLR-induced change and ambient change.

- **Ambient Change:** Each transect is assigned a normal distribution defined by the mean and standard deviation of simulated shoreline change (Section 3.5). A Boolean flag indicates whether the trend exceeds the detectability threshold of 15 m, classifying the coast as either stable or unstable.
- **SLR-Induced Change:** For each transect and SSP-year combination, projected shoreline change is represented by 100 ensemble-based samples derived from climate-model-driven SLR scenarios.

In total, 274,517 transects contain both SLR and AC data. These transects are included in the analysis, representing almost 27.500 km of sandy coastline.

3.6.2. Sampling Method and Combined Distribution

Total projected shoreline change was estimated using a Monte Carlo sampling approach, applied to each transect included in both dataset components, across all Shared Socioeconomic Pathways and time horizons. A minimum of 500 iterations were performed per case, with a maximum of 10,000 iterations allowed. Sampling continued until convergence was achieved, defined as a change in the sample mean below a tolerance threshold of 0.01.

For each iteration:

- A value for AC was drawn from a normal distribution defined by the mean and standard deviation of historical trend extrapolation.
- A value for SLR-induced retreat was randomly sampled from the 100-member SLR ensemble distribution.
- The two values were summed to produce one realization of combined shoreline change.

This process resulted in a probabilistic distribution of total shoreline change for each transect, scenario, and time horizon. If no detectable ambient trend was present (i.e., below the resolution threshold), only the SLR-induced component was used in the combined projection.

3.6.3. Output

The output consists of probabilistic shoreline change projections for each transect, year, and SSP. These projections reflect the combined effect of ambient shoreline trends and SLR-induced retreat.

For each case, the following summary statistics were extracted:

- Median projected shoreline change (p_{50}),
- 5th percentile (p_5) and 95th percentile (p_{95}), defining the 90% confidence interval,
- Full sample distribution, retained for use in downstream exposure analysis (Section 3.7).

These outputs form the basis for assessing spatial patterns of coastal erosion risk under different climate scenarios.

3.7. Quantifying Asset Exposure to Projected Shoreline Retreat

This section outlines the methodology used to estimate the exposure of built assets to future shoreline retreat across Europe. By combining shoreline change projections with coastal infrastructure data, the analysis identifies buildings located within projected retreat zones under various SSP scenarios and time horizons.

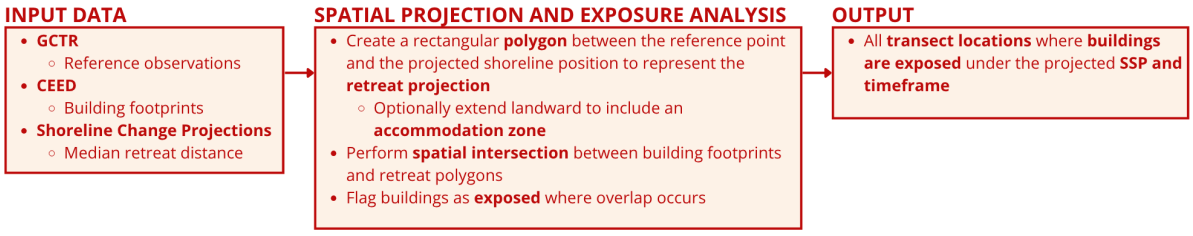

Figure 3.12: Workflow for quantifying coastal asset exposure by intersecting projected shoreline retreat zones with building footprint data under multiple SSP scenarios

3.7.1. Input Data

The exposure assessment integrates the following geospatial datasets:

- **Coastal European Exposure Database (CEED):** Georeferenced building footprints and infrastructure features along the European coastline (Koks et al., 2023).
- **Global Coastal Transect Repository:** Shore-normal transects spaced at 100 m intervals, including fixed reference points and orientation data (Calkoen et al., 2025).

- **Shoreline Change Projections:** Median retreat distances at transect level for each SSP-year combination, derived from the combined shoreline change model (see section 3.6).

3.7.2. Spatial Projection of Shoreline Change and Exposure Analysis

To spatially represent shoreline retreat, a retreat zone was constructed for each transect based on the following steps:

1. The most recent shoreline position was used as a reference point.
2. Median projected shoreline retreat was applied along a shore-normal transect line.
3. A rectangular polygon was created between the reference point and the projected shoreline position to represent the retreat zone.
4. A lateral space of 50 m was added on both sides to account for transect width.
5. Optionally, the retreat zone was extended landward by an accommodation buffer, representing a margin between the shoreline and infrastructure.

This procedure generated a spatial layer of retreat polygons, one per transect, for each scenario-year combination (SSP and time horizon).

Exposure was assessed by spatially intersecting the projected retreat polygons with CEED building footprints. A transect was classified as exposed if any part of it overlapped with a retreat zone.

For each transect, the following attributes were recorded:

- Transect ID, scenario (SSP), and year,
- Reference point coordinates and projected shoreline change,
- Presence or absence of exposed buildings (binary).

No differentiation was made between buildings based on type, use, or value, exposure was considered in spatial terms only. An example of this process, with and without the accommodation buffer, is illustrated in Figure 3.13.

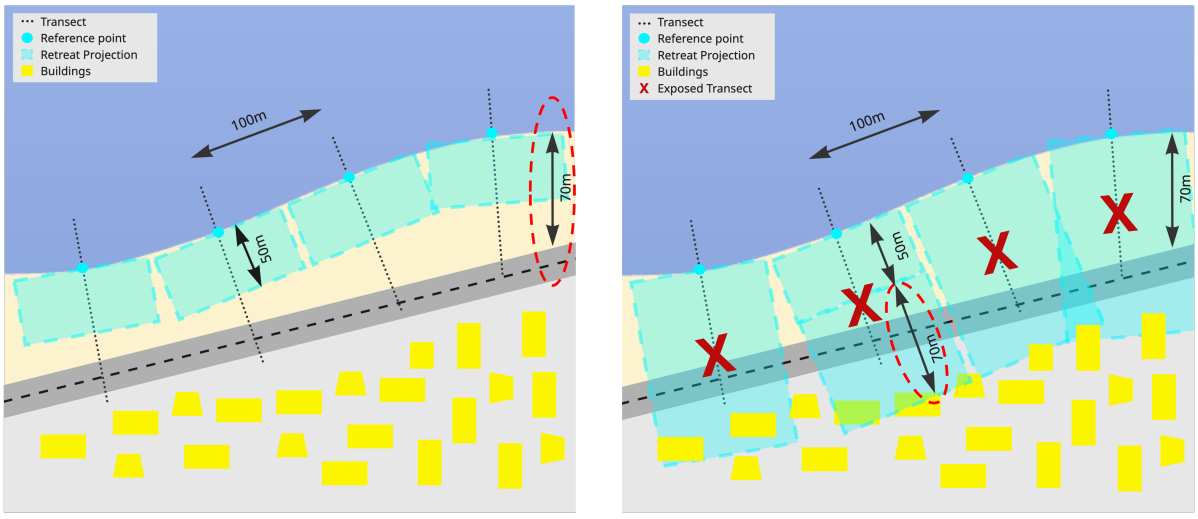

(a) Retreat projection zone without accommodation space (red dashed circle).

(b) Retreat projection zone with accommodation space (red dashed circle).

Figure 3.13: Schematic overview of the shoreline retreat projection method. Each retreat zone is constructed along shore-normal transects, with an optional landward extension to account for infrastructure-free space (Lansu et al., 2024), here referred to as the accommodation space or buffer.

3.7.3. Output

The output consists of transect-level exposure records, indicating whether and where buildings intersect projected shoreline retreat zones. These results can support coastal risk assessments and inform man-

agement strategies at local, regional, and national scales. They also serve as the basis for identifying high-risk locations.

3.8. Identification of High-Risk Beaches

To inform spatial adaptation strategies, this thesis identifies high-risk beaches based on projected shoreline retreat and building exposure under different sea-level rise scenarios. The analysis is conducted for two time horizons, 2050 and 2100, and across multiple Shared Socioeconomic Pathways to reflect a range of climate futures.

In this thesis, a high-risk beach is defined as a continuous stretch of sandy coastline with at least 10 adjacent transects (equivalent to 1 km) where each transect meets the following conditions:

- **Exposure:** At least one built structure intersects the projected retreat polygon (binary).
- **Retreat definition:** Exposure can be assessed using retreat polygons based solely on shoreline change, or optionally extended landward by an accommodation buffer to reflect space between the shoreline and infrastructure.

This binary definition provides a transparent and reproducible approach to identifying locations where the retreat of the shoreline is likely to directly affect built assets. It moves beyond general erosion trends by explicitly incorporating both the spatial extent of erosion and the presence of vulnerable structures.

The resulting high-risk beach stretches are then evaluated using the Nourishment Suitability Assessment Model, which assesses the alignment between their characteristics and policy context and the historical conditions under which nourishment has been implemented.

The outcomes of this analysis are presented in the following chapters:

- Chapter 4: Documents the characteristics and spatial patterns of historical nourishment practices.
- Chapter 5: Presents shoreline retreat projections and identifies high-risk beaches across scenarios.
- Chapter 6: Combines both components in a synthesis by showcasing three high-risk beaches and evaluating their suitability for nourishment as a response to future coastal erosion.

Overview of the Methodological Workflow

Concluding the methodology chapter, Figure 3.14 provides an overview of the analytical workflow from transects to exposure assessment. It illustrates how shoreline retreat projections are integrated with spatial building data to assess future coastal exposure.

This figure provides a concise overview of the sequential steps taken and serves as a conceptual bridge to the results and synthesis chapters that follow.

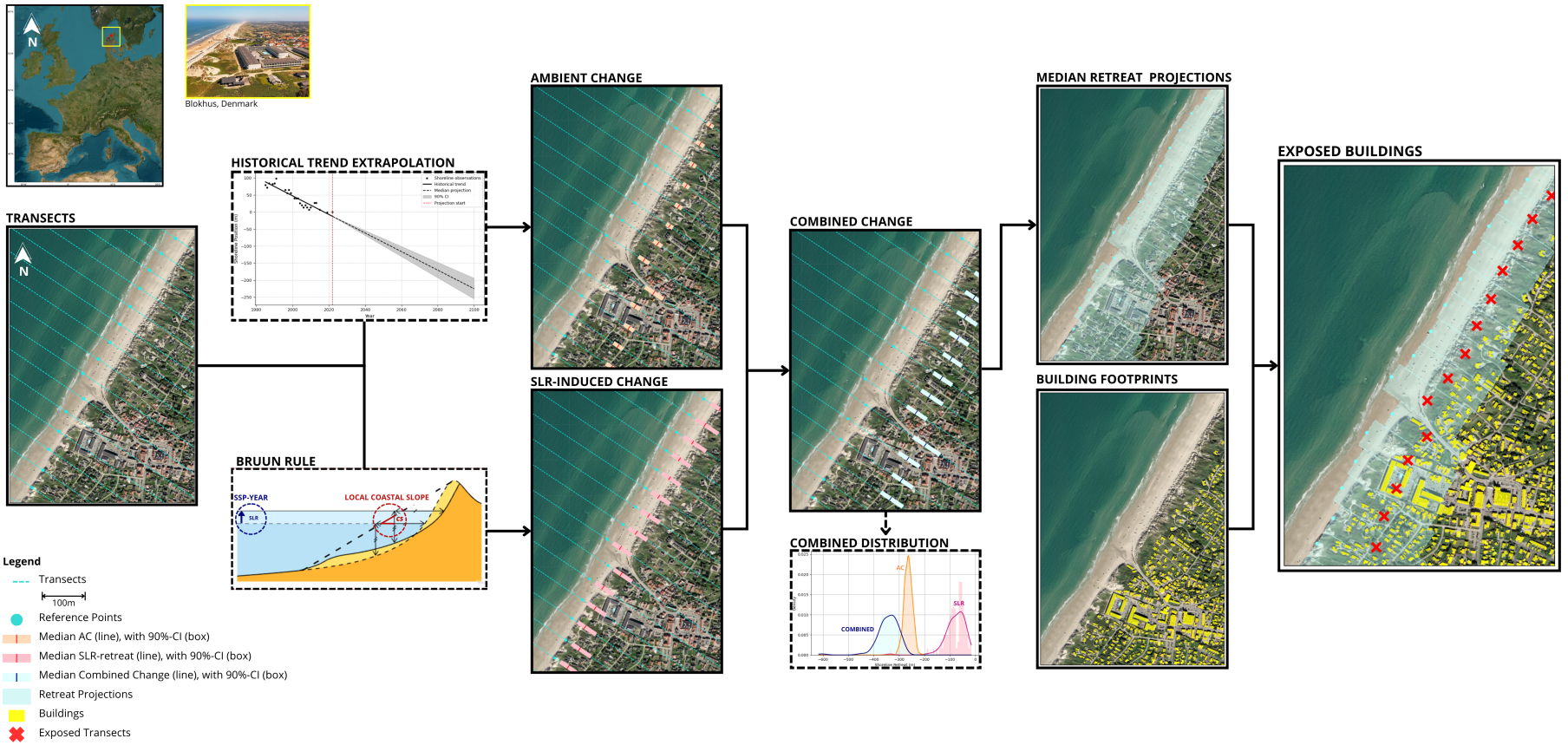

Figure 3.14: Overview of the methodological workflow, showing how shoreline retreat projections are integrated with building exposure data and historical nourishment patterns to inform the Nourishment Suitability Assessment Model (NSAM). Projections correspond to SSP2-4.5 for 2100

4

Results I: Historical Nourishments

Overview

By analysing the nourishment database, this chapter uncovers the spatial distribution, implementation motives, and coastal contexts, such as borrow area, nourishment type, and coastal type, under which nourishments have historically been applied across Europe.

Nourishment Activity

- **1,060 records** mapped across diverse coastal settings, with up to **70 years** of records in countries like the Netherlands and Germany.
- The **Netherlands alone accounts for over 70%** of total nourishment volume (~460 million m³), followed by **Germany** and **Portugal**.
- **Volume increases** in countries with more experience and established coastal management practices.

Nourishment Characteristics

- **Offshore borrow areas** dominate, followed by sediment from inlet and channel sources.
- Nourishments are primarily applied to **dune sediment plain coasts**.
- **Shoreline response varies:** most nourished beaches remain stable or accrete, while only **7%** exhibit an erosion-to-erosion pattern (i.e. 'sawtooth').
- **Proactive and reactive strategies** are applied across Europe.

Key Factors Suitability

- **Coastal type**
- **Coastal policy**
- **Sediment availability**
- **Knowledge and experience**

This chapter presents the main findings from the analysis of historical coastal nourishment interventions across Europe. The results are based on a harmonised database, integrated with satellite-derived shoreline trends and coastal typologies.

4.1. Overview of Nourishment Activities in Europe

This section provides a summary of the geographic and temporal distribution of nourishment interventions across Europe, based on the compiled dataset. It contextualises the diversity of coastal settings, data coverage, and national documentation efforts.

Figure 4.1 presents the number of nourishment records, temporal coverage, and reported volumes per national dataset. The Netherlands accounts for over 70% of the total nourished volume, more than 460×10^6 m^3, followed by Germany and Portugal. Coverage extends over 50 years in France, and over 70 years in the Netherlands, Germany, and Portugal.

Figure 4.2 shows the mapped locations of 1,060 nourishment records linked to the Global Coastal Transect Repository, each including at least a start year and reported fill volume. The interventions span a variety of coastal settings, including the North Sea, Baltic, Atlantic, Mediterranean, and Adriatic coasts. High concentrations occur along the Dutch and German shorelines, where beach nourishment is applied frequently and at scale as part of ongoing coastal management strategies.

Appendix C.1 presents the nourishment volumes per country. It shows a clear trend of increasing

volumes in countries with more experience and established knowledge in implementing nourishments.

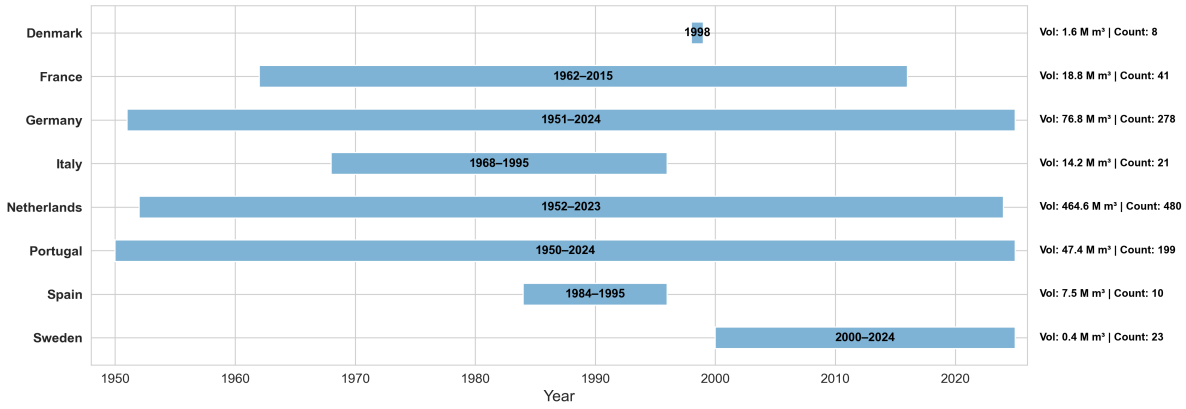

Figure 4.1: Number of nourishment records per country. This reflects national documentation efforts and data availability.

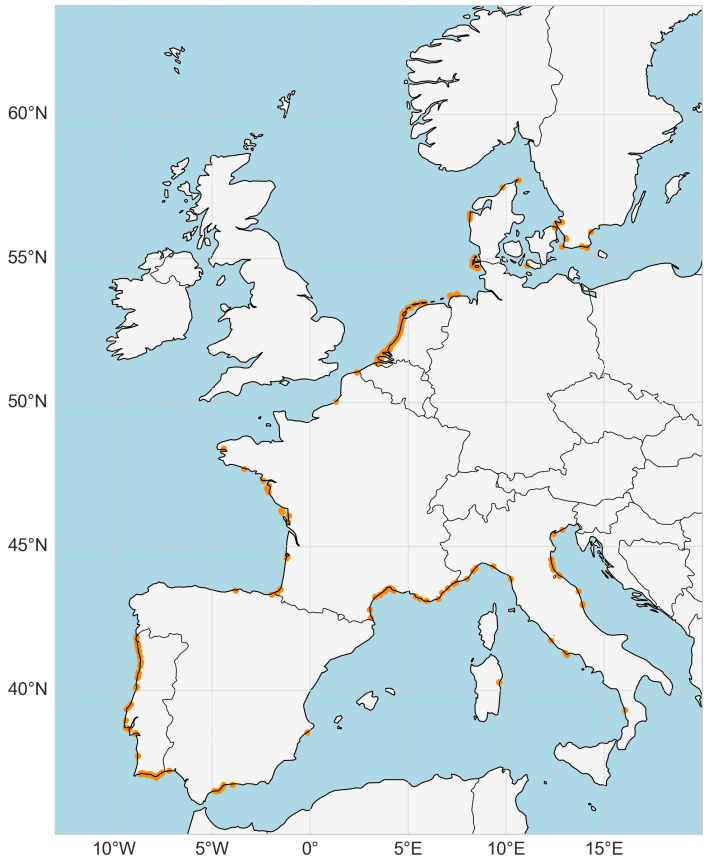

Figure 4.2: Geographic distribution of nourishment records across Europe. Locations are linked to the Global Coastal Transect Repository and span diverse coastal environments.

4.2. Typologies and Characteristics of Coastal Nourishments

This section explores the physical characteristics, strategic intent and coastal conditions of nourishment practices across Europe. Rather than assessing effectiveness, the focus is on identifying how nourishments have been applied, by purpose, type, material source, and coastal setting, and how shoreline

conditions vary prior to intervention. These insights form the foundation for evaluating nourishment suitability as an adaptation strategy in later sections.

4.2.1. Classification by Purpose, Type, and Borrow Area

To understand how nourishment strategies vary across European coasts, the dataset was analysed using five core attributes: nourishment purpose, type, borrow area, shore type, and coastal type. These relationships are visualised by both total nourished volume and the number of nourishment records, reflecting the scale and frequency of interventions respectively.

Figure 4.3 shows the relationship between borrow area and nourishment type. Offshore borrow areas account for over 479×10^6 m^3 of nourished sediment, largely from Dutch projects. Coastal protection and shoreline stability dominate as primary purposes, particularly in high-volume interventions along dune coasts.

Figure 4.4 presents the same relationships by nourishment count. 27% of nourishment records (with known borrow source) use material from inlets and channels, mainly for smaller-scale interventions, like those in Portugal. This contrast highlights how different borrow strategies are deployed based on project scale and context.

Additional national-level visualisations and coastal classifications are provided in section C.2 and section C.3.

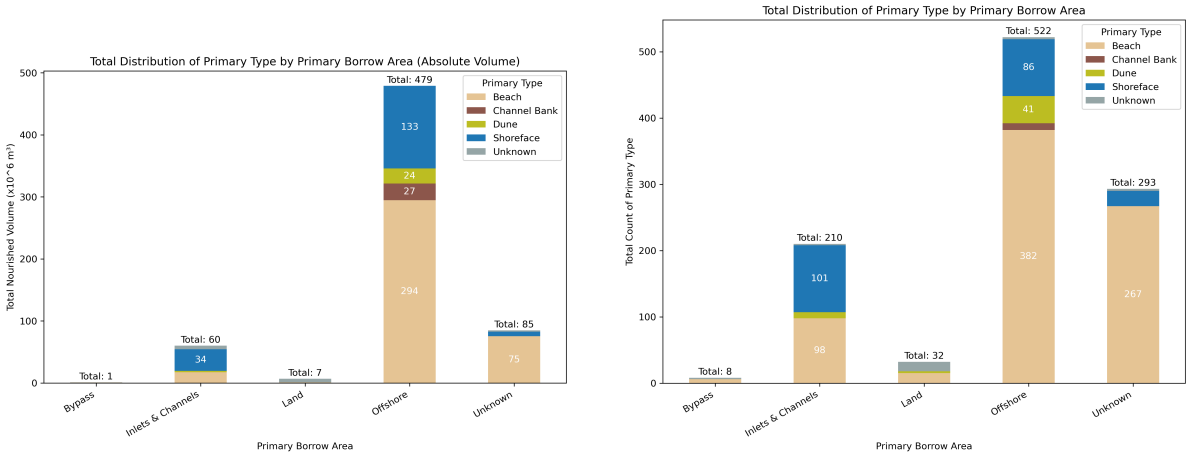

(a) By total nourished volume

(b) By number of nourishment projects

Figure 4.3: Relationship between primary borrow area and nourishment type, shown by (left) total nourished volume and (right) project count. Offshore borrow dominates in high-volume nourishments, especially in the Netherlands.

4.2.2. Shoreline Behaviour Before Nourishment

To understand shoreline conditions preceding nourishment, trends were analysed across 169 sites retained after applying data quality filters described in subsection 3.2.3. Sites were grouped by total nourishment volume to explore whether pre-intervention shoreline trends vary with the scale of nourishment.

Figure 4.5 shows shoreline change trends prior to nourishment, categorized by nourishment volume and filtered by three thresholds of minimum observational coverage (5, 10, and 15 observations). These thresholds correspond to minimum detectable trend magnitudes of $|T| > 3$, 1.5, and 1 m/yr, respectively, ensuring increasing confidence in the reported trends.

The results indicate that erosive trends are most frequently associated with smaller nourishments. In contrast, medium-scale nourishments (0.5–2 Mm^3) often coincide with stable or accreting shorelines. This suggests that nourishment is not always a direct response to active erosion but may also serve pre-emptive or sediment-redistribution purposes.

This pattern is particularly evident along the Dutch coast, as highlighted in the spatial distribution

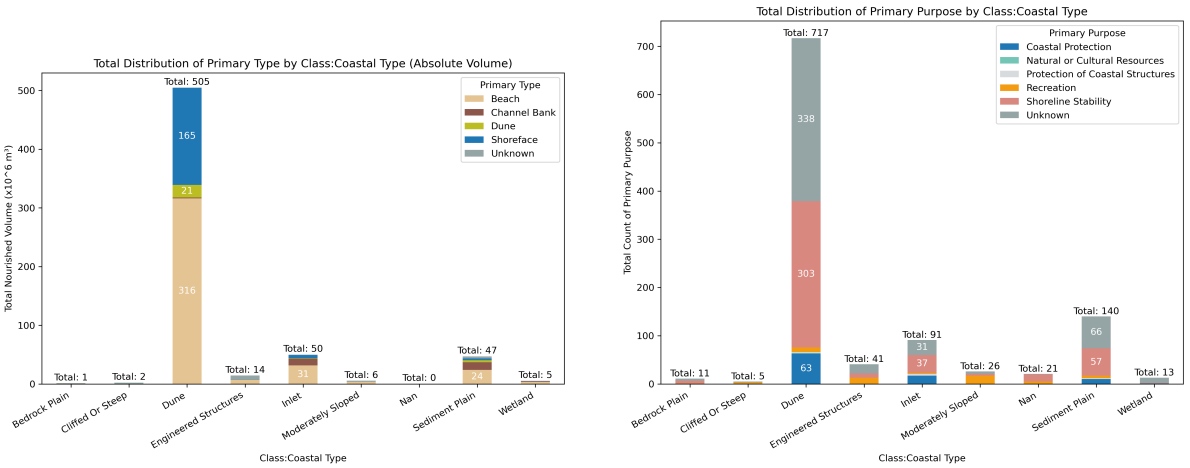

(a) By total nourished volume

(b) By number of nourishment projects

Figure 4.4: Relationship between coastal type and nourishment type, shown by (left) total nourished volume and (right) project count. Dune and sediment plain coasts dominate in both scale and frequency, primarily through beach and shoreface nourishments.

map in Figure C.27, where longshore drift contributes to downdrift accretion even in the absence of recent interventions.

To assess whether the overall accretion signal is disproportionately influenced by Dutch transects, the analysis was repeated excluding all data from the Netherlands. As shown in Figure C.28, the share of accretive trends drops notably, while erosive trends become dominant. This supports the interpretation that Dutch sediment redistribution has a substantial effect on trend classification in the full dataset.

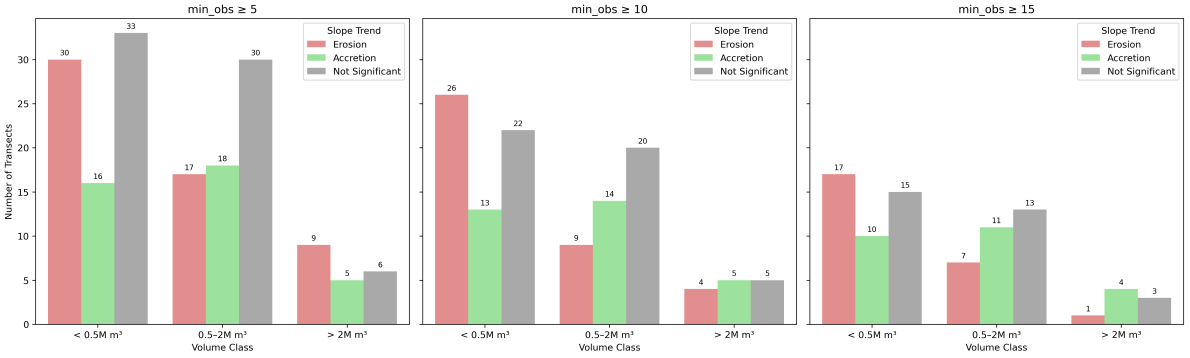

Figure 4.5: Distribution of shoreline slope trends prior to nourishment, grouped by total nourishment volume. Bars show the number of transects classified as erosive, accretive, or not significant, across three minimum observation thresholds.

Overall, the findings demonstrate that nourishment interventions have been applied under a range of coastal conditions. While erosion remains the most common driver, stable and accreting sites have also been targeted.

Additional supporting figures are included in section C.4.

4.2.3. Shoreline Behaviour at Nourished Beaches

To further explore how nourishments interact with shoreline change, interventions were classified based on pre- and post-nourishment trends. The results reveal a diverse set of behavioural archetypes, moving beyond the traditional expectation of a singular ”sawtooth” erosion–jump-erosion pattern.

Figure 4.6 shows fitted shoreline trends before and after nourishment for each archetyp. The colours indicate trend direction and annotations highlighting the number of transects and repeated interventions

to distinguish single from cumulative effects.

The most common archetype is a transition from erosion to accretion ($n = 16$), followed by *Not Significant* → *Accretion* ($n = 15$) and *Not Significant* → *Not Significant* ($n = 15$).

Several cases showed the *Accretion* → *Accretion* ($n = 13$) and *Accretion* → *Not Significant* ($n = 12$) archetypes.

Conversely, classical erosion-based archetypes are less dominant: only six transects follow the *Erosion* → *Erosion* pattern, and just eleven show *Erosion* → *Not Significant*. Only one transect exhibits *Accretion* → *Erosion*, indicating that nourishment-induced destabilisation is rare in this dataset.

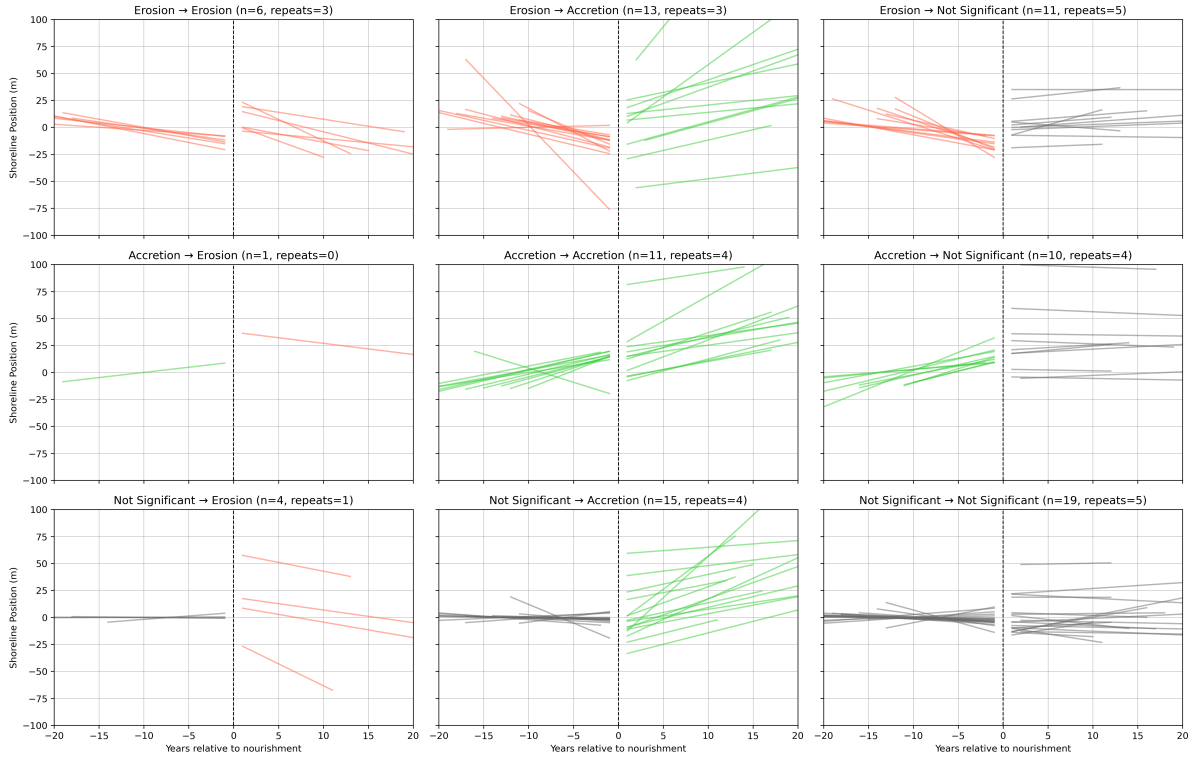

Figure 4.6: Fitted shoreline trends before and after nourishment, grouped by archetype. Colours indicate trend direction and significance: erosion (red), accretion (green), and not significant (grey). Year zero denotes the timing of nourishment. The number of transects and number of repeated nourishments are noted per panel.

4.2.4. Governance Context and Strategic Application

The diversity of nourishment patterns and archetypes observed in this study reflects differences in national governance structures. Institutional maturity, policy orientation, and decision-making frameworks strongly influence whether nourishment is deployed reactively or strategically. This section contextualises the findings within a comparative governance perspective across Europe.

Table 4.1 summarises the distribution of responsibilities and the policy role of nourishment in selected countries.

Governance clearly shapes how and when nourishment is applied. Medium- to large-scale interventions more frequently occur on stable or accreting shorelines, suggesting a proactive, strategic use. This is most evident in countries like the Netherlands, where long-established national programmes aim to maintain sediment balance and coastal form. By contrast, countries with less institutionalised systems, such as Sweden, tend to apply nourishment reactively, primarily in response to erosion.

These contrasts highlight how governance capacity affects not only the frequency of nourishment, but also its purpose and timing. Recognising this distinction is essential for assessing site suitability, as institutional readiness strongly influences the viability of long-term, nourishment-based adaptation strategies.

Table 4.1: Governance responsibility and policy role of beach nourishment in selected European countries.

Country	Responsibility for coastal safety and erosion	Policy role of beach nourishment	Source
Belgium (Flanders)	Regional (federal state) level	Core part of the Master Plan for Coastal Safety, complementing structural measures.	Bontje et al. (2016)
Denmark	Varies by location: national, municipal, or landowner level	Promoted by the Danish Coastal Authority as a key soft protection method.	Bontje et al. (2016)
France	Shared across administrative levels under national strategy	Common and institutionalized, but not universally preferred.	Cerema (2023)
Germany	Federal government and coastal states	Common along the North Sea; limited by sediment supply in the Baltic.	Bontje et al. (2016)
Italy	Regional authorities, with national support	Once widespread, now reduced due to sediment shortages and environmental limits.	Pranzini (2018)
Portugal	National government, with local and private roles; coastal land up to 50 m inland is state-owned	Central to policy since the 1990s; port authorities are key actors.	Pinto et al. (2020)
Spain	National policy, implemented regionally	Widely used for tourism, but reactive and lacks national coordination.	MITECO (2022)
Sweden	Municipalities and landowners	Emerging strategy, not yet widely adopted.	Bontje et al. (2016)
The Netherlands	National government and regional water boards	Preferred and institutionalized for coastal maintenance.	Bontje et al. (2016)
United Kingdom (England)	National frameworks with local implementation	In use since the 1950s; now part of site-specific technical strategies.	Bontje et al. (2016)

4.3. NSAM: Key Factors Enhancing Suitability

This section presents the empirical results that inform the Nourishment Suitability Assessment Model. It identifies the coastal characteristics and contextual factors most frequently associated with historical nourishment practices. The assumption is that locations where nourishments have previously been implemented are, by precedent, more likely to be suitable for future nourishment under similar conditions.

The model is structured around four key factors that were identified in section 3.3 and are consistently associated with the majority of past nourishment practices:

1. **Coastal Type:** Sites located on sediment plains or within dune-backed systems are frequently observed in the dataset and show higher suitability for nourishment-based adaptation.
2. **Coastal Policy:** Countries with established national programmes have implemented more nourishment interventions. Nourishment has been applied in both proactive and reactive contexts, indicating suitability across varying pre-nourishment trends.
3. **Sediment Availability:** Access to offshore borrow areas or sediment deposits within inlets and channels improves the logistical feasibility and cost-effectiveness of nourishment operations.
4. **Knowledge and Experience:** Areas with documented prior interventions and the use of local knowledge exhibit higher frequencies and volumes of nourishment, contributing to suitability.

5

Results II: Shoreline Projections and Exposure

Overview

By extrapolating historical trends and modelling SLR-induced erosion, this chapter projects where, when, and under which climate scenarios the European coast is expected to retreat. The median of the combined projections is spatially intersected with exposure data to identify the location of high-risk beaches.

Shoreline Change Projections

- **Ambient change:**
  - **41%** of the historically unstable coasts are **eroding**
  - EU **median AC** is accretive, **+17.4m** by 2100, however, strong local/regional variation (e.g., inlets/deltas)
- Over **98%** of transects projected to **erode** due to **SLR** under all SSPs and time horizons**;** median changes reaches **-45m** in 2100 under SSP2-4.5
- **84–87%** of sandy coasts retreat under combined projections (AC + SLR), with median retreat up to -80.2m (SSP5-8.5, 2100)
- **Strong regional variation:** North Sea, southern Baltic and Atlantic most affected
- Mediterranean coasts show **lower retreat** rates and narrower uncertainty, but SLR identified as **risk to infrastructure**

Identification of High-Risk Beaches

- **High-risk beaches** are defined as **≥ 1km contiguous beach segments** with building exposure due to erosion
- Number of high-risk beaches ranges from **10 to 841** depending on SSP, time horizon and accommodation space
- Up to **3,690 km of coast** is identified as exposed under SSP5-8.5 with 70m accommodation space
- The **size of the buffer zone** drives the number of high-risk beaches more than SLR scenario or time horizon
- **Nourished coasts** generally **do not appear as high risk** on the map due to their historical accretion signal but remain dependent on continued intervention for resilience

This chapter presents the results of the shoreline change projections alongside the corresponding exposure assessment. The analysis is conducted at the European scale, with selected regional examples, such as the Holland coast near Zandvoort, the Danish town of Blokhus, and Moncofa in Spain, highlighting key spatial patterns and local variations. The second part of the chapter focuses on the exposure assessment, which integrates the combined shoreline change projections to identify areas at greatest risk.

5.1. Shoreline Change Projections

This section presents the results of probabilistic shoreline change projections across Europe, using the methods described in Sections 3.4–3.6. Shoreline change is evaluated under different climate and socioeconomic scenarios, and for multiple time horizons. The projections are used to identify areas at risk and serve as the basis for subsequent exposure and suitability assessments. The full set of projections, along with high-resolution spatial distribution maps, can be found in Appendix C.5.

5.1.1. Selection of Evaluated Scenarios

To maintain focus and avoid duplication, only a subset of the projection outputs is included in the main results. Specifically:

- The **SSP2-4.5** scenario, shown for **2050** and **2100**, serves as the reference pathway, representing moderate emissions and socioeconomic trends.
- For comparison, the **SSP5-8.5** scenario is included only for the year **2100**, representing fossil-fueled development and high emmisions
- Projections for SSP1-2.6 and intermediate years under SSP5-8.5 are provided in Appendix C.5.

This selection allows for evaluation of both gradual and extreme change trajectories, while maintaining clarity and conciseness in the results.

5.1.2. Ambient Change Projections

Ambient shoreline change represents the extrapolated continuation of historical shoreline movement based on satellite observations spanning 1984–2024. These projections are scenario-independent and reflect observed dynamics without accounting for future climate forcing.

At the European scale, the spatial pattern of ambient change becomes increasingly heterogeneous over time, with both accretion and erosion occurring along different parts of the coastline. While the overall median trend is accretive, substantial local variation is observed.

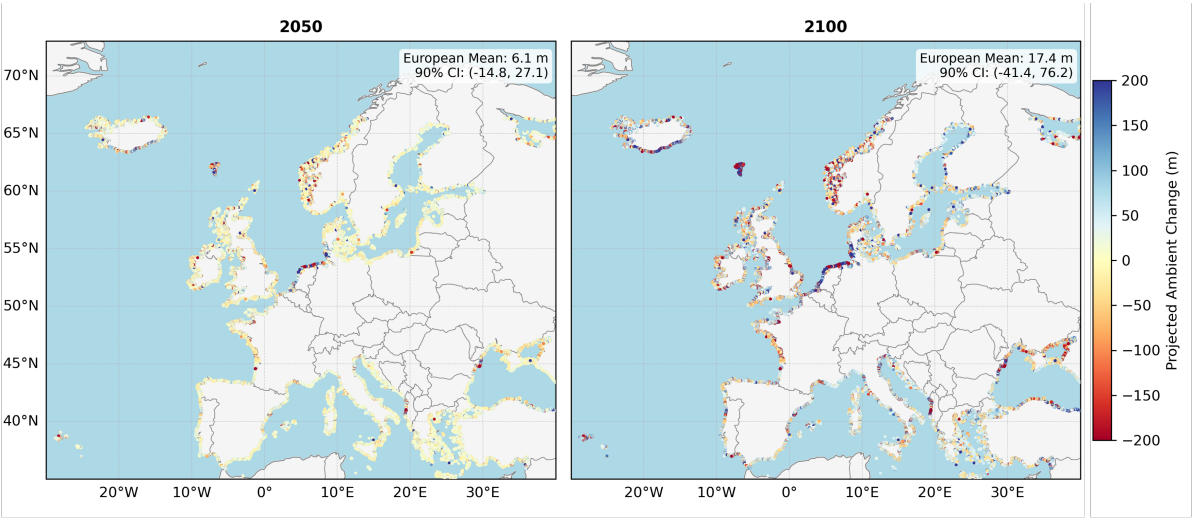

Figure 5.1: Projected ambient-induced shoreline change (p_{50}) for 2050 and 2100. Only transects with a valid historical trend (see section 3.5) are shown.

Zooming in to the regional scale, distinct patterns emerge. Along the Holland coast (from Scheveningen to Zandvoort, approximately 35 km of coastline), the projections indicate a median shoreline advance of 170 m by 2100, with a 90% confidence interval ranging from 131 m to 207 m. Although this coast is historically erosional (Mulder et al., 2011; van Rijn, 1995), the accretive signal (corresponding to a measured change rate of approximately 2 m/year over the observation period) reflects the impact of extensive nourishment activities in recent decades. These nourishments are captured in the historical trend and extrapolated forward, resulting in projected shoreline advance.

In contrast, along the Danish coast near Blokhus, where no significant interventions have occurred, the projections indicate continued erosion, with a median shoreline retreat of −23 m by 2100. Localised accretion can also be observed in parts of this stretch.

These regional examples illustrate how European-scale assessments can mask important localised patterns of erosion. Multiple erosion hotspots emerge, defined as contiguous 2.5 km segments with erosion rates exceeding 0.5 m/year. As shown in Figure 5.3, these hotspots can exhibit projected median shoreline retreat values ranging from approximately −25 m to −100 m by 2050.

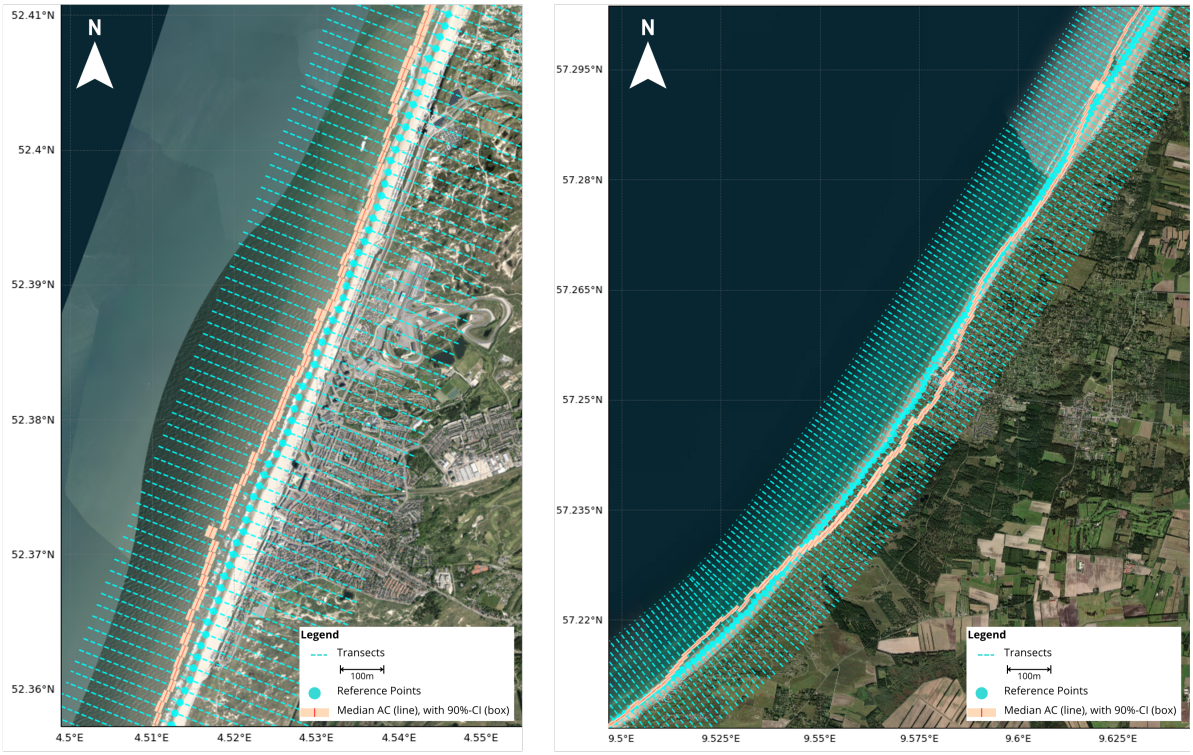

Figure 5.2: Projected ambient shoreline change by 2100 along the Holland coast (left) and near Blokhus, Denmark (right). The Holland coast shows shoreline advance due to the continuation of nourishment-driven accretion, while the Blokhus coast exhibits ongoing natural erosion in the absence of major interventions.

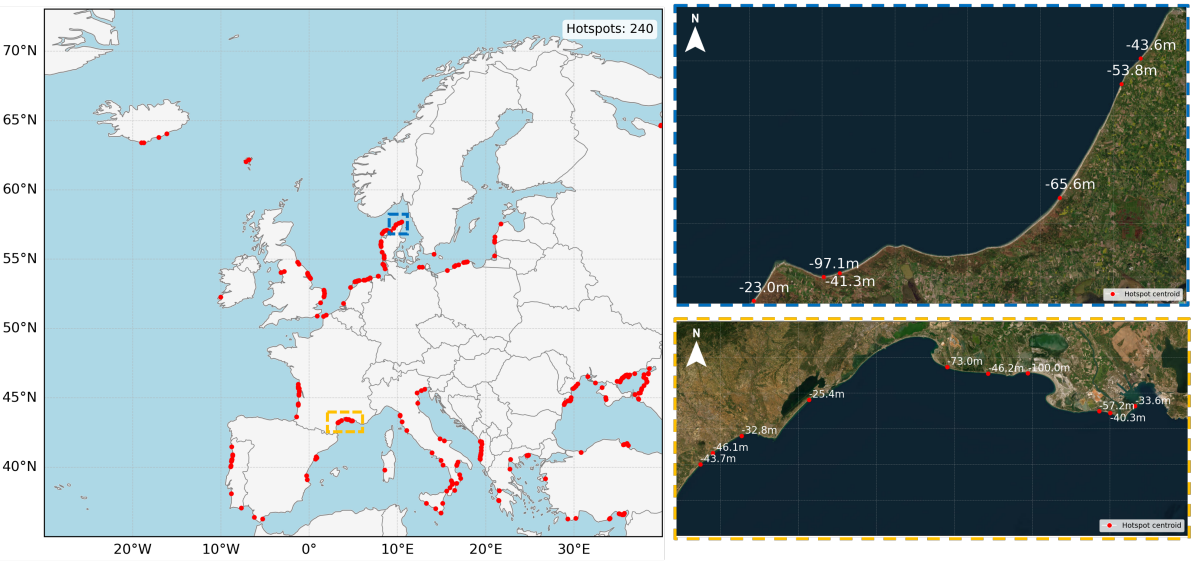

Figure 5.3: Left: Localised erosion hotspots in ambient shoreline change projections for 2050, defined as 2.5 km segments exceeding 0.5 m/year erosion. Right: Zoom-in on hotspots in Denmark (top) and France (bottom). Values correspond to the projected median shoreline retreat (m) in 2050.

Several consistent regional patterns can be observed:

- Shoreline accretion along the Dutch Holland coast, particularly between Hoek van Holland and Den Helder.
- The most severe erosion hotspots occur at inlets and barrier islands, such as in the Wadden Sea, and along the Atlantic coasts of France and Portugal.
- High erosion rates are observed at river deltas, including the Rhone (France) and Ebro (Spain) deltas.
- Localised erosion hotspots along the Mediterranean coastline.
- Increasing spatial heterogeneity and widening confidence intervals towards 2100, driven by the continued divergence of projected trends.

In summary, these patterns highlight the spatially variable nature of ambient shoreline change and underscore the importance of regional analyses in identifying areas most at risk.

5.1.3. SLR-Induced Change Projections

Sea-level rise projections were derived by applying the Bruun Rule, using local coastal slope data and sea-level projections from CMIP6 ensemble models. This approach yields a varied spatial pattern of projected shoreline retreat across Europe.

At the European scale, almost all coastlines are projected to retreat due to sea-level rise, placing increasing pressure on already unstable, erosional coasts and introducing new pressures on historically more stable stretches of shoreline. As depicted in Figure 5.4, under SSP2-4.5, median shoreline retreat increases from −18.0 m in 2050 to −45.2 m by 2100. When considering only retreating transects, the average retreat is similar, reaching −18.3 m and −46.0 m for 2050 and 2100, respectively (see Appendix C.5).

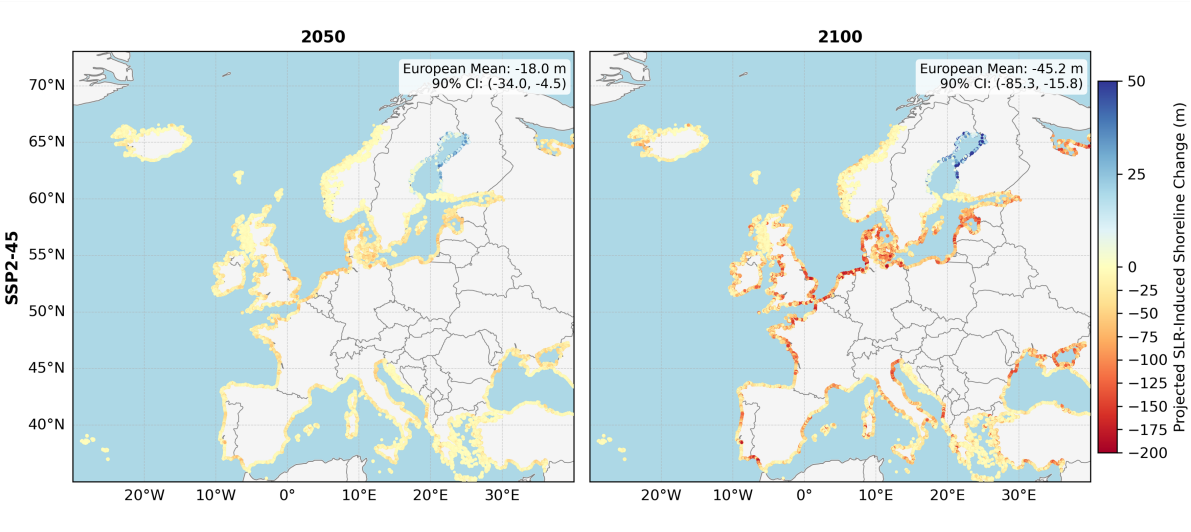

Figure 5.4: SLR-induced shoreline change (p_{50}) under SSP2-4.5 for 2050 and 2100.

Zooming in to the regional scale reveals important local contrasts between ambient and SLR-driven dynamics. For example, along the coast of Spain between Castelló de la Plana and Valencia, ambient change projections suggest accretion, with a median shoreline advance of 37 m by 2100. However, SLR-induced retreat dominates, with a median projected shoreline retreat of −73 m (90% confidence interval: −131 m to −31 m) under SSP2-4.5. Figure 5.5 illustrates part of this stretch near Moncofa, where the projections show clear SLR-driven retreat and associated confidence intervals. Even under the lowest retreat projections, infrastructure in this area is expected to become exposed.

Under the high-emissions scenario (SSP5-8.5), the magnitude of projected shoreline retreat increases substantially. The average median retreat across Europe reaches −63.1 m by 2100 (Figure 5.6).

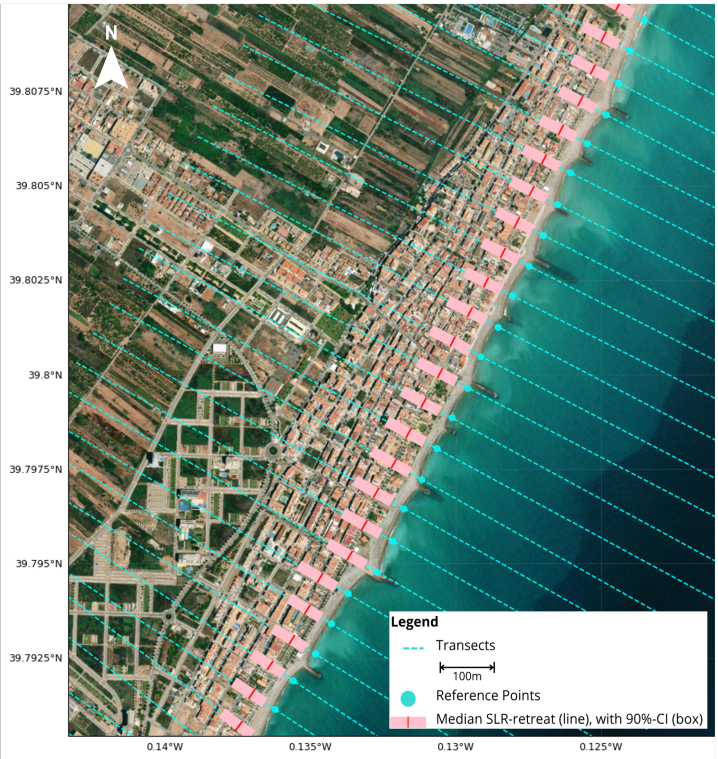

Figure 5.5: Projected SLR-induced shoreline retreat near Moncofa (Spain) under SSP2-4.5 by 2100. The figure shows median retreat values and corresponding 90% confidence intervals, highlighting areas where infrastructure is projected to become exposed.

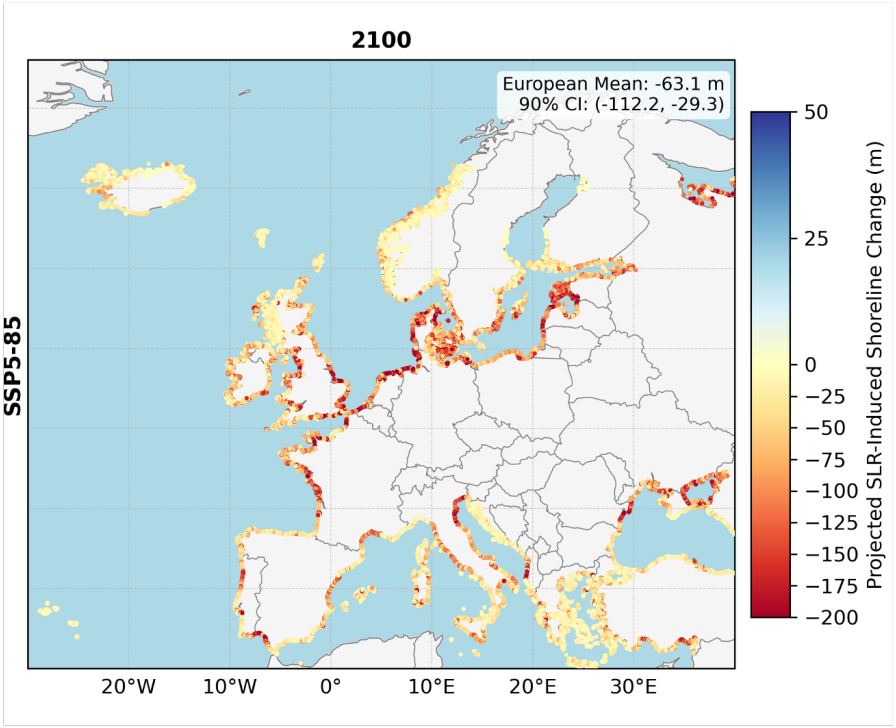

Figure 5.6: SLR-induced shoreline retreat (p_{50}) under the SSP5-8.5 scenario for 2100.

In summary, several consistent regional patterns of SLR-induced retreat can be identified:

- Greater retreat along the North Sea coasts and the southern Baltic Sea.
- Local shoreline advance in parts of northern Baltic regions, driven by relative sea-level fall due to changes in the gravitational pull.
- More localised and severe retreat along southern Spain and the southern Portuguese border.

5.1.4. Combined Shoreline Change Projections

The combined shoreline change projections integrate both ambient change and SLR-induced retreat. Where a valid ambient trend is available, the two components are combined probabilistically. Where no ambient trend could be detected, only SLR-induced retreat is used. This approach ensures a consistent and representative treatment of projected shoreline change across all transects.

At the European scale, the combined projections reveal substantial spatial variability in both retreat magnitude and uncertainty. As shown in Figure 5.7, areas with high ambient accretion partially offset SLR-induced retreat, while regions with ambient erosion experience amplified shoreline loss. The figure illustrates median projected change (p_{50}) and the width of the 90% confidence intervals under SSP2-4.5 for 2050 and 2100.

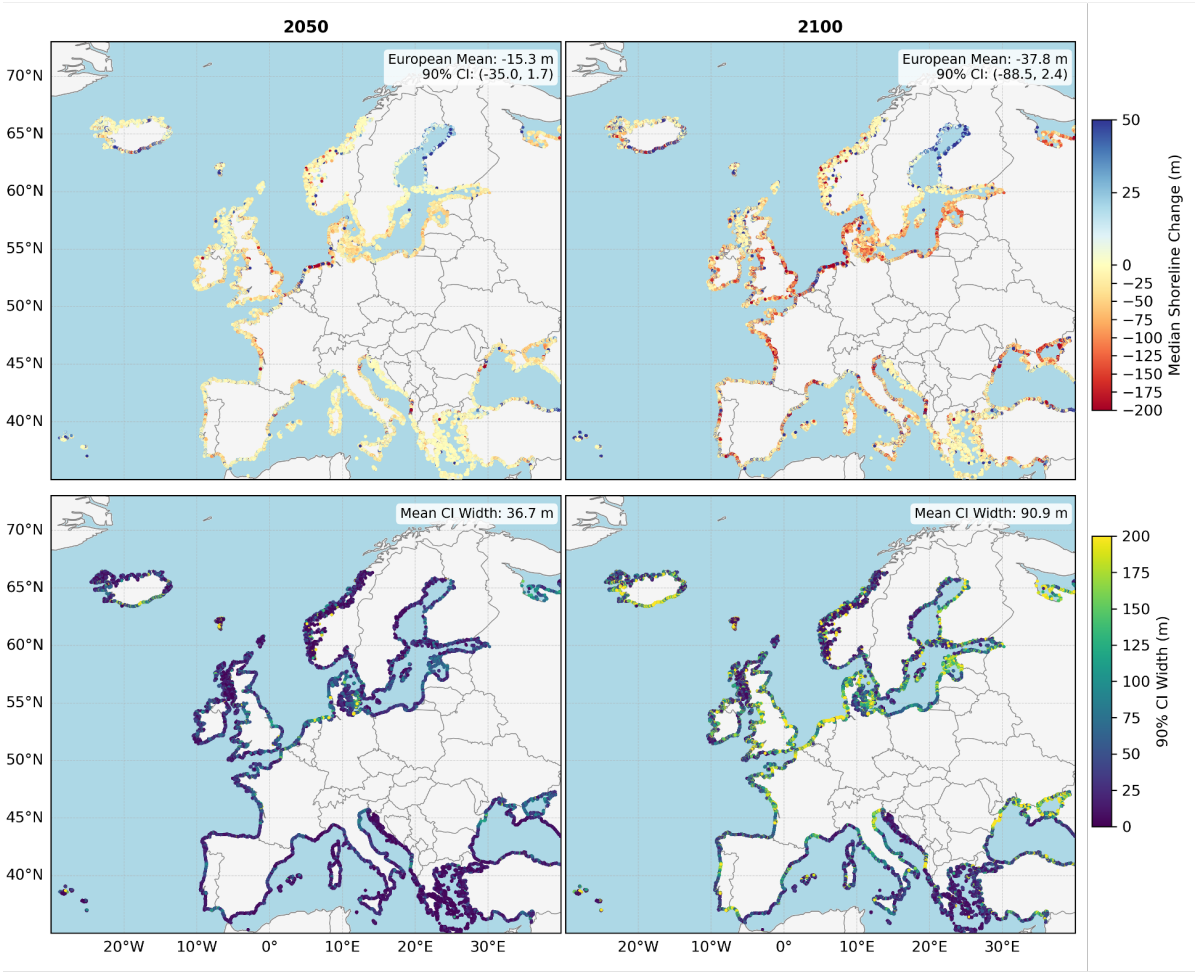

Figure 5.7: Combined shoreline change under SSP2-4.5. Top row: projected change (p_{50}) for 2050 and 2100. Bottom row: corresponding width of the 90% confidence intervals.

Zooming in to the regional scale highlights how combined projections reflect both natural processes and human interventions. Figure 5.8 presents three representative locations introduced earlier: Moncofa (Spain), Zandvoort (Netherlands), and Blokhus (Denmark). These examples illustrate different management histories and shoreline responses.

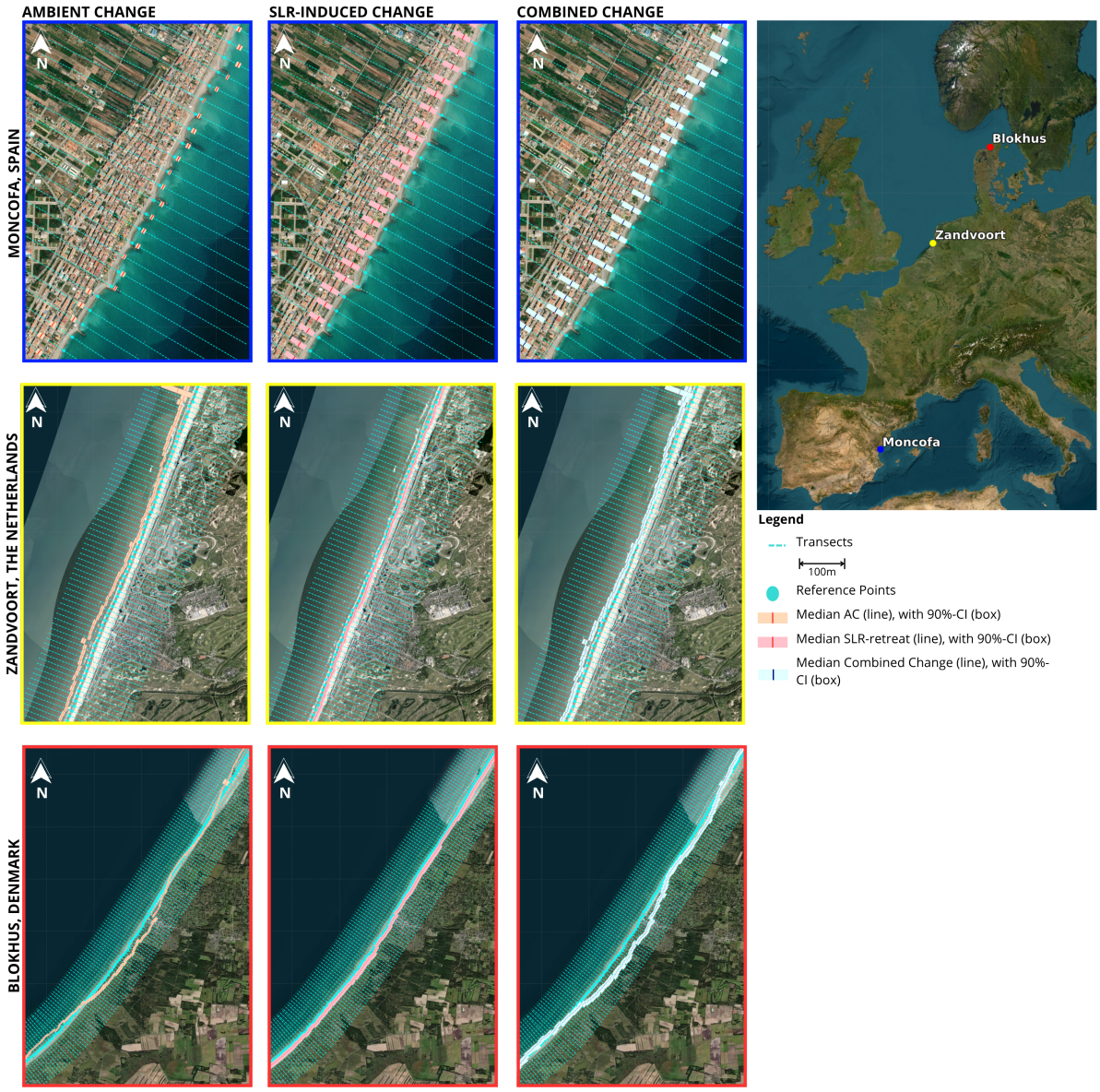

Figure 5.8: Combined shoreline change projections for three coastal sites by 2100 under SSP2-4.5. The panels show projected median ambient change (left), SLR-induced retreat (centre), and combined change (right) for Moncofa (Spain, top row), Zandvoort (Netherlands, middle row), and Blokhus (Denmark, bottom row). The map on the right indicates the location of these sites within Europe. Boxes and lines denote median projections and 90% confidence intervals.

Moncofa represents a hard-engineered shoreline, characterised by groyne fields, where localised accretion is evident in ambient trends, but SLR-induced retreat dominates overall projections. Zandvoort exemplifies a nourished coast, where sustained interventions have so far offset SLR impacts, although maintaining this resilience will require continued nourishment at a scale comparable to that of the past 70 years. Blokhus illustrates a naturally eroding coastline, where retreat is projected to intensify further under rising sea levels in the absence of interventions.

By 2100, several general patterns emerge:

- Areas with greater projected retreat often correspond to wider confidence intervals, reflecting higher uncertainty.
- The combined spatial pattern strongly resembles that of ambient change in regions with strong ambient trends.
- Average shoreline change values are slightly lower than pure SLR projections due to the contribution of accretive ambient trends.

Northern Europe, particularly along the North Sea, Baltic Sea, and Atlantic coasts, shows larger retreat values and broader confidence intervals compared to southern regions. In contrast, the Mediterranean coastline generally exhibits lower retreat rates and narrower uncertainty bounds.

Under the high-emissions scenario (SSP5-8.5), both retreat magnitudes and associated uncertainties increase further (Figure 5.9). The figure illustrates median retreat and confidence interval width for retreating transects. Full results for all scenarios and time horizons are provided in Appendix C.5.

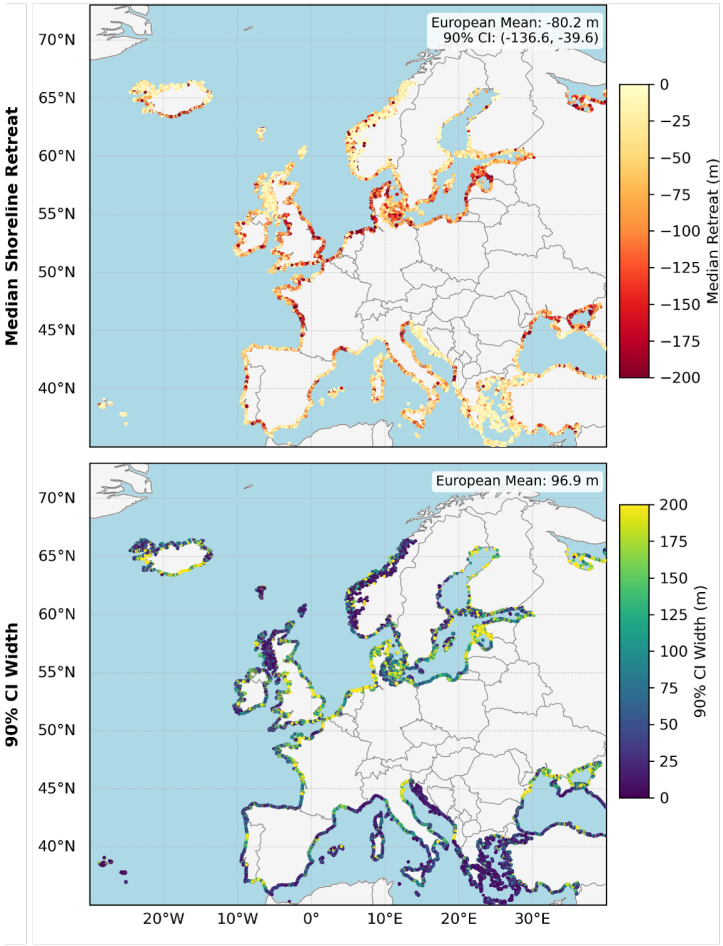

Figure 5.9: Projected shoreline retreat under SSP5-8.5 by 2100. Top row: median combined shoreline retreat (p_{50}). Bottom row: corresponding width of the 90% confidence interval. Only retreating transects are shown.

Data Summary Shoreline Projections

Table 5.1 provides an overview of the transect inventory and projected shoreline change under different model components and emission scenarios. It includes the total number of transects, the subset with valid ambient and/or SLR data, and the number and length of transects projected to be eroding under each scenario. The summary is structured to distinguish between ambient-only, SLR-only, and combined shoreline change projections across time and scenario levels.

Table 5.1: Summary of Coastal Transects and Projected Shoreline Change by Scenario

Description	SSP	Year	No. of Transects	Coastline Length (km)	Percentage
General Inventory					
Transects in Europe (GCTR)	-	-	1,388,990	138,899	-
Of which sandy transects	-	-	412,818	41,282	29.7%
Sandy transects with SLR	-	-	283,479	28,348	68.7%
Sandy transects with AC	-	-	377,208	37,721	91.4%
Stable / Unstable	-	-	*235,836 / 141,372*	*23,584 / 14,137*	*62.5%/ 37.5%*
Sandy transects with AC and SLR	-	-	274,517	27,452	66.5%
Ambient Change Only					
Unstable eroding coast	-	-	58,300	5,830	41.2%
SLR-Induced Change Only					
Eroding coast	1–2.6	2030	279,436	27,944	98.6%
Eroding coast	1–2.6	2050	279,143	27,914	98.5%
Eroding coast	1–2.6	2100	279,026	27,903	98.4%
Eroding coast	2–4.5	2030	279,042	27,904	98.4%
Eroding coast	2–4.5	2050	279,790	27,979	98.7%
Eroding coast	2–4.5	2100	280,160	28,016	98.8%
Eroding coast	5–8.5	2030	279,159	27,916	98.5%
Eroding coast	5–8.5	2050	279,537	27,954	98.6%
Eroding coast	5–8.5	2100	280,693	28,069	99.0%
Combined AC + SLR-Induced Change					
Eroding coast	1–2.6	2030	244,942	24,494	89.2%
Eroding coast	1–2.6	2050	231,192	23,119	84.2%
Eroding coast	1–2.6	2100	224,857	22,486	81.9%
Eroding coast	2–4.5	2030	245,347	24,535	89.4%
Eroding coast	2–4.5	2050	233,279	23,328	85.0%
Eroding coast	2–4.5	2100	230,976	23,098	84.1%
Eroding coast	5–8.5	2030	245,480	24,548	89.4%
Eroding coast	5–8.5	2050	235,626	23,563	85.8%
Eroding coast	5–8.5	2100	238,348	23,835	86.8%

5.2. Identification of High-Risk Beaches

This section identifies high-risk beaches based on the median projected shoreline retreat under selected climate scenarios. The analysis builds on the shoreline projections described earlier, using outputs from the SSP2-4.5 scenario for the years 2050 and 2100, and from the high-emission SSP5-8.5 scenario for 2100. Shoreline change is projected relative to a fixed reference point per transect, as detailed in subsection 3.7.2.

To evaluate exposure, either the projected shoreline change can be directly referenced to the transect's fixed point, or an additional accommodation buffer can be applied. This buffer represents the minimum beach width required between the shoreline and the first line of infrastructure. Following Lansu et al. (2024), a representative value of 70 m is used to reflect conditions in densely populated coastal areas

of the Northern Hemisphere. For comparison, a 0 m buffer is also applied to illustrate direct exposure under the projected shoreline position. These two values (0 m and 70 m) are used consistently across the European-scale assessment.

In practice, the appropriate accommodation buffer may vary depending on national coastal policies. For example, in Portugal, the first 50 m of coastal land is state-owned and subject to public easement, providing a policy-relevant buffer for shoreline management (Pinto et al., 2020). Such regional distinctions are considered in localized analyses (see chapter 6).

Hotspots are defined as coastal segments with at least 10 consecutive transects (equivalent to a minimum of 1 km) where the projected shoreline position, including any buffer, intersects with built infrastructure. These serve as a proxy for high-risk beaches with exposure along continuous stretches. This approach promotes spatial consistency and filters out isolated retreat points.

5.2.1. Quantification of Exposure

Table 5.2 provides an overview of high-risk beach segments (hotspots) across scenarios, years, and accommodation buffer assumptions. The table summarizes the number of identified hotspots, their mean length, the total length of exposed transects (including all intersected transects regardless of hotspot status), and the proportion of eroding transects with intersecting buildings.

Without accommodation buffers, relatively few hotspots are identified. For example, under SSP2-4.5 in 2050, only 10 discrete hotspots emerge, with a mean length of 1,210 m and a total exposed length of 406 km (1.7% of all eroding transects). Applying a 70 m buffer substantially increases both the number and length of high-risk segments, yielding 506 hotspots, a mean length of 1,653 m, and 2,719 km exposed (11.6% of eroding transects). This demonstrates that the extent of high-risk beaches is more sensitive to accommodation assumptions than to emissions scenario or time horizon.

By 2100, this pattern intensifies. Under SSP2-4.5, a buffer of 70 m results in 731 hotspots spanning 3,321 km and covering 14.4% of eroding transects. Similarly, SSP5-8.5 produces 841 hotspots and 3,690 km of exposed length (15.5%).

The ten most critical hotspots in terms of direct, near-term exposure (under SSP2-4.5, 2050, no buffer) include Storekongsmark (Denmark); Wissant and Hameau du Nord (France); Isola del Lido (Venice, Italy); Alcúdia (Mallorca) and Casablanca (Spain); and Bexhill-on-Sea, Bridlington, Llandudno, and Sheerness (United Kingdom). Some of these are densely populated, tourist-dependent areas, while others are smaller coastal towns.

Table 5.2: Overview of high-risk beach hotspots under different SSP scenarios, years, and accommodation buffer assumptions. **Mean length** refers only to hotspot segments; **total exposed length** includes all transects intersecting buildings within the buffer zone.

SSP	Year	Buffer (m)	No. of Hotspots	Mean Length per Hotspot (m)	Total Length of Exposed Transects (km)	% of Eroding Transects with Buildings
2–4.5	2050	0	10	1,210	406	1.7%
2–4.5	2050	70	506	1,653	2,719	11.6%
2–4.5	2100	0	164	1,543	1,295	5.6%
2–4.5	2100	70	731	1,707	3,321	14.4%
5–8.5	2100	0	263	1,617	1,760	7.4%
5–8.5	2100	70	841	1,780	3,690	15.5%

5.2.2. Spatial Distribution of High-Risk Beaches

Figure 5.10 illustrates the spatial distribution of high-risk beaches under SSP2-4.5 in 2050 and SSP5-8.5 in 2100, both assuming a 70 m accommodation buffer. Red markers indicate hotspot locations, with brighter areas reflecting regions of denser clustering of high-risk transects. Nourishment sites (plotted in yellow) are overlaid to provide spatial context regarding existing coastal intervention measures. These nourishment locations help identify where previous management efforts may have reduced exposure

or where protective measures coincide with high-risk zones. This highlights areas where sustained or enhanced interventions could be critical to mitigating future risk.

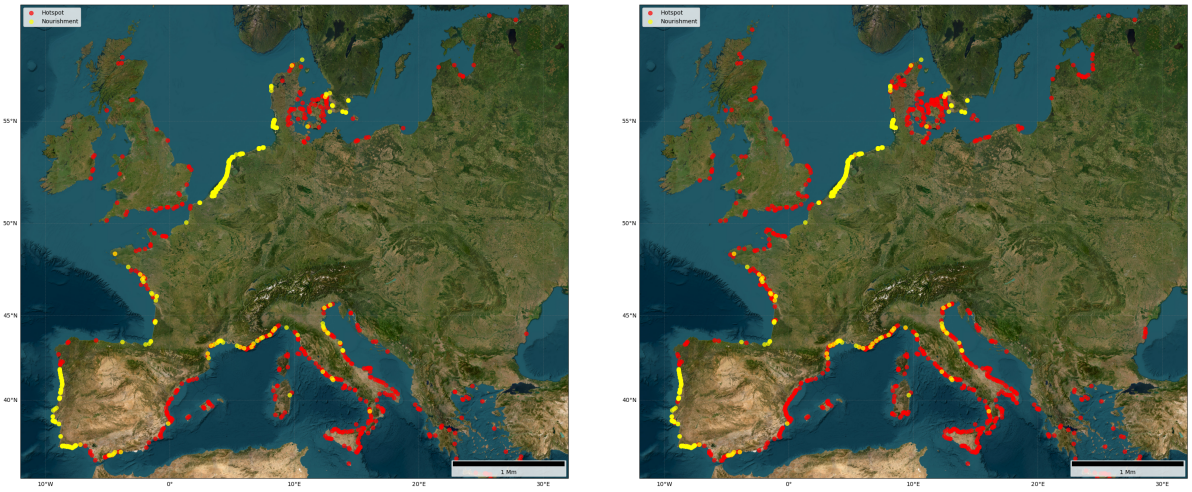

(a) SSP2-4.5, 2050, with 70 m buffer

(b) SSP5-8.5, 2100, with 70 m buffer

Figure 5.10: Spatial distribution of high-risk beaches (hotspots) under two scenarios, SSP2-4.5 in 2050 and SSP5-8.5 in 2100, both with 70 m accommodation space. Red markers represent hotspot centroids; yellow markers indicate nourishment locations. Densely clustered red points highlight areas of concentrated exposure risk.

6

Synthesis and Application

Overview

By combining shoreline retreat projections, exposure analysis, and a structured suitability framework, this chapter demonstrates how the NSAM supports context-specific adaptation planning at high-risk beaches across Europe.

NSAM: Traffic Light Classification

- Evaluates **nourishment suitability** based on four key factors:
  - Coastal type
  - Coastal policy
  - Sediment availability
  - Knowledge & experience
- Uses a factor-specific **traffic light system** to reflect **alignment** with conditions at **historically nourished sites**
- Provides **first-order screening** to prioritise high-risk beaches for detailed feasibility studies

Evaluation of the Showcases

- **Three** showcases illustrate different **planning horizons**, **scenarios**, and **governance contexts**
- 3 show cases are evaluated:
  - **Storekongsmark, Denmark:** Physical and institutional barriers despite technical capacity
  - **Islantilla, Spain:** Favourable morphology but fragmented governance and uncertain sediment sources
  - **Bacton, UK:** Strong alignment of conditions and strategic value enabling large-scale nourishment
- Shows how the NSAM informs **site-specific adaptation** strategies for **different climate scenarios**

This chapter synthesises findings on projected shoreline retreat, exposure of built environments, and historical nourishment practices to evaluate beach nourishment as a potential adaptation strategy. It demonstrates the potential of a first-order suitability analysis using the Nourishment Suitability Assessment Model. The model provides a structured, empirical framework for evaluating the nourishment suitability of high-risk beaches, based on physical, institutional, and practical criteria. The location of these high-risk beaches is determined through the shoreline projections and exposure analysis (chapter 5).

6.1. Operationalising the NSAM: Traffic Light Classification

Building on the key suitability factors identified in section 4.3, this section presents the full NSAM as a first-order classification tool for coastal nourishment suitability. The model draws on empirical patterns in historical practice and contextual enabling conditions.

The NSAM evaluates four core factors:

- **Coastal Type:** Physical characteristics, such as sandy sediment plains or dune-backed systems.
- **Coastal Policy:** National or regional programmes supporting nourishment interventions.
- **Sediment Availability:** Access to borrow areas, including offshore sources and inlets or channels.
- **Knowledge and Experience:** Institutional capacity and history of successful implementation.

Each factor is assessed independently using historical nourishment records, geospatial indicators, and policy review. A traffic light classification reflects how closely local conditions align with those of historically nourished sites:

- **Green – High suitability:** Strong alignment with historical nourishment contexts. For example, green for sediment availability indicates validated, accessible sources.
- **Orange – Moderate or uncertain suitability:** Partial alignment or context-dependent suitability, reflecting data gaps, variable conditions, or the need for further feasibility assessment.
- **Red – Low suitability:** The enabling condition is absent or weakly represented in the local context. This signals that one of the key enabling conditions is not met rather than infeasibility.

This factor-specific traffic light system provides a transparent, structured first-order indication to identify sites with the most suitable conditions for nourishment. It is not a substitute for detailed feasibility studies, but rather a tool to prioritise where such studies may be most warranted. The NSAM is visualised in Figure 6.1, with detailed descriptions for each factor and classification.

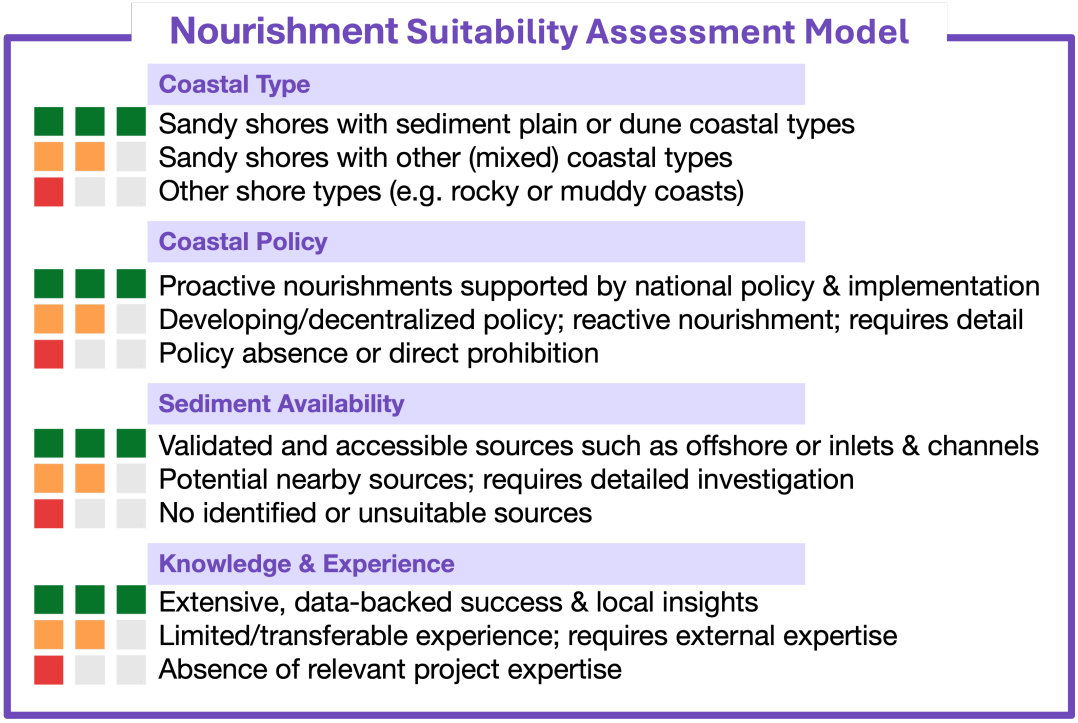

Figure 6.1: Factor-specific traffic light classification used in the Nourishment Suitability Assessment Model. Each key factor is evaluated independently based on empirical patterns in historical nourishment practice.

6.2. Evaluation of the Showcases

To demonstrate the application of the NSAM, this chapter presents three regional showcases that reflect diverse physical settings, policy contexts, and coastal management approaches. Each combines local shoreline retreat projections with suitability factors to explore if, how, and where nourishment could serve as an adaptation strategy under contrasting futures.

The cases span different planning horizons, climate scenarios, and accommodation space assumptions, highlighting that nourishment strategies must align with local conditions, objectives, and scenario choices:

1. A near-term exposure scenario in Denmark — SSP2-4.5 in 2050 with 0 m accommodation space;
2. A moderate, long-term planning scenario in Spain — SSP2-4.5 in 2100 with 50 m accommodation space;

3. A high-impact scenario in the United Kingdom — SSP5-8.5 in 2100 with 100 m accommodation space.

The selected sites, Storekongsmark (Denmark), Islantilla (Spain), and Bacton (United Kingdom), illustrate how the NSAM supports context-specific planning and helps coastal managers assess where nourishment may offer a viable adaptation response. Each case combines projected shoreline change with a step-by-step application of the suitability framework.

6.2.1. Showcase 1: Storekongsmark, Denmark

This first showcase examines Storekongsmark, a 1.4 km shoreline with buildings close to the coast, under SSP2-4.5 in 2050 assuming no inland accommodation space. Identified as one of Europe's 10 high-risk beaches facing near-term exposure, the site highlights the need not only to locate critical areas but also to apply tools like the NSAM to quickly assess potential adaptation options. As shown in Figure 6.2, critical infrastructure lies in close proximity to the projected retreat zone, underscoring the urgency of effective intervention.

Figure 6.2: Storekongsmark, Denmark: Local exposure and transect analysis under SSP2-4.5 (2050) without accommodation space. Left: Exposed built environment and projection lines. Right: Location within the European hotspot map for this scenario.

Suitability Assessment

Coastal type ■■

The transects are sandy with mixed morphology, classified as sediment plain and partly cliffed or steep (GCTR). While sandy stretches may be suitable for nourishment, the cliffed sections pose technical and environmental challenges, requiring local feasibility assessments.

Coastal policy ■■

Denmark applies a mixed governance model. The Danish Coastal Authority (DCA) offers national guidance and technical expertise, but implementation responsibility rests with municipalities and private landowners (Danish Coastal Authority, 2019). This decentralised structure results in only moderate policy support for nourishment, as decisions depend on local prioritisation and funding (Bontje et al., 2016).

Sediment availability ■■■
Offshore sediment sources are well-documented and regularly monitored, providing reliable material for nourishment (Staudt et al., 2021).

Knowledge and experience ■■■
Denmark has significant institutional capacity, with nourishment projects and monitoring dating back to the 1980s.

In summary, while sediment availability, technical capacity, and institutional knowledge are favourable, geomorphological constraints and decentralised governance reduce overall suitability for nourishment at Storekongsmark. This case illustrates how even well-resourced settings can face physical and institutional barriers to implementing nourishment.

6.2.2. Showcase 2: Islantilla, Spain

This second showcase focuses on Islantilla, a 5 km shoreline along Spain's Huelva coast, under SSP2-4.5 in 2100 with 50 m accommodation space. As a tourism-dependent resort town, beach preservation is economically critical, with wide beaches forming a key asset for the local economy. The site currently lacks substantial erosion control structures, aside from small groynes in nearby areas, providing an opportunity to evaluate the potential of nourishment in a relatively unmodified setting. As shown in Figure 6.3, future retreat highlights the need for proactive adaptation planning.

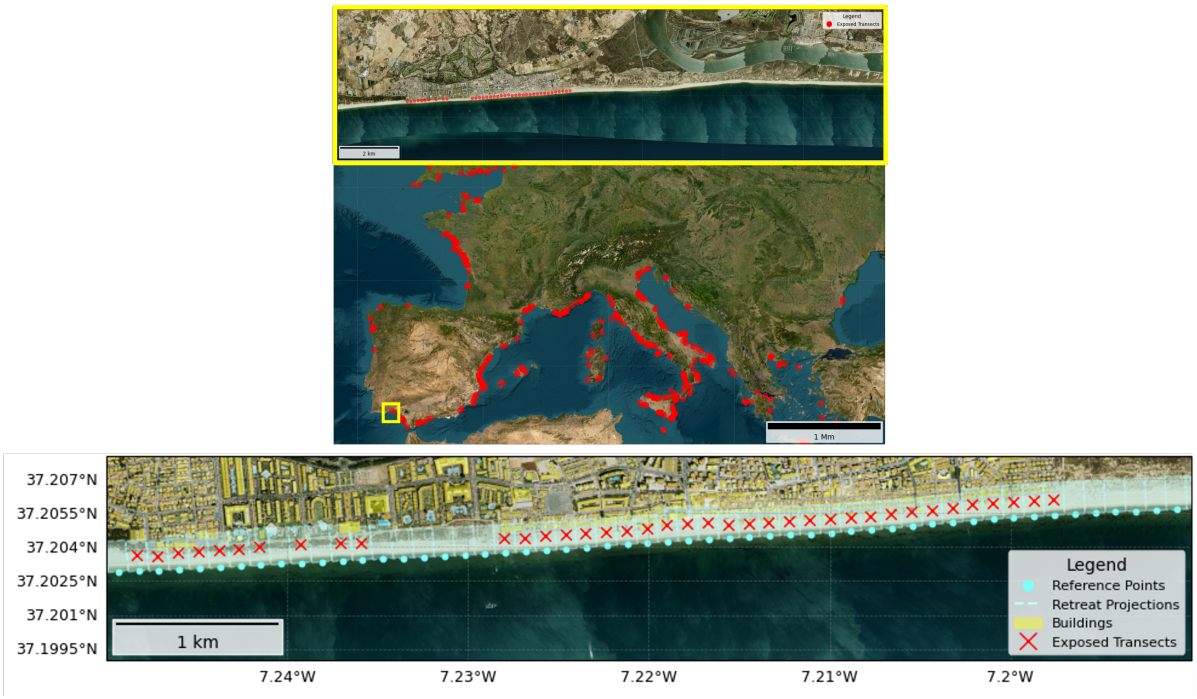

Figure 6.3: Islantilla, Spain: Local exposure and transect analysis under SSP2-4.5 (2100) with 50 m accommodation space. Left: Exposed built environment and projection lines. Right: Location within the European hotspot map for this scenario.

Suitability Assessment

Coastal type ■■■
The site consists of sediment plains backed by dune systems, as classified in the GCTR dataset, offering good physical suitability for nourishment.

Coastal policy ■■
Spain's national coastal management framework is defined by the Coastal Act, overseen by the Ministry for the Ecological Transition and Demographic Challenge (MITECO). While national policy recognises nourishment as a soft defence option, implementation is largely decentralised, with regional and local

authorities responsible for project delivery. This often results in reactive, tourism-driven interventions rather than long-term risk reduction, as no dedicated national funding stream exists for systematic beach nourishment (MITECO, 2022).

Sediment availability ■■
Potential sources include maintenance dredging from the Rio Piedras inlet; however, no confirmed offshore borrow areas exist near Islantilla, limiting the suitability of nourishment without further investigation.

Knowledge and experience ■■
Spain has experience with nourishment in high-tourism areas, but long-term monitoring and integration into structured adaptation plans remain limited (Staudt et al., 2021).

In summary, Islantilla combines favourable geomorphological conditions with economic incentives for beach preservation. However, fragmented governance, uncertain sediment sources, and a reactive policy environment limit readiness for large-scale, sustained nourishment as part of a proactive adaptation strategy.

6.2.3. Showcase 3: Bacton, United Kingdom

This showcase examines Bacton on the Norfolk coast under SSP5-8.5 in 2100 with 100 m accommodation space. The site spans over 5 km of coastline, where erosion poses a direct threat to residential areas and infrastructure south of the gas terminal, as visualised in Figure 6.4. The orange dashed circle marks the location of the gas terminal.

This case illustrates how UK coastal policy targets national protection efforts where the value of at-risk assets justifies major investment. The 2019 Bacton Sandscaping project was a major beach nourishment intervention aimed at safeguarding the gas terminal from coastal erosion, while also providing protection to the nearby communities of Bacton and Walcott (Borsje et al., 2024).

Importantly, the exposure assessment does not flag transects at the gas terminal as high risk, likely because the sandscaping project has influenced the historical signal and offset SLR projections. This underscores the importance of accounting for past adaptation efforts when identifying high-risk beaches.

The scenario is particularly illustrative under a high fossil-fuel future, where safeguarding critical energy infrastructure remains a strategic priority.

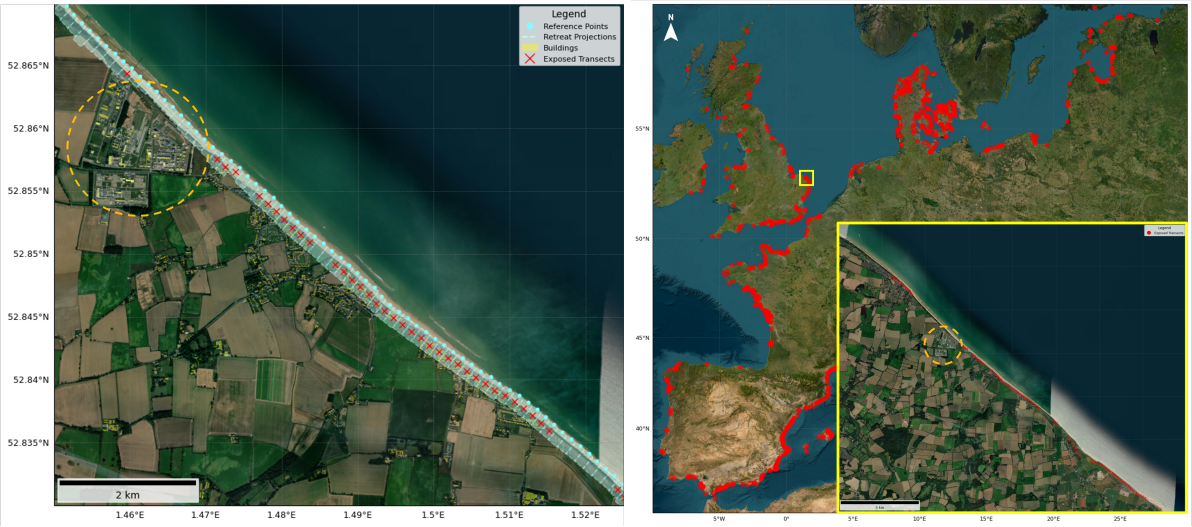

Figure 6.4: Bacton, UK: Local exposure and transect analysis under SSP5-8.5 (2100) with 100 m accommodation space. Left: Exposed built environment and projection lines. Right: Location within the European hotspot map. The orange dotted line marks the Bacton gas terminal.

Suitability Assessment

Coastal type ■■■

The site features sediment plains, dune-backed stretches, and some moderate sloped coastal types, highly suitable for nourishment.

Coastal policy ■■■

Strong national policy support exists through Shoreline Management Plans, which define objectives for each coastal cell. The Bacton gas terminal is a priority site, supported by both local authorities and national agencies (Environment Agency, 2020).

Sediment availability ■■■

The 2019 project confirms the presence of established offshore borrow areas with suitable sediment characteristics and demonstrates the feasibility of large-scale sediment placement (Borsje et al., 2024).

Knowledge and experience ■■■

The UK has extensive nourishment experience dating back to the 1950s (Hanson et al., 2002), with the Bacton Sandscaping project now serving as a reference for innovative, large-scale interventions.

In summary, Bacton exemplifies a highly suitable site for nourishment, where favourable physical conditions combine with the presence of a critical economic asset to justify major intervention. Here, geomorphology, governance, sediment access, and institutional capacity align to support long-term adaptation within the UK's targeted coastal protection framework.

7

Discussion

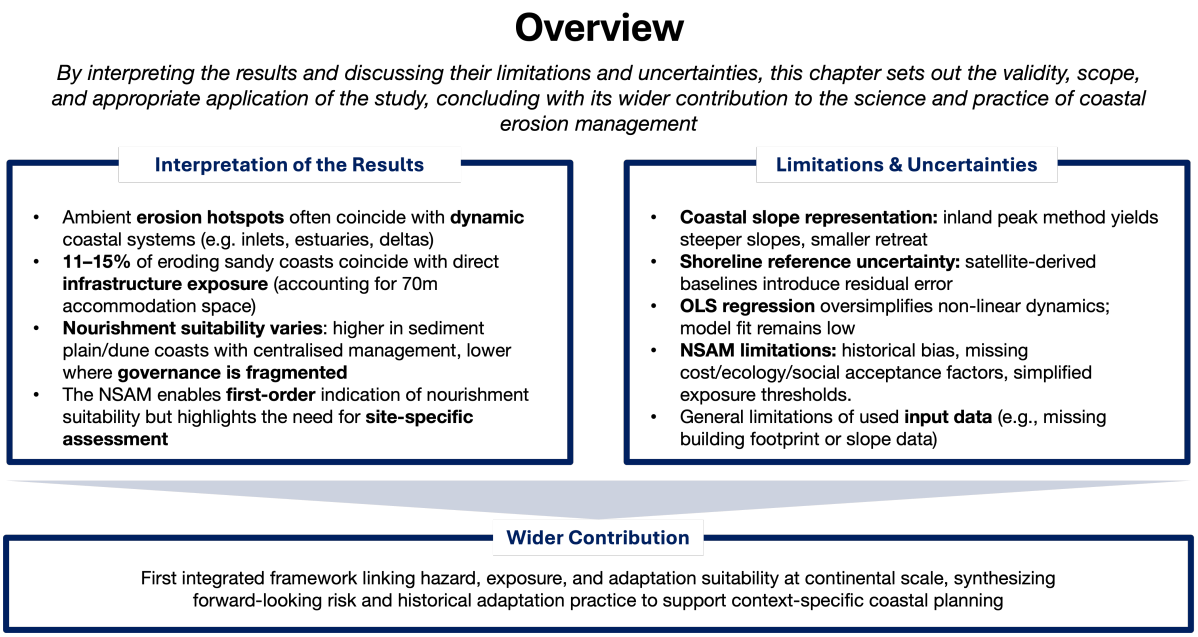

This chapter reflects on the main findings of the study by interpreting the projected shoreline changes, assessing patterns of exposure, and evaluating the suitability of beach nourishment as an adaptation measure. It compares outcomes with existing literature, critically reviews methodological choices, and highlights key limitations. Finally, it considers the implications of these results for coastal adaptation planning and outlines the wider contribution to research and policy.

7.1. Interpretation of the Results

This section provides an interpretation of the findings presented in chapter 4 and chapter 5. It begins by examining the projected shoreline changes, followed by an assessment of the identified exposure, and concludes with a discussion on the suitability of beach nourishment as an adaptation strategy.

7.1.1. Shoreline Change Projections: Patterns and Drivers

Ambient Shoreline Change Model results indicate that, under current ambient trends, the European coastline is, on average, accreting, with a median change of 6.1 m by 2050 and 17.4 m by 2100. However, this continental-scale signal masks substantial local variability. Erosion hotspots are observed along the Atlantic coast of France and Portugal, in the North Sea from the Wadden Sea area up to

Denmark, and across parts of the Mediterranean, particularly between Marseille and Béziers (France). This pattern reflects the spatially heterogeneous nature of historical coastal change across Europe.

A closer inspection reveals that many of these erosion hotspots are near coastal inlets, estuaries, and deltas, such as the Rhône (France), Ebro (Spain), Vlieland-Terschelling inlet (Netherlands), and Gironde estuary (France). Erosive trends in these settings are primarily driven by the dynamic nature of these coastal systems. The detection method applied in this study identifies such areas as dynamic, serving as an indicator of variable shoreline behaviour. However, because of their inherent variability, these systems are not well represented by the linear regression model used to detect and extrapolate long-term trends. This leads to relatively high residual errors, as discussed further in subsection 7.2.2 (Antolínez et al., 2016).

When comparing the identified erosion hotspots with those reported by Luijendijk et al. (2018), who define hotspots as contiguous sandy shoreline segments of at least 5 km, comparable results are found (e.g., Nebel Island, Germany; Esbjerg, Denmark; Venice, Italy). In addition, the use of a shorter minimum segment length of 2.5 km resulted in the identification of a greater number of hotspots. This choice improves spatial resolution for continental-scale analysis compared to global-scale studies and enables the detection of smaller, locally significant erosion features, such as those near Aveiro (Portugal) or along the southern coast of Italy.

In contrast, the persistent accretion signal observed along the Dutch coast is likely the result of long-standing beach nourishment practices. As described by Armstrong and Lazarus (2019), similar trends along the U.S. Atlantic coast have been linked to extensive nourishment activity, which can mask underlying erosional patterns. In the Netherlands, regular nourishments have been carried out to maintain the coastline at its 1990 position (Lodder & Slinger, 2022). This long-term intervention masks natural long-term trends, and an accretive signal is detected by the model, illustrating the model's sensitivity to anthropogenic influences. These findings emphasize the importance of interpreting ambient trends within the context of historical coastal management. The nourishment database developed in this study may serve as a valuable resource for identifying and adjusting for such human-driven trends in future analyses (for example, see Figure 5.10).

Other human activities, such as reduced sediment supply from river damming, large-scale land reclamation, and the construction of hard structures that constrain natural dynamics, can also mask natural shoreline trends. While these factors were not examined in detail here, they represent important considerations for future research. It is also important to note that ambient shoreline change reflects part of the sediment balance along the coast, where erosion in one location can contribute to accretion elsewhere, particularly in areas influenced by anthropogenic interventions. This redistribution helps explain why the median European signal shows net accretion despite the presence of local erosion hotspots. However, not all eroded sediment contributes to visible accretion alongshore; some may be transported offshore beyond the depth of closure, where it is effectively lost from the active coastal profile. The extent to which the observed accretion signal reflects natural sediment dynamics, as opposed to the influence of nourishments or other human interventions, cannot be determined with certainty in this study. A detailed assessment of sediment pathways was beyond the scope of this thesis but represents an important direction for future research.

Sea-Level Rise-Induced Shoreline Change When sea-level rise is considered in isolation, nearly all sandy coastlines across Europe are projected to experience net erosion by the end of the century. Over 98% of transects show shoreline retreat across all projection years and emission scenarios. The remaining transects, located in the northern part of the Baltic Sea, experience a relative fall in sea level due to changes in gravitational pull following ice cap melt (Weisse et al., 2021). The physical processes underlying this phenomenon are outside the scope of this study, which focuses on the mitigation of coastal erosion.

Under SSP2-4.5, the 90% confidence interval of projected shoreline change ranges from −34.0 m to −4.5 m by mid-century, and from −85.3 m to −15.8 m by 2100. Under SSP5-8.5, projections range from −36.5 m to −5.6 m at mid-century, and from −111.6 m to −28.5 m by 2100. These projections are consistent with previous large-scale modelling efforts, such as those by Vousdoukas et al. (2020) and Athanasiou et al. (2020), although median values for Europe are slightly lower in this study. For

example, the median projected SLR-induced shoreline retreat is −45.2 m under SSP2-4.5 and −62.5 m under SSP5-8.5, compared to −54 m and −97 m in 2100, respectively, reported by Athanasiou et al. (2020).

This difference is likely due to methodological choices, particularly the use of a steeper coastal slope in this study as opposed to the nearshore slope commonly applied in previous models. The implications of slope definition are discussed further in subsection 7.2.1.

Combined Shoreline Change When ambient and SLR-induced shoreline change are combined, the European median becomes slightly more erosive compared to the SLR-only scenario. These projections are generated through Monte Carlo sampling, which captures the additive effects of both components and their respective uncertainties. This indicates that while ambient trends can be locally accretive, they are generally insufficient to counteract the dominant erosive influence of sea-level rise.

An interesting outcome is that, although the median shoreline retreat intensifies over time, the number of eroding transects decreases. This is primarily due to processes in the northern Baltic region, where falling sea level, driven by changes in gravitational pull from melting ice caps, and vertical land uplift from glacial isostatic adjustment act together to offset sea-level rise. As a result, more transects in this region shift from projected erosion to accretion over time. Whether these processes should be treated as fully independent is discussed further in subsection 7.2.2.

A related observation is that the combined median shoreline retreat increases significantly when focusing solely on transects projected to erode. While the Europe-wide median retreat under SSP5-8.5 in 2100 is −55.0 m when considering all transects, this value deepens to −80.2 m when calculated for eroding transects only. This difference reflects compensation from accretive ambient changes in certain regions, which partially offsets the overall retreat signal when all transects are included.

In areas with unstable ambient trends (e.g., dynamic coasts), such as parts of the Holland coast, the 90% confidence interval for total shoreline change widens. This is particularly evident where ambient accretion and SLR-induced retreat oppose each other, increasing projection variance. Since ambient change is only included when historical shoreline movement exceeds 15 m, it often reflects larger and more uncertain extrapolations.

The overall CI width arises from the interaction of ambient and SLR-induced components. Ambient trend uncertainty is modelled as a normal distribution based on regression residuals, while SLR-induced change is sampled from 100 CMIP6 ensemble members. Figure 7.1 illustrates this for a transect along the Holland coast under SSP2-4.5, where opposing trends contribute to a wider combined distribution. This highlights the need to account for both directional trends and uncertainty ranges when interpreting model outputs.

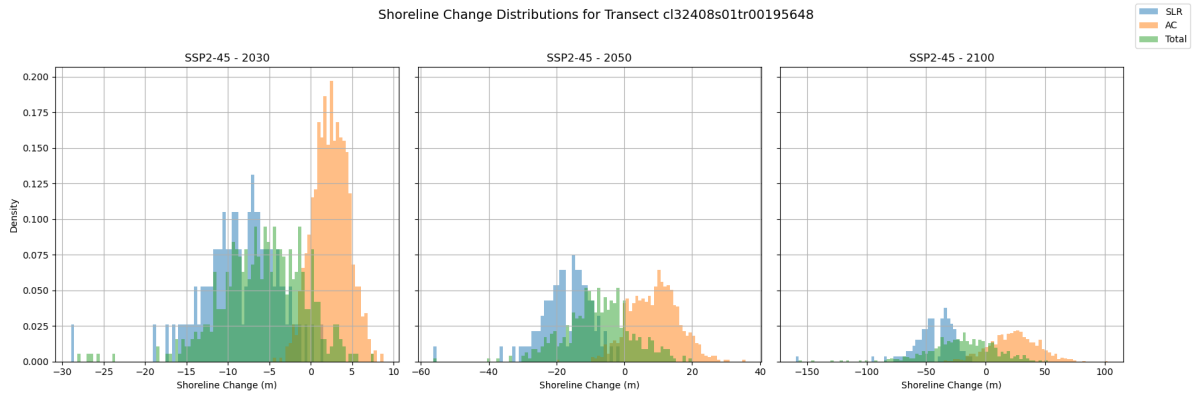

Figure 7.1: Distribution of shoreline change components for an accreting transect along the Holland coast under SSP2-4.5 at three time steps (2030, 2050, 2100). SLR-induced change (blue), ambient trend (orange), and their combined effect (green) are shown. Opposing trends contribute to a wider total distribution.

To further illustrate the variability at finer spatial scales, the zoomed-in combined shoreline change projections for three coastal sites (Figure 5.8) illustrate that transect-level projections can diverge

from the broader regional signal. For example, at Zandvoort (the Netherlands), one northern transect shows a stronger accretive trend with a wider confidence interval than neighbouring transects. Such local differences may arise from limitations in the shoreline detection method (e.g., composite image processing) or other data inconsistencies. Similar small-scale deviations are also observed in the SLR-induced signal, where coarse-resolution sea-level rise data (approximately 111 km at the equator) or coastal data (1 km spatial scale) are downscaled to the transect level (100 m spatial scale).

While these local anomalies should be considered when interpreting individual transect projections, they do not diminish the reliability of projections at the regional scale (for example, the dominant trend across stretches longer than 1 km). Future research could address this by systematically quantifying variability between consecutive transects and statistically assessing the confidence of local projections.

7.1.2. Exposure Assessment: Identification of High-Risk Beaches

Not all eroding coastlines result in the immediate exposure of infrastructure. To assess where erosion is likely to threaten built assets, this study used the Coastal European Exposure Database to evaluate the spatial overlap between projected eroding coastlines and the location of existing infrastructure. The analysis shows that only a subset of eroding transects intersects with areas of high exposure.

Under SSP2-4.5 in 2050, over 23,000 km of sandy coastline (85%) is projected to erode. In densely populated European regions, the median distance between the shoreline and the first line of infrastructure is approximately 70 m (Lansu et al., 2024). This value is used in this study as the accommodation space threshold for identifying exposed infrastructure. Based on this threshold, around 2,700 km of the projected eroding coastline intersects with building footprints, representing 11.6% of the total eroding length. By 2100, this share increases to about 3,300 km (14.4%) under SSP2-4.5 and nearly 3,700 km (15.5%) under SSP5-8.5.

These results indicate that although a substantial portion of Europe's eroding coastline currently does not directly threaten infrastructure, more than 3,300 km of sandy coast is projected to intersect with built assets by 2100. While this length grows modestly under higher emissions scenarios, it shows that most eroding transects with infrastructure present are expected to contribute to elevated exposure, even under moderate pathways.

To better quantify the severity of exposure, this analysis also identified exposure hotspots, defined as contiguous coastal segments of at least 1 km where projected shoreline retreat intersects with infrastructure. The minimum segment length ensures spatial continuity and serves as a proxy for the scale of at-risk assets, under the assumption that longer exposed segments are more likely to include substantial infrastructure.

The number of exposure hotspots is considerably smaller than the total length of exposed transects, which helps further narrow the set of priority areas for adaptation. For example, in 2050 under SSP2-4.5 with a 70 m buffer, 506 hotspots are identified, covering 836 km, compared to 2,719 km of total exposed coastline. By 2100, the number of hotspots increases to 731 (1,248 km) under SSP2-4.5 and 841 (1,497 km) under SSP5-8.5, while the total exposed lengths are 3,321 km and 3,690 km, respectively. This distinction highlights the value of hotspot detection for identifying discrete, spatially concentrated areas of elevated exposure within the broader European context.

While hotspot identification provides valuable insight into where infrastructure may be affected by coastal erosion, the approach has limitations. The analysis is based solely on building footprints and does not account for differences in building type, height, or density. For example, high-density urban areas with multi-storey buildings, such as Scheveningen (the Netherlands), may have a footprint comparable to smaller coastal settlements, such as Skagen (Denmark), even though the potential consequences of erosion would differ substantially. Furthermore, the method assumes uniform vulnerability across all structures. In reality, buildings respond differently depending on factors such as construction type, foundation design, and maintenance. A more comprehensive risk assessment would require the inclusion of vulnerability curves or damage functions that relate hazard intensity to expected damage or loss, consistent with standard risk frameworks (Cardona et al., 2012; Jongman et al., 2012).

7.1.3. Suitability of Nourishment as Adaptation

The suitability of beach nourishment as an adaptation strategy varies considerably across Europe's high-risk coastal zones. This variability reflects both physical conditions and institutional frameworks, as captured by the NSAM. The study focuses on high-risk sandy coastlines, which exhibit high to moderate suitability depending on the coastal type situated behind them. Consequently, national governance structures and policy traditions emerge as critical determinants of practical suitability. Countries with strong, centralised coastal management and established nourishment programmes, such as the United Kingdom, demonstrate high suitability. This is largely due to consistent policy support, long-term planning, and secured funding mechanisms. In contrast, suitability tends to be lower in regions where responsibility for coastal defence is fragmented or devolved to individual landowners, as in Denmark, or where interventions are predominantly reactive, as seen in parts of Spain.

The analysis highlights an important simplification in the assessment: high-risk beaches are identified using a binary criterion based solely on the presence or absence of buildings. This binary approach implies that the incentive to nourish these beaches is also treated as binary. Such simplification overlooks variations in economic value, strategic importance, and the density of at-risk assets along these segments. A more nuanced assessment would incorporate socio-economic indicators and risk-based prioritisation to better capture the actual drivers of nourishment decisions (see subsection 7.2.3).

This study provides a first-of-its-kind synthesis of historical nourishment practices at the European scale and demonstrates the value of linking these records to a continental-scale suitability assessment. The selected showcases illustrate the diversity of coastal and governmental contexts in which nourishment could be applied. However, it is important to recognise that other coastal adaptation strategies might, in some cases, be more suitable or preferred. Although this study focuses on nourishment as the key adaptation strategy, it acknowledges that nourishment may not always represent the best solution. Material constraints (e.g. lack of sediment that matches native characteristics), spatial constraints (e.g. insufficient space for soft solutions to protect the hinterland), and environmental constraints (e.g. the presence of protected areas) can all limit its applicability. When addressing coastal erosion, it is essential to balance decisions against all local factors and consider a range of potential solutions. However, a comprehensive evaluation of alternative strategies lies beyond the scope of this research.

7.2. Methodological Limitations and Uncertainties

This section critically evaluates key methodological decisions made in this study and the associated uncertainties they introduce. The discussion is organized thematically to highlight sources of model sensitivity and structural simplification.

7.2.1. Input Data Uncertainty

Coastal Slope Representation

This study employs coastal slopes derived from Athanasiou et al. (2024), defined as the gradient between the depth of closure and the nearest inland elevation peak. This choice departs from earlier definitions, such as the nearshore slope (i.e., the slope from the depth of closure to the shoreline) (Bruun, 1962), which has been used in previous global studies (e.g., Vousdoukas et al. (2020)). The coastal slope, by contrast, represents the full active beach profile, covering both submerged and subaerial components, and therefore more accurately captures the zone affected by sea-level rise and retreat (see Figure 2.4. This approach is more consistent with the mass-conservation principle of the Bruun Rule and aligns with Zhang et al. (2004), who defined the landward limit of the active beach at the berm or dune crest.

Nonetheless, this slope definition introduces important uncertainties. The DeltaDTM product used to identify inland peaks may misrepresent the true morphological break (e.g., berm crest or dune ridge), potentially leading to overestimated slopes and thus underestimated retreat. Although the nearest inland elevation peak does not always correspond precisely to these features, this approach still incorporates the entire active profile into the Bruun Rule's mass-conservation principle. Overall, it typically yields steeper slope values (Figure B.1), and because the Bruun Rule links shoreline retreat inversely to slope, this results in smaller projected retreat magnitudes. Furthermore, the use of 1 km-spaced slope indicators may oversimplify terrain in morphologically complex areas, reducing accuracy and consistency in retreat projections across Europe, an acknowledged limitation of large-scale studies of this kind.

In addition, this study assigned each transect a single representative local slope value from Athanasiou et al. (2024), without accounting for uncertainty within the coastal slope. A sensitivity analysis on sediment plain coasts demonstrates that using a single fixed slope (e.g., 0.01) results in a median projected retreat of −21.1 m. In contrast, when slope uncertainty is represented by the observed variability within this coastal type, the resulting distribution yields a broader range of retreat values and a smaller median of −6.2 m (see Figure 7.2). This highlights how applying a single slope value can distort both central estimates and tail risks, potentially skewing adaptation priorities.

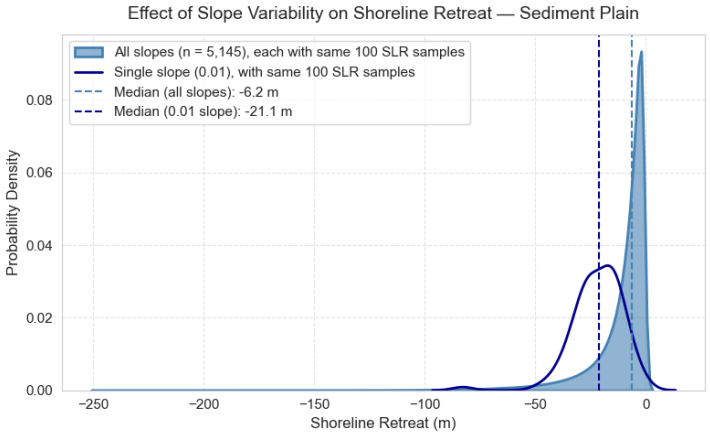

Figure 7.2: Kernel density estimate of shoreline retreat projections under SLR for sediment plain coasts. The solid line shows retreat values derived from a single fixed slope of 0.01, while the shaded area illustrates the distribution of retreat outcomes when accounting for observed slope variability across all transects ($n = 5{,}145$), each combined with the same 100-member SLR ensemble. The wider distribution highlights increased tail risk and underscores the importance of incorporating slope variability to improve the robustness of ensemble-based shoreline retreat modelling.

Shoreline Reference Point

Shoreline change in this study is measured relative to a fixed historical reference point derived from Landsat satellite composites. Although these composites provide subpixel precision (e.g., 15 m (Hagenaars et al., 2017)), residual positional errors arise from factors such as horizontal geolocation error, seasonal averaging, and morphological variability. These sources of uncertainty represent a combination of aleatory variability (e.g., due to natural morphological fluctuations) and epistemic uncertainty (Walker et al., 2003)(e.g., due to limitations in geolocation accuracy and image processing; see Hagenaars et al. (2017) and Luijendijk et al. (2018)). Such uncertainties propagate through all retreat projections and can, in some cases, particularly for short-term horizons (e.g., 2030, 2050) or gentle-slope environments, be of comparable magnitude to the projected retreat itself.

Accounting for these uncertainties explicitly in future modelling, such as through spatial confidence intervals on reference points, could improve the robustness of projections, particularly for infrastructure-focused or near-term risk assessments.

7.2.2. Structural Modelling Assumptions

Linear Regression for Ambient Change

This study uses ordinary least squares (OLS) regression to estimate ambient shoreline trends. While OLS is widely applied in continental-scale analyses (Crowell et al., 1997; Le Cozannet et al., 2019), it reduces complex, often non-linear coastal dynamics to a single linear trajectory. Alternative approaches, including machine learning methods and non-linear models, have been explored (e.g., Calkoen et al. (2021)), but OLS remains the standard within coastal management frameworks, such as Dutch coastal monitoring and policy (Baart, 2013).

This simplification does not capture non-linear behaviours such as storm-driven variability, sediment supply changes, or episodic human interventions (e.g., nourishment resets) especially in dynamic coastal systems (e.g., inlets, deltas or estuaries). Moreover, the resulting confidence intervals represent only aleatory uncertainty, random variation around the fitted line, and do not account for epistemic uncertainty associated with model structure, assumptions, or potential misspecification (Walker et al.,

2003).

To assess the appropriateness of the linear model across different coastal settings, a sensitivity analysis compared OLS model fit (R^2) for two groups: the full set of sandy transects and a subset classified as "sediment plain + dune" coasts, for which linear regression is considered more suitable as processes are expected to exhibit more gradual and approximately linear behaviour over time. As shown in Figure 7.3, the full dataset (left panel) exhibits low fit, with a mean R^2 of 0.21 and median of 0.12 across 295,031 transects. Isolating unstable coasts (ambient change > 15 m) improves the mean fit to 0.43, though overall performance remains modest.

The sediment plain + dune subset (right panel) shows somewhat better fit: for all transects in this group ($n = 161{,}032$), the mean R^2 is 0.26 (median = 0.17), rising to a mean of 0.48 (median = 0.47) for the unstable subset ($n = 68{,}432$). This suggests that linear regression describes historical shoreline dynamics more effectively for soft, sandy coasts such as sediment plains and dunes.

However, sediment plain and dune coasts represent only about half of Europe's sandy transects and rely on geomorphic classifications derived from machine-learning detection, which introduces additional epistemic uncertainty (Calkoen et al., 2025). Therefore, this study retains the full sandy coastline dataset for consistency and completeness. As a result, OLS-based ambient projections should be interpreted as indicative baselines, suitable for large-scale assessments and relative comparisons, but not as precise forecasts, particularly in engineered or highly variable coastal environments.

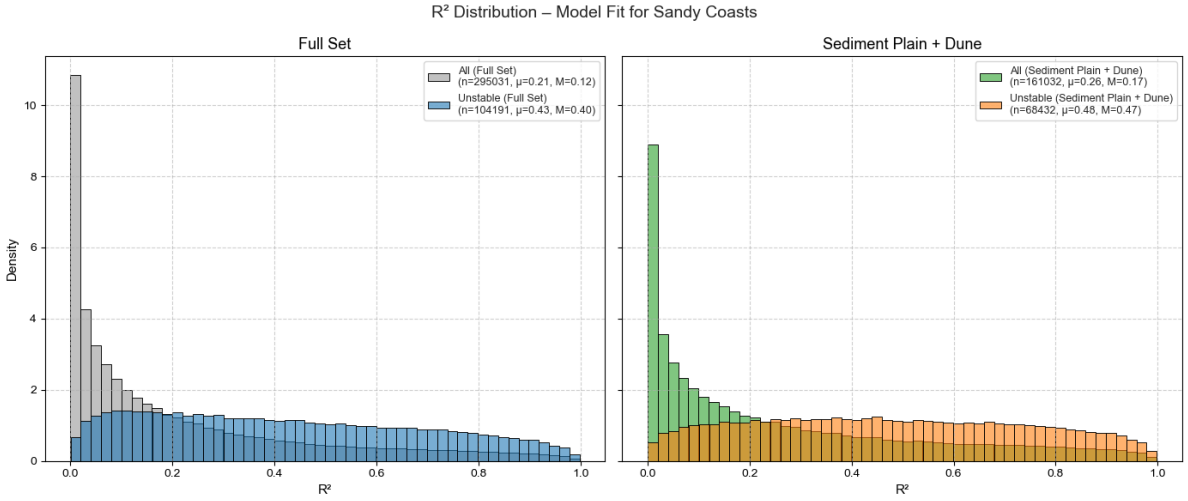

Figure 7.3: R^2 distribution of OLS model fit for ambient shoreline trends. Left: All sandy transects (full set). Right: Sediment plain + dune subset. Mean (μ) and median (M) values shown for both full and dynamic subsets. Results suggest linear regression performs somewhat better in stable morphodynamic environments, though overall fit remains low.

Independence of Ambient and SLR-Induced Change

This model assumes that ambient shoreline change and SLR-induced retreat are statistically independent. This allows their effects to be combined via Monte Carlo sampling, with ambient trends added to SLR-driven projections. The assumption is supported by studies showing weak or no correlation between historical shoreline change and sea-level rise across diverse coastal settings (Le Cozannet et al., 2014, 2019; Webb & Kench, 2010).

However, this independence may not hold under future conditions. In sediment-starved systems and low-lying deltas, rising seas increasingly interact with sediment dynamics and coastal morphology, leading to compound effects (Blum & Roberts, 2009; Ranasinghe et al., 2012). Temporal mismatches between baseline periods for ambient trends (2021–2024) and SLR projections (1995–2014) further complicate the separation of drivers. In regions with strong glacial isostatic adjustment, such as the Baltic, the combined effect of land uplift and sea level fall can exaggerate shoreline advance (Weisse et al., 2021).

Future modelling should consider harmonising baselines and incorporating process-based approaches to

better account for potential coupling between SLR and ambient coastal change.

Use of the Bruun Rule

The Bruun Rule is applied here to estimate shoreline retreat under sea-level rise due to its simplicity and low data requirements (Zhang et al., 2004). However, its quantitative accuracy has long been debated (J. A. G. Cooper & Pilkey, 2004; Ranasinghe et al., 2012). A key criticism is that it relies on idealised assumptions, such as the presence of an equilibrium beach profile, cross-shore sediment transport dominance, and sediment conservation, that are seldom satisfied in real-world settings (Ranasinghe, 2016). Moreover, the Bruun Rule does not account for alongshore processes, human interventions, or sediment supply limitations, which restrict its applicability on engineered, inlet-interrupted, or sediment-starved coasts (J. A. Cooper et al., 2020).

Although appropriate for first-order, large-scale assessments, the Bruun Rule often overestimates retreat and fails to capture spatial variability and key sources of uncertainty when compared to process-based models (Le Cozannet et al., 2019; Ranasinghe et al., 2012). Therefore, results derived from it should be interpreted with caution, particularly when applied to local-scale or policy-relevant decision-making.

7.2.3. Limitations of the Nourishment Suitability Assessment Model

While the Nourishment Suitability Assessment Model (NSAM) offers a rapid, first-order tool for identifying where beach nourishment may be a suitable adaptation strategy, several limitations constrain its applicability, particularly at local scales.

A key limitation is the model's reliance on historical nourishment patterns from a subset of countries with available data. As such, NSAM reflects existing institutional practices, technical capacity, and policy preferences rather than objective or optimal criteria for nourishment suitability. This biases results toward regions with a history of nourishment and under-represents potential in under-resourced or newly exposed areas.

The model further omits critical decision factors, such as cost-effectiveness, ecological impact, and public acceptance, which are essential in real-world planning. Nourishment projects can be expensive and may cause unintended ecological consequences, such as habitat disruption or sediment imbalances (de Schipper et al., 2021). Moreover, local opposition to repeated beach works or coastal reshaping using nourishment can affect the feasibility, particularly when contrasted with hard engineering solutions. These dimensions require local engagement and interdisciplinary assessment that cannot be captured through historical patterns alone.

In terms of spatial representation, NSAM simplifies nourishment interventions by mapping them to transect-level points, despite the fact that they often span broader coastal stretches. The lack of consistent volume or footprint data prevents more nuanced analysis, potentially distorting the apparent intensity or coverage of nourishment activity, especially in heavily managed areas.

Additionally, the NSAM evaluates exposure hotspots detected using a binary exposure method, which leads to a binary nourishment incentive without accounting for variations in asset value or infrastructure density. This overlooks the diversity of real-world decision-making contexts, as illustrated by the Bacton gas terminal showcase. Future work should integrate spatial asset data and governance indicators to better reflect actual incentive structures.

Finally, while NSAM is appropriate for continental-scale prioritisation, it is not intended for local-scale design or engineering decisions. Its simplified assumptions and inputs make it a useful first assessment tool, but detailed, site-specific modelling, stakeholder consultation, and expert judgement are needed for implementation. Particularly, the model does not address sediment dynamics, such as the sourcing, placement, and morphological evolution of nourished material, which are critical for the long-term effectiveness and environmental impact of nourishment strategies, as highlighted in the literature review. Incorporating these processes in future work would help improve assessments of local feasibility and performance.

7.2.4. Input Data Limitations

A final limitation of this study arises from the inherent constraints of the core datasets on which the analyses are based. As introduced in chapter 3, these datasets include the Global Coastal Transect Sys-

tem, ShorelineMonitor, and Global Coastal Transect Repository (Calkoen et al., 2025), complemented by AR6 sea-level rise projections (IPCC, 2023b), coastal slope data (Athanasiou et al., 2024), and the Coastal European Exposure Database (Koks et al., 2023). While the providers of these datasets have made considerable efforts to minimise data gaps, certain limitations inevitably influence the results of this study.

First, while differences in the spatial coverage of the ShorelineMonitor and Global Coastal Transect Repository introduce only a minor gap in the combined shoreline change dataset, the largest reduction in usable transects arises from the coastal slope filter and the spatial join threshold. As shown in Table 5.1, only 66.5% of sandy transects in Europe have valid data for both ambient change and sea-level rise components. This is primarily due to the retention of transects with naturally occurring coastal slopes and the exclusion of transects that could not be matched during the spatial join, given that the transects used by Athanasiou et al. (2024) are spaced at 1 km intervals. This incomplete coverage introduces uncertainty and may limit the representativeness of the projections at the continental scale.

Second, although the CEED building footprint data offer extensive spatial coverage across Europe, not all building footprints are fully captured (e.g., Aldeburgh, UK). In areas where data are missing or incomplete, exposure hotspots may be under-identified. A detailed evaluation of CEED spatial completeness was beyond the scope of this study, but this limitation should be considered when interpreting the exposure results.

Key Points

The limitations outlined above do not undermine the validity of this study but instead clarify its scope and appropriate application. The modelling framework is well suited for continental-scale prioritisation, exposure identification, and comparative analysis of coastal erosion risk. However, its outputs are not intended for direct use in local-scale planning or engineering design without further refinement.

Among the various uncertainties, two stand out as particularly consequential: the representation of coastal slope and the assumption of statistical independence between ambient shoreline change and SLR-induced retreat. Both influence projected shoreline change and, by extension, the prioritisation of adaptation measures. Inaccurate slope estimates may systematically under- or overestimate retreat magnitudes, while assuming independence may obscure important process interactions in sediment-starved or uplift-dominated regions.

Addressing these issues should be a central focus of future work. Incorporating higher-resolution topographic and morphological datasets, harmonising baseline periods, and moving toward coupled, process-based or probabilistic models will enhance both the accuracy and credibility of shoreline change projections. As coastal adaptation increasingly requires site-specific, multi-dimensional assessments, refining these foundational components will be essential to bridge the gap between regional-scale risk modelling and actionable local decision-making.

7.3. Wider Contribution

This study advances the science and practice of coastal erosion management under climate change by integrating high-resolution shoreline change modelling with infrastructure exposure analysis and a first-order suitability assessment for beach nourishment across Europe. It addresses a persistent gap in previous research, where hazard projections and adaptation suitability have often been treated in isolation.

The primary innovation lies in bridging physical risk assessment with policy-relevant decision support. By combining shoreline projections with a Nourishment Suitability Assessment Model, this study identifies not only where coastal retreat is likely to lead to asset exposure, but also where soft interventions may be both physically and institutionally viable. This integrated approach supports more strategic, context-aware adaptation planning across the continent.

Methodologically, the study introduces several advances:

- It applies ensemble based modelling to capture uncertainty in sea-level rise impacts.
- It incorporates locally derived coastal slopes to better reflect profile geometry in Bruun Rule

applications.

- It leverages historical nourishment records to ground adaptation suitability in observed practice, rather than theoretical potential.

These innovations contribute to a more realistic and spatially nuanced understanding of coastal risk, helping to shift from generic hazard-based maps toward actionable prioritisation tools for adaptation planning.

While focused on Europe, the NSAM framework is conceptually transferable to other regions seeking to implement nature-based erosion mitigation. Its transparency, scalability, and grounding in geomorphology, institutional context, and historical precedent make it well suited for global comparisons, national planning, and early-stage suitability assessment. As policy increasingly shifts toward ecosystem-based and anticipatory adaptation, tools that combine physical realism with governance relevance, such as NSAM, will play a vital role. This study offers a replicable model for linking scientific projections with implementable strategies, while underscoring the need for local data, stakeholder engagement, and interdisciplinary refinement to translate large-scale assessments into effective on-the-ground action.

8

Conclusion

This thesis aims to answer the central question:

Where and to what extent are nourishments suitable to mitigate coastal erosion under changing climate conditions?

The research addressed this by focusing on two key links in the climate adaptation chain: the physical impacts of future shoreline retreat, and the suitability of nourishments as a nature-based response. This was done by developing high-resolution projections of future coastal erosion risk. These projections were then combined with a newly developed database of historical nourishment practices to create a practical framework for assessing where nourishments are likely to be suitable.

A core contribution of this thesis is the development of detailed shoreline change projections for European sandy beaches under different climate scenarios. Using satellite-derived shoreline data and geospatial tools, historical trends were probabilistically extrapolated into the future. These were combined with AR6 sea-level rise projections and local coastal slopes to estimate shoreline change under mild, moderate, and extreme conditions. Over 81% of Europe's sandy coastlines face erosion under all climate scenarios, with a projected median change of -37.8 m under SSP2-4.5 by 2100, increasing to -80.2 m under SSP5-8.5 when only accounting for eroding beaches. These projections provide spatially explicit, probabilistic insight into where erosion is expected to occur, at 100 m transect resolution.

By referencing these future shorelines to a fixed baseline, this study identified at which transects direct exposure of built assets is present. While 84% of the beaches are projected to erode under SSP2-4.5, only 5.6% of these beaches directly intersect with buildings when the future shoreline is projected. However, exposure rises to 14.4% when a representative accommodation space of 70 m is applied, reflecting the median distance between the shoreline and the first line of infrastructure. Under higher emissions scenarios, this number increases further, identifying up to 841 (1,479 km) exposure hotspots by 2100. This assessment shows not only where erosion will occur but also where it could affect infrastructure, highlighting urgent targets for adaptation.

To understand where nourishments could realistically be part of that response, this research collected 1,060 nourishment records from across Europe. These show that nourishments are not applied uniformly across all sandy beaches. Most are found on sedimentary plain and dune coasts, serving both reactive and proactive purposes, ranging from shoreline stability to recreation. Offshore sourced sand is the dominant source, and countries with more technical knowledge and experience tend to make more use of nourishments. This indicates that the presence of institutional capacity and supportive governance is just as important as physical need when it comes to the use of nourishments.

Based on this historical evidence, a Nourishment Suitability Assessment Model was developed to enable a first-order indication of whether nourishment is likely to be a suitable strategy for a given location. The model incorporates four key factors: coastal type, sediment availability, policy environment, and

knowledge & experience. While the NSAM provides a practical and fast first assessment, it has clear limitations. The model is based on historical nourishment patterns and reflects the institutional practices and experiences of the countries represented in the database. It does not account for trade-offs between costs, nor does it integrate ecological impacts, physical design or the social acceptance of nourishments. These aspects require further research and local engagement before implementation.

The framework was applied in three showcase areas, demonstrating how NSAM can be used in practice to assess nourishment suitability at different sites. This synthesis of forward-looking erosion risk and backward-looking adaptation practice helps bridge the gap between impact assessment and action. It shows that while many coasts are at risk, not all are equally suitable for nourishment, and a context-specific approach is necessary.

In sum, this thesis shows that large parts of Europe's sandy coastlines are likely to retreat under future climate conditions, and that nourishments can be a useful adaptation strategy, but only under the right conditions. The projections and tools developed here offer a concrete, data-driven starting point for coastal planners and policymakers to identify where nourishments are most likely to be suitable. Moving forward, the NSAM could be expanded to integrate ecological and social dimensions and linked to broader coastal adaptation strategies that take into account long-term resilience, regional coordination, and sustainability.

9

Recommendations

This research aimed to provide continental-scale projections of shoreline retreat, integrated exposure assessment, and a first-order indication of nourishment suitability, based on historical precedent, across Europe. While the study offers valuable insights, several opportunities exist for future research to build on these foundations and enhance the accuracy of the projections, representativeness exposure assessment, and practical relevance for coastal adaptation planning.

The recommendations are grouped into two main areas: (i) methodological improvements to reduce uncertainty and strengthen the technical basis of the shoreline projections and exposure assessment, and (ii) expansion of the adaptation and management perspective beyond nourishment alone.

9.1. Methodological Improvements

The methods in this study combined established and novel approaches, including probabilistic extrapolation of ambient trends, ensemble-based modelling of SLR-induced retreat, and building-level exposure quantification using footprint data. Future research could advance this framework in several ways:

- **Enhance uncertainty quantification in shoreline change models.** While this study accounted for parameter uncertainty in ambient change through Monte Carlo sampling of the trend, and evaluated SLR-induced retreat using 100-member SLR ensembles, future work could further incorporate model (aleatory) uncertainty. This includes representing natural variability in both the linear regression of ambient trends and the application of the Bruun Rule for SLR-induced retreat. Moreover, future models should move beyond the assumption of statistical independence between ambient shoreline change and SLR-induced retreat, as this may obscure important process interactions. Rather than relying solely on deterministic assumptions, such as an equilibrium profile or linear dynamics, future models should reflect the inherent variability and potential coupling of coastal system responses.
- **Improve input data quality and resolution.** Reducing input uncertainty, for example, through higher-resolution coastal slope data or satellite imagery, would improve shoreline change projections. Propagating input uncertainty explicitly (e.g., accounting for variability in slope) could provide more robust confidence intervals. Additionally, errors introduced when linking projections to spatial reference points should be quantified. Generating spatial confidence intervals for shoreline positions and applying resampling techniques would strengthen spatial impact estimates.
- **Leverage neighbouring transect data for consistency checks.** Incorporating spatial coherence by assessing how individual transect projections align with neighbouring transects within the same coastal stretch could provide a valuable quality control measure, helping to identify outliers or inconsistencies.
- **Strengthen exposure data foundations.** Improving the completeness and resolution of infrastructure datasets, and incorporating attributes such as building type, height, use, and economic

value, would enhance risk-based prioritisation of adaptation measures.

- **Expand and standardise nourishment records.** Developing more comprehensive and standardised datasets on nourishment practices would strengthen the empirical foundation of the NSAM and better represent the diversity of coastal management approaches across Europe.

9.2. Broadening Adaptation and Management Perspectives

While this study focused on nourishment as an adaptation strategy, future research could extend the framework to support a more integrated view of coastal adaptation. Potential directions include:

- **Integrate alternative strategies for non-sandy coasts.** The traffic light framework could be adapted to propose context-appropriate measures where nourishment is unsuitable, such as managed realignment, hard defences, or hybrid solutions, based on combined physical and institutional criteria.
- **Position nourishment within a broader decision-support context.** Rather than viewing nourishment in isolation, the NSAM could form part of a multi-criteria toolset that helps planners weigh adaptation options against objectives such as cost-effectiveness, ecological value, and social acceptance.
- **Explore dynamic adaptation pathways.** Future studies could link suitability assessments with dynamic, long-term adaptation pathways that enable flexible sequencing of measures in response to changing risks and priorities.

These recommendations aim to support the continued refinement of large-scale coastal risk assessments and their integration into practical adaptation planning, while acknowledging the complexity of translating large-scale projections and suitability analysis into local actionable strategies.

Finally, the nourishment database compiled in this study offers valuable opportunities for future research. The dataset could be expanded and refined, for example by representing the full spatial extent of each nourishment intervention, enabling deeper analysis of shoreline behaviour at nourished coasts. By combining the nourishment records with the ShorelineMonitor time series, future work could systematically investigate the different behavioural pathways that nourished coasts follow over time. This study's initial findings suggest that nourishments are not always placed on actively eroding coasts, and that post-nourishment shoreline trajectories display a range of behaviours, not only the classical sawtooth pattern of erosion, jump, and renewed erosion. Exploring these patterns in detail would improve understanding of nourishment dynamics and support more targeted, evidence-based coastal management strategies.

References

Adriadapt. (2022, February). Beach nourishment.

Anthony, E. J., Cohen, O., & Sabatier, F. (2011). Chronic offshore loss of nourishment on Nice beach, French Riviera: A case of over-nourishment of a steep beach? *Coastal Engineering*, *58*(4), 374–383. https://doi.org/10.1016/j.coastaleng.2010.11.001

Antolínez, J. A. A., Méndez, F. J., Camus, P., Vitousek, S., González, E. M., Ruggiero, P., & Barnard, P. (2016). A multiscale climate emulator for long-term morphodynamics (MUSCLE-morpho). *Journal of Geophysical Research: Oceans*, *121*(1), 775–791. https://doi.org/10.1002/2015JC011107

Armstrong, S. B., & Lazarus, E. D. (2019). Masked Shoreline Erosion at Large Spatial Scales as a Collective Effect of Beach Nourishment. *Earth's Future*, *7*(2), 74–84. https://doi.org/10.1029/2018EF001070

Athanasiou, P., van Dongeren, A., Giardino, A., Vousdoukas, M. I., Ranasinghe, R., & Kwadijk, J. (2020). Uncertainties in projections of sandy beach erosion due to sea level rise: an analysis at the European scale. *Scientific Reports*, *10*(1). https://doi.org/10.1038/s41598-020-68576-0

Athanasiou, P., Van Dongeren, A., Giardino, A., Vousdoukas, M., Gaytan-Aguilar, S., & Ranasinghe, R. (2019). Global distribution of nearshore slopes with implications for coastal retreat. *Earth System Science Data*, *11*(4), 1515–1529. https://doi.org/10.5194/essd-11-1515-2019

Athanasiou, P., Van Dongeren, A., Pronk, M., Giardino, A., Vousdoukas, M., & Ranasinghe, R. (2024). Global Coastal Characteristics (GCC): A global dataset of geophysical, hydrodynamic, and socioeconomic coastal indicators. *Earth System Science Data*, *16*(7), 3433–3452. https://doi.org/10.5194/essd-16-3433-2024

Baart, F. (2013). *C O N F I D E N C E I N C O A S TA L F O R E C A S T S* (tech. rep.).

Barbier, E. B., Hacker, S. D., Koch, E. W., Stier, A. C., & Silliman, B. R. (2024). Estuarine and Coastal Ecosystems and Their Services. In *Treatise on estuarine and coastal science (second edition)* (pp. 14–34). Elsevier. https://doi.org/10.1016/B978-0-323-90798-9.00104-9

Bird, E., & Lewis, N. (2014, September). *SPRINGER BRIEFS IN EARTH SCIENCES Beach Renourishment* (tech. rep.). https://doi.org/https://doi.org/10.1007/978-3-319-09728-2

Blum, M. D., & Roberts, H. H. (2009, July). Drowning of the Mississippi Delta due to insufficient sediment supply and global sea-levelrise. https://doi.org/10.1038/ngeo553

Bontje, L. ; Fredriksson, C. ; & Wang, Z. ; (2016, January). *Coastal erosion and beach nourishment in Scania as issues in Swedish coastal policy* (tech. rep.). http://www.tidskriftenvatten.se/article.asp?articleID=4788

Borchert, S. M., Osland, M. J., Enwright, N. M., & Griffith, K. T. (2018). Coastal wetland adaptation to sea level rise: Quantifying potential for landward migration and coastal squeeze. *Journal of Applied Ecology*, *55*(6), 2876–2887. https://doi.org/10.1111/1365-2664.13169

Borsje, R., Flikweert, J., Goodliffe, R., & Hesk, P. (2024). Bacton Sandscaping – Initial Performance of a Mega Nourishment. *Coasts, Marine Structures and Breakwaters 2023: Resilience and adaptability in a changing climate*, 1471–1488. https://doi.org/10.1680/cmsb.67042.1471

Bosboom, J., & Stive, M. (2023, January). *Coastal Dynamics*. TU Delft OPEN Publishing. https://doi.org/10.5074/T.2021.001

Box, G., & Cox, D. (1964). An Analysis of Transformations. *Journal of the Royal Statistical Society*, *26*(2).

Bruun, P. (1962). Sea level rise as a cause of shore erosion. *Journal of the Waterways and Harbors Division*, *88*(1), 117–130.

Bujan, N., Cox, R., & Masselink, G. (2019). From fine sand to boulders: Examining the relationship between beach-face slope and sediment size. *Marine Geology*, *417*. https://doi.org/10.1016/j.margeo.2019.106012

Calkoen, F., Luijendijk, A., Rivero, C. R., Kras, E., & Baart, F. (2021). Traditional vs. Machine-learning methods for forecasting sandy shoreline evolution using historic satellite-derived shorelines. *Remote Sensing*, *13*(5), 1–21. https://doi.org/10.3390/rs13050934

Calkoen, F., Luijendijk, A., Vos, K., Kras, E., & Baart, F. (2025). Enabling coastal analytics at planetary scale. *Environmental Modelling and Software*, *183*. https://doi.org/10.1016/j.envsoft.2024.106257

Cardona, O.-D., van Aalst, M. K., Birkmann, J., Fordham, M., McGregor, G., Perez, R., Pulwarty, R. S., Lisa Schipper, E. F., Tan Sinh, B., Décamps, H., Keim, M., Davis, I., van Aalst, M., Birkmann, J., Fordham, M., McGregor, G., Perez, R., Pulwarty, R., Schipper, E., … Midgley, P. (2012). *Coordinating Lead Authors: Lead Authors: Review Editors: Contributing Authors:: Determinants of risk: exposure and vulnerability. In: Managing the Risks of Extreme Events and Disasters to Advance Climate Change Adaptation 2 Determinants of Risk: Exposure and Vulnerability* (tech. rep.). Australia.

Castelle, B., Kras, E., Masselink, G., Scott, T., Konstantinou, A., & Luijendijk, A. (2024). Satellite-derived sandy shoreline trends and interannual variability along the Atlantic coast of Europe. *Scientific Reports*, *14*(1). https://doi.org/10.1038/s41598-024-63849-4

Cazenave, A., & Cozannet, G. L. (2014). Sea level rise and its coastal impacts. *Earth's Future*, *2*(2), 15–34. https://doi.org/10.1002/2013ef000188

Cerema. (2023, June). *Méthodes souples – Retour d'expériences pour le littoral* (tech. rep.). Ministère de la Transition écologique et de la cohésion des territoires. www.cerema.fr

Coco, G., Senechal, N., Rejas, A., Bryan, K. R., Capo, S., Parisot, J. P., Brown, J. A., & MacMahan, J. H. (2014). Beach response to a sequence of extreme storms. *Geomorphology*, *204*, 493–501. https://doi.org/10.1016/j.geomorph.2013.08.028

Coelho, C., Lima, M., & Ferreira, M. (2022). A Cost–Benefit Approach to Discuss Artificial Nourishments to Mitigate Coastal Erosion. *Journal of Marine Science and Engineering*, *10*(12). https://doi.org/10.3390/jmse10121906

Cooper, J. A., Masselink, G., Coco, G., Short, A. D., Castelle, B., Rogers, K., Anthony, E., Green, A. N., Kelley, J. T., Pilkey, O. H., & Jackson, D. W. (2020, November). Sandy beaches can survive sea-level rise. https://doi.org/10.1038/s41558-020-00934-2

Cooper, J. A. G., & Pilkey, O. H. (2004). Sea-level rise and shoreline retreat: Time to abandon the Bruun Rule. *Global and Planetary Change*, *43*(3-4), 157–171. https://doi.org/10.1016/j.gloplacha.2004.07.001

Crowell, M., Douglas, B. C., & Leatherman, S. P. (1997). On forecasting future US shoreline positions: a test of algorithms. *Journal of Coastal Research*, *13*(4), 1245–1255.

Danish Coastal Authority. (2019). *A coastal oriented Policy Brief from the Interreg North Sea Building with Nature project* (tech. rep.).

de Schipper, M. A., Ludka, B. C., Raubenheimer, B., Luijendijk, A. P., & Schlacher, T. A. (2021, January). Beach nourishment has complex implications for the future of sandy shores. https://doi.org/10.1038/s43017-020-00109-9

Dean, R. G. (1991). *Equilibrium Beach Profiles: Characteristics and Applications* (tech. rep.).

Dean, R. G. (2002). *Beach Nourishment: Theory and Practice*. World Scientific.

Deltares & Rijkswaterstaat. (n.d.). CoastViewer: Interactive Coastal Data Viewer.

Elko, N. A., & Wang, P. (2007). Immediate profile and planform evolution of a beach nourishment project with hurricane influences. *Coastal Engineering*, *54*(1), 49–66. https://doi.org/10.1016/j.coastaleng.2006.08.001

Environment Agency. (2020). *National Flood and Coastal Erosion Risk Management Strategy for England* (tech. rep.).

EUROSION. (2004). *Living with coastal erosion in Europe: Sediment and Space for Sustainability PART II-Maps and statistics* (tech. rep.).

Gares, P. A., Wang, Y., & White, S. A. (2006). Using LIDAR to monitor a beach nourishment project at Wrightsville Beach, North Carolina, USA. *Journal of Coastal Research*, *22*(5), 1206–1219. https://doi.org/10.2112/06A-0003.1

Gijsman, R., Visscher, J., & Schlurmann, T. (2018). *A method to systematically classify design characteristics of sand nourishments* (tech. rep.). https://doi.org/https://doi.org/10.15488/9261

Goncalves, R. M., & Awange, J. L. (2017). Three Most Widely Used GNSS-Based Shoreline Monitoring Methods to Support Integrated Coastal Zone Management Policies. *Journal of Surveying Engineering*, *143*(3). https://doi.org/10.1061/(asce)su.1943-5428.0000219

Griggs, G., & Reguero, B. G. (2021, August). Coastal adaptation to climate change and sea-level rise. https://doi.org/10.3390/w13162151

Hagenaars, G., Luijendijk, A., De Vries, S., & Boer, W. (2017). *LONG TERM COASTLINE MONITORING DERIVED FROM SATELLITE IMAGERY* (tech. rep.). APA.

Hallermeier, R. J. (1978). USES FOR A CALCULATED LIMIT DEPTH TO BEACH EROSION. *Coastal Engineering Proceedings*, (16), 88. https://doi.org/10.9753/icce.v16.88

Hamm, L., Capobianco, M., Dette, H. H., Lechuga, A., Spanhoff, R., & Stive, M. J. F. (2002). *A summary of European experience with shore nourishment* (tech. rep.). www.elsevier.com/locate/coastaleng

Hanson, H., Brampton, A., Capobianco, M., Dette, H. H., Hamm, L., Laustrup, C., Lechuga, A., & Spanhoff, R. (2002). *Beach nourishment projects, practices, and objectives-a European overview* (tech. rep.). www.elsevier.com/locate/coastaleng

Hinkel, J., Nicholls, R. J., Tol, R. S., Wang, Z. B., Hamilton, J. M., Boot, G., Vafeidis, A. T., McFadden, L., Ganopolski, A., & Klein, R. J. (2013). A global analysis of erosion of sandy beaches and sea-level rise: An application of DIVA. *Global and Planetary Change*, *111*, 150–158. https://doi.org/10.1016/j.gloplacha.2013.09.002

IPCC. (2023a, June). Technical Summary. In *Climate change 2021 – the physical science basis* (pp. 35–144). Cambridge University Press. https://doi.org/10.1017/9781009157896.002

IPCC. (2023b, July). *IPCC, 2023: Climate Change 2023: Synthesis Report. Contribution of Working Groups I, II and III to the Sixth Assessment Report of the Intergovernmental Panel on Climate Change [Core Writing Team, H. Lee and J. Romero (eds.)]. IPCC, Geneva, Switzerland.* (P. Arias, M. Bustamante, I. Elgizouli, G. Flato, M. Howden, C. Méndez-Vallejo, J. J. Pereira, R. Pichs-Madruga, S. K. Rose, Y. Saheb, R. Sánchez Rodríguez, D. Ürge-Vorsatz, C. Xiao, N. Yassaa, J. Romero, J. Kim, E. F. Haites, Y. Jung, R. Stavins, … C. Péan, Eds.; tech. rep.). Intergovernmental Panel on Climate Change. https://doi.org/10.59327/IPCC/AR6-9789291691647

Jackson, L. P., & Jevrejeva, S. (2016). A probabilistic approach to 21st century regional sea-level projections using RCP and High-end scenarios. *Global and Planetary Change*, *146*, 179–189. https://doi.org/10.1016/j.gloplacha.2016.10.006

Jongman, B., Kreibich, H., Apel, H., Barredo, J. I., Bates, P. D., Feyen, L., Gericke, A., Neal, J., Aerts, J. C., & Ward, P. J. (2012). Comparative flood damage model assessment: Towards a European approach. *Natural Hazards and Earth System Science*, *12*(12), 3733–3752. https://doi.org/10.5194/nhess-12-3733-2012

Koks, E., De Plaen, J., & Colmenares, M. (2023, October). *CoCliCo Research and Innovation Action (RIA) High-resolution pan-European exposure database* (tech. rep.). VU Amsterdam. Amsterdam.

Kriebel, D. L., & Dean, R. G. (1993). Convolution Method for Time-Dependent Beach-Profile Response. *Journal of Waterway, Port, Coastal, and Ocean Engineering*, *119*(2), 204–226. https://doi.org/10.1061/(ASCE)0733-950X(1993)119:2(204)

Lansu, E. M., Reijers, V. C., Höfer, S., Luijendijk, A., Rietkerk, M., Wassen, M. J., Lammerts, E. J., & van der Heide, T. (2024). A global analysis of how human infrastructure squeezes sandy coasts. *Nature Communications*, *15*(1). https://doi.org/10.1038/s41467-023-44659-0

Le Cozannet, G., Bulteau, T., Castelle, B., Ranasinghe, R., Wöppelmann, G., Rohmer, J., Bernon, N., Idier, D., Louisor, J., & Salas-y-Mélia, D. (2019). Quantifying uncertainties of sandy shoreline change projections as sea level rises. *Scientific Reports*, *9*(1). https://doi.org/10.1038/s41598-018-37017-4

Le Cozannet, G., Garcin, M., Yates, M. L., Idier, D., Yates, M., & Meyssignac, B. (2014). Approaches to evaluate the recent impacts of sea-level rise on shoreline changes. *Earth-Science Reviews*, *138*, 47–60. https://doi.org/10.1016/j.earscirev.2014.08.005{\"{i}}

Lodder, Q., & Slinger, J. (2022). The 'Research for Policy' cycle in Dutch coastal flood risk management: The Coastal Genesis 2 research programme. *Ocean and Coastal Management*, *219*. https://doi.org/10.1016/j.ocecoaman.2022.106066

Luijendijk, A., Hagenaars, G., Ranasinghe, R., Baart, F., Donchyts, G., & Aarninkhof, S. (2018). The State of the World's Beaches. *Scientific Reports*, *8*(1). https://doi.org/10.1038/s41598-018-24630-6

Marchand, M. (n.d.). *CONCEPTS AND SCIENCE FOR COASTAL EROSION MANAGEMENT CONCISE REPORT FOR POLICY MAKERS* (tech. rep.).

McGranahan, G., Balk, D., & Anderson, B. (2007). The rising tide: Assessing the risks of climate change and human settlements in low elevation coastal zones. *Environment and Urbanization*, *19*(1), 17–37. https://doi.org/10.1177/0956247807076960

Mentaschi, L., Vousdoukas, M. I., Pekel, J. F., Voukouvalas, E., & Feyen, L. (2018). Global long-term observations of coastal erosion and accretion. *Scientific Reports*, *8*(1). https://doi.org/10.1038/s41598-018-30904-w

Mentaschi, L., Vousdoukas, M. I., Voukouvalas, E., Dosio, A., & Feyen, L. (2017). Global changes of extreme coastal wave energy fluxes triggered by intensified teleconnection patterns. *Geophysical Research Letters*, *44*(5), 2416–2426. https://doi.org/10.1002/2016GL072488

Merkens, J. L., Reimann, L., Hinkel, J., & Vafeidis, A. T. (2016). Gridded population projections for the coastal zone under the Shared Socioeconomic Pathways. *Global and Planetary Change*, *145*, 57–66. https://doi.org/10.1016/j.gloplacha.2016.08.009

MITECO. (2022). *National Strategic Plan for Coastal Protection Considering the Effects of Climate Change* (tech. rep.). Government of Spain. https://www.miteco.gob.es/es/costas/temas/proteccion-costa/estrategias-proteccion-costa/

Mongelli, F. P., Ceglar, A., & Scheid, B. A. (2024). Why Do We Need to Strengthen Climate Adaptations? Scenarios and Financial Lines of Defence. *ECB Working Paper Series*, *No. 2024/3005*. https://doi.org/10.2139/ssrn.5060437

Mulder, J. P., Hommes, S., & Horstman, E. M. (2011). Implementation of coastal erosion management in the Netherlands. *Ocean and Coastal Management*, *54*(12), 888–897. https://doi.org/10.1016/j.ocecoaman.2011.06.009

Neumann, B., Vafeidis, A. T., Zimmermann, J., & Nicholls, R. J. (2015). Future coastal population growth and exposure to sea-level rise and coastal flooding - A global assessment. *PLoS ONE*, *10*(3). https://doi.org/10.1371/journal.pone.0118571

Nicholls, R. J. (2011). Planning for the impacts of sea level rise. *Oceanography*, *24*(2), 144–157. https://doi.org/10.5670/oceanog.2011.34

Nicholls, R. J., Birkemeier, W. A., & Lee, G.-H. (1998). *Evaluation of depth of closure using data from Duck, NC, USA* (tech. rep.).

Nicholls, R. J., & Cazenave, A. (2010, June). *Sea-Level Rise and Its Impact on Coastal Zones* (tech. rep.). https://www.science.org

Nordstrom, K. F. (2005). Beach nourishment and coastal habitats: Research needs to improve compatibility. *Restoration Ecology*, *13*(1), 215–222. https://doi.org/10.1111/j.1526-100X.2005.00026.x

Osborne, J. W. (2010). *Improving your data transformations: Applying the Box-Cox transformation* (tech. rep.). https://www.researchgate.net/publication/284261483

Pianca, C., Holman, R., & Siegle, E. (2015). Shoreline variability from days to decades: Results of long-term video imaging. *Journal of Geophysical Research: Oceans*, *120*(3), 2159–2178. https://doi.org/10.1002/2014JC010329

Pinto, C. A., Silveira, T. M., & Teixeira, S. B. (2020). Beach nourishment practice in mainland Portugal (1950–2017): Overview and retrospective. *Ocean and Coastal Management*, *192*. https://doi.org/10.1016/j.ocecoaman.2020.105211

Pranzini, E. (2018, April). Shore protection in Italy: From hard to soft engineering … and back. https://doi.org/10.1016/j.ocecoaman.2017.04.018

Qiu, Y., Gopalakrishnan, S., Klaiber, H. A., & Li, X. (2020). Dredging the sand commons: the economic and geophysical drivers of beach nourishment. *Climatic Change*, *162*(2), 363–383. https://doi.org/10.1007/s10584-020-02757-8

Ranasinghe, R. (2016, September). Assessing climate change impacts on open sandy coasts: A review. https://doi.org/10.1016/j.earscirev.2016.07.011

Ranasinghe, R., Callaghan, D., & Stive, M. J. (2012). Estimating coastal recession due to sea level rise: Beyond the Bruun rule. *Climatic Change*, *110*(3-4), 561–574. https://doi.org/10.1007/s10584-011-0107-8

Ranasinghe, R., & Turner, I. L. (2006). Shoreline response to submerged structures: A review. *Coastal Engineering*, *53*(1), 65–79. https://doi.org/10.1016/j.coastaleng.2005.08.003

Roy, R., Monju, M. H., Tan, M. L., Rahman, M. S., Kundu, S., Rahman, M. S., Talukder, B., & Bhuyan, M. S. (2023). Determining synergies and trade-offs between adaptation, mitigation and development in coastal socio-ecological systems in Bangladesh. *Environmental Development*, *48*. https://doi.org/10.1016/j.envdev.2023.100936

Schoonees, T., Gijón Mancheño, A., Scheres, B., Bouma, T. J., Silva, R., Schlurmann, T., & Schüttrumpf, H. (2019). Hard Structures for Coastal Protection, Towards Greener Designs. *Estuaries and Coasts*, *42*(7), 1709–1729. https://doi.org/10.1007/s12237-019-00551-z

Slott, J. M., Murray, A. B., Ashton, A. D., & Crowley, T. J. (2006). Coastline responses to changing storm patterns. *Geophysical Research Letters*, *33*(18). https://doi.org/10.1029/2006GL027445

Speybroeck, J., Bonte, D., Courtens, W., Gheskiere, T., Grootaert, P., Maelfait, J. P., Mathys, M., Provoost, S., Sabbe, K., Stienen, E. W., Van Lancker, V., Vincx, M., & Degraer, S. (2006, June). Beach nourishment: An ecologically sound coastal defence alternative? A review. https://doi.org/10.1002/aqc.733

Spoto, F., Sy, O., Laberinti, P., Martimort, P., Fernandez, V., Colin, O., Hoersch, B., & Meygret, A. (2012). Overview Of Sentinel-2. *2012 IEEE International Geoscience and Remote Sensing Symposium*, 1707–1710. https://doi.org/10.1109/IGARSS.2012.6351195

Staudt, F., Gijsman, R., Ganal, C., Mielck, F., Wolbring, J., Hass, H. C., Goseberg, N., Schüttrumpf, H., Schlurmann, T., & Schimmels, S. (2021, April). The sustainability of beach nourishments: a review of nourishment and environmental monitoring practice. https://doi.org/10.1007/s11852-021-00801-y

Stive, M. J. F., Aarninkhof, S. G. J., Hamm, L., Hanson, H., Larson, M., Wijnberg, K. M., Nicholls, R. J., & Capobianco, M. (2002). *Variability of shore and shoreline evolution* (tech. rep.). https://doi.org/https://doi.org/10.1016/S0378-3839(02)00126-6

van Duin, M. J., Wiersma, N. R., Walstra, D. J., van Rijn, L. C., & Stive, M. J. (2004). Nourishing the shoreface: Observations and hindcasting of the Egmond case, The Netherlands. *Coastal Engineering*, *51*(8-9), 813–837. https://doi.org/10.1016/j.coastaleng.2004.07.011

van Egmond, E. M., van Bodegom, P. M., Berg, M. P., Wijsman, J. W., Leewis, L., Janssen, G. M., & Aerts, R. (2018). A mega-nourishment creates novel habitat for intertidal macroinvertebrates by enhancing habitat relief of the sandy beach. *Estuarine, Coastal and Shelf Science*, *207*, 232–241. https://doi.org/10.1016/j.ecss.2018.03.003

van Oudenhoven, A. P., Aukes, E., Bontje, L. E., Vikolainen, V., van Bodegom, P. M., & Slinger, J. H. (2018). 'Mind the Gap' between ecosystem services classification and strategic decision making. *Ecosystem Services*, *33*, 77–88. https://doi.org/10.1016/j.ecoser.2018.09.003

van Rijn, L. (1995). Sand budget and coastline changes of the central coast of Holland between Den Helder and Hoek van Holland, period 1964-2040.

van de Wal, R., Melet, A., Bellafiore, D., Camus, P., Ferrarin, C., Oude Essink, G., Haigh, I. D., Lionello, P., Luijendijk, A., Toimil, A., Staneva, J., & Vousdoukas, M. (2024). Sea Level Rise in Europe: Impacts and consequences. *State of the Planet*, *3-slre1*, 1–33. https://doi.org/10.5194/sp-3-slre1-5-2024

van der Werf, J. J., Huisman, B. J., Price, T. D., Larsen, B. E., de Schipper, M. A., McFall, B. C., Krafft, D. R., Lodder, Q. J., & Ruessink, B. G. (2025, August). Shoreface nourishments: Research advances and future perspectives. https://doi.org/10.1016/j.earscirev.2025.105138

Vitousek, S., Buscombe, D., Vos, K., Barnard, P. L., Ritchie, A. C., & Warrick, J. A. (2023). The future of coastal monitoring through satellite remote sensing. *Cambridge Prisms: Coastal Futures*, *1*. https://doi.org/10.1017/cft.2022.4

Vos, K., Splinter, K. D., Palomar-Vázquez, J., Pardo-Pascual, J. E., Almonacid-Caballer, J., Cabezas-Rabadán, C., Kras, E. C., Luijendijk, A. P., Calkoen, F., Almeida, L. P., Pais, D., Klein, A. H., Mao, Y., Harris, D., Castelle, B., Buscombe, D., & Vitousek, S. (2023). Benchmarking satellite-derived shoreline mapping algorithms. *Communications Earth and Environment*, *4*(1). https://doi.org/10.1038/s43247-023-01001-2

Vousdoukas, M. I., Mentaschi, L., Voukouvalas, E., Verlaan, M., & Feyen, L. (2017). Extreme sea levels on the rise along Europe's coasts. *Earth's Future*, *5*(3), 304–323. https://doi.org/10.1002/2016EF000505

Vousdoukas, M. I., Ranasinghe, R., Mentaschi, L., Plomaritis, T. A., Athanasiou, P., Luijendijk, A., & Feyen, L. (2020, March). Sandy coastlines under threat of erosion. https://doi.org/10.1038/s41558-020-0697-0

Walker, W., Harremoës, P., Rotmans, J., van der Sluijs, J., van Asselt, M., Janssen, P., & Krayer von Krauss, M. (2003). Defining Uncertainty: A Conceptual Basis for Uncertainty Management in Model-Based Decision Support. *Integrated Assessment*, *4*(1), 5–17. https://doi.org/10.1076/iaij.4.1.5.16466

Webb, A. P., & Kench, P. S. (2010). The dynamic response of reef islands to sea-level rise: Evidence from multi-decadal analysis of island change in the Central Pacific. *Global and Planetary Change*, *72*(3), 234–246. https://doi.org/10.1016/j.gloplacha.2010.05.003

Weisse, R., Dailidiene, I., Hünicke, B., Kahma, K., Madsen, K., Omstedt, A., Parnell, K., Schöne, T., Soomere, T., Zhang, W., & Zorita, E. (2021, August). Sea level dynamics and coastal erosion in the Baltic Sea region. https://doi.org/10.5194/esd-12-871-2021

Wulder, M. A., Roy, D. P., Radeloff, V. C., Loveland, T. R., Anderson, M. C., Johnson, D. M., Healey, S., Zhu, Z., Scambos, T. A., Pahlevan, N., Hansen, M., Gorelick, N., Crawford, C. J., Masek, J. G., Hermosilla, T., White, J. C., Belward, A. S., Schaaf, C., Woodcock, C. E., … Cook, B. D. (2022). Fifty years of Landsat science and impacts. *Remote Sensing of Environment*, *280*, 113195. https://doi.org/10.1016/J.RSE.2022.113195

Zhang, K., Douglas, B. C., & Leatherman, S. P. (2004). *GLOBAL WARMING AND COASTAL EROSION* (tech. rep.). www.ipcc.ch

A

Supplementary Literature Review

A.1. Physical Drivers of Coastal Erosion

Bird and Lewis (2014) identified 15 distinct factors contributing to coastal erosion:

1. Reduction in sediment supply from eroding cliffs
2. Reduction of fluvial sediment supply to the coast
3. Reduction of sediment supply from the sea floor
4. Reduction of sand supply from inland dunes
5. Submergence and increased wave attack
6. Increased wave energy because of increased storminess
7. Losses of beach sediment alongshore
8. A change in the angle of incidence of waves
9. Interception of longshore drift by breakwaters
10. Increased losses of beach sediment to the back shore
11. Beach weathering, including attrition of beach sediment
12. A rise in the beach water table
13. Removal of beach sediment by run-off
14. Increased scour by wave reflection from an artificial structure
15. Extraction of sand and shingle from the beach

A.2. Methodologies for Projecting Future Erosion

The analysis by Vousdoukas et al. (2020) incorporates all three distinct components of shoreline retreat: ambient shoreline change, sea-level rise-induced retreat, and storm-induced erosion. Each component is driven by specific physical processes, as detailed below.

Ambient Shoreline Change

Ambient shoreline change arises from a combination of natural and anthropogenic factors. Key contributors include alongshore sediment transport, reduced sediment supply from rivers, and human interventions, such as ports or groynes, which disrupt natural sediment dynamics and exacerbate downstream erosion.

In this research, historical shoreline dynamics from datasets by Luijendijk et al. (2018) and Mentaschi et al. (2018), spanning 1984–2015, are analyzed. These data are used to represent ambient shoreline variations, and a probabilistic methodology is applied to project future trends. Synthetic shoreline

position series are generated using Monte Carlo sampling, producing robust probability density functions for shoreline changes over the 21st century.

Sea-Level Rise-Induced Shoreline Retreat

The impact of sea-level rise on shoreline retreat is calculated using the Bruun rule as specified in Equation A.1 (Bruun, 1962):

$$R = \frac{1}{\tan\beta}\text{SLR} \tag{A.1}$$

Here, R represents the retreat distance, SLR denotes sea-level rise, and $\tan\beta$ is the active profile slope. The projections of regional SLR from Jackson and Jevrejeva (2016) are used. The SLR projections account for major global factors such as ocean self-attraction and loading, (globally averaged) steric, and dynamic sea-level changes, ice mass balance from glaciers, ice sheets, and land-water storage, but exclude localized vertical land movements like subsidence from groundwater pumping. The dataset by Athanasiou et al. (2019) provides the active profile slope, in previous studies this was assumed to be constant (Hinkel et al., 2013). To find the most offshore boundary of the active profile, the Hallermeier (1978) formula, adopted by Nicholls et al. (1998) for longer timescales is used. Given by:

$$d_c = 2.28H_{e,t} - 68.5(\frac{H_{e,t}^2}{gT_{e,t}^2}) \tag{A.2}$$

Here, $H_{e,t}$ represents the significant wave height that is surpassed for only 12 hours per t years, $T_{e,t}$ is the corresponding wave period, and g denotes the gravitational acceleration. In this context, t refers to the period from 1980 to 2100. The landward boundary of the active profile is determined by the berm or dune crest, or the farthest offshore point at mean sea level (MSL). The active profile length, L_b, is defined as the cross-shore distance between the depth of closure and the landward boundary. The slope of the profile is expressed as $\tan\beta = \frac{d_c}{L_b}$.

Waves are modeled using WAVEWATCH-III for the period 1980–2100, driven by six Global Climate Models (GCMs) from CMIP5 (Mentaschi et al., 2017; Vousdoukas et al., 2017).

Storm-Induced Erosion

Storm-induced erosion, driven by extreme storm events, is modeled using the KD93 convolution erosion model (Kriebel & Dean, 1993). This model, based on the equilibrium profile concept, estimates shoreline retreat and sand volume loss due to storm-induced waves and surges. It relies on two sets of inputs:

1. **Hydrodynamic variables:** Significant wave height (H_s), peak wave period (T_p), wave incidence angle (α_w), storm surge (η_s), tidal level (η_{tide}), and event duration.
2. **Beach profile parameters:** Dune height (D), berm height (B), berm width (W), and the beach-face slope ($\tan\beta_f$).

Figure 2.6 illustrates the projections of shoreline changes under RCP4.5 and RCP8.5 for 2050 and 2100, showing increasing erosion trends with higher greenhouse gas concentrations.

A.3. Adaptation Strategies for Coastal Erosion

Retreat

The retreat strategy involves relocating infrastructure and communities away from high-risk areas, allowing natural processes to continue with minimal interference. While it is a sustainable long-term solution, retreat often faces significant social, economic, and political challenges, such as public resistance and high relocation costs.

Accommodation

Accommodation strategies adapt human activities and infrastructure to coexist with coastal erosion and rising sea levels. This includes measures like flood-resilient designs, elevating buildings, and modifying agricultural practices. Accommodation allows continued use of coastal regions but requires substantial investments and ongoing adaptation to changing conditions.

Protection

Protection strategies are further divided into:

- **Hard Protection:** Includes seawalls, groynes, and breakwaters that create physical barriers against erosion and flooding. These structures provide immediate and robust protection but can disrupt natural sediment dynamics, often leading to unintended consequences such as increased erosion downstream.
- **Soft Protection:** Involves environmentally friendly approaches like beach nourishment and dune restoration, which work with natural processes. Although more sustainable, these methods require regular maintenance and may be less effective in areas exposed to high wave energy.

Preserving Fixed Coastlines

In specific cases, such as the preservation of the 1990 coastline in the Netherlands, sand nourishment has been the primary strategy for maintaining stable coastlines. This approach leverages natural sediment dynamics to balance ecological, economic, and protective needs, ensuring long-term stability.

Advantages, Limitations, and Trade-offs

Each strategy presents specific benefits and drawbacks. Retreat is the most sustainable option but is socially and politically challenging. Accommodation supports continued use of coastal areas but involves significant adaptation efforts. Hard protection provides immediate results but incurs high environmental costs, while soft protection is more sustainable yet demands consistent maintenance. The choice of strategy depends on a comprehensive evaluation of site-specific conditions, including physical, legal, and socio-economic factors.

By integrating these strategies, coastal management plans can be tailored to address the unique challenges posed by climate change, ensuring the protection of vulnerable coastal regions while balancing ecological and societal needs.

B

Supplementary Methodological Details

B.1. Metadata Fields and Data Types

Table B.1: Final Database Structure, alphabetical order

Column Name	dtype	Description
D50_native/borrow (mm)	float64	Median grain size of native or borrow material (in mm)
borrow_area	string	Location or description of the sediment source for nourishment
borrow_area_flag	string	Classification of the borrow area (e.g., offshore, inlet, channel)
coastal_defense	string	Classification of coastal protection function (e.g., flood prevention, erosion mitigation)
common_country_name	string	Full country name where nourishment was conducted
country	string	Two-letter country code (ISO 3166-1 alpha-2)
departement	string	Administrative region or department (mainly for French data)
deposit_type	string	Type of nourishment deposit (e.g., beach, dune, shoreface)
end_date	datetime64	End date of the nourishment project
geometry	geometry	Geospatial point geometry of the nourishment location
lat	float64	Latitude coordinate in decimal degrees (EPSG:4326)
length	float64	Length of the nourished coastal section (in meters)
location	string	Cleaned and standardized location name
lon	float64	Longitude coordinate in decimal degrees (EPSG:4326)
method	string	Method of nourishment (e.g., direct placement, rainbowing)
municipality	string	Municipality or local administrative unit of the nourishment site
nourishment_id	string	Unique identifier for each nourishment record
performance	string	Post-nourishment performance assessment (if available)
placement_depth	string	Depth or elevation where sediment was placed
primary_borrow_area	string	Most relevant borrow area type after standardization
primary_purpose	string	Most relevant nourishment purpose after standardization
primary_type	string	Most relevant nourishment type after standardization
purpose	string	Original description of nourishment purpose(s)
purpose_flag	string	Flag representing standardized nourishment purpose classification
responsible_body	string	Name of the organization responsible for the nourishment project
responsible_body_category	string	Category of responsible organization (e.g., national agency, research institute)
source	string	Original data source (e.g., scientific paper, agency dataset)
start_date	datetime64	Start date of the nourishment project
transect_id	string	Identifier from the Global Coastal Transect System (GCTS) matched to this nourishment
type_flag	string	Flag representing standardized nourishment type classification
vol	float64	Nourishment volume (in 10^3 m^3)
vol_per_metre	float64	Volume per meter of coastline (in 10^3 m^3/m)
year	int64	Start year extracted as a 4-digit integer

B.2. Excluded Nourishment Records

Table B.2: Nourishment projects excluded due to being over 100m from the nearest transect.

Country	Location	Lat	Lon	Transect ID	Nourishment ID	Distance (m)
France	Lido de Sète	43.66	3.69	cl32409s00tr00513433	31b8a43c98304d62ae5fa5fbf1999f1a	21885.00
Spain	Oran Beach	43.30	-8.38	cl30793s00tr00473353	5ed7fa8cbc2c4c91a3f1715f87b73169	763.30
Denmark	Agger Tange	55.69	11.71	cl32430s00tr00034663	4224049b5bfd4d26b5743732427f22b5	2437.20
Denmark	Agger Tange	55.69	11.71	cl32430s00tr00034663	f60802bb022142aab5b527bd40c569a2	2437.20
Denmark	Harboore Tange	55.69	11.71	cl32430s00tr00034663	145c676e046a4a97b040419810b4cfb3	2437.20
Denmark	N. Holmsland Tange	55.69	11.71	cl32430s00tr00034663	bd29ee83b05b4561b4a4820bc6ea1c3a	2437.20
Denmark	S. Holmsland Tange	55.69	11.71	cl32430s00tr00034663	703be7f591a7402387ebd2f99790ce3b	2437.20
Denmark	Hald Strand	55.69	11.71	cl32430s00tr00034663	8f79ef2fabda41b8abb5a7839a4a93d4	2437.20
Italy	Fiume Esino – Fosso Rubiano (AN)	40.79	14.46	cl32263s00tr00071239	389e468d440b4373acdc96f2a5310b1c	3859.40
Italy	Land Sourcellino	40.79	14.46	cl32263s00tr00071239	2fec9427b009446db018fb5b451b3fb2	3859.40
Italy	Nettuno	40.92	14.46	cl32263s00tr00058139	e62e2e5ed49c4ad893f3f447447a6101	15387.20
Italy	Cecina Mare	40.79	14.46	cl32263s00tr00071239	39d4f1a843eb4f17bdfeefa482ee72cc	3859.40
Italy	Le Gorette	40.79	14.46	cl32263s00tr00071239	fdad801db19843149dd3c9fecdb329ce	3859.40
Italy	Formia	40.94	14.24	cl32263s00tr00052239	c7b4211228494b47b564d889fd198c8b	9547.40
Italy	Terracina	40.83	14.19	cl32263s00tr00039739	8fa9424a97f14805857b76a99438c836	1673.40
Italy	Minturno-Scauri	40.79	14.46	cl32263s00tr00071239	82839e91f9c44449ab4a15a6021f4e71	3859.40
Netherlands	Slufterdam	51.95	4.02	cl32408s01tr00262548	34c9e1ab9acc4084a7e4975ccadb4ac4	1735.80
Netherlands	Slufterdam	51.95	4.02	cl32408s01tr00262548	a6849ec13abd4af88f96db7ca4743d24	2130.10
Netherlands	Slufterdam	51.95	4.02	cl32408s01tr00262548	e9a38e50dd1f4a77be24a6dc288092bb	1735.80
Netherlands	Slufterdam	51.95	4.02	cl32408s01tr00262448	9b7a5781b9e64ff2a4abeaab320f003a	1972.30
Netherlands	Slufterdam	51.94	4.02	cl32408s01tr00262348	5101b3c58be7417c824a49fb12a3397b	817.70
Netherlands	Slufterdam	51.95	4.01	cl32408s01tr00256148	e69cf0b0ca844da492c1a7af040defd7	1898.10
Netherlands	Slufterdam	51.94	4.02	cl32408s01tr00262448	0a1fea395289474880d93b6f6ce839ac	1166.00
Netherlands	MV2 Kustfundament	51.97	4.01	cl32408s01tr00248848	fcaa2a3eb7a1457ba349d8eb5f49fb29	451.80
Netherlands	MV2 Kustfundament	51.97	4.02	cl32408s01tr00248748	d453078bb5c44a98b0e83f9df6343d0a	505.70
Netherlands	MV2 Kustfundament	51.96	4.02	cl32408s01tr00248648	3a91ef030ab340df8094386341f26fbd	2222.50
Netherlands	MV2 Kustfundament	51.94	4.02	cl32408s01tr00262448	b910eb1b59f14d56a6b6d09b00a359fe	1166.00
Netherlands	MV2 Kustfundament	51.97	4.01	cl32408s01tr00248848	9da1aeeb23a64f4690bcab25343e8c05	451.80
Netherlands	MV2 Kustfundament	51.97	4.02	cl32408s01tr00248748	6b5447e847aa40769b6530ff7d46a9ed	505.70
Netherlands	MV2 Kustfundament	51.94	4.02	cl32408s01tr00262348	55e01e3d3dc04e1ead713af9b61e3674	645.70
Netherlands	MV2	51.97	4.01	cl32408s01tr00248748	4c181475c6424ebe8e8fd38e3f1e393f	812.30
Netherlands	MV2	51.93	4.02	cl32408s01tr00261648	2cb56978d8584b9ab32dfe2d51021bc4	182.50
Netherlands	MV2 Kustfundament	51.93	4.02	cl32408s01tr00261648	01b52a41b2b04538b1c671b6dcde2d35	182.50

Continued on next page

Country	Location	Lat	Lon	Transect ID	Nourishment ID	Distance (m)
Netherlands	MV2 Kustfundament	51.97	4.02	cl32408s01tr00248648	4a51a84a1fee448284f493658335ee80	516.90
Netherlands	Maasvlakte 2	51.96	3.98	cl32408s01tr00254748	640259df4b564c499c564d50fb9b2b5b	376.20
Netherlands	Maasvlakte 2	51.96	3.98	cl32408s01tr00254748	ff37429d5d9642848fde1d2f8402f2e8	376.20
Netherlands	Maasvlakte 2	51.96	3.98	cl32408s01tr00254748	0642741224c9401a84a8bc879d664843	376.20
Netherlands	Maasvlakte 2	51.93	4.02	cl32408s01tr00261648	0110b73522d844078c4bf5ea975ce7ae	182.50
Netherlands	Maasvlakte 2	51.97	4.01	cl32408s01tr00248748	2f03e58df2e94657b1d44e829f204abe	812.30
Netherlands	Maasvlakte 2	51.95	4.01	cl32408s01tr00256148	b4135168bba846269b0f840ca1951bad	2362.30
Netherlands	Maasvlakte 2	51.96	4.01	cl32408s01tr00248748	5ccb2257b9bb4289b0947e638945c1ac	2136.60

B.3. EDA: SLR-Induced Change Input

This appendix provides an overview of the exploratory data analysis (EDA) conducted to validate the slope dataset used in the SLR-induced retreat calculations. It includes analysis of slope value distributions, their relationship to coastal type, and the spatial matching process between slopes and transects. The figures help justify the slope filtering thresholds and spatial join radius of 750 m applied in the main analysis.

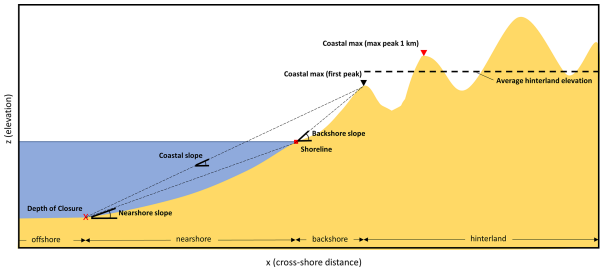

Figure B.1: Schematic representation of the coastal slope and the nearshore slope. Reprinted from Athanasiou et al. (2024).

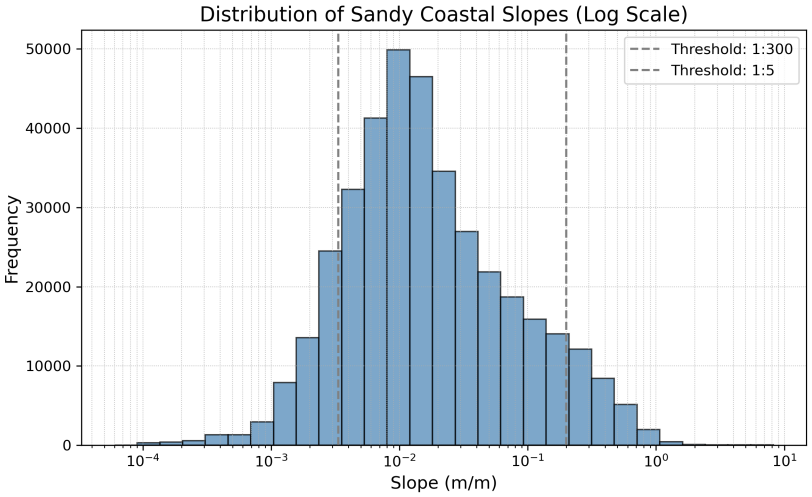

Figure B.2: Histogram of raw coastal slope values (log-binned). Values are filtered to the physically plausible range for sandy coastlines (1/5 to 1/300), consistent with the literature (Vousdoukas et al., 2020).

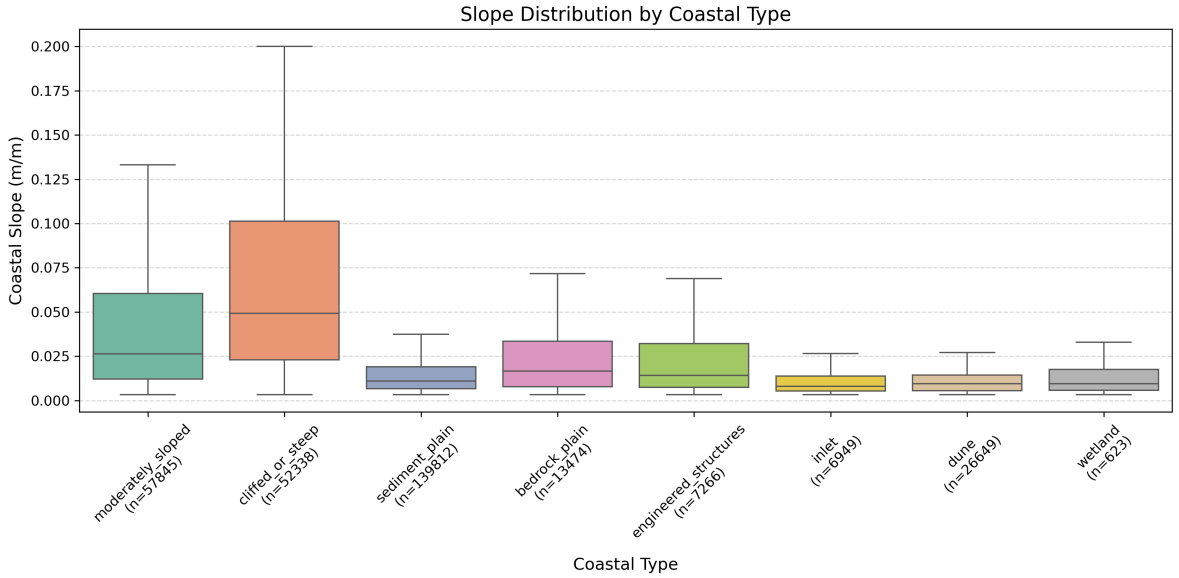

Figure B.3: Boxplot of slope values stratified by coastal type. Sandy systems (e.g., dunes, sediment plains) show expected slope distributions within the retained range. This confirms internal consistency between coastal classification and slope assignment.

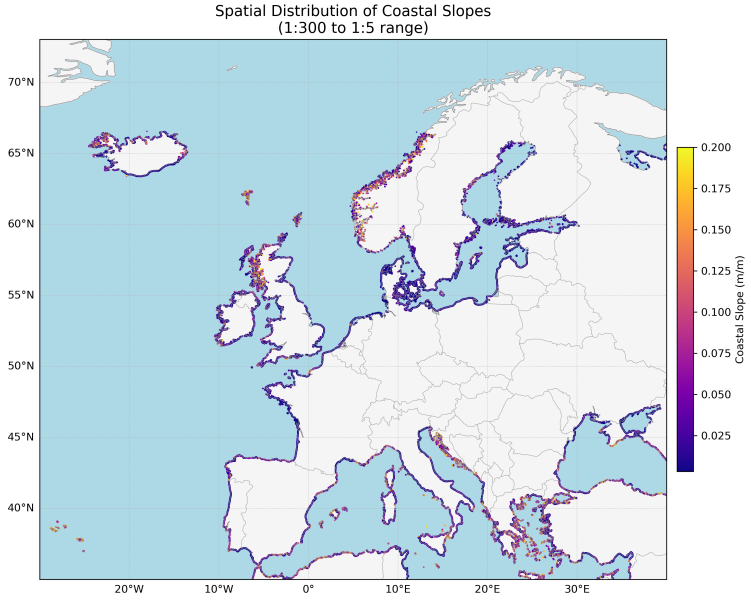

Figure B.4: Spatial distribution of transects with matched slope values (within the valid slope range and 750 m join radius). Gaps highlight areas where transects were excluded due to missing or mismatched slope data.

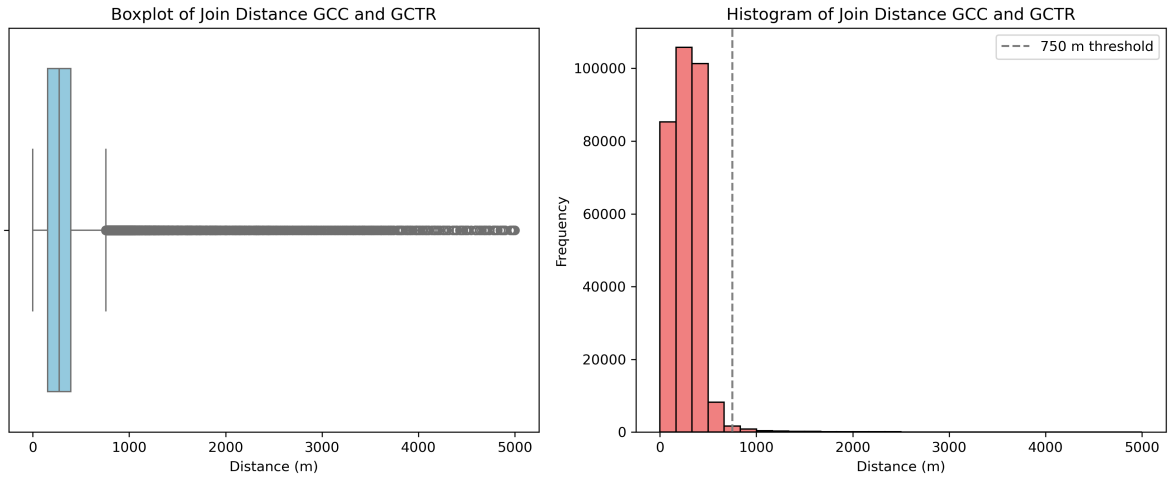

Figure B.5: Boxplot and histogram of spatial join distances between transects and slope points. The applied threshold of 750 m (dashed line) reflects a trade-off between sample coverage and spatial accuracy.

B.4. Ambient Change: Model Validation

This appendix provides supporting figures for the validation of the ambient shoreline change model. To assess the reliability of the linear regression approach, we examined two key metrics across all transects: the coefficient of determination (R^2) and the root mean squared error (RMSE). Density plots of both metrics are shown below, followed by example trend fits for a stable and an unstable shoreline transect. These visualizations support the statistical evaluation presented in Section 3.5.2 and confirm that model performance is better in areas with stronger shoreline trends.

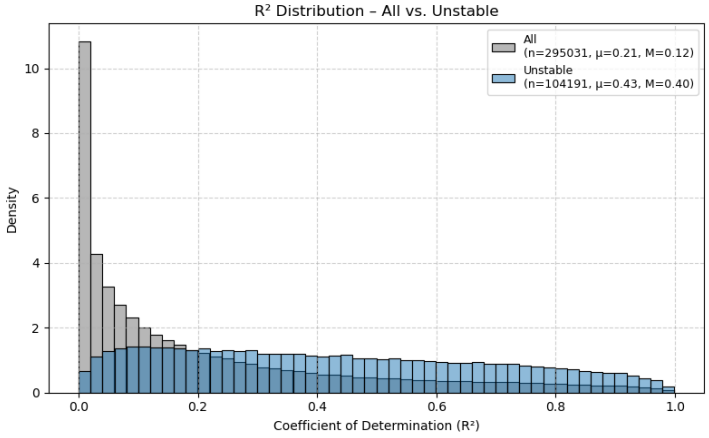

Figure B.6: Density distribution of R^2 values across all ambient shoreline change transects. The distribution is right-skewed, with most values concentrated below 0.4, reflecting weak explanatory power for stable coasts with minimal change.

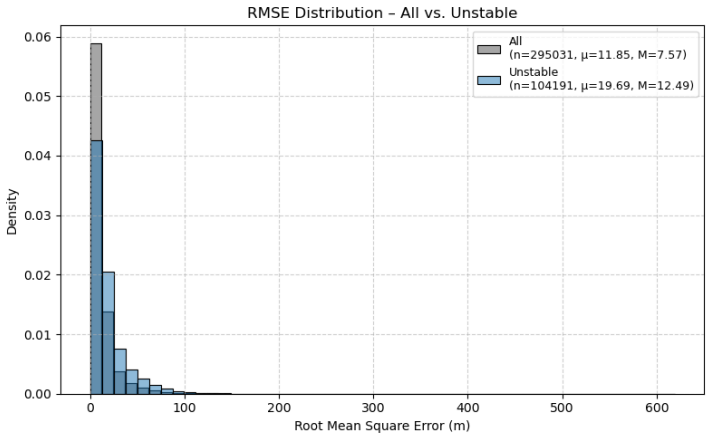

Figure B.7: Density distribution of RMSE values across all transects. Lower RMSE values are associated with low-magnitude shoreline change, while higher RMSE values occur in areas with larger observed shifts, such as erosive hotspots.

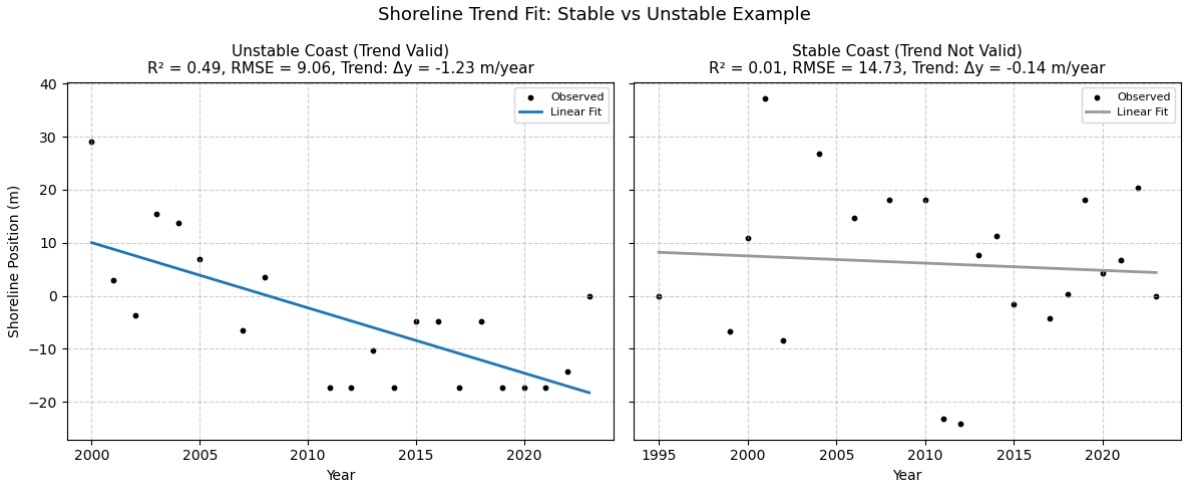

Figure B.8: Example model fit for two transects: one classified as stable (top) and one as unstable (bottom). The stable transect shows a near-horizontal trend line with low variance explained, while the unstable transect displays a clear directional trend and stronger model fit.

B.5. Distributions Shoreline Change

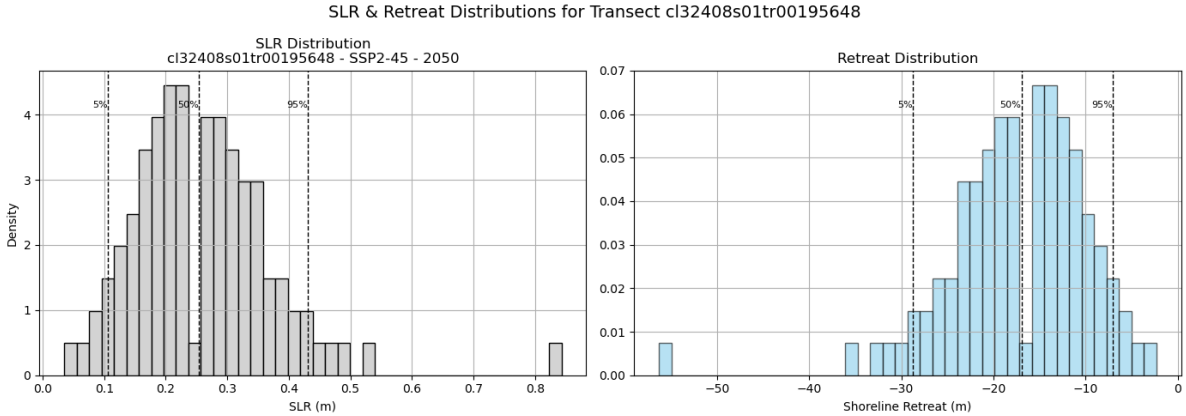

Figure B.9: left: sea-level rise ensemble distribution. Right: the corresponding retreat distribution for this transect

C

Supplementary Results

C.1. Annual and cumulative nourishment volumes per Country

Below are the annual and cumulative nourishment volumes plotted per country:

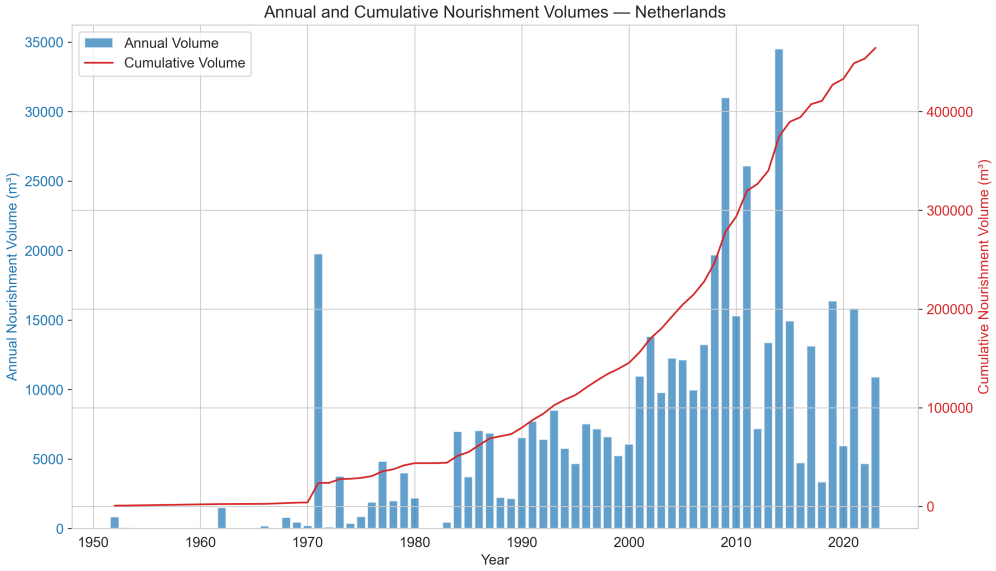

Figure C.1: Annual and cumulative nourishment volumes for the Netherlands.

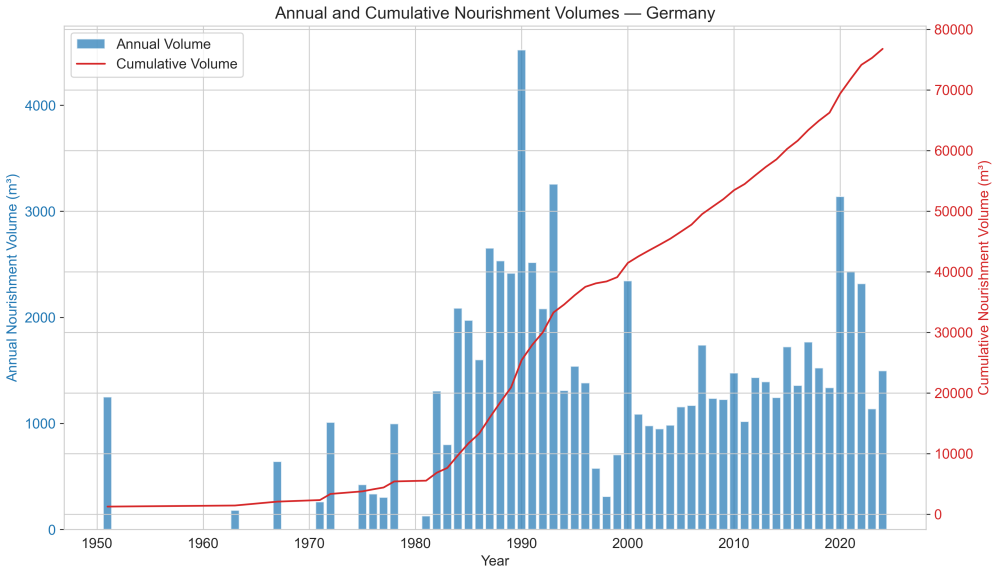

Figure C.2: Annual and cumulative nourishment volumes for Germany.

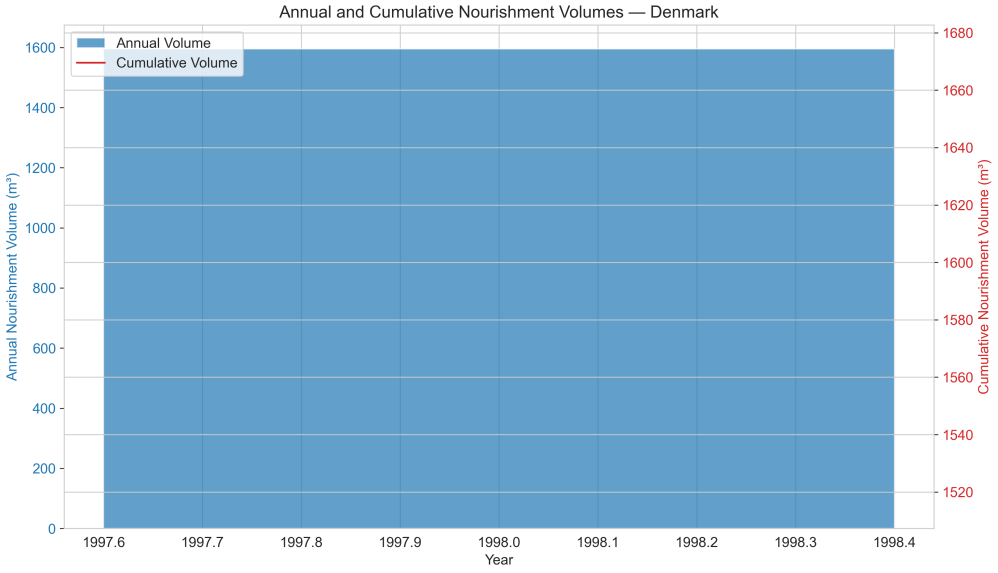

Figure C.3: Annual and cumulative nourishment volumes for Denmark.

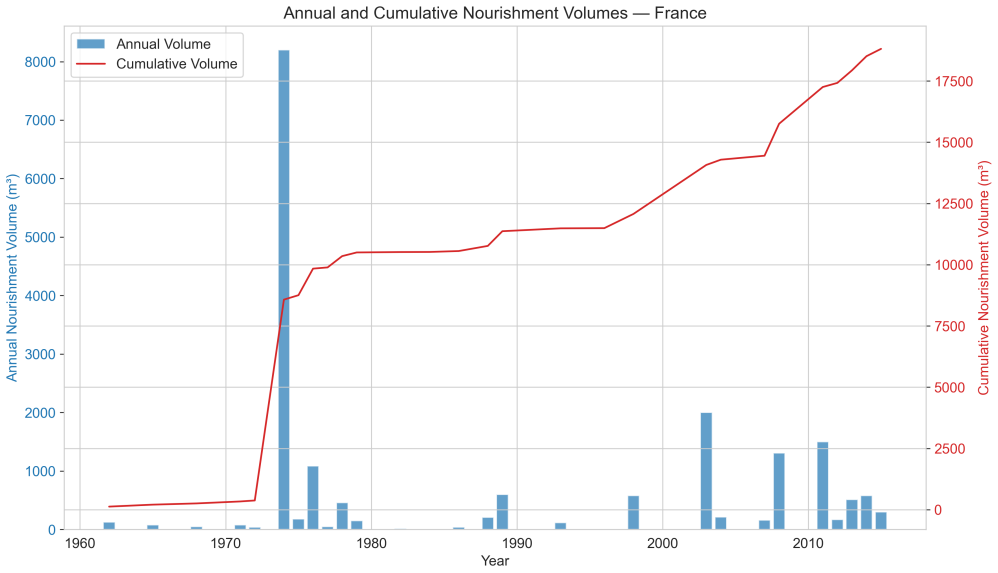

Figure C.4: Annual and cumulative nourishment volumes for France.

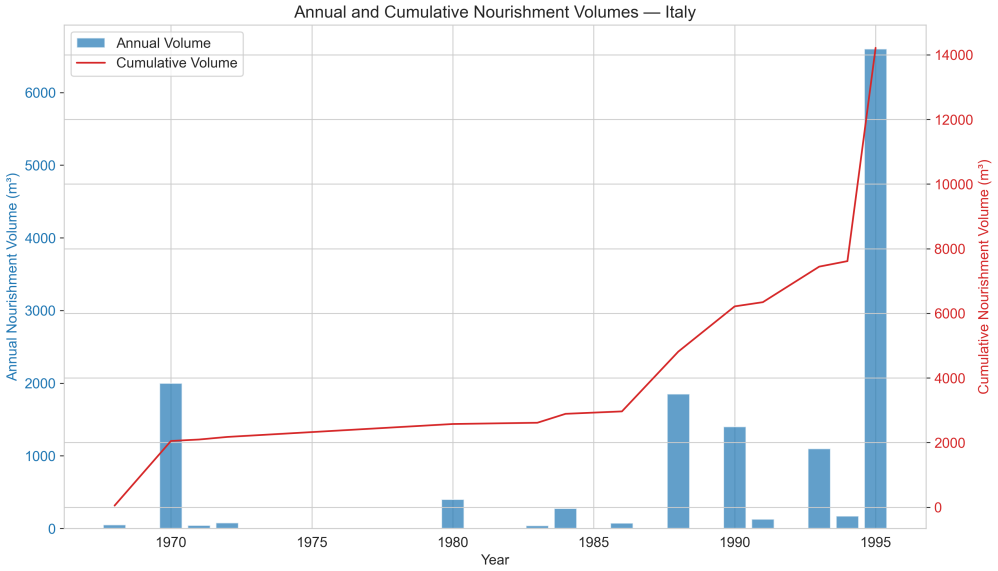

Figure C.5: Annual and cumulative nourishment volumes for the Italy.

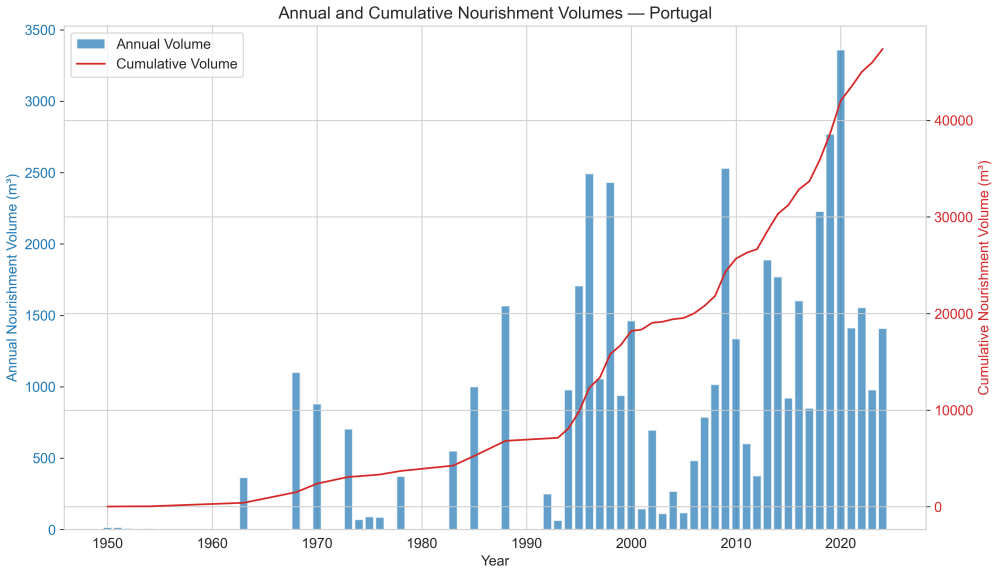

Figure C.6: Annual and cumulative nourishment volumes for Portugal.

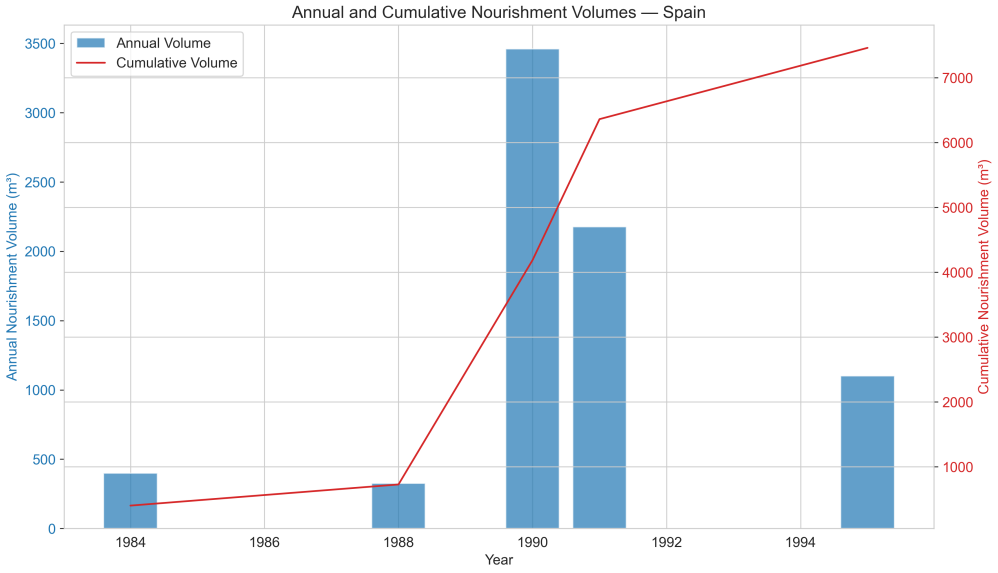

Figure C.7: Annual and cumulative nourishment volumes for Spain.

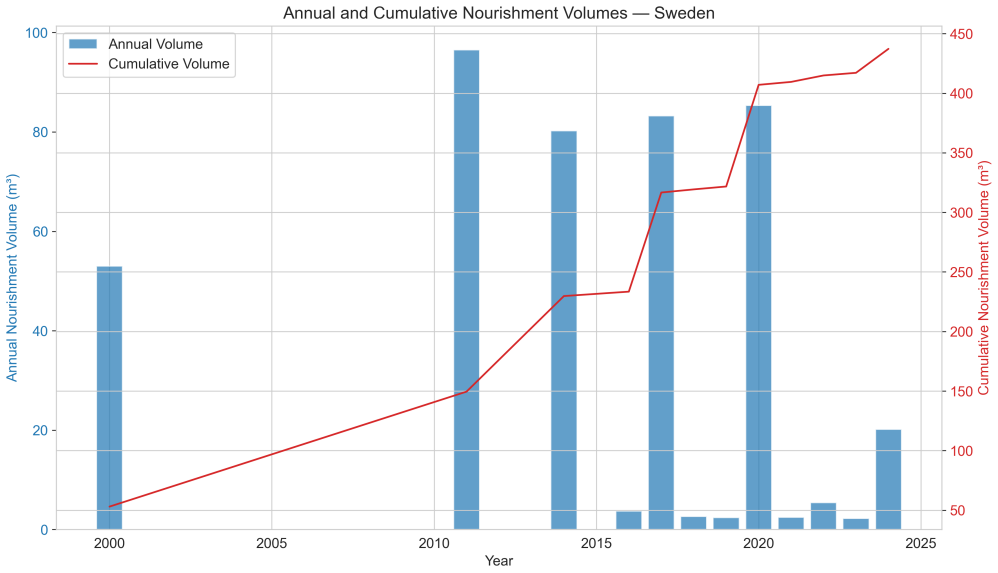

Figure C.8: Annual and cumulative nourishment volumes for Sweden.

C.2. Stacked Bar Charts of Nourishments by Country

This appendix includes the full classification of shoreline typologies by nourishment count and volume, separated by borrow source and intervention type. Bar charts per country are provided to illustrate national variation in strategic focus.

Denmark

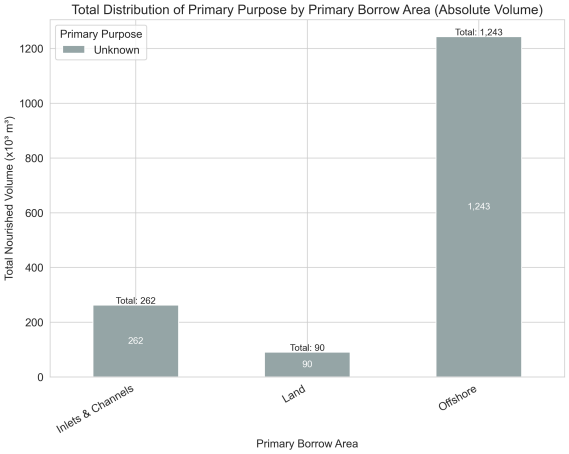

(a) Primary Borrow Area vs. Primary Purpose

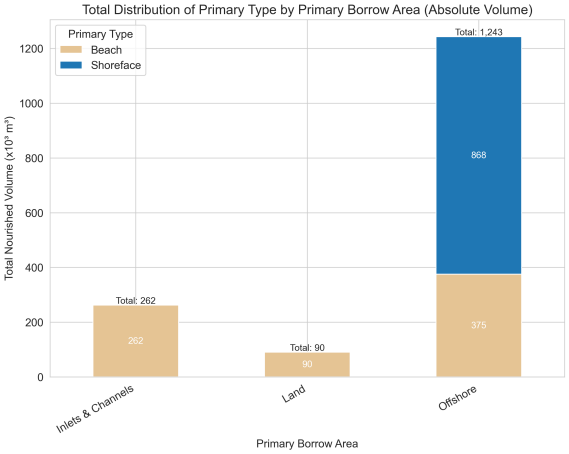

(b) Primary Borrow Area vs. Primary Type

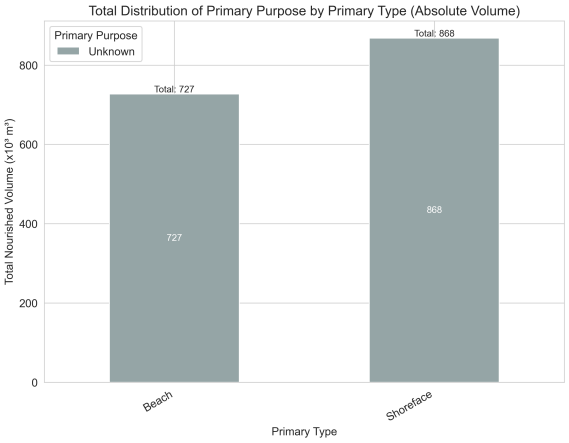

(c) Primary Type vs. Primary Purpose

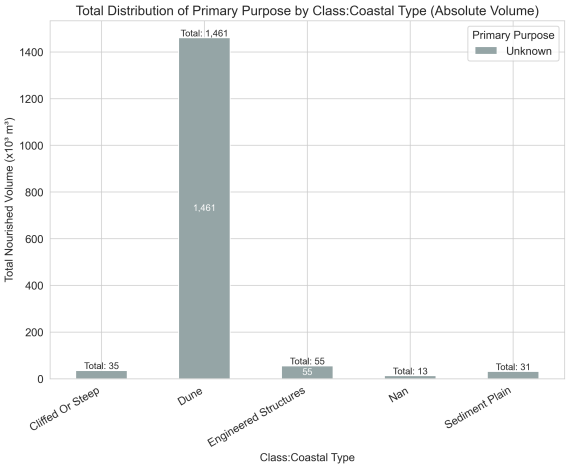

(d) Coastal Type vs. Primary Purpose

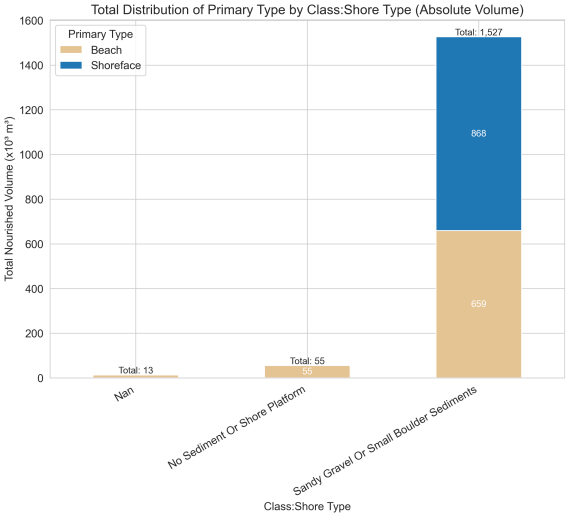

(e) Shore Type vs. Primary Type

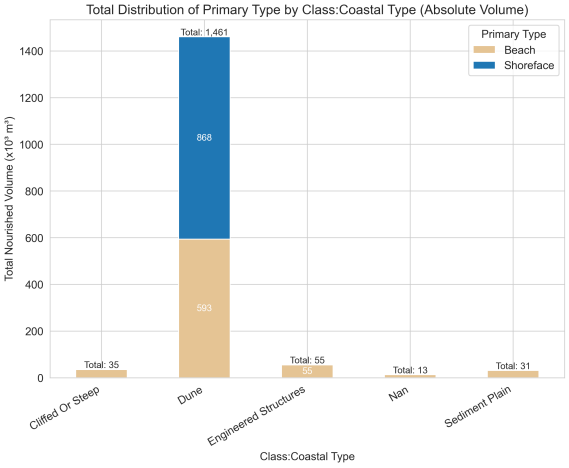

(f) Coastal Type vs. Primary Type

Figure C.9: Stacked Bar Charts Based on Nourished Volumes – Denmark

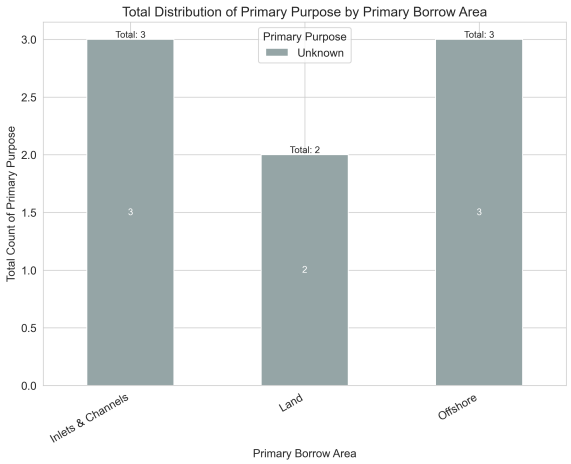

(a) Primary Borrow Area vs. Primary Purpose

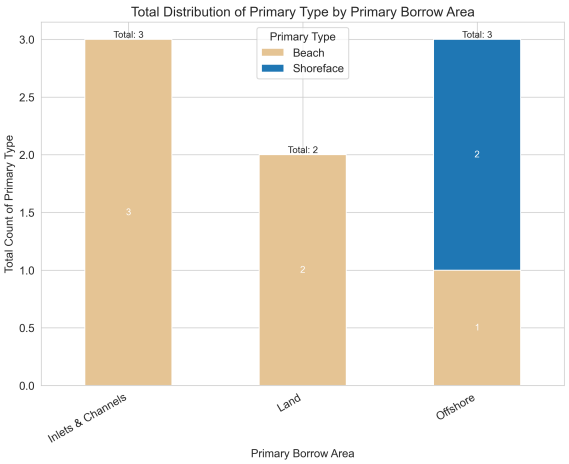

(b) Primary Borrow Area vs. Primary Type

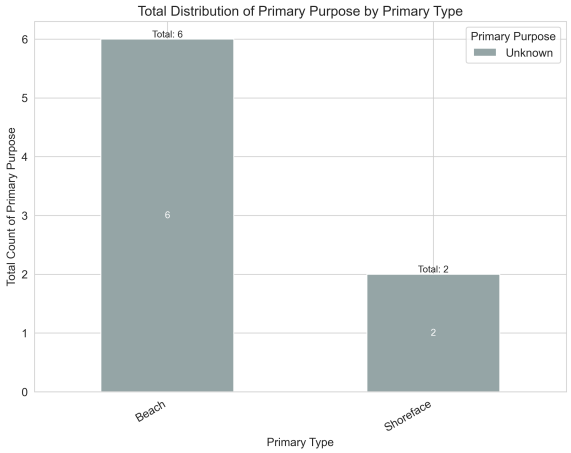

(c) Primary Type vs. Primary Purpose

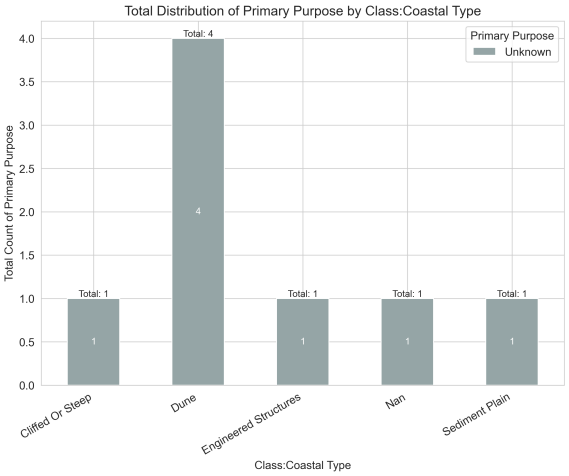

(d) Coastal Type vs. Primary Purpose

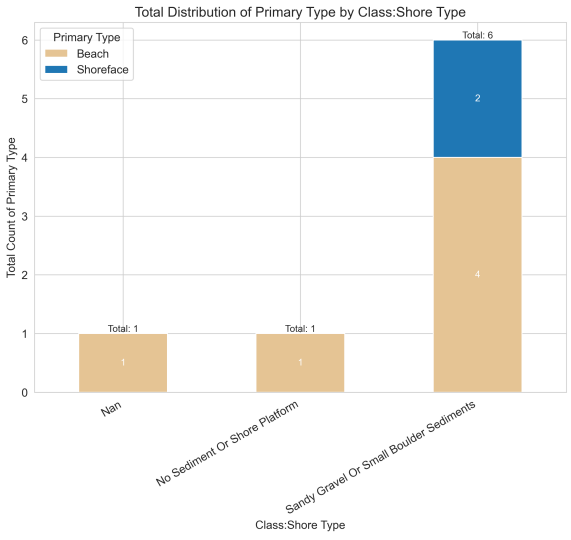

(e) Shore Type vs. Primary Type

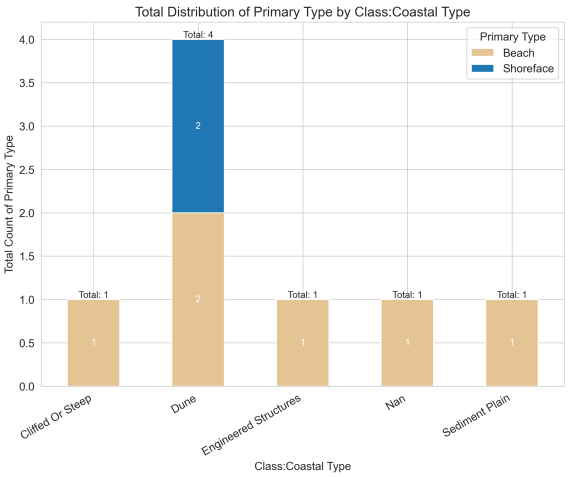

(f) Coastal Type vs. Primary Type

Figure C.10: Stacked Bar Charts Based on Nourishment Count – Denmark

France

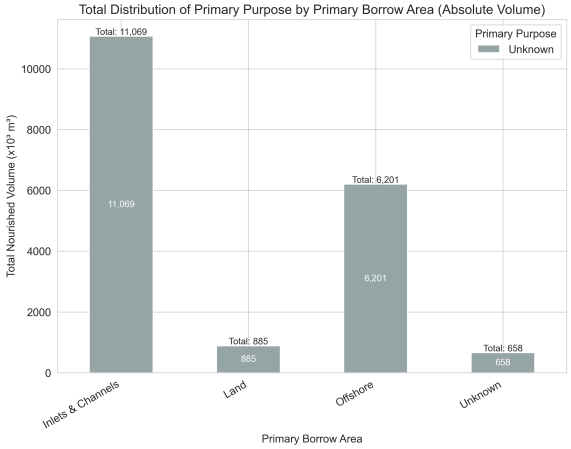

(a) Primary Borrow Area vs. Primary Purpose

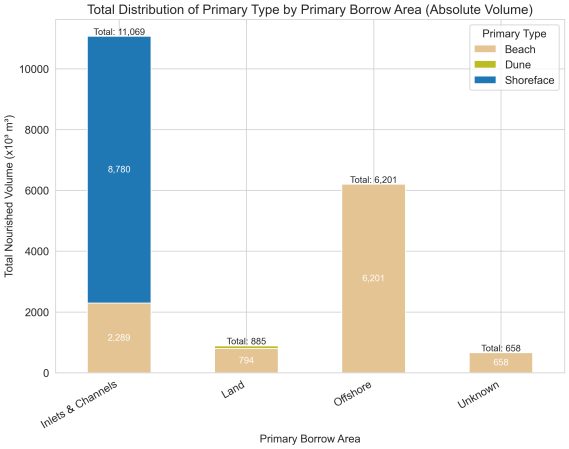

(b) Primary Borrow Area vs. Primary Type

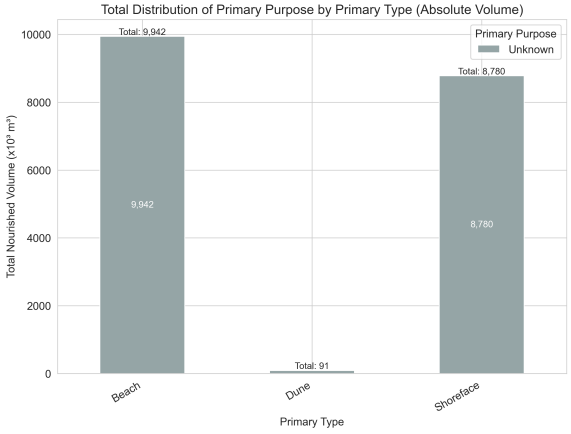

(c) Primary Type vs. Primary Purpose

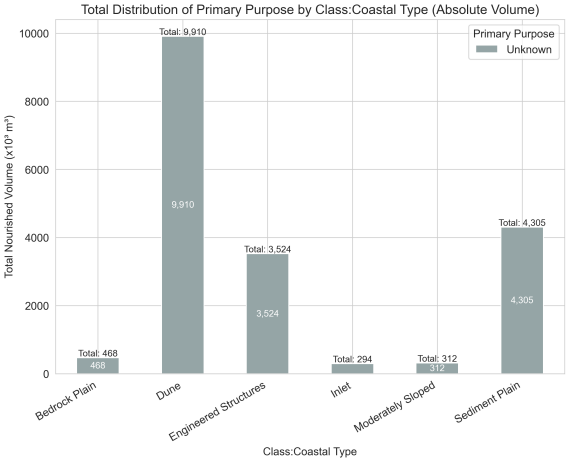

(d) Coastal Type vs. Primary Purpose

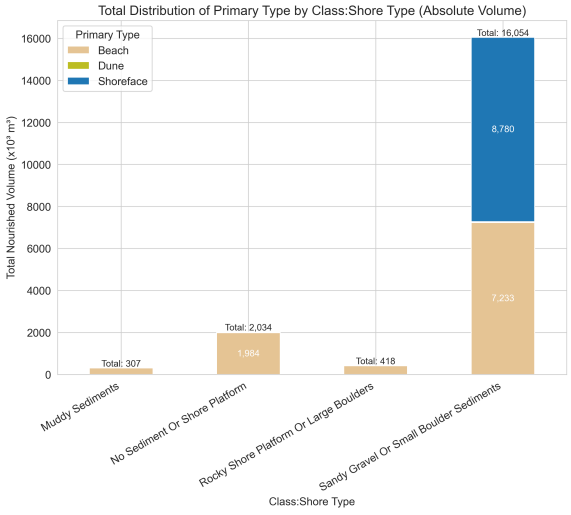

(e) Shore Type vs. Primary Type

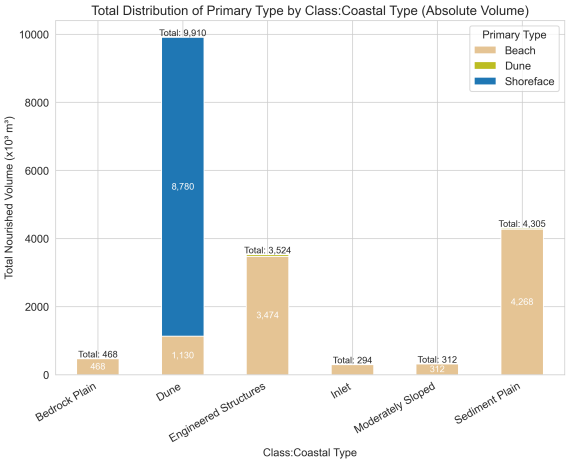

(f) Coastal Type vs. Primary Type

Figure C.11: Stacked Bar Charts Based on Nourished Volumes – France

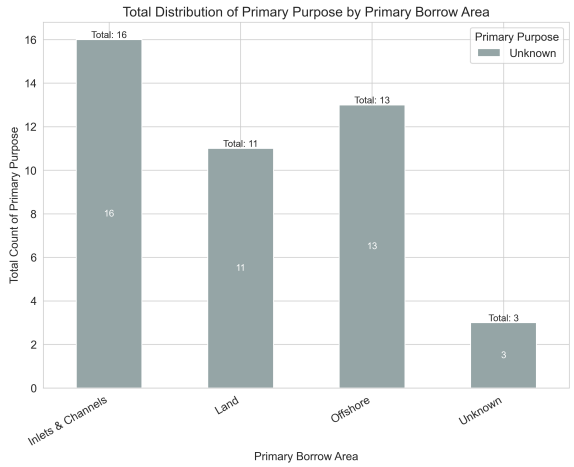

(a) Primary Borrow Area vs. Primary Purpose

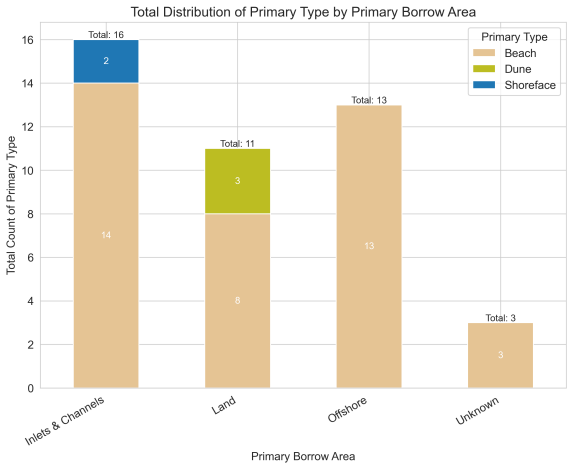

(b) Primary Borrow Area vs. Primary Type

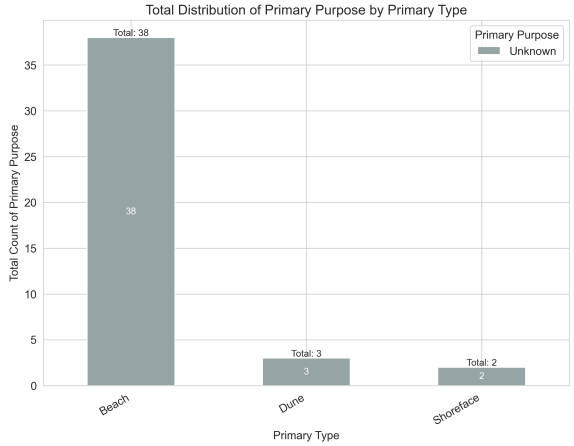

(c) Primary Type vs. Primary Purpose

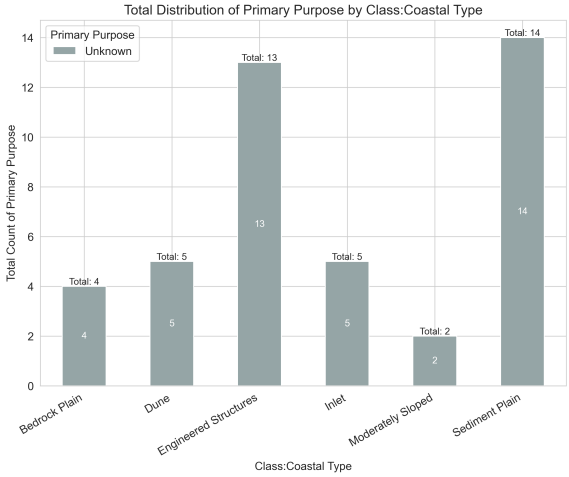

(d) Coastal Type vs. Primary Purpose

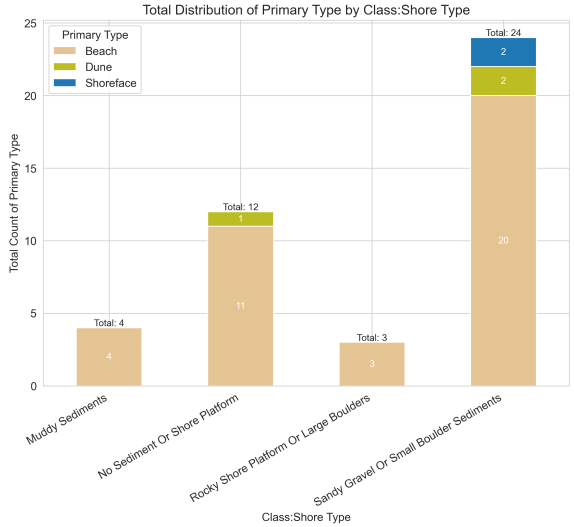

(e) Shore Type vs. Primary Type

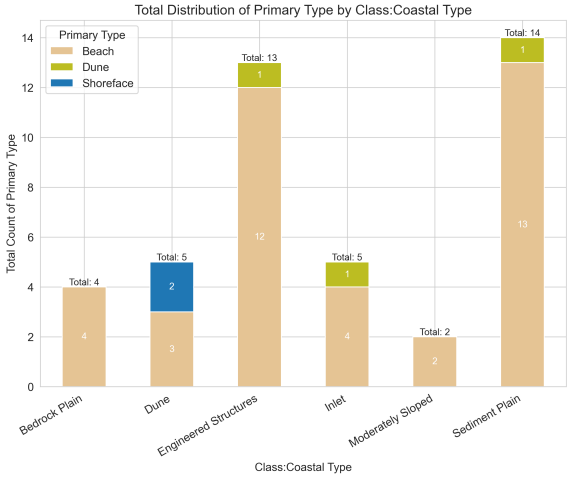

(f) Coastal Type vs. Primary Type

Figure C.12: Stacked Bar Charts Based on Nourishment Count – France

Germany

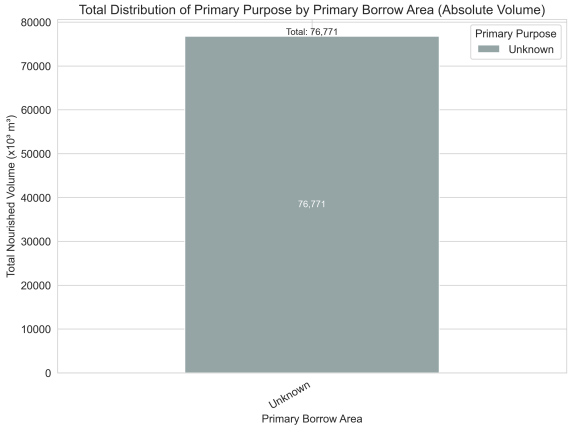

(a) Primary Borrow Area vs. Primary Purpose

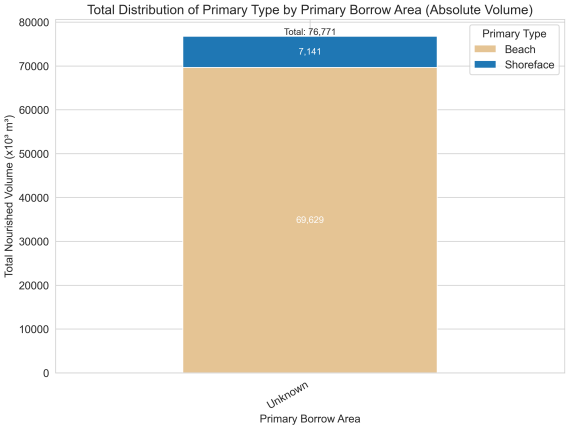

(b) Primary Borrow Area vs. Primary Type

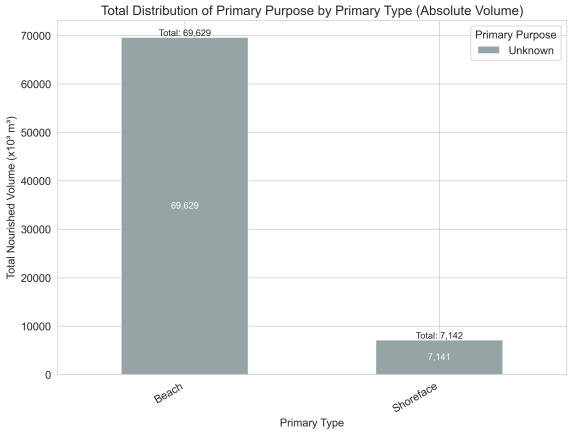

(c) Primary Type vs. Primary Purpose

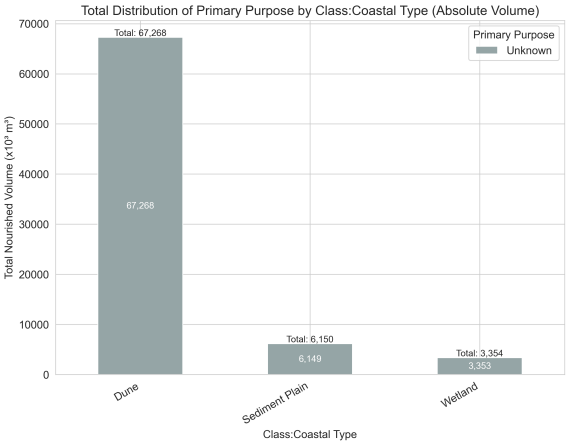

(d) Coastal Type vs. Primary Purpose

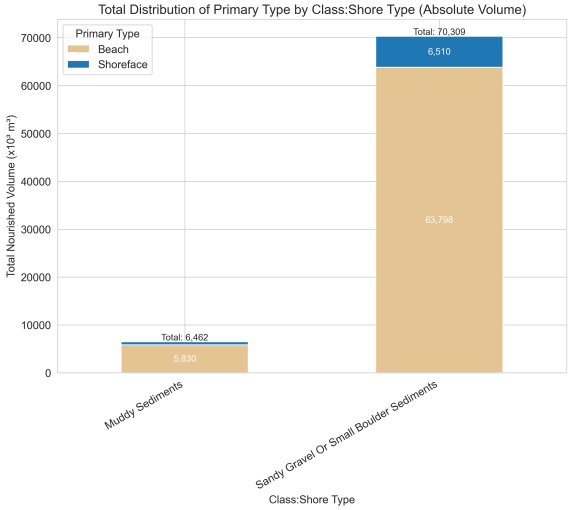

(e) Shore Type vs. Primary Type

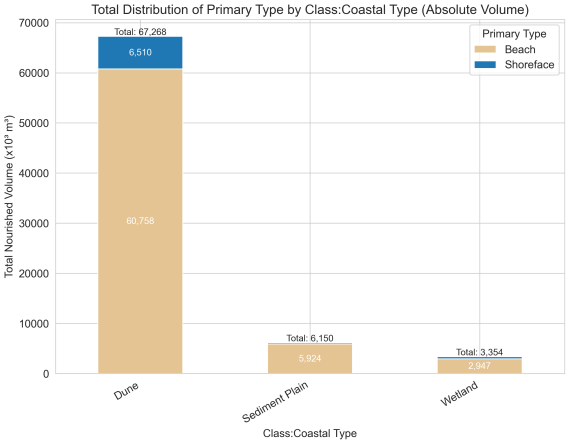

(f) Coastal Type vs. Primary Type

Figure C.13: Stacked Bar Charts Based on Nourished Volumes – Germany

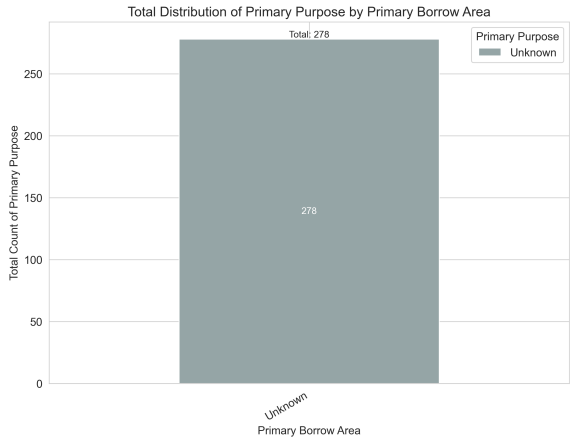

(a) Primary Borrow Area vs. Primary Purpose

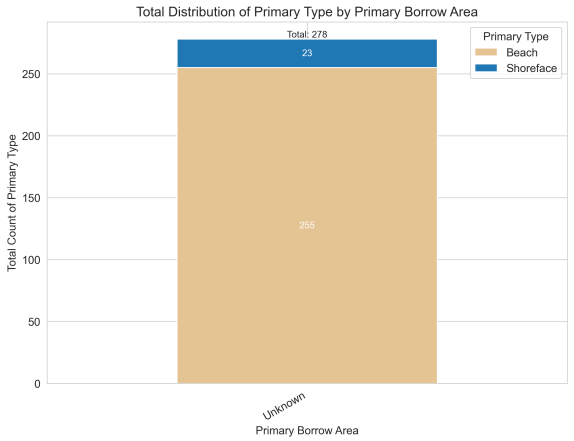

(b) Primary Borrow Area vs. Primary Type

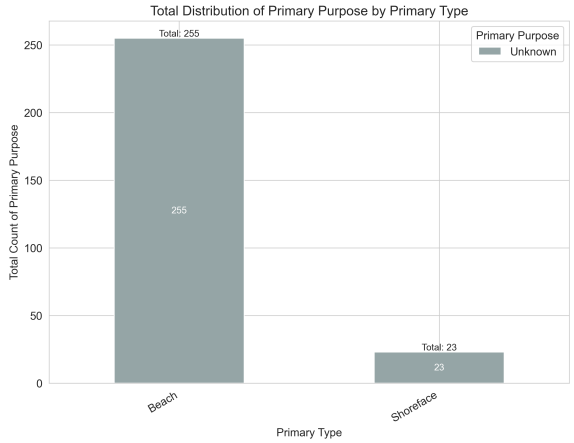

(c) Primary Type vs. Primary Purpose

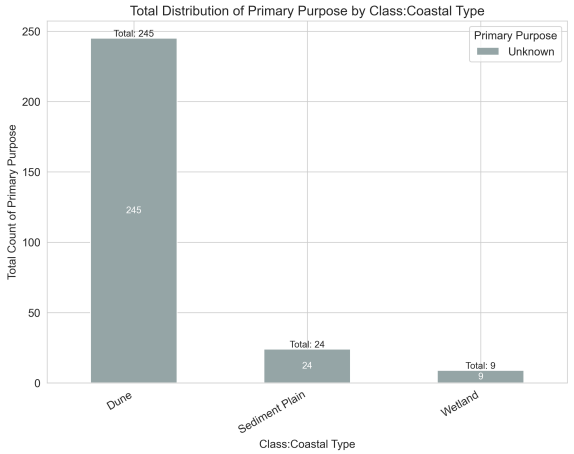

(d) Coastal Type vs. Primary Purpose

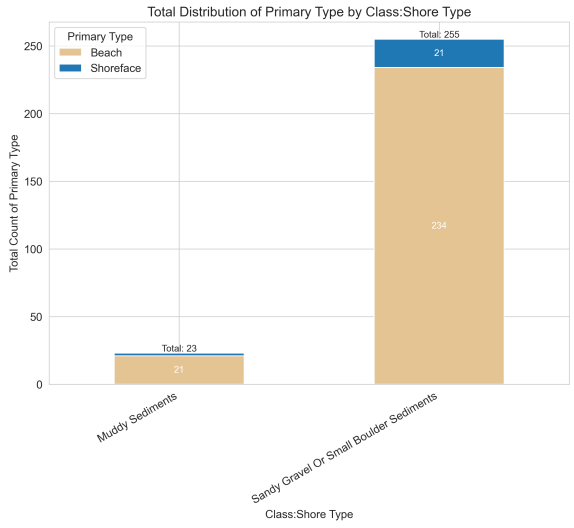

(e) Shore Type vs. Primary Type

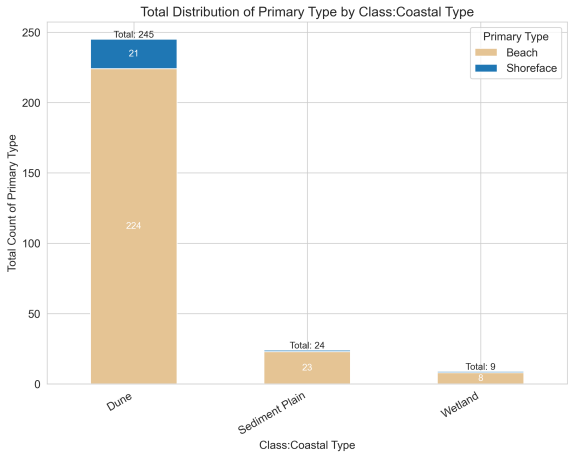

(f) Coastal Type vs. Primary Type

Figure C.14: Stacked Bar Charts Based on Nourishment Count – Germany

Italy

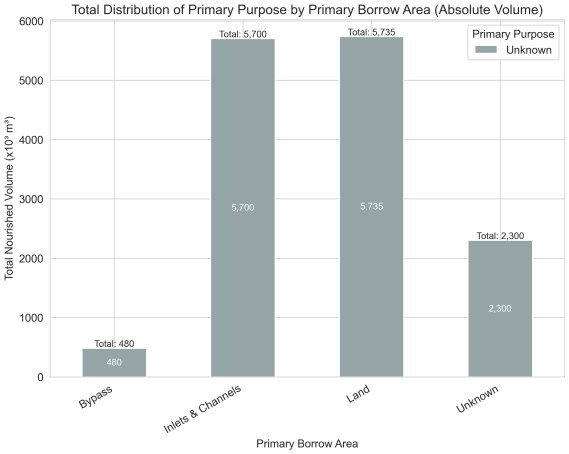

(a) Primary Borrow Area vs. Primary Purpose

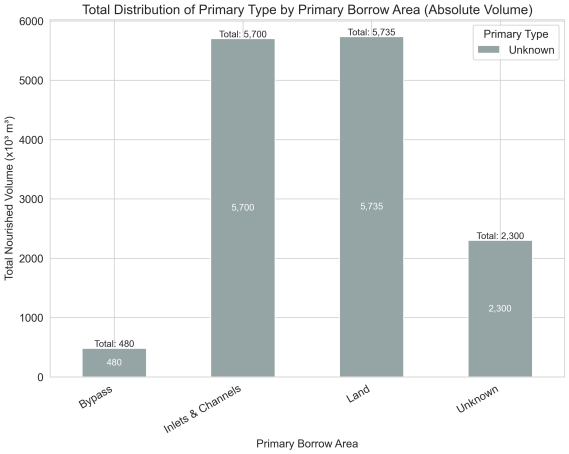

(b) Primary Borrow Area vs. Primary Type

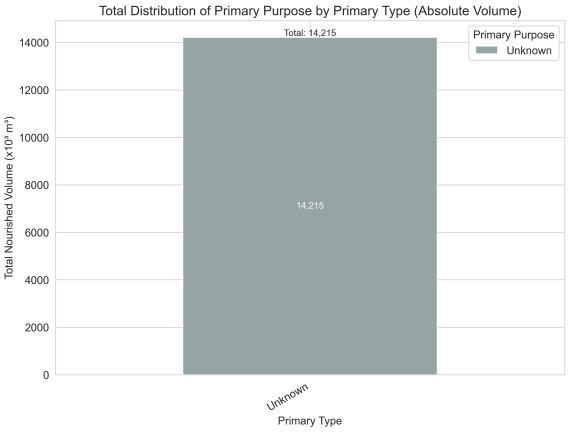

(c) Primary Type vs. Primary Purpose

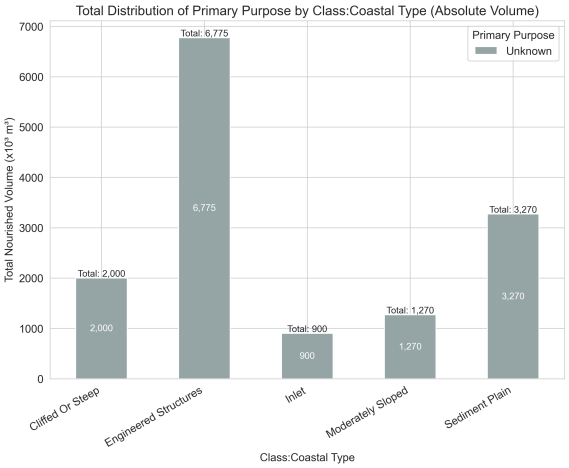

(d) Coastal Type vs. Primary Purpose

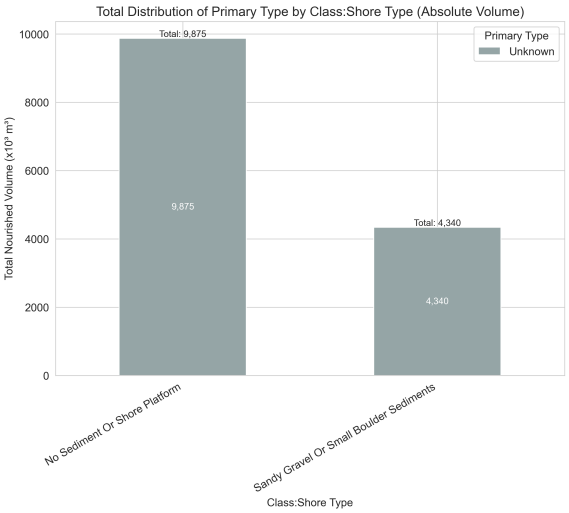

(e) Shore Type vs. Primary Type

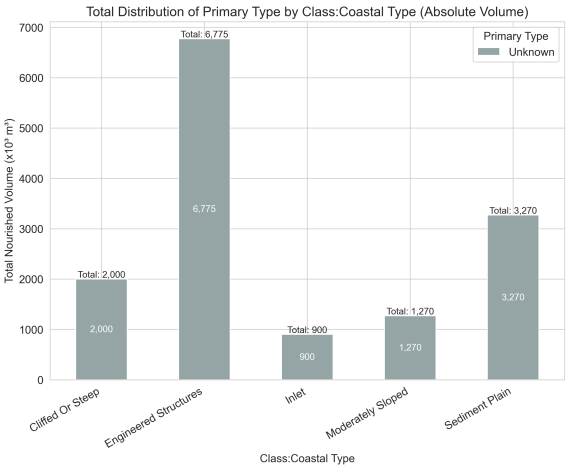

(f) Coastal Type vs. Primary Type

Figure C.15: Stacked Bar Charts Based on Nourished Volumes – Italy

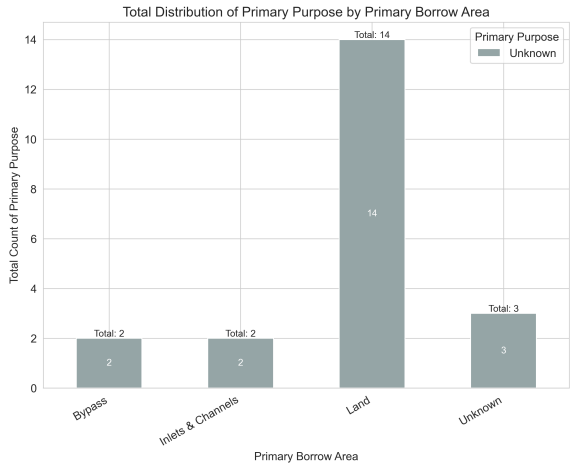

(a) Primary Borrow Area vs. Primary Purpose

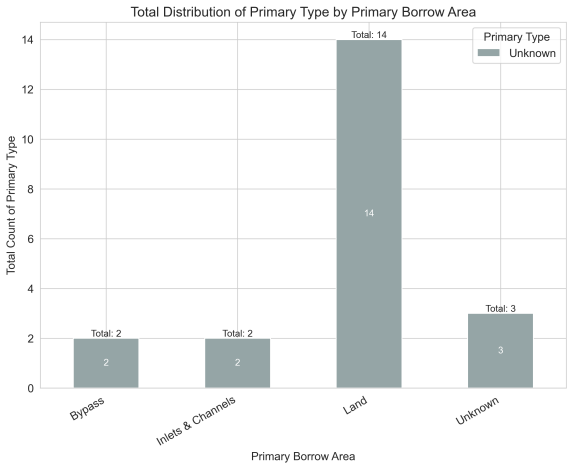

(b) Primary Borrow Area vs. Primary Type

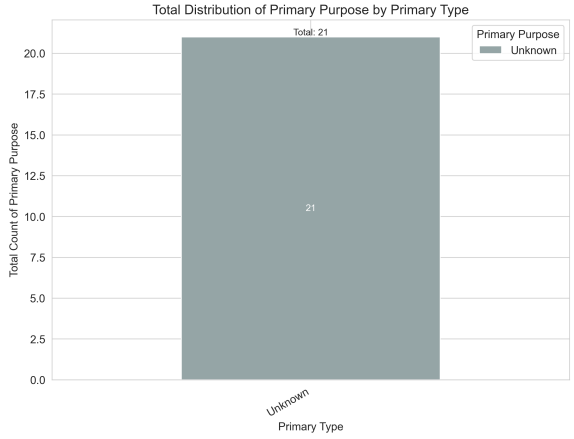

(c) Primary Type vs. Primary Purpose

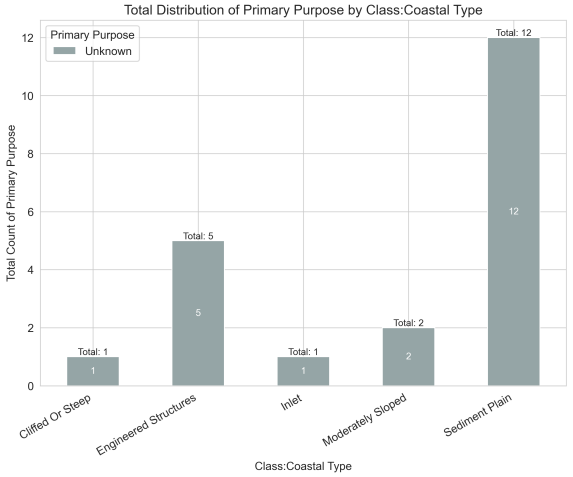

(d) Coastal Type vs. Primary Purpose

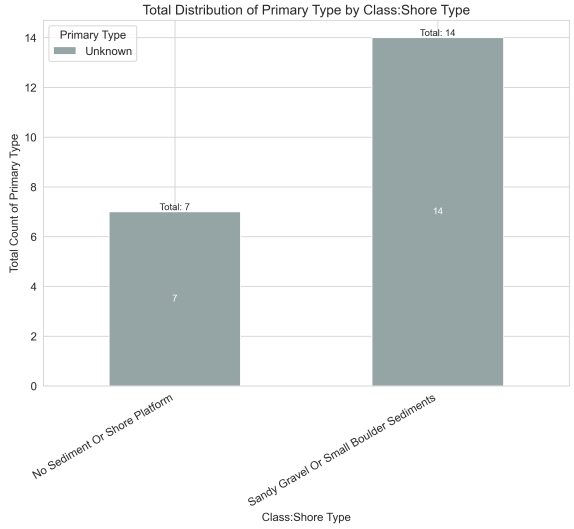

(e) Shore Type vs. Primary Type

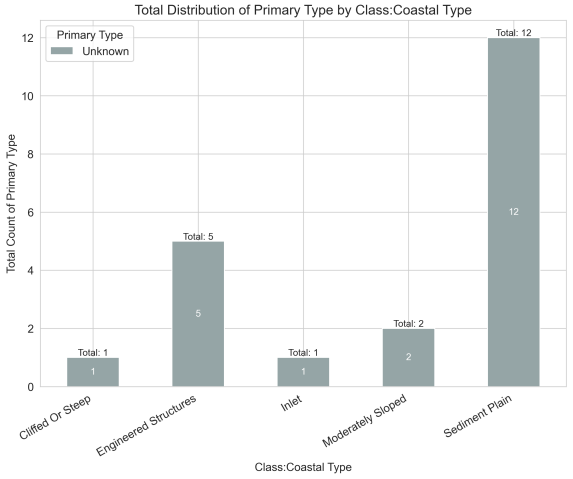

(f) Coastal Type vs. Primary Type

Figure C.16: Stacked Bar Charts Based on Nourishment Count – Italy

Netherlands

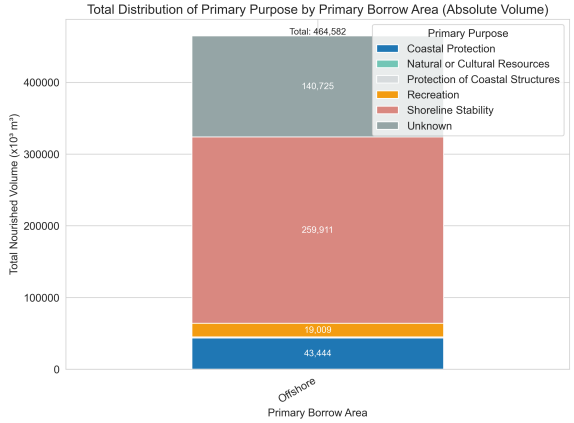

(a) Primary Borrow Area vs. Primary Purpose

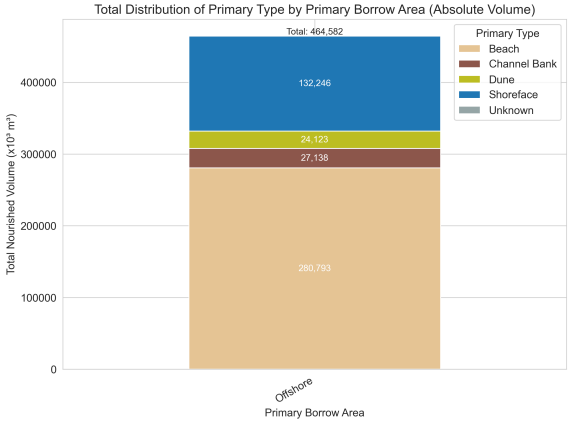

(b) Primary Borrow Area vs. Primary Type

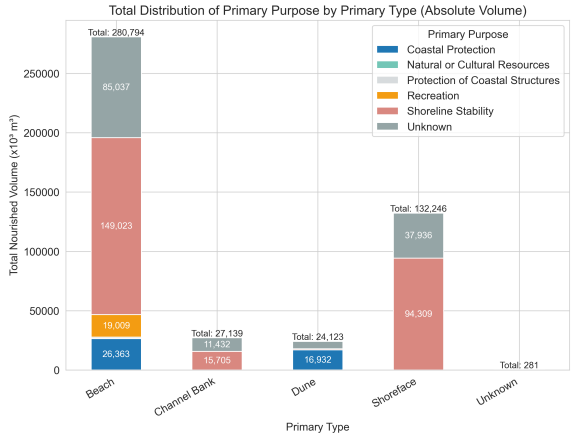

(c) Primary Type vs. Primary Purpose

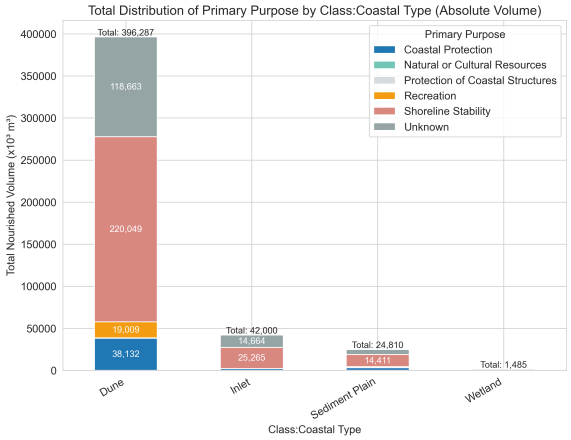

(d) Coastal Type vs. Primary Purpose

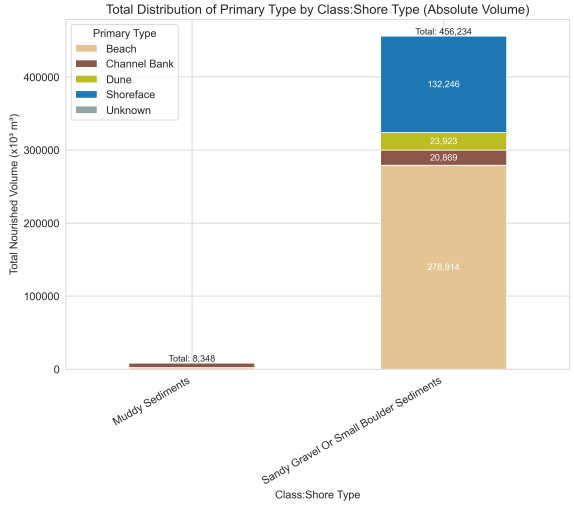

(e) Shore Type vs. Primary Type

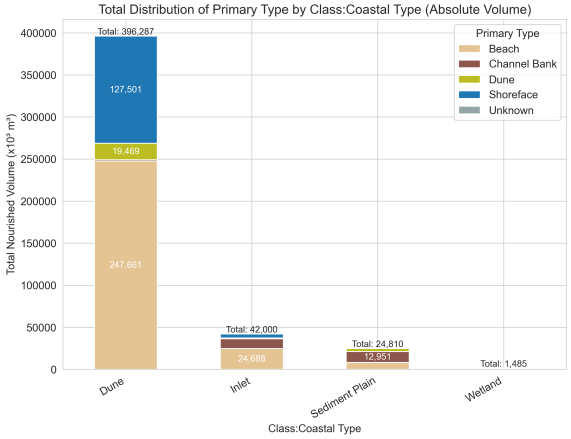

(f) Coastal Type vs. Primary Type

Figure C.17: Stacked Bar Charts Based on Nourished Volumes – Netherlands

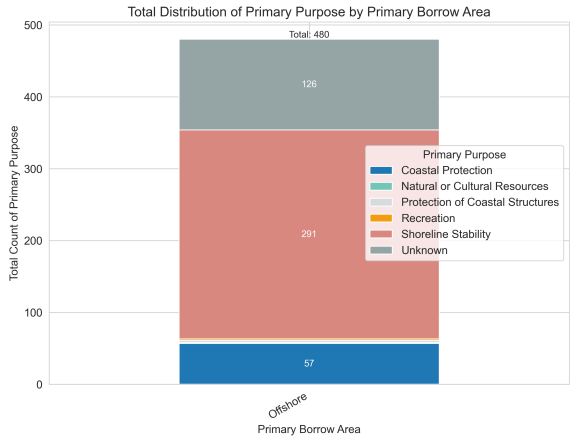

(a) Primary Borrow Area vs. Primary Purpose

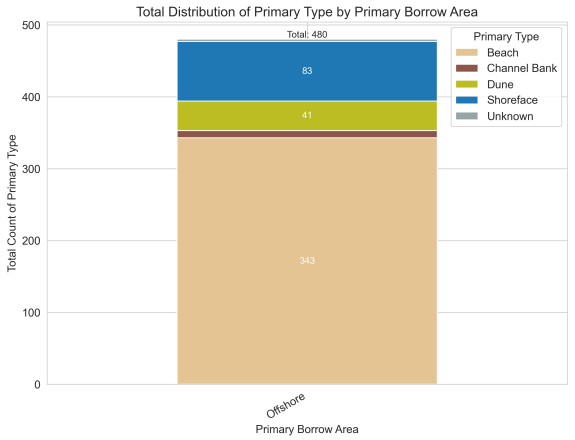

(b) Primary Borrow Area vs. Primary Type

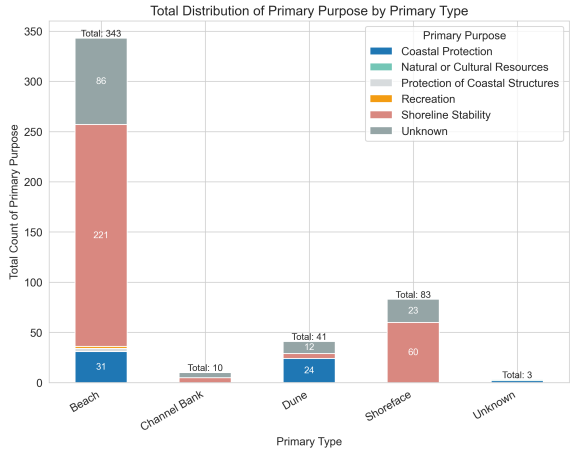

(c) Primary Type vs. Primary Purpose

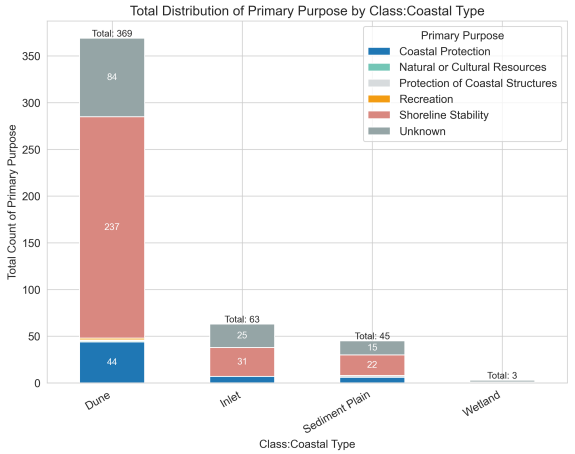

(d) Coastal Type vs. Primary Purpose

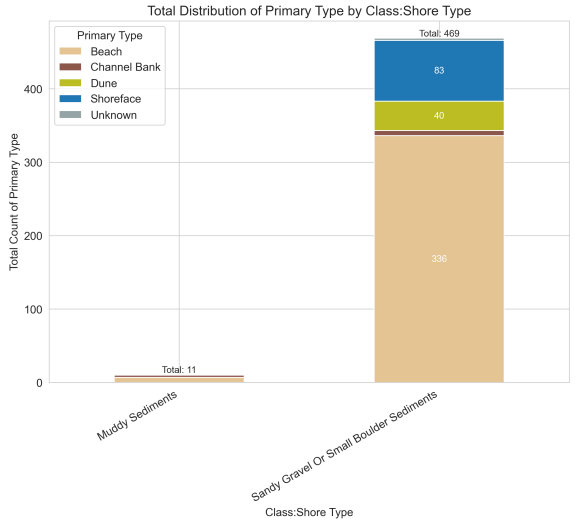

(e) Shore Type vs. Primary Type

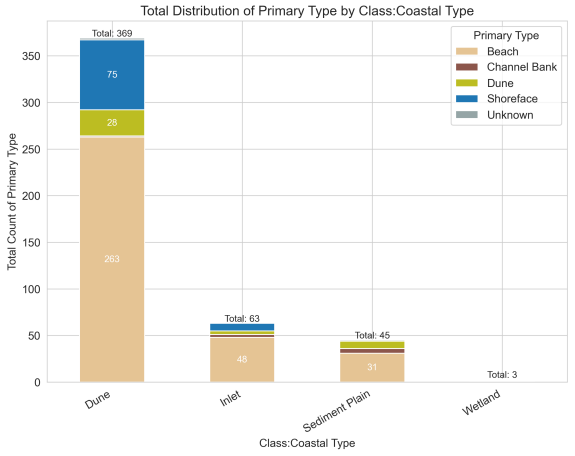

(f) Coastal Type vs. Primary Type

Figure C.18: Stacked Bar Charts Based on Nourishment Count – Netherlands

Portugal

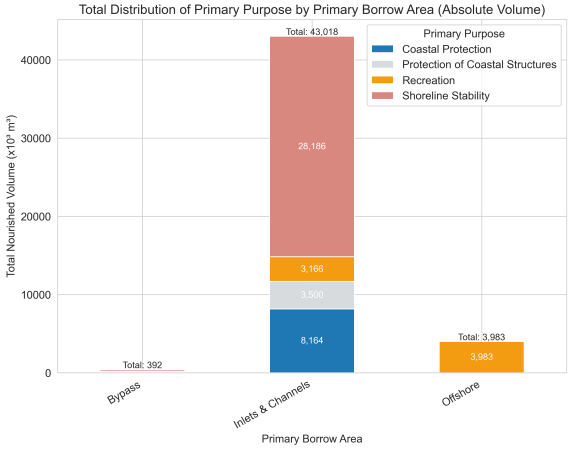

(a) Primary Borrow Area vs. Primary Purpose

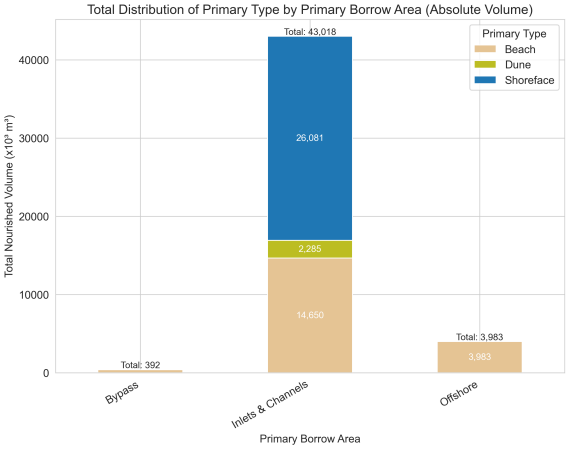

(b) Primary Borrow Area vs. Primary Type

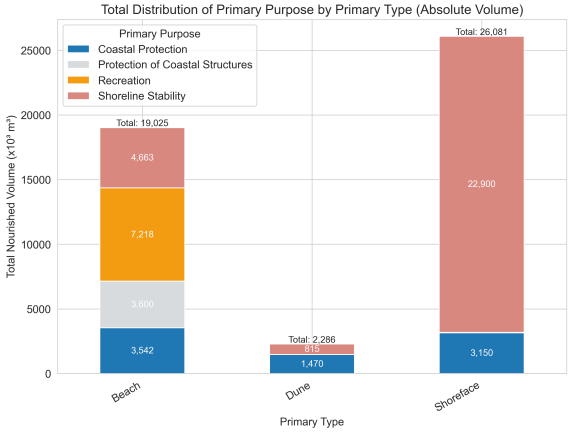

(c) Primary Type vs. Primary Purpose

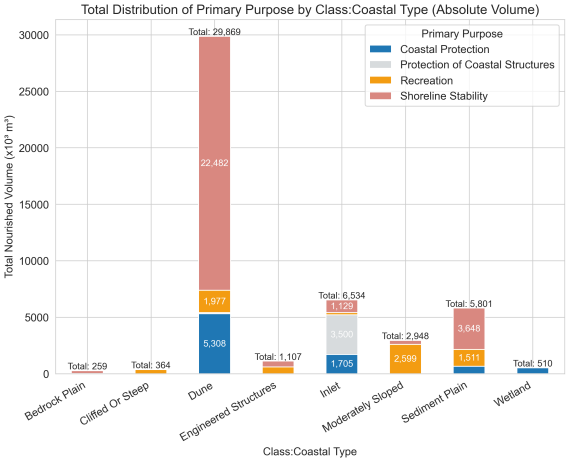

(d) Coastal Type vs. Primary Purpose

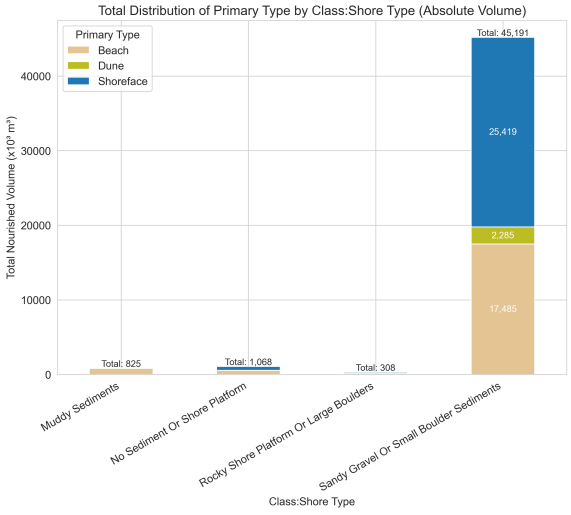

(e) Shore Type vs. Primary Type

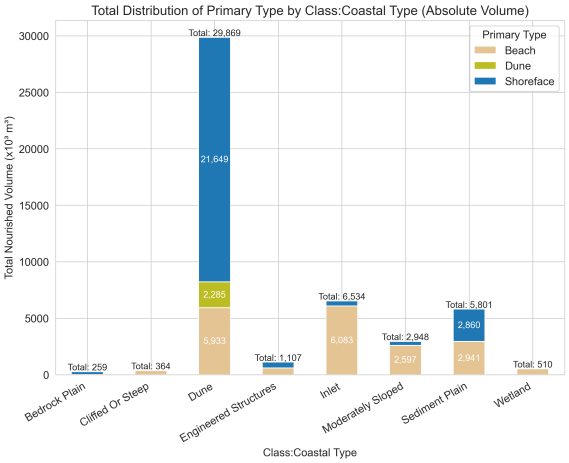

(f) Coastal Type vs. Primary Type

Figure C.19: Stacked Bar Charts Based on Nourished Volumes – Portugal

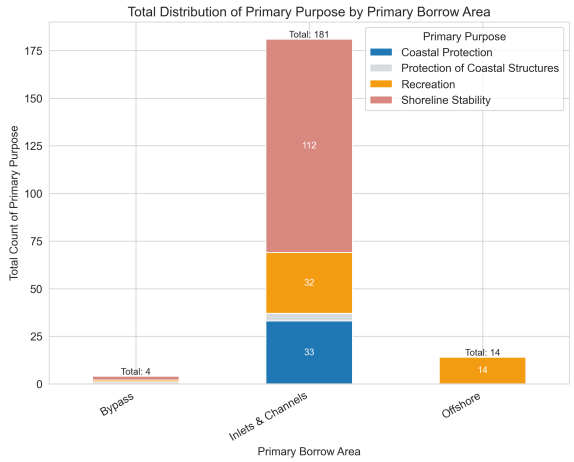

(a) Primary Borrow Area vs. Primary Purpose

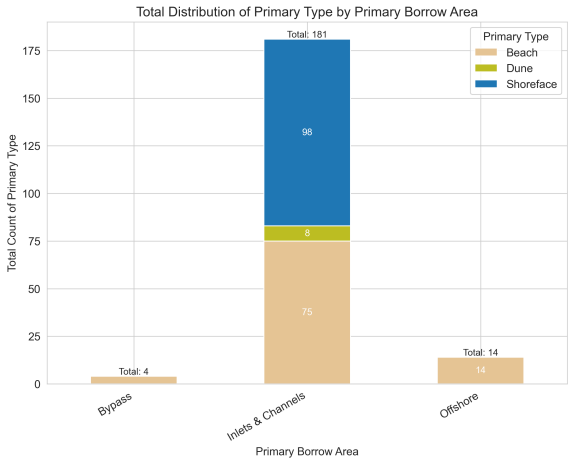

(b) Primary Borrow Area vs. Primary Type

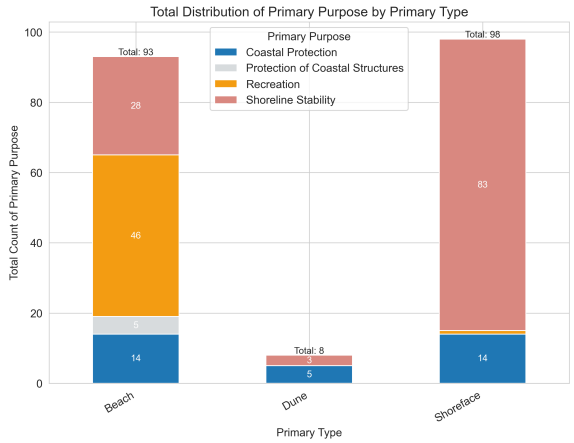

(c) Primary Type vs. Primary Purpose

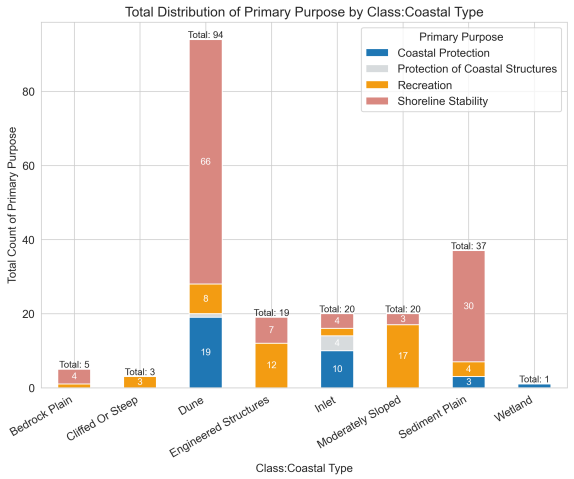

(d) Coastal Type vs. Primary Purpose

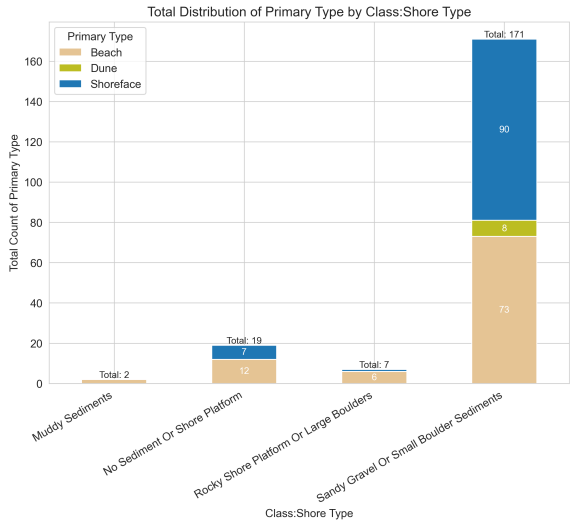

(e) Shore Type vs. Primary Type

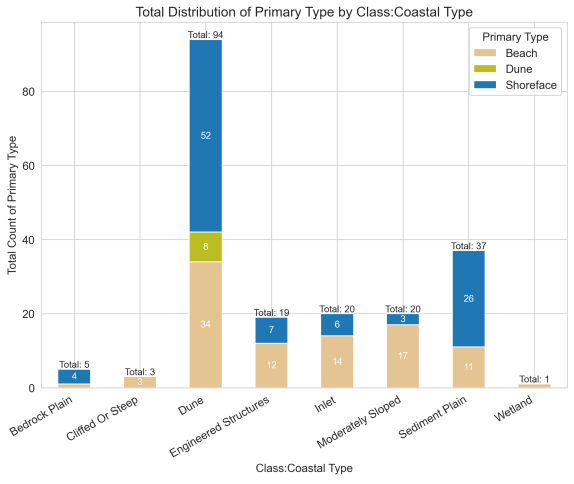

(f) Coastal Type vs. Primary Type

Figure C.20: Stacked Bar Charts Based on Nourishment Count – Portugal

Spain

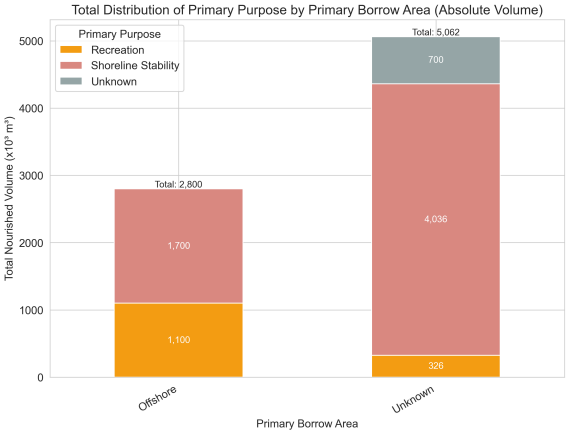

(a) Primary Borrow Area vs. Primary Purpose

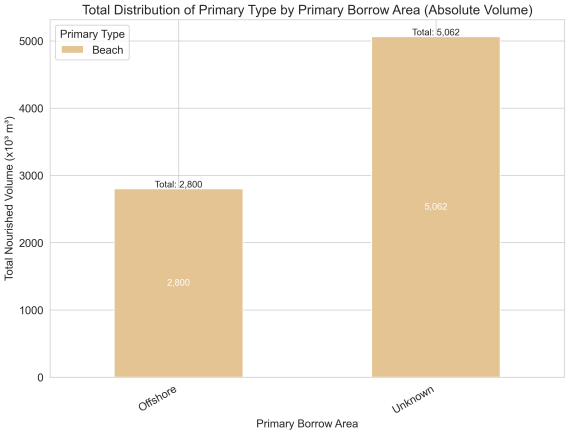

(b) Primary Borrow Area vs. Primary Type

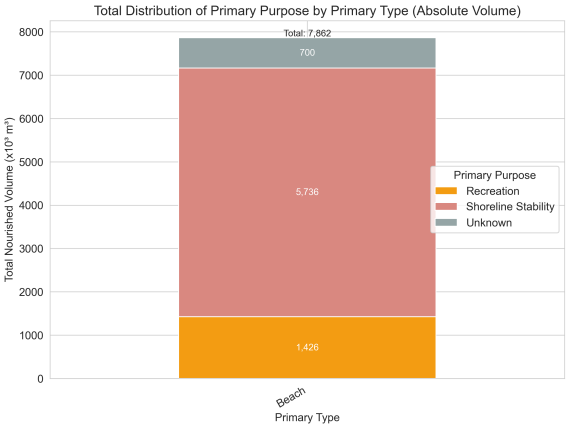

(c) Primary Type vs. Primary Purpose

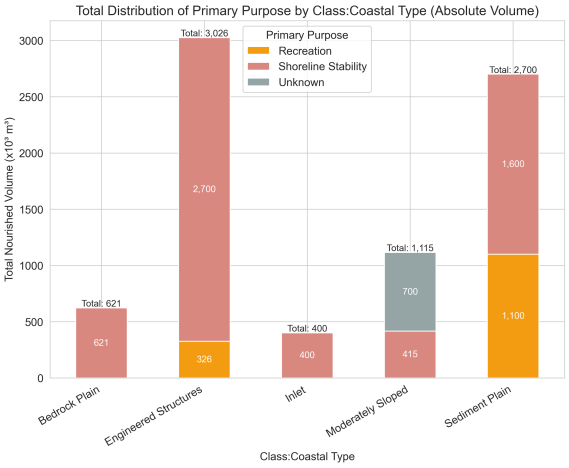

(d) Coastal Type vs. Primary Purpose

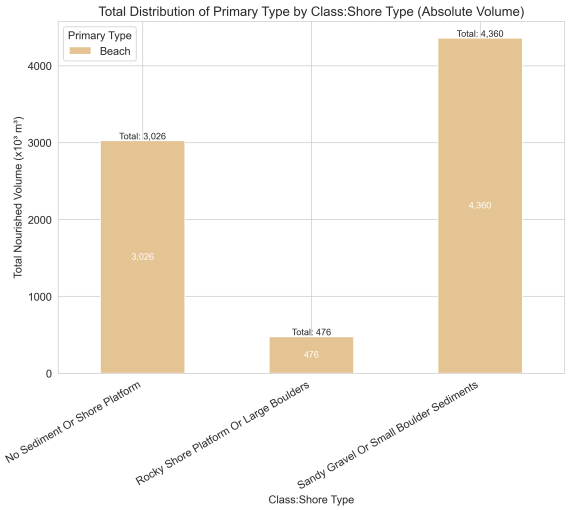

(e) Shore Type vs. Primary Type

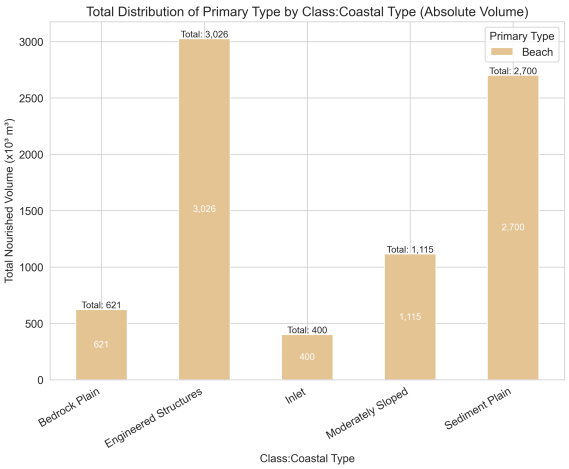

(f) Coastal Type vs. Primary Type

Figure C.21: Stacked Bar Charts Based on Nourished Volumes – Spain

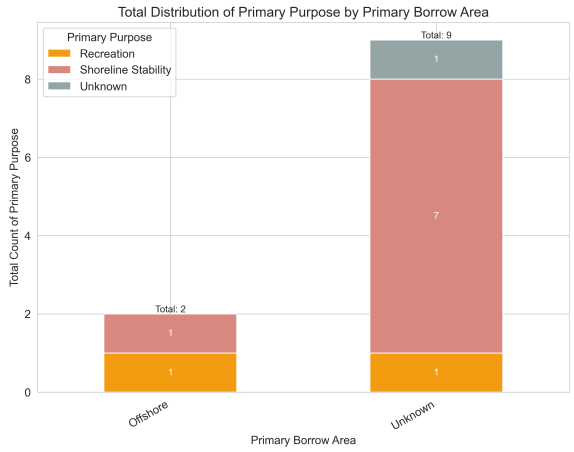

(a) Primary Borrow Area vs. Primary Purpose

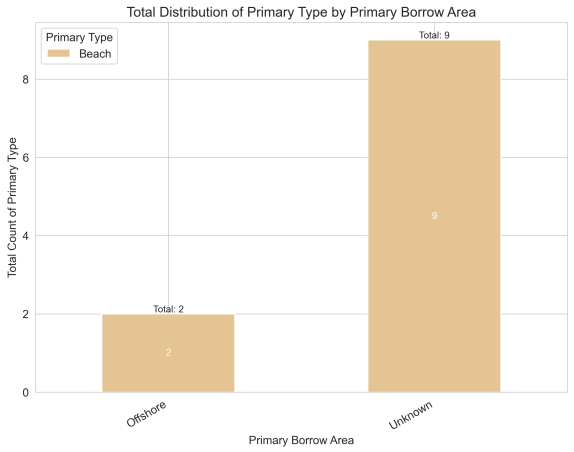

(b) Primary Borrow Area vs. Primary Type

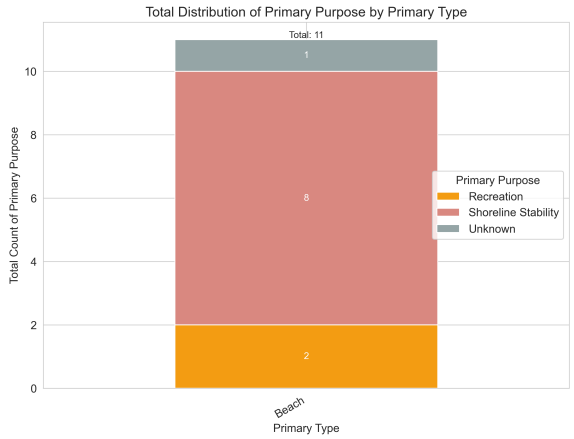

(c) Primary Type vs. Primary Purpose

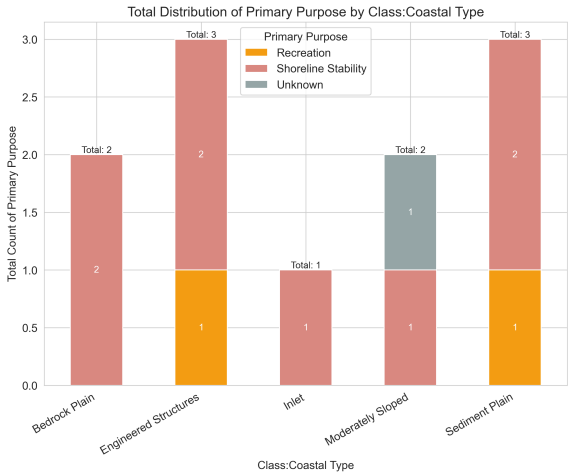

(d) Coastal Type vs. Primary Purpose

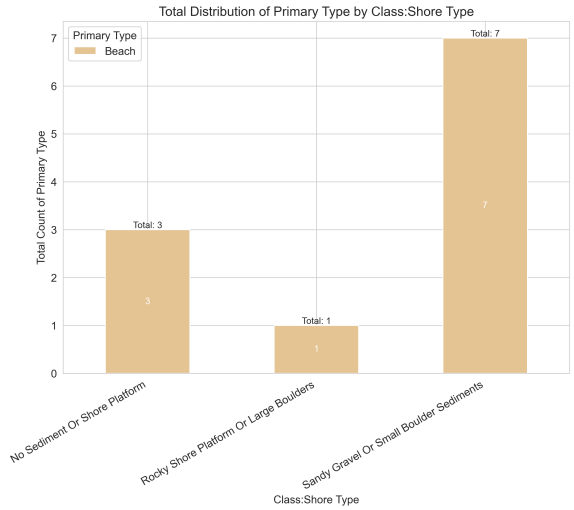

(e) Shore Type vs. Primary Type

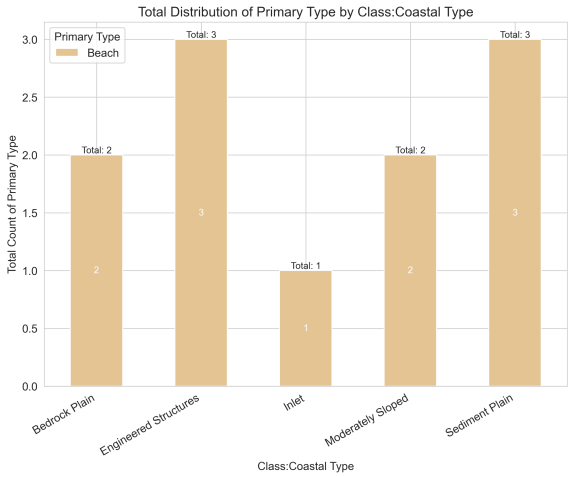

(f) Coastal Type vs. Primary Type

Figure C.22: Stacked Bar Charts Based on Nourishment Count – Spain

Sweden

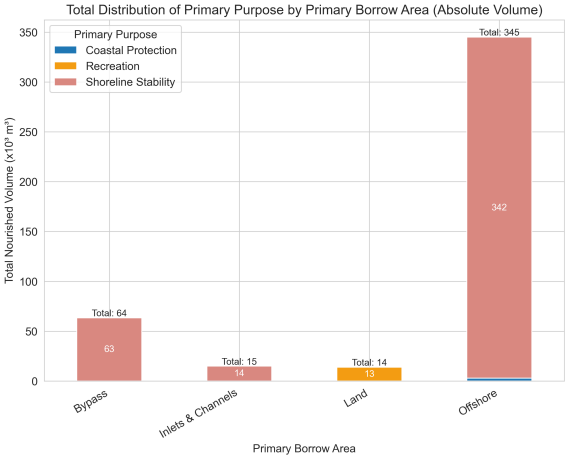

(a) Primary Borrow Area vs. Primary Purpose

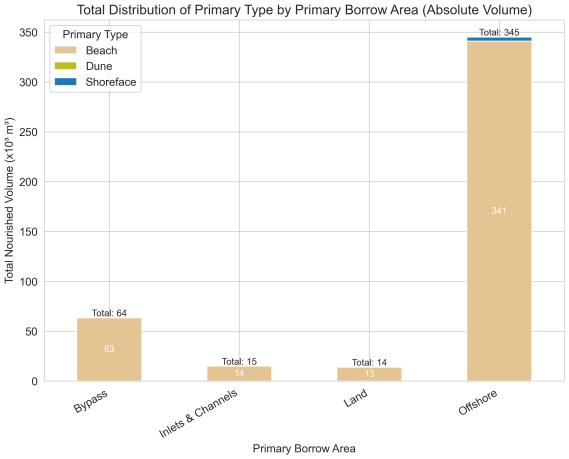

(b) Primary Borrow Area vs. Primary Type

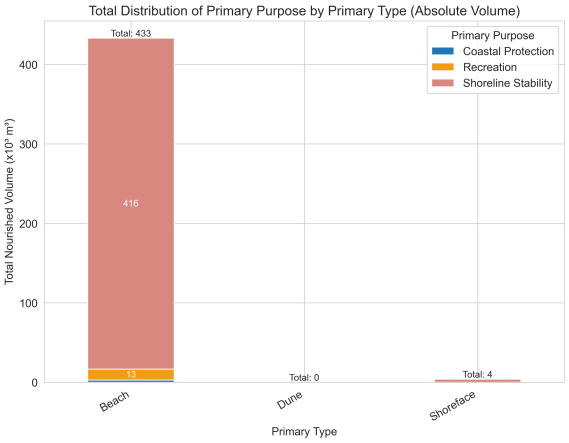

(c) Primary Type vs. Primary Purpose

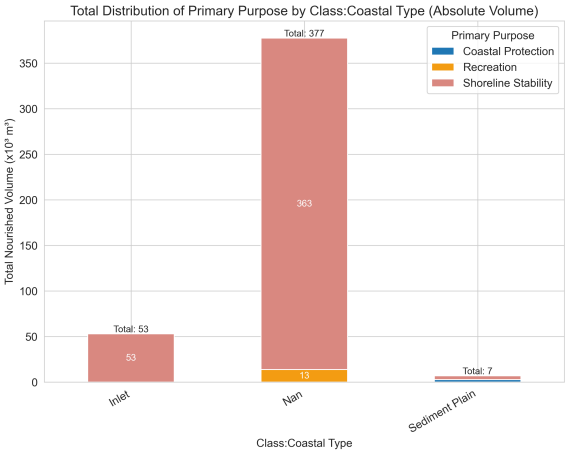

(d) Coastal Type vs. Primary Purpose

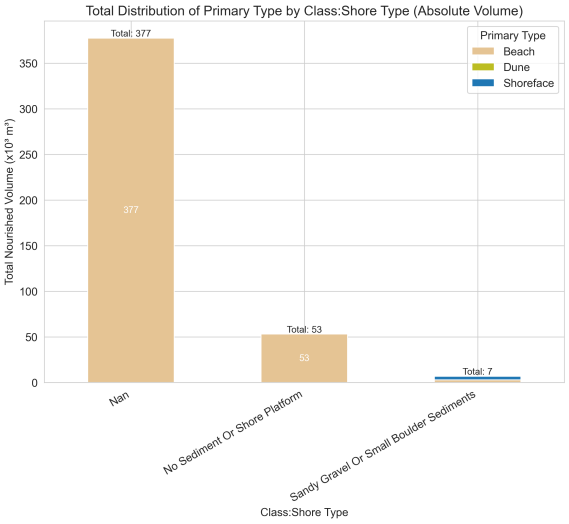

(e) Shore Type vs. Primary Type

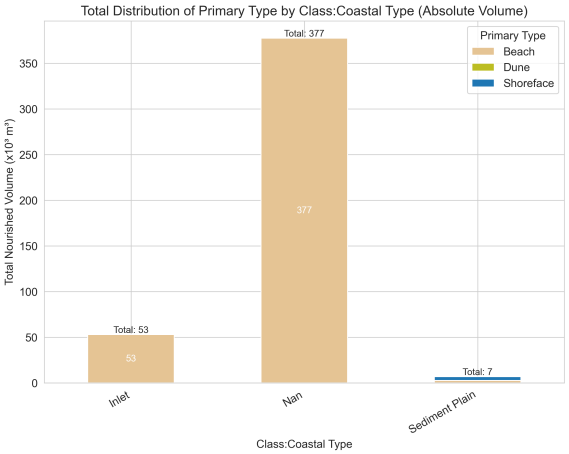

(f) Coastal Type vs. Primary Type

Figure C.23: Stacked Bar Charts Based on Nourished Volumes – Sweden

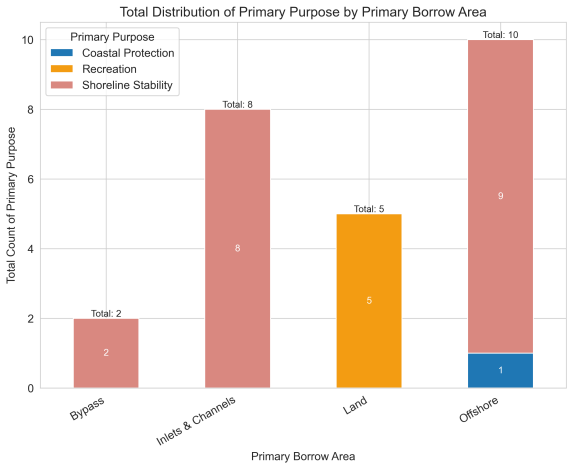

(a) Primary Borrow Area vs. Primary Purpose

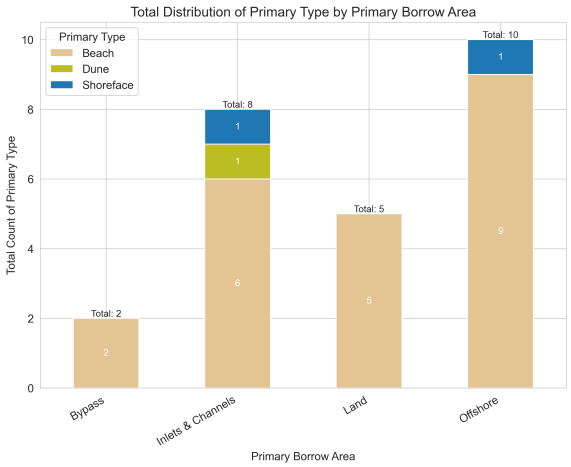

(b) Primary Borrow Area vs. Primary Type

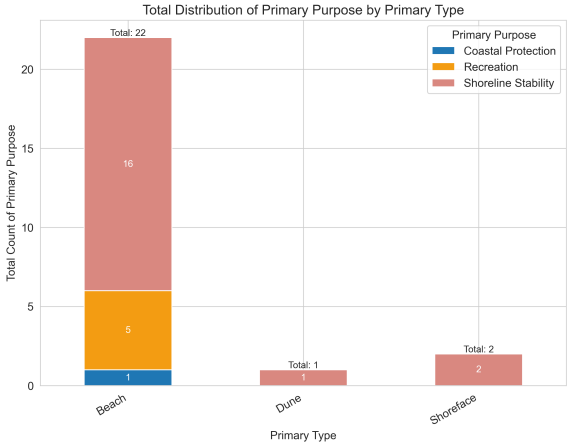

(c) Primary Type vs. Primary Purpose

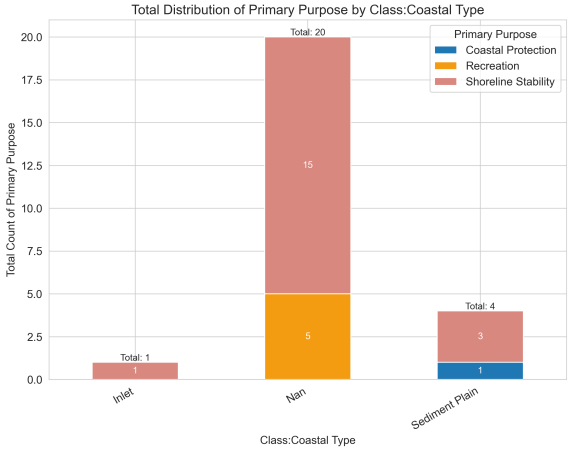

(d) Coastal Type vs. Primary Purpose

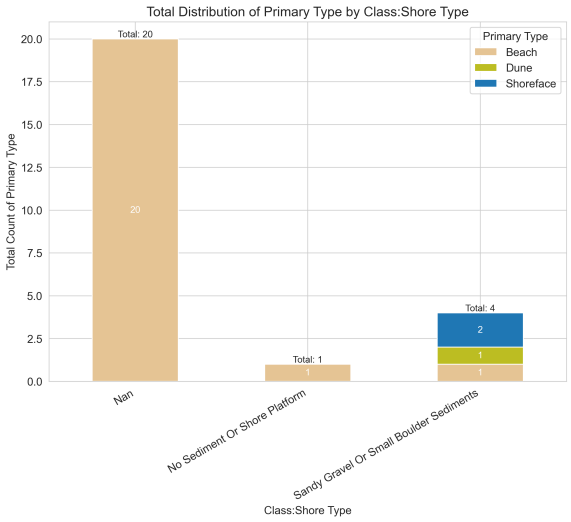

(e) Shore Type vs. Primary Type

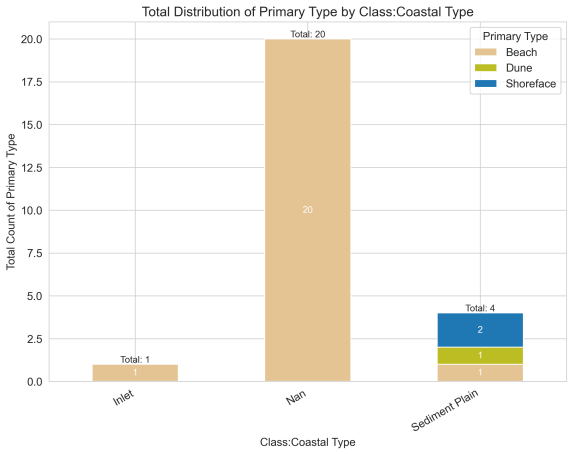

(f) Coastal Type vs. Primary Type

Figure C.24: Stacked Bar Charts Based on Nourishment Count – Sweden

C.3. Distribution Shore- and Coastal Types

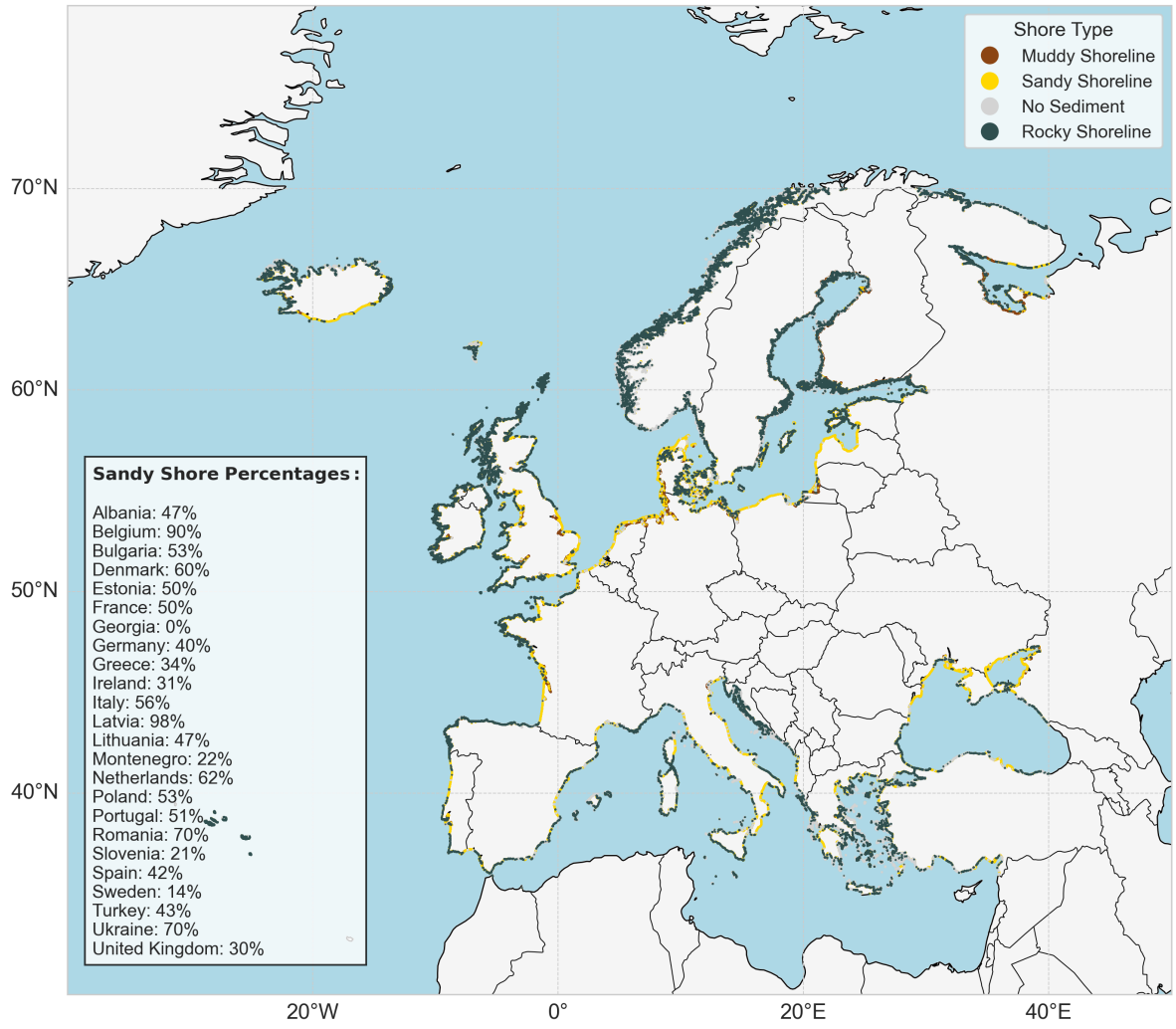

Figure C.25: Distribution of shore types across Europe. The percentage of sandy shorelines per country is included in the left corner. This figure highlights the regional focus of the analysis, which is limited to sandy coasts.

Figure C.26: Distribution of coastal types within sandy shorelines across Europe. This plot shows the variety of geomorphological contexts in which nourishments are applied.

C.4. Detailed Analysis of Nourishment Dynamics

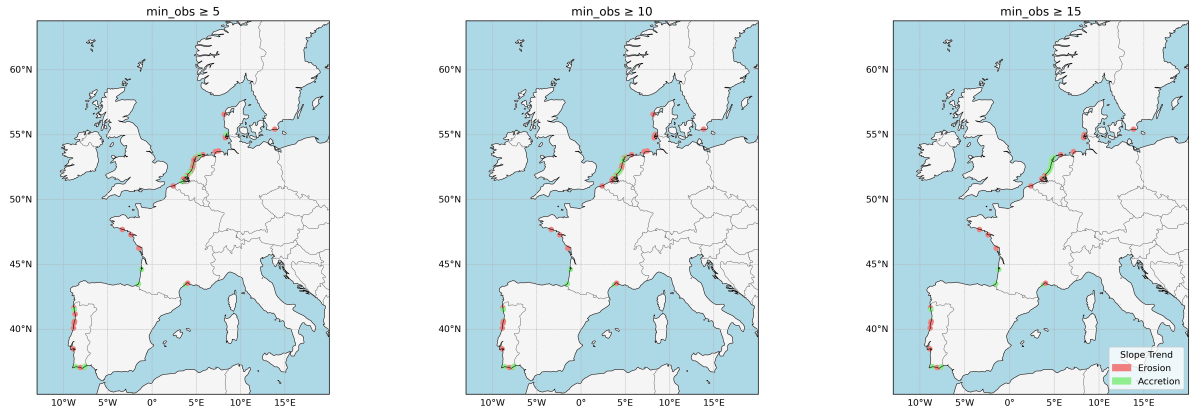

Figure C.27: Spatial distribution of transects showing erosive (red) and accretive (green) shoreline trends prior to nourishment, for three levels of observational coverage.

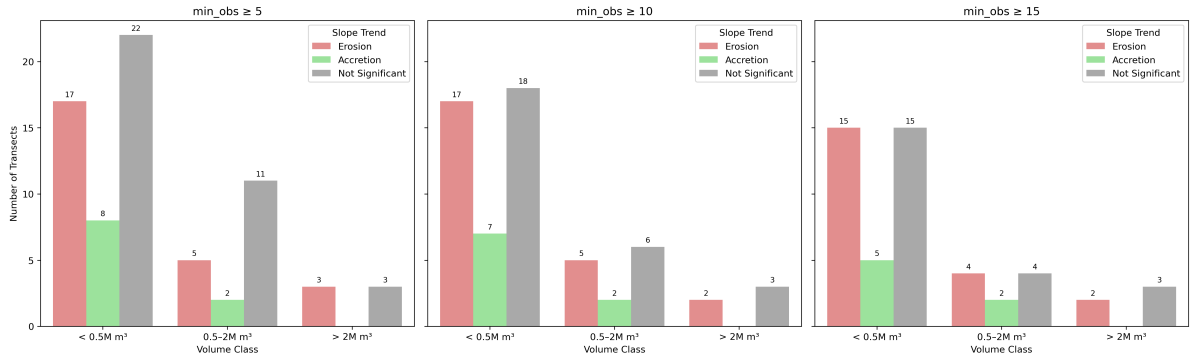

Figure C.28: Pre-nourishment slope trend classification by nourishment volume class, excluding all transects along the Dutch coast.

C.5. Projection outputs

This appendix presents all projection outputs. It begins with ambient shoreline change across the three time steps, followed by sea-level rise (SLR)-induced **change** for all scenarios and years, as well as SLR-induced **retreat**. Finally, combined **change** and **retreat** projections are included.

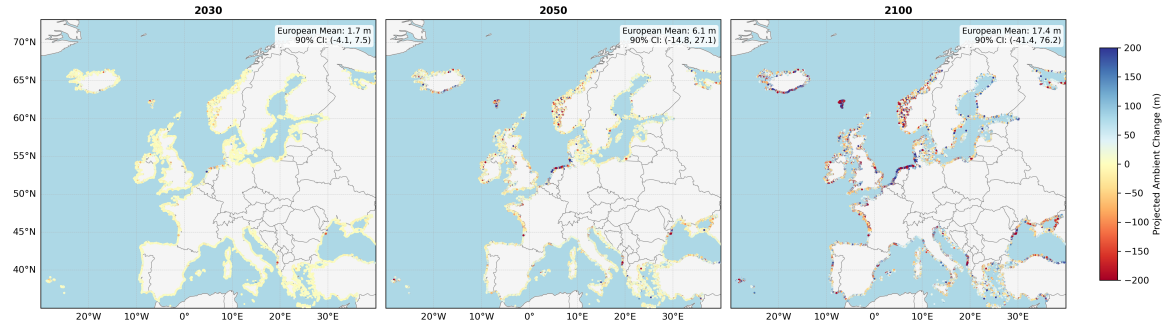

Figure C.29: Ambient shoreline change across all time steps.

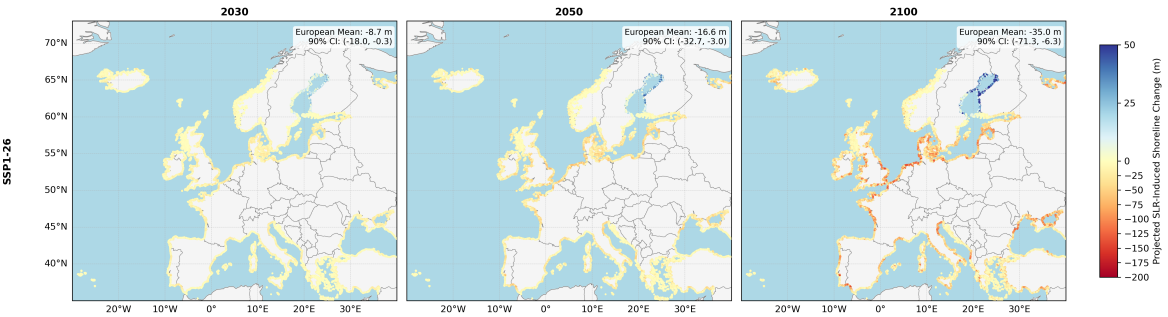

Figure C.30: Isolated SLR-only shoreline change under SSP1-2.6.

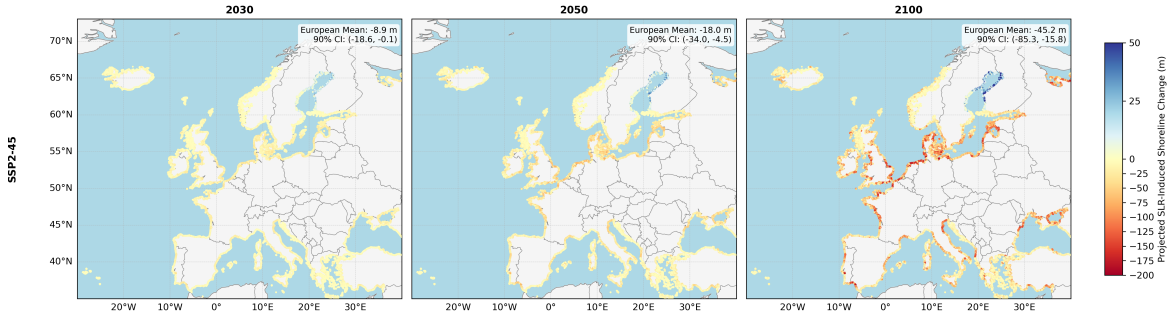

Figure C.31: Isolated SLR-only shoreline change under SSP2-4.5.

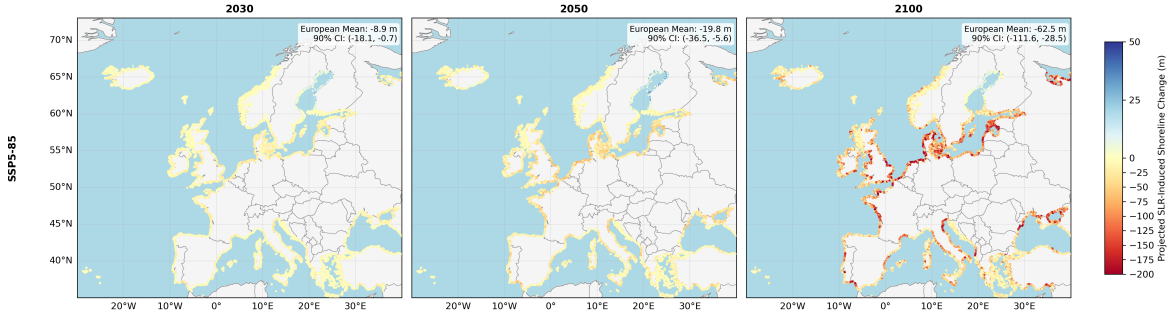

Figure C.32: Isolated SLR-only shoreline change under SSP5-8.5.

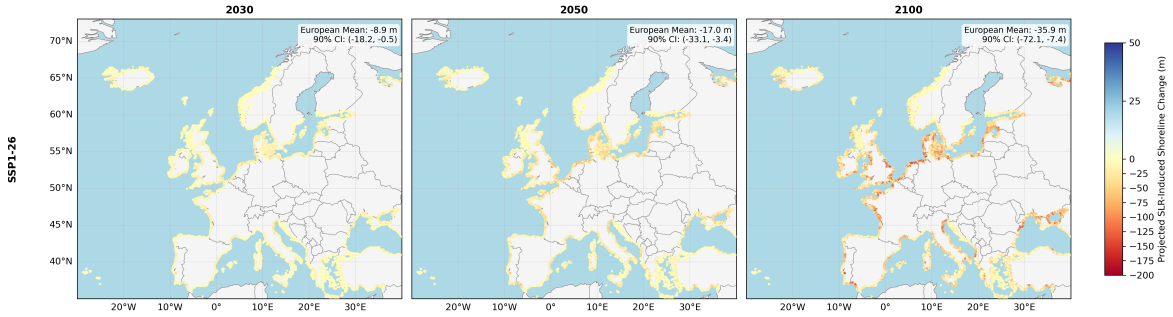

Figure C.33: Isolated SLR-only shoreline retreat under SSP1-2.6.

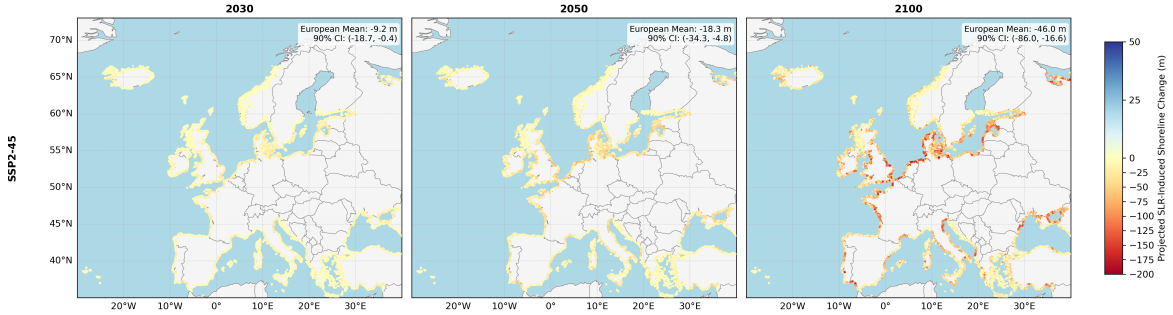

Figure C.34: Isolated SLR-only shoreline retreat under SSP2-4.5.

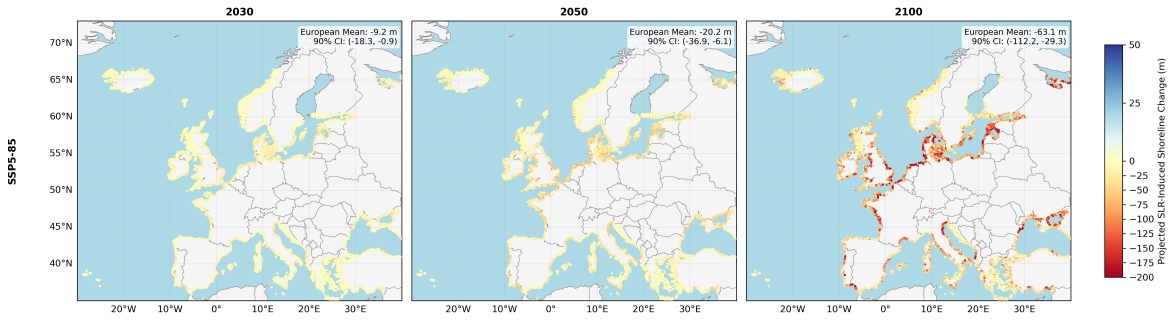

Figure C.35: Isolated SLR-only shoreline retreat under SSP5-8.5.

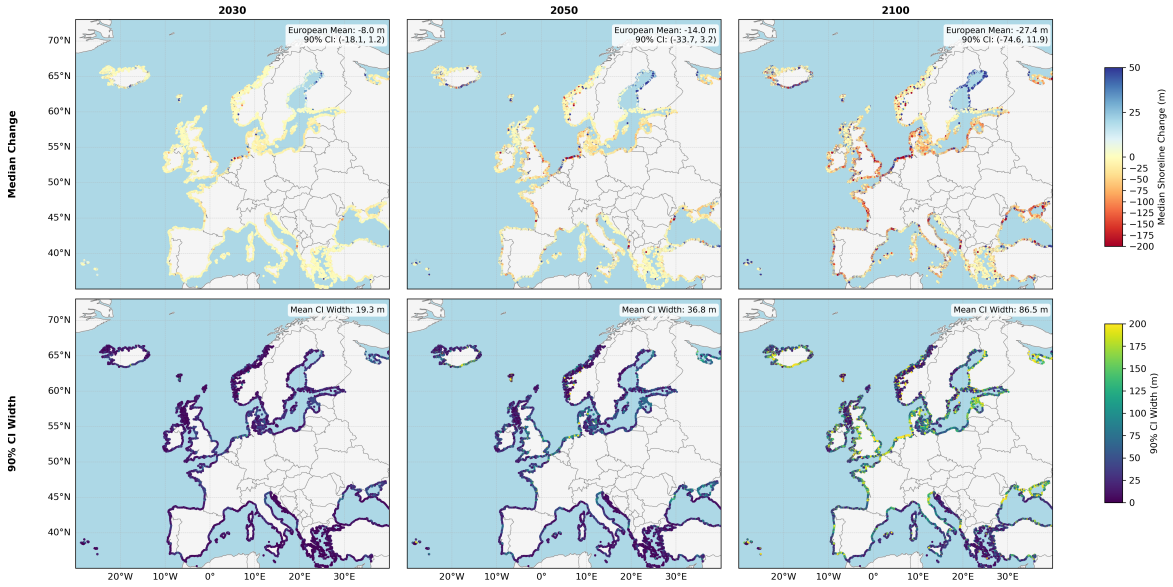

Figure C.36: Combined shoreline change and 90% confidence interval under SSP1-2.6.

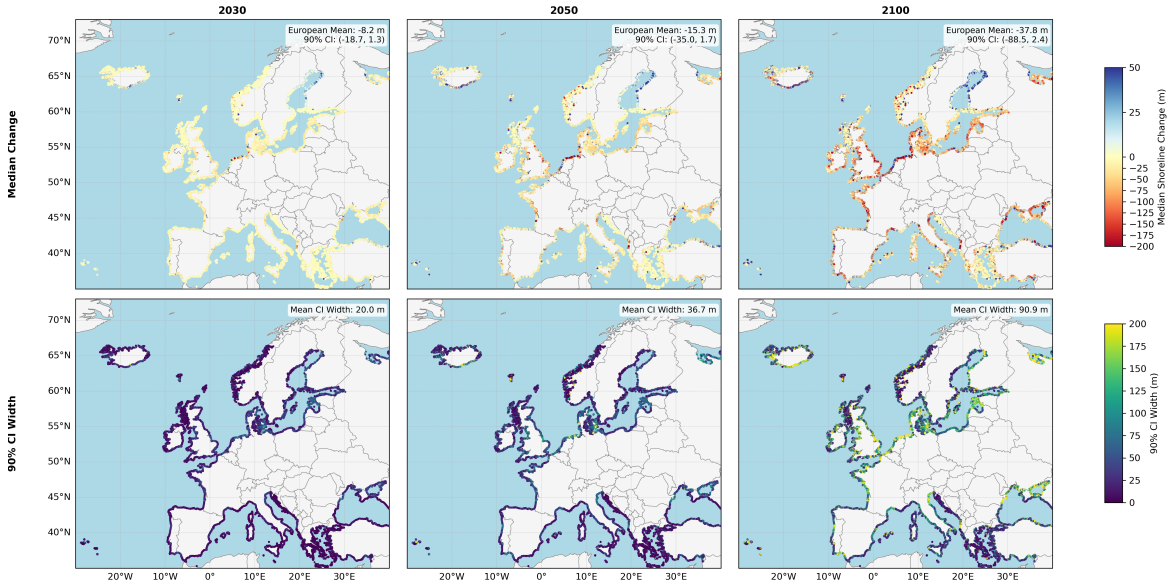

Figure C.37: Combined shoreline change and 90% confidence interval under SSP2-4.5.

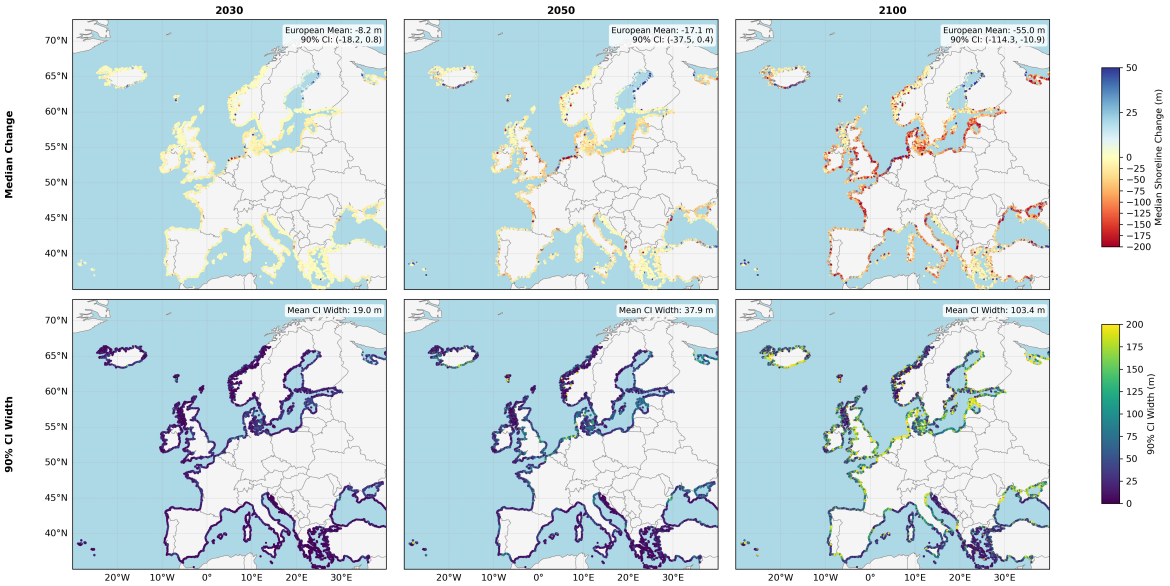

Figure C.38: Combined shoreline change and 90% confidence interval under SSP5-8.5.

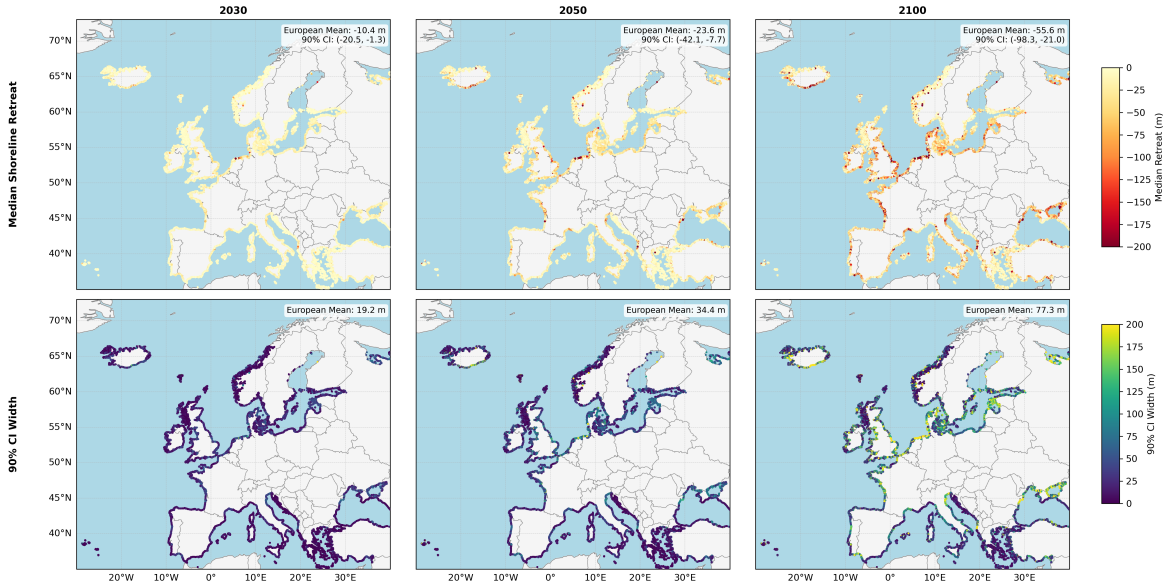

Figure C.39: Combined shoreline retreat and 90% confidence interval under SSP1-2.6.

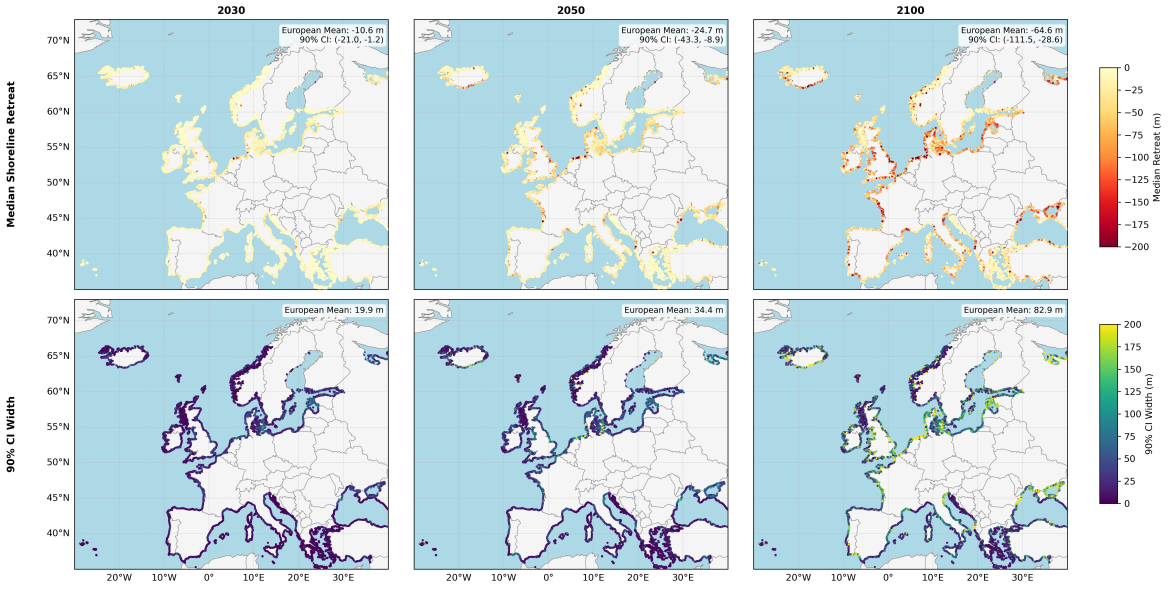

Figure C.40: Combined shoreline retreat and 90% confidence interval under SSP2-4.5.

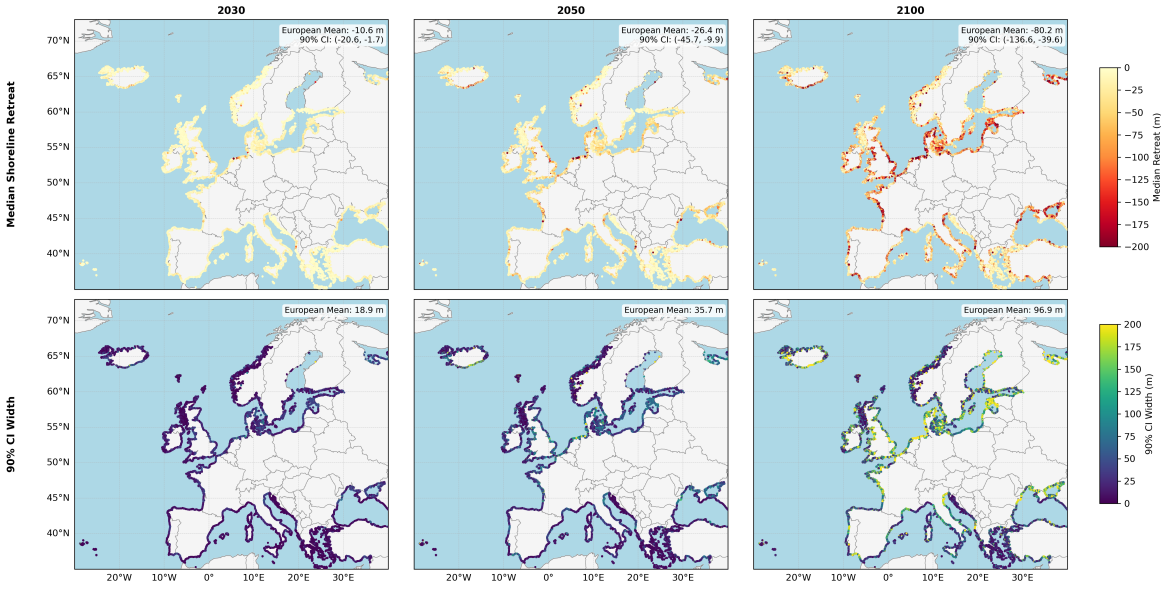

Figure C.41: Combined shoreline retreat and 90% confidence interval under SSP5-8.5.